UNIVERSITY OF SALERNO

DEPARTMENT OF CHEMISTRY AND BIOLOGY "A. ZAMBELLI"

Ph.D Course in Chemistry (XXXIV Cycle)

Thesis on

Identification of polyphenols in grape pomace and new synthetic approaches to 2,3-diaryl-2,3- dihydrobenzofurans, useful active ingredients against degenerative diseases

Tutor:

Prof. Paolo LUPATTELLI

Ph.D. Student:

Teresa LAURITA

Ph.D. Coordinator:

Prof. Claudio PELLECCHIA

ACADEMIC YEAR 2020-2021

INDEX

To Irene, my little princess and great warrior.

LIST OF ABBREVIATIONS

GP = Grape pomace
SO_2 =Sulfure dioxide
MeOH = Methanol
EtOH = Ethanol
H_2O = Water
DHB = Dihydrobenzofuran
H_2O_2 = Hydrogen peroxide
$FeCl_3$*H_2O = Ferric chloride* water
Tf_2O = Trimethan sulfoni acid
NIS = N-iodiosuccinimide
BBr_3 = Borono tribromide
PPh_3 = Triphenylphosphine
DEAD = Diethyl azodicarboxylate
THF = Tetrahydrofuran
p-TsOH = *p*-Toluensulfonic acid
ZnI_2 = Zinc iodide
$PdCl_2$ = Palladium chloride
CH_2Cl_2 = Dichloreomethane
MnO_2 = Manganese dioxide
BBr_3 = Borono tribromide
KOH = Potassium hydroxide
CH_3CN = Acetonitrile
t-BuOH = *tert*-butyl alcohol
$MgBr_2$ = Magnesium bromide
NO_2 = Nitrogen group
CF_3 = Trifluoromethyl gropup
OCH_3 = Methoxyl group
K_2CO_3 = Potassium carbonate
CuI = Copper iodide
PhMgBr = Phenylmagnesium bromide
BF_3 = Boron trifluoride
PhLI = Phenyllithium
$PhBF_3K$ = Potassium phenyltrifluoroborate
$ArB(OH)_2$ = Aryl boronic acid
Et_2ZN = Diethyl zinc
BCl_3 = Boron trichloride
$HCOONH_2$ = Nitromethane
$NaBH_2$ = Sodium borohydrine
i-PrOH = Isopropyl alcohol
TFA = Trifluoroacetic acid
n-Bu_4F = tetra-*n*-butylammonium fluoride
CsF = Cesium fluoride
$TiCl_4$ = Titanium tetrachloride
$NaHCO_3$ = Sodium bicarbonate
HCl = Hydrochloric acid
EtOAc = Ethyl acetate
EP = Petroleum ether
Et_2O = Diethyl ether
Na_2SO_4 = Sodium solfate
$Pd(OAc)_2$ = Palladium diacetate
NH_4Cl_4 = Ammonium chloride
$AlCl_3$ =Alluminium chloride
Nai = SOdium iodide
EOM.CL = Chloromthyl ethyl ether
LiOTf = Lithium triflate
HFIP = Hexafluoro-2-propanol
AcOH = Acetic acid
AgTFA = Silver trifluoroacetate
$AgCO_3$ = Silver carbonate
NaOH = SOdium hydroxide
Et_3N = Triethylamine
Ac_2O = Acetic anhydride
I_2 = Iodide
$PhI(OAc)_2$ = (Diacetoxyiodo)benzene

GENERAL INTRODUCTION

Natural products, including plants, animals and minerals have been the basis of treatment of human diseases.[1]
Historically, most of the new drugs have been generated from natural products (secondary metabolites) and their derivatives.
Before 20th century, crude and semi-pure extracts of plants, animals, microbes and minerals represented the only medications available to treat human illnesses. The 20th century revolutionized the use of drugs, by the receptor theory of drug action. The idea that the effect of drug in human body is mediated by specific interactions of the molecule with biological macromolecules led scientist to the conclusion that individual chemical compounds in extracts, rather than some mystical "power of life" are the factors required for the biological activity of the drug. This led to the beginning of a totally new era in pharmacology, as pure, isolated chemicals, instead of extracts, became the standard treatments for diseases. Indeed, many bioactive compounds, responsible for the effects of crude extract drugs, were discovered and their chemical structure elucidated.

Classical examples of drugs discovered this way are morphine, the active agent in *Opium*, and digoxin, a heart stimulant originating from flower *Digitalis lanata*.
Nevertheless, natural products present challenges for drug discovery, as isolation and characterization together with, in most cases, too small quantities for a complete biological evaluation.
The organic synthesis of natural products has been demonstrated to be a valuable approach to obtain sufficient material for research and applications. In addition, by synthesis it is possible to design and obtain analogs or substructures of natural products for structure-activity studies, in order to achieve compounds with desired properties for applications in pharmaceutical, agricultural, and food industries.

Among natural compounds, in the last years, phenolic compounds have aroused great interest in the scientific community for their protective and beneficial role for human body.
Special attention has been paid to the total phenolic content of grape pomace, in particular to specific compounds, *i.e. trans*-resveratrol and its derivatives. Recently such grape pomace extracts were studied in disease prevention and treatment,[2] highlighting their high biotechnological potential and paving the way for alternative uses, in particular as food supplements, new drugs or cosmetics for humans.

Instead, on a synthetic standpoint the 2,3-dihydrobenzofuran ring-system, which constitutes the core skeleton of different resveratrol oligomers, has recently received significant attention.[3] Regio-and stereoselective approaches were described which allow the preparation of good

[1] a) Lahlou, M. *Expert Opin. Drug Discov*., **2007**, *2*, 697-705. b) Patwardhan, B.; Vaidya, A. D. B.; Chorghade, M. *Curr. Sci*., **2004**, *86*, 789-799.
[2] a) Koutelidakis, A.; Charalampia, D. *Moj Food Process. Technol*., **2016**, *3*, 262-265. b) Averilla, J. N.; Oh, J.; Kim, H.J.; Kim, J. S.; Kim, J.S. *Food Sci Biotechnol.*, **2019**, *28*, 1607-1615.
[3] Laurita, T.; D'Orsi, R.; Chiummiento, L.; Funicello, M.; Lupattelli, P. *Synthesis* **2020**, *52*, 1451-1477

quantities of these natural compounds or analogs for broad-spectrum biological and pharmacological analysis.

AIM OF Ph.D. PROJECT

The aim of this Ph.D. project is based on three different studies:

1. Analysis of total phenolic compounds and in particular of *trans*-resveratrol into three different samples of grape pomace (work done in "*OSUN SOLUTIONS Srl"*, Lauria, (Pz), Italy)

2. New synthetic approach for stereo- and entantioselective synthesis of *trans* 2,3-diaryl-2,3-dihydrobenzofurans systems, via regio- and diastereoselective arylation of *trans* 2.3-diaryloxiranes (work done in "*University of Basilicata"*, Potenza, Italy);

3. Metal-catalyzed C-H functionalization of diarylacetaldehydes: access to a new potential key intermediate for synthesis of 2,3-diaryl- 2,3-dihydrobenzofurans (work done in "*Université de Strasbourg"*, Strasbourg, France).

CHAPTER 1. GRAPE POMACE: A SOURCE OF BIOACTIVE PHENOLIC COMPOUNDS

1.1 Introduction

Grape is the world's largest fruit crop with an annual production of more than 70 million tons.[4] Grapes and products obtained therefrom, such as wine, grape juice, jams and raisins, have then an obvious economic importance. Eighty percent of the worldwide grape production is used in winemaking. The wine industry produces millions of tons of residues, that is grape pomace (GP), after fermentation, which represents a waste management issue both ecologically and economically.

When grape berries are processed for winemaking, the skins and seeds are usually in contact with the fermenting broth for several days. Thus, grapes are subjected to a slight but prolonged extraction with a hydroethanol mixture that provides the red wine with a variable content of polyphenols. However, the residue remaining after fermentation (i.e., GP), which mainly consists of skins and seeds, still contains high levels of polyphenols.[5] The phenolic content of GP depends on multiple factors, including climate, degree of ripeness, berry size, grapevine variety and on the characteristics of the winemaking, e.g. maceration time, temperature, intensity and duration of pressing, used SO_2 doses.

Phenolic compounds are secondary metabolites, which are produced *via* the shikimic acid pathway in higher plants and microorganisms. They contain benzene rings, with one or more hydroxyl substituents, and range from simple phenolic molecules to highly polymerized compounds.[6] In food science, natural phenolics are generally classified into classes and sub-classes, based on the similarity of their chemical structures, that is, the types of building blocks that appear as repeated units. Four major classes of polyphenols found in foods are phenolic acids, flavonoids, lignans and stilbenes (Figure 1).

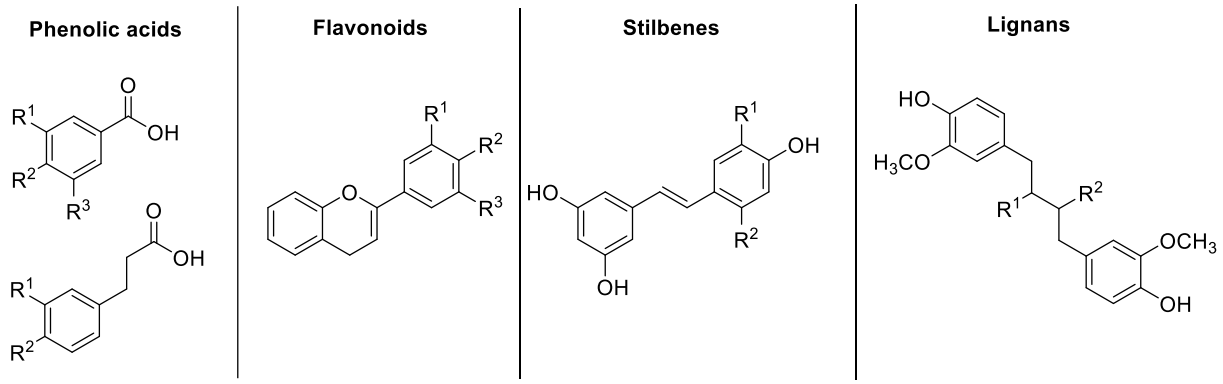

Figure 1 Phenolic acids, flavonoids, lignans and stilbenes structures

[4] F.-F.S.D., FAOSTAT-FAO Statistical Database
[5] Fontana, A. R.; Antoniolli, A.; Bottini, R. *J. Agric. Food Chem*, **2013**, *61*, 8987-9003.
[6] Shahidi, F. & Naczk, M. *"Phenolics in food and Nutraceuticals", FL: CRC Press LLC*. **2004**, 443–482.

These polyphenols have shown several health-promoting proprieties. Epidemiological studies have revealed an inverse relationship between chronic diseases and phenolic compounds nutrition intake. In fact, phenolic groups are able of accepting an electron, forming phenoxyl radicals, rather stable, interrupting chain oxidative reactions in cellular components.[7] Also, polyphenols possibly offer a significant protection against cancer, diabetes, cardiovascular diseases, asthma, hypertension, neurological disorders (such as Alzheimer's disease), psychiatric and in general cognitive diseases.[8] The possible mechanisms of polyphenols bioactivity are based on their antioxidant activity, but plethora of studies points out potential effect on metabolic pathways and on the expression of specific genes.

Thanks to these health proprieties, bioactive phenolic compounds extracted from grape pomace may provide great opportunities for adding value to wine residues, contributing to the development of novel functional foods and supplements, helping in the prevention of the development of serious chronic diseases, besides promoting sustainable development through revalorization of waste residues[9] and decreasing environmental impact.

One of the major active polyphenolic compounds found in grape pomace is resveratrol. Resveratrol is a stilbenoid polyphenol, possessing two phenol rings linked to each other by an ethylene bridge. The chemical structure of resveratrol (3,5,4′-trihydroxystilbene) is identified in two isomeric forms, *cis*- and *trans*-resveratrol (Figure 2). *Trans* form is dominant in terms of its prevalence and different biological activities are attributed to it, namely in inducing cellular responses such as cell cycle arrest, differentiation, apoptosis, and to enhance cancer cells anti-proliferation.[10]

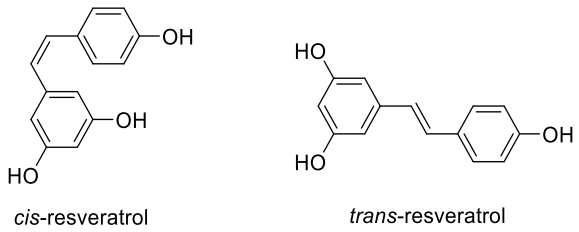

cis-resveratrol *trans*-resveratrol

Figure 2 Chemical structure of *cis*- and *trans*-resveratrol

This compound is classified as a phytoalexin,[11] a substance synthesized *de novo* by plants in response to a stress, injury, ultraviolet irradiation and/or fungal infection.

Resveratrol was first isolated from white hellebore (*Veratrum grandiflorum* O. Loes) roots in 1940, then from *Polygonum cuspidatum* roots in 1963, a plant used in traditional Chinese and Japanese Medicine as anti-inflammatory and anti-platelet agent. This natural polyphenol has been detected in more than 70 plant species, and is also found in discrete amounts in red wines

---

[7] Pandey, K. P.; Rizvi, S. I. *Oxid. Med. Cell Longev.*. **2009**, *2*, 270–278.

[8] a) Fraga, C. G.; Galleanoa, M.; Verstraetenc, S. V. et al. *Molec. Asp. of Medicine* **2010**, *3*1, 435–445. b) Rio, D. D.; Costa, L. G.; Lean, M. E. J. et al. *Nutrit. Metabol. and Cardiov. diseases*. **2010**, *20*, 1–6.

[9] Dimou, C.; Kopsahelis, N.; Papadaki, A. et al. *Int. Food Res. J.* **2015**, *73*, 81–87.

[10] a) Akinwumi, B.C.; Bordun, K.M.; Anderson, H.D. *Int. J. Mol.* Sci. **2018**, *19*, 792. b) Anisimova, N.Y.; Kiselevsky, M.V.; Sosnov, A.V.; Sadovnikov, S.V.; Stankov, I.N.; Gakh, A.A. Trans-, *Chem. Cen. J.* **2011**, *5*, 88. c) Orallo, F. *Curr. Med. Chem*. **2006**, *13*, 87–98.

[11] Ahuja, I.; Kissen, R.; Bones, A. M. *Trends Plant Sci.* **2012**, *17*, 73-90.

and various human foods. High concentrations are present in grapes, possibly because of *Vitis vinifera* response to fungal infection.

Interest in *trans*-resveratrol as a human supplement arose from the "French Paradox", reported for the first time in 1992[12] from Renaud and De Lorgeril, stating that the French population shows a low cardiovascular diseases expected rate, although it consumes high quantities of saturated fats, together with red wine.

Trans-resveratrol, as the other phenolic compounds, is produced in grape skins and some of this solubilizes into red wine during fermentation. According to Vincenzi *et al.*[13] the concentration of resveratrol in red wine is too low for therapeutic effect because most of resveratrol remains in winery waste. This led to investigation of resveratrol as a nutraceutical supplement at increased does, opening up the possibility of producing a resveratrol-based product from grape solid winery waste.[14]

Several studies have associated various human health effects to resveratrol, such as:

- Cardioprotective effects: resveratrol protection against cardiovascular illnesses has been associated to the lowering of lipid peroxidation and improvement of serum cholesterol profile as well as triglyceride concentration; reduction of platelet aggregation; vasodilatation and lowering of blood pressure.[15] Antiatherosclerotic action, protection of endothelial cells against apoptosis, induction of neovascularisation of the infarcted myocardium and diminishing of smooth muscle cell (SMC) proliferation have also been revealed.
- Antioxidant effects: they depend upon the arrangement of functional groups on aromatic ring. Thus, the hydroxyl groups in 3,4,5 positions influence several mechanisms of antioxidant activity, such as radical scavenging and metal ion chelation abilities.[16] In addition, resveratrol's antioxidant properties have successfully been employed to protect cells against hydrogen peroxide-induced oxidative stress,[17] in which the pre-tratment with resveratrol promoted cell survival and protection against UV-irradiation-induced cell death.
- Neuroprotective effects: resveratrol has several neuroprotective roles in various neurodegenerative impairments, such as Alzheimer's, Huntington's and Parkinson's diseases, amyotrophic lateral sclerosis and alcohol-induced neurodegenerative disorders. This protective effects seem to be related mainly to its antioxidant activity, since oxidative stress appears to be closely related to major neuronal pathologies.[18]
- Anti-inflammatory effects: the key mediators of the inflammatory processes are the prostaglandins (PGs). Resveratrol has been shown to dose-dependently inhibit induced

---

[12] Renaud, S., and de Lorgeril, M. *Lancet*, **1992**, 339, 1523–1526.

[13] Vincenzi, S.; Tomasi, D.; Gaiotti, F.; Lovat, L.; Giacosa, S.; Torchio, F.; Río Segade, S.; Rolle, L. *J. Enol. Vitic.* **2013**, *34*, No 1.

[14] a) Beres, C.; Costa, G.N.S.; Cabezudo, I.; Silva-James, N.K.: Teles, A.S.C.: Cruz, A.P.G.: Mellinger-Silva, C.; Tonon, R. V.; Cabral, L.M.C.; Freitas, S.P., *Waste Manag.* **2017**, *68*, 581-594. b) Devesa-Rey, R.; Vecino, X.; Varela-Alende, J.L.; Barral, M.T.; Cruz, J.M.; Moldes, A.B. *Waste Manag*. **2011**, *31*, 2327-2335.

[15] a) Bradamante. S.; Barenghi, L.; Villa, A. *Cardiovasc. Drug Rev.* **2004**, *22*, 169-188. b)

[16] Stivala, L.A.; Savio, M.; Carafoli, F.; Perucca, P.; Bianchi, L.; Maga, G.; Forti, L.; Pagnoni, U.M.; Albini, A.; Prosperi, E.; et al. *J. Biol. Chem*., **2001**, *276*, 22586–22594.

[17] Konyalioglu, S.; Armagan, G.; Yalcin, A.; Atalayin, C.; Dagci, T. *Neural Regen. Res*., **2013**, 8, 485–495.

[18] Sun, A. Y.; Wang, Q.; Simonyi, A.; Sun, G. Y. *Mol. Neutrobiol.* **2010**, *41*, 375-383.

production of PGE_2 in human peripheral blood leukocytes, while *in vivo*, resveratrol significantly decreased levels of rat PGD_2. In the *in vitro* and *in vivo* models, resveratrol decreased the expression of cyclooxygenase-2 (COX-2), an enzyme that catalyzes PG synthesis and is induced by inflammation. Resveratrol has been observed to decrease induced COX-2 activity by inhibiting the expression of the enzyme *via* signal transduction pathways. [19]

Nuclear factor-κB (NF-κB), a transcription factor, regulates genes involved in inflammation and tumorigenesis. Inhibition of NF-κB activity is a possible mechanism by which resveratrol exerts its anti-inflammatory activity. Inhibition of TNF-induced NF-κB activation by resveratrol has been observed in several cell lines. The exact mechanism by which resveratrol inhibits NF-κB activation remains uncertain.[20]

- Anticancer effects: resveratrol is able to inhibit all carcinogenesis stages (e.g., initiation, promotion and progression).[21] Many studies[22] also provided evidence that resveratrol not only acts a chemopreventive agent, but also displays chemotherapeutic properties linked to its anti-inflammatory, antioxidant, pro-apoptosis and anti-proliferative actions. Its antiproliferative action occurs by activating cell cycle and inducing of apoptosis. Several studies[23] have suggested that the anti-proliferative effects of resveratrol on cancer cells is the result of a metabolic conversion of resveratrol to piceatannol (Figure 3) by cytochrome P450 1B1 (CYP1B1). CYP1B1 is a gene highly expressed in cancerous tissue and not much in physiological ones.

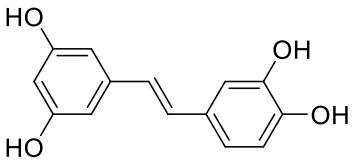

piceatannol

Figure 3 Structure of piacetannol

Give that these bioactive compounds are strongly correlated with a broad spectrum of beneficial effects, the investigation of their content in the GP extracts constitutes basic information for the evalutation of the feasibility of their use in the food and pharmaceutical industries.

---

[19] Richard, N.; Porath, D.; Radspieler, A.; Schwager J. *Mol Nutr Food Res*, **2005**, *49*, 431–42.

[20] King, E., R.; Bomser, A., J.; Min, D., B. *Comprehensive Reviews in Food Science and Food Safety*, **2006**, *5*, 65-70.

[21] Varoni, E.M.; Lo Faro, A.F.; Sharifi-Rad, J.; Iriti, M. *Front. Nutr.*, **2016**, *3*, 8.

[22] a) Pezzuto, J.M. *Pharm. Biol.*, **2008**, *46*, 443–573. b) Van Ginkel, P.R.; Sareen, D.; Subramanian, L.;Walker, Q.; Darjatmoko, S.R.; Lindstrom, M.J.; Kulkarni, A.; Albert, D.M.; Polans, A.S. *Clin. Cancer Res*., **2007**, *13*, 5162–5169.

[23] a) Wolter, F.; Clausnitzer, A,; Akoglu, B.; Stein, J. *J. Nutr.***220**, *132*, 298-302. b) Larrosa, M.; Tomás-Barberán, F. A.; Espín, J. C.; *Eur. J. Nutr.* **2004**, *43*, 275-284.

1.2 Goal of the work

A part of my doctoral work was done at *Osun Solution S.r.l.* (Lauria, Italy), a laboratory specialized in chemical-physical and microbiological analyses in the food sector and offers a complete outsourcing service from the study of formulas of new products, to the identification and characterization of new ecotypes of medicinal plants to be used as nutraceuticals.

In this laboratory, the goal of the work was to determinate the content of total phenolic compounds and of *trans*-resveratrol into three different varieties of grape pomace using two different extraction procedures.

1.3 Materials and methods

1.3.1 Chemicals and samples

The *trans*- resveratrol standard (99%) was purchased from PhytoLab (Germany), the Gallic acid standard from Merck kGaA (China) and *Folin-Ciocalteau* reagent from Titolchimica s.p.a. (Italy). All solvent used for extraction and analyses were analytic grade. Methanol, water and acetonitrile were purchased from Honeywell (United States) and Ethanol 96° from Carlo Erba (Italy).

The studies were carried out on three grape pomace (GP) cultivars: Aglianico del vulture (Barile, Italy, 2019), Yuko (Japanese grown in Modena, Italy, 2019) and Piedirosso (Quarto, Italy, 2020).

1.3.2 Extraction procedures

Two different extraction procedures were used to prepare the grape pomace extracts.

- Extraction in laboratory was carried out with a classical procedure putting the matrices in alcoholic aqueous solution at reflux

  Aglianico del Vulture: 25 g of pulverized dry pomace were weighed into a 250 mL flat-bottomed flask and extracted with 125 mL of 80% aqueous EtOH under stirring at 80°C for 2 hours. The extract was separated by filtration under vacuum and the material was re-extracted twice using the same procedure. The combined extracts were concentrated first by evaporation under reduced pressure and finally in the vacuum dryng oven, to get the dry extract (Figure 4 **A**).

- Extraction in industry was carried out by spray-drying microencapsulation using maltodextrin as carrier material

  Piedirosso: the fresh red pomace (50 % humidity) was extracted with 80% aqueous EtOH in a percolator at room temperature for 7 days in a static way. The extract was discharged and filtered and the pomace was statically extracted again with 80% EtOH at room temperature in a percolator for 5 days. The extract was discharged, the pomace was pressed and the extract was filtered, obtaining a fluid extract. The two extracts were combined, concentrated, pasteurized and filtered. 45% of maltodextrin was added on the total

theoretical dry extract and everything was dried using a spray dryer, to obtain the dry powder extract (Figure 4 **B**).

Yuko: the dry pomace (5% humidity) was extracted 4 times with 80% aqueous EtOH at room temperature in a percolator for 6 hours under stirring. The extract was drained and filtered. The extracts were combined, concentrated, pasteurized and filtered. 66% of maltodextrin was added to the total extract and dried using a spray dryer, to get the dry powder extract (Figure 4 **C**).

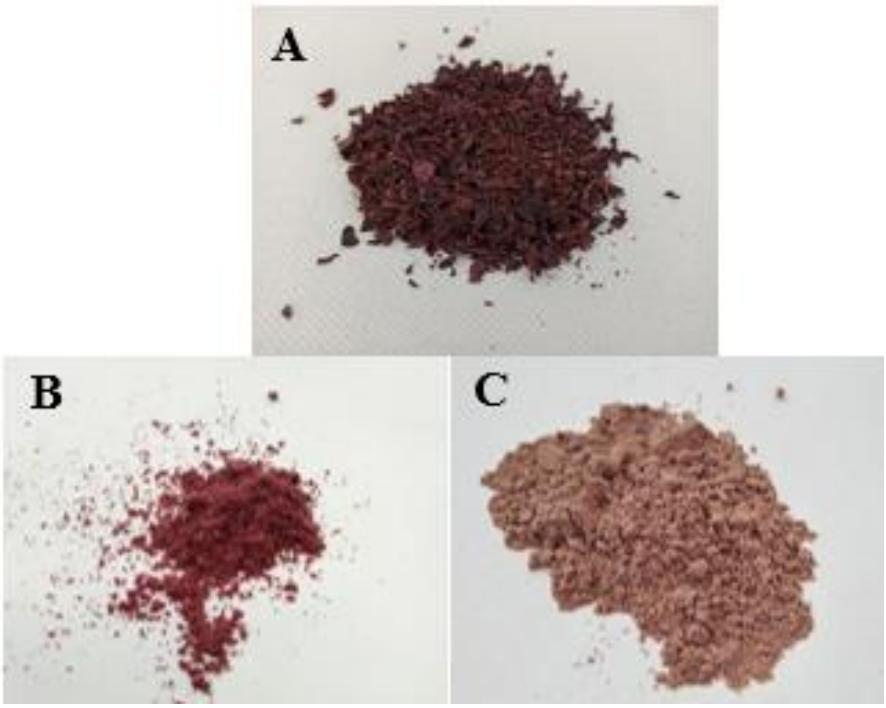

Figure 4 Grape pomace extract of Aglianico del Vulture (**A**), Piedirosso (**B**) and Yuko (**C**)

1.3.3 Spectrophotometric determination of total soluble polyphenols: instrumentation and conditions

The amount of the total soluble polyphenols in the extracts was determined spectrophotometrically using UV-1800 SHIMADZU Spectrophotometer according to the *Folin-Ciocalteau* (*FC*) method.

The *FC* colorimetry is based on a chemical reduction of the reagent, a mixture of tungsten and molybdenum oxide. The product of the metal oxide reduction has a blue color that exhibits a broad light absorption maximum at 760 nm. The intensity of light absorption at that wavelength is proportional to the concentration of phenolics. In this work was employed a *FC* method supplied by nVH Italy Srl:

Blank solution: Mixture of 1.0 mL of phosphomolybdotungtic reagent and 12.0 mL of water diluted to 25.0 mL with a 290 g/L solution of sodium carbonate. After 30 minutes this solution was used as compensation liquid for the measure of samples and standards.

Reference solution A: 10 mg of Gallic acid is poured in 100.0 mL of water. 2.0 mL of this solution is stirred with 1.0 mL of phosphomolybdotungtic reagent and 10.0 mL of water and the solution is diluted to 25.0 mL with a 290 g/L solution of sodium carbonate. After 30 minutes the absorbance at 760 nm is measured, using blank solution as compensation liquid.

Reference solution B: 5.0 mL of reference solution A is added to 10.0 mL of water. 2.0 mL of this solution is mixed with 1.0 mL of phospdomolybdotungstic reagent and 10.0 mL of water and diluted to 25.0 mL with a 290 g/L solution of sodium carbonate. After 30 minutes the absorbance at 760 nm is measured, using blank solution as compensation liquid.

Reference solution C: 5.0 mL of reference solution A is added to 20.0 mL of water. 2.0 mL of this solution is mixed with 1.0 mL of phospdomolybdotungstic reagent and 10.0 mL of water and diluted to 25.0 mL with a 290 g/L solution of sodium carbonate. After 30 minutes the absorbance at 760 nm is measured, using blank solution as compensation liquid.

Test solution: To 15 mg of grape to be examined 80 mL of water is added in a 100 mL volumetric flask and sonicated for 10 minutes. The mixture is cooled and brought to volume with water. 2.0 mL of this solution is mixed with 1.0 mL of phospdomolybdotungstic reagent and 10.0 mL of water and diluted to 25.0 mL with a 290 g/L solution of sodium carbonate. After 30 minutes the absorbance at 760 nm is measured, using blank solution as compensation liquid.

Total phenolic content of the extracts were determined by the help of standard curve and it was expressed as percentage content of total polyphenols as gallic acid from the expression:

$$\frac{C \times t \times V}{m} \times 100$$

Where

C = concentration of polyphenols as Gallic acid in the test solution, determinated from calibration curve, in mg/mL;

t = percentage content of Gallic acid in Gallic acid reference substance;

V = dilution of the test solution, in milliliters;

m = mass of the extract to be examined, in milligrams.

1.3.4 HPLC instrumentation and conditions

Analyses of *trans*-resveratrol in the extract were carried out using UV/VIS SHIMADZU – SPD-20° detector and two SHIMADZU – LC-20AT pumps. The separation was performed with C18 Lichrospher column (250 X 4,6 mm; 5 µm particle size). The mobile phase consisted of 2% (v/v) acetic acid in water (eluent A) and 0.5% acetic acid in water and acetonitrile (50:50, v/v;

eluent B) using a gradient program as follows: : from 10 to 24% B (20 min), from 24 to 30% B (20 min), from 30 to 55% B (20 min), from 55 to 100% B (15 min), 100% B isocratic (8 min), from 100 to 10% B (2 min). Total run time was 90 min. The solution of samples was filtered on 0.45 µm nylon filters before injection. The injection volume for all samples was 20 µL. Monitoring was performed at 320 nm.[24] Quantification of *trans*-resveratrol in the extract was determined using a calibration curve of the corresponding standard.

1.4 Results and discussion

1.4.1 Spectrophotometric determination of total soluble polyphenols: instrumentation and conditions

The concentration (C) and the measured absorbance (A) of the reference solutions are given in Table. Standard curve was obtained from plotting of light absorption (y) against different concentration of gallic acid (x) and are shown in Figure 5.

Table 1 Concentration and measured absorbance of reference standard solutions

	C (mg/mL)	Abs.
Ref. A	0.112	0.954
Ref. B	0.056	0.395
Ref. C	0.028	0.113

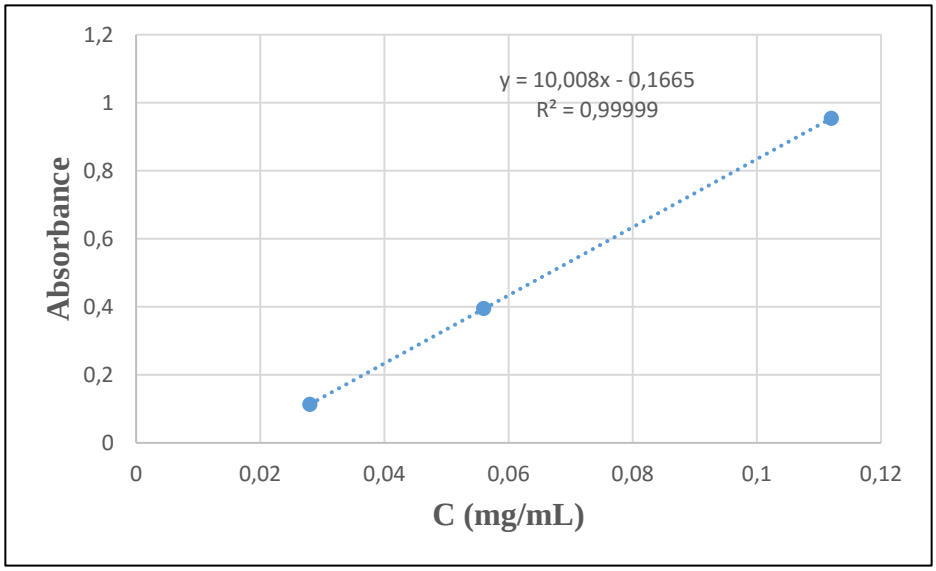

Figure 5 Calibration curve of standard gallic acid

The results in terms of absorbance of the three kind of grape pomace extracts, which were plotted on gallic acid curve, were showed in the following Table 2. The samples were measured

[24] Kammerer D., Claus A., Carle R., Schieber A. *J. Agric. Food Chem* **2004**, *52*, 4360-4367.

in triplicates and the results (Table 2) was expressed as percentage content of total polyphenols as gallic acid ± standard deviation (SD).

Table 2 Total polyphenols content of grape pomace extracts

Samples	% $_{\text{polyphenols tot}}$ ± SD
Aglianico del Vulture	36.0 ± 0.6
Yuko	7.1 ± 0.4
Piedirosso	10.7 ± 0.4

It has to be noted that the result obtained for the GP extract of "Aglianico del Vulture" are hardly comparable to those obtained for the GP extracts of "Yuko" and "Piedirosso", due to the two different extraction methodology.

The percentage of total polyphenols obtained for the GP of "Aglianico del Vulture" is in agreement with the results obtained in previous research on different red grape pomace extracted with similar methodology.[25]

Regarding the GP of "Yuko" and "Piedirosso" extracted applying the same methodology the percentage of total polyphenols are quite similar. The slightly higher value in the GP of "Piedirosso" probably depends on grapevine variety, in fact usually the content of polyphenols is higher in the red pomace than in the white ones.

A significant result of our analyses is that the total polyphenols content of wine pomaces is very good, so considering their innumerable beneficial properties for human health, these wine byproducts could be a potential matrices for the formulation of new drugs and supplements food.

1.4.2 Quantification of trans-resveratrol by HPLC-UV

A preliminary study was devoted to find the better chromatographic conditions to obtain good separation of *trans*-resveratrol. After testing various methods, both with isocratic[26] and gradient elution,[27] which gave bad results, the best separation of the compound was obtained using the system above described in Materials and methods (*section 1.3.4*).[24]

In order to quantify the *trans*-resveratrol present in the grape pomace extracts, a calibration curve of the standard was built analyzing a series of standards across a range of concentrations near the expected concentration of the analyte in the samples.

1 mg of *trans*-resveratrol standard was exactly weighted and solved in a 1:1 mixture of MeOH/H_2O in a 10 mL volumetric flask, thus obtaining a 0.1 mg/mL solution. This solution

[25] a) Butkhup, L.; Chowtivannakul, S.; Gaensakoo, R.; Prathepha, S.; Samappito. S. *S. Afr. J. EnoL Vitic*., **2010**, *31*, 89-98. b) Negro, C.; Tommasi, A.; Miceli, A. *Bioresour. Technol.*, **2003**, *87*, 41-44.

[26] Pascual-Marti M.C., Salvador A., Chafer A., Berna A. *Talanta* **2001**, *54*, 735-740.

[27] Silva M. A., Ky I., Jourdes M., Teissedre P.-L. **2012**, *234*, 361-365; Giusti F., Caprioli G., Ricciutelli M., Vittori S., Sagratini G. *Food Chem.* **2016**, *221*, 689-697.

was then diluted 1:10, 1:100, 1:200, 1:1000 in volumetric flasks with the same solvent mixture in order to obtain 0.01, 0.001, 0.0005, 0.0001 mg/mL solutions, respectively. The solutions in the range between 0.01 and 0.0001 mg/mL were analyzed in duplicates by HPLC-UV. Retention times (t_R) and the peak area for each standard are reported in Table 3.

Table 3 t_R, concentrations and areas of *trans*-resveratrol in the calibration curve

t_R (min)	C (mg/mL)	A_{Medium}
51.67 ± 0.58	0.01	2109310
50.90 ± 0.58	0.001	238841
50.29 ± 1.57	0.0005	119813
50.31 ± 0.09	0.0001	24588

The plot of the instrument response, based on the peak area under the curve of the standards Vs. its concentration, showed a linear relationship and a very good correlation of determination R^2, as shown in Figure 6.

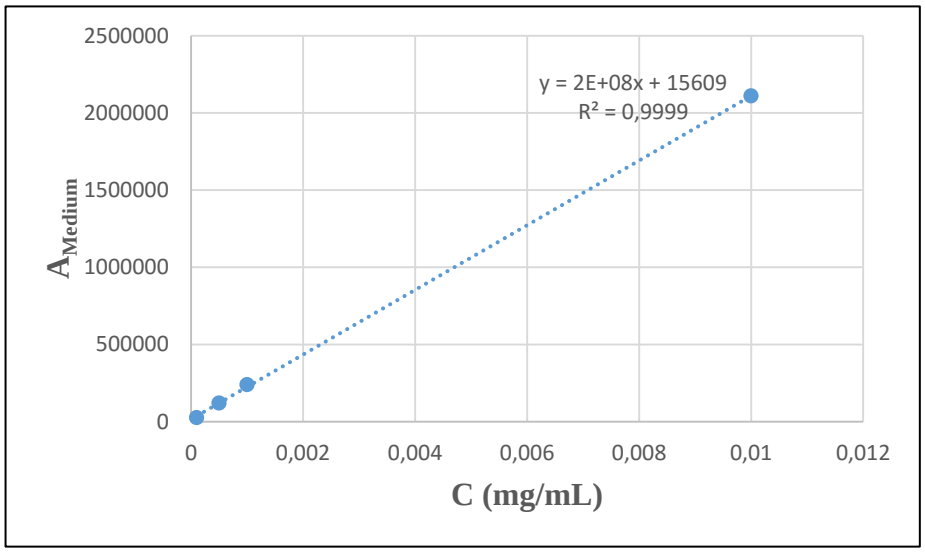

Figure 6 Calibration curve of standard *trans*-resveratrol

The samples were prepared by dissolving of 600 mg of the grape pomace extract in a 20 mL volumetric flask with a 1:1 solution of MeOH/H_2O, obtaining a concentration of 30 mg/mL. *Trans*-resveratrol was identified by comparison of its retention times with that of the standard, so before the analysis of each extract, the chromatographic run of the standard was done. The experiments on each extract were carried out in duplicate in order to evaluate the variability of the measurements. The obtained chromatograms for each experiment of GP extract of *"Aglianico del Vulture"*, *"Yuko"* and *"Piedirosso"* are shown in Figure 7, 8 and 9, respectively.

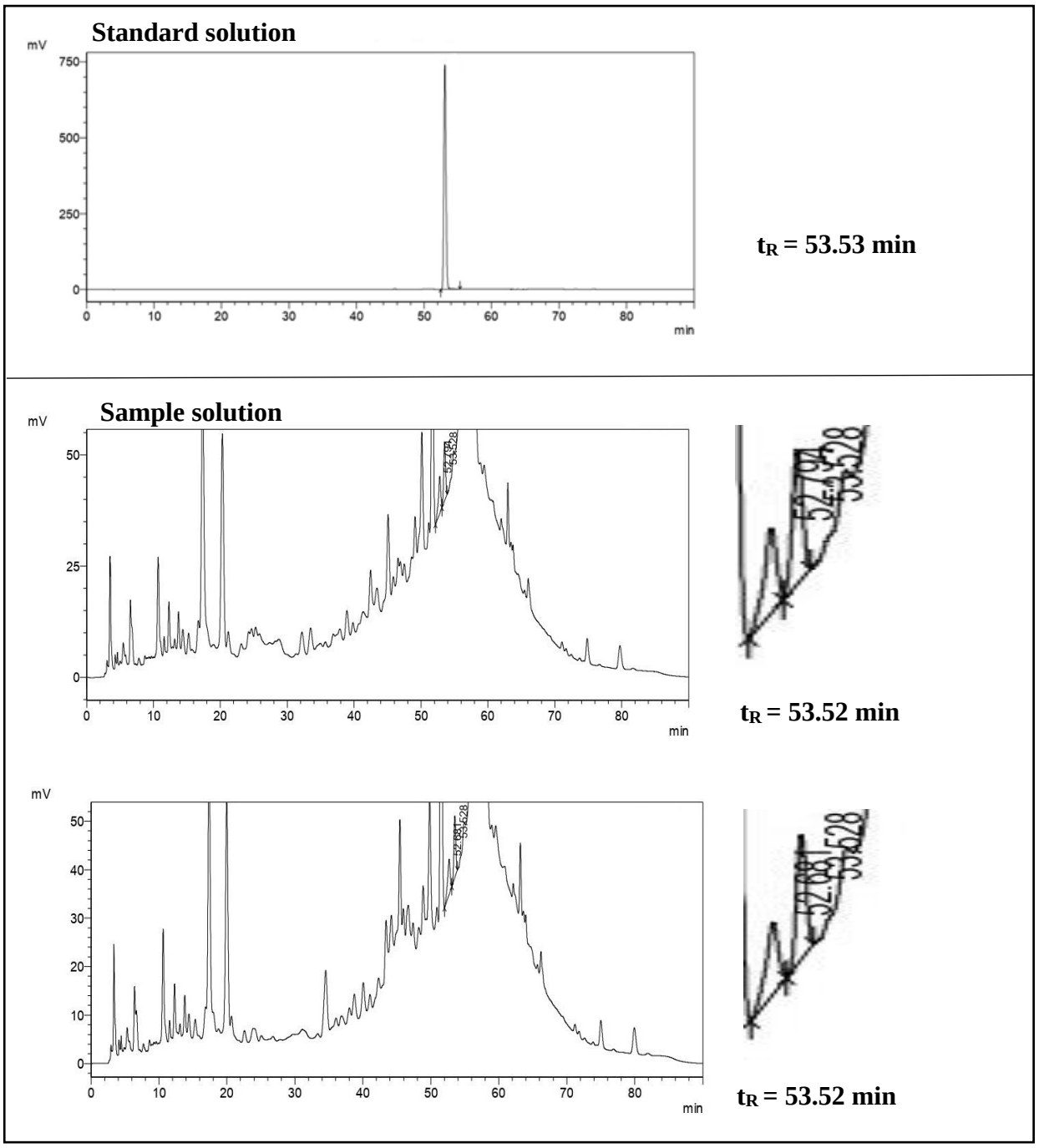

Figure 7 Chromatograms of standard and of "*Aglianico del Vulture"* grape pomace extract

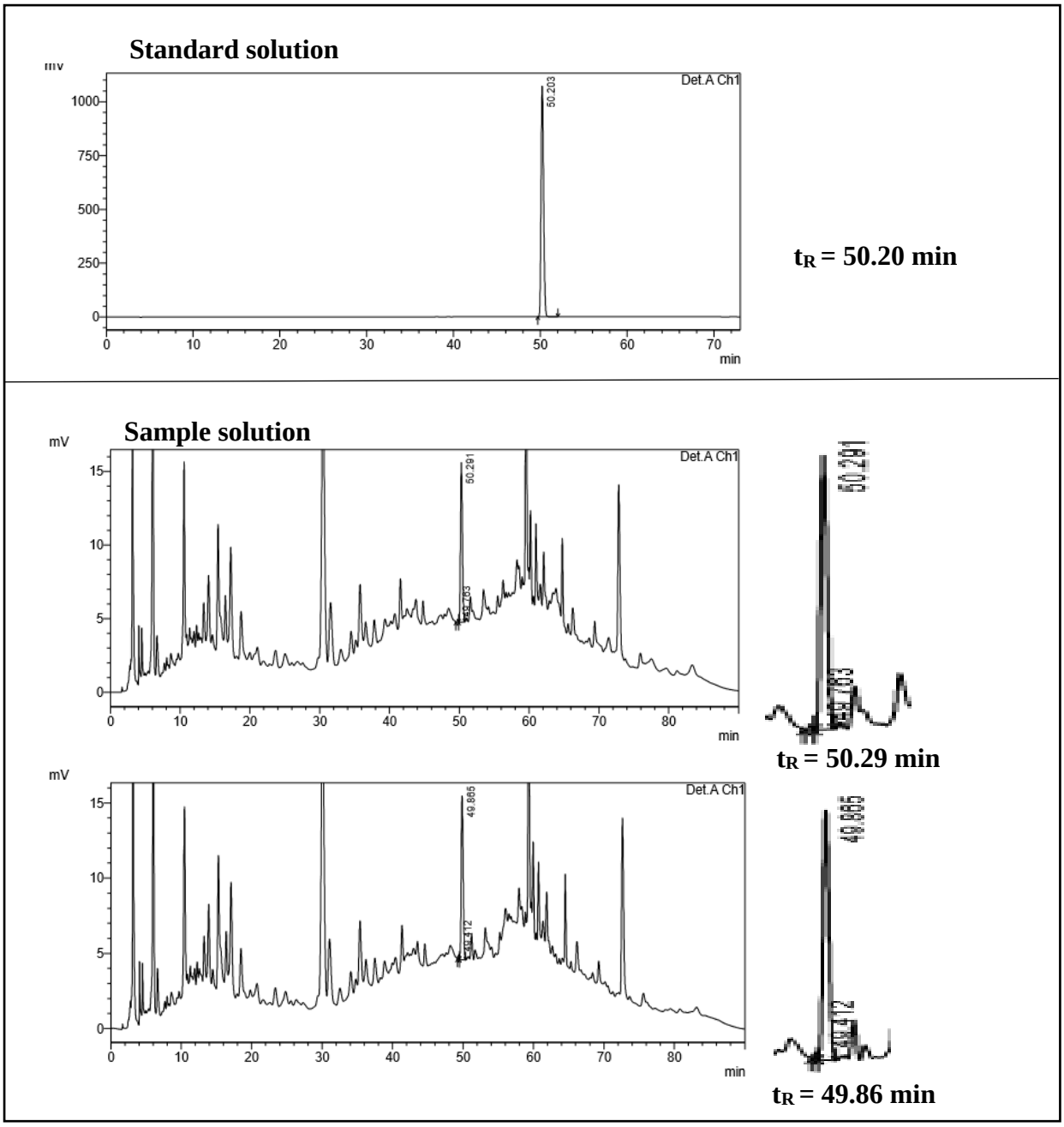

Figure 8 Chromatograms of standard and of "*Yuko"* grape pomace extract

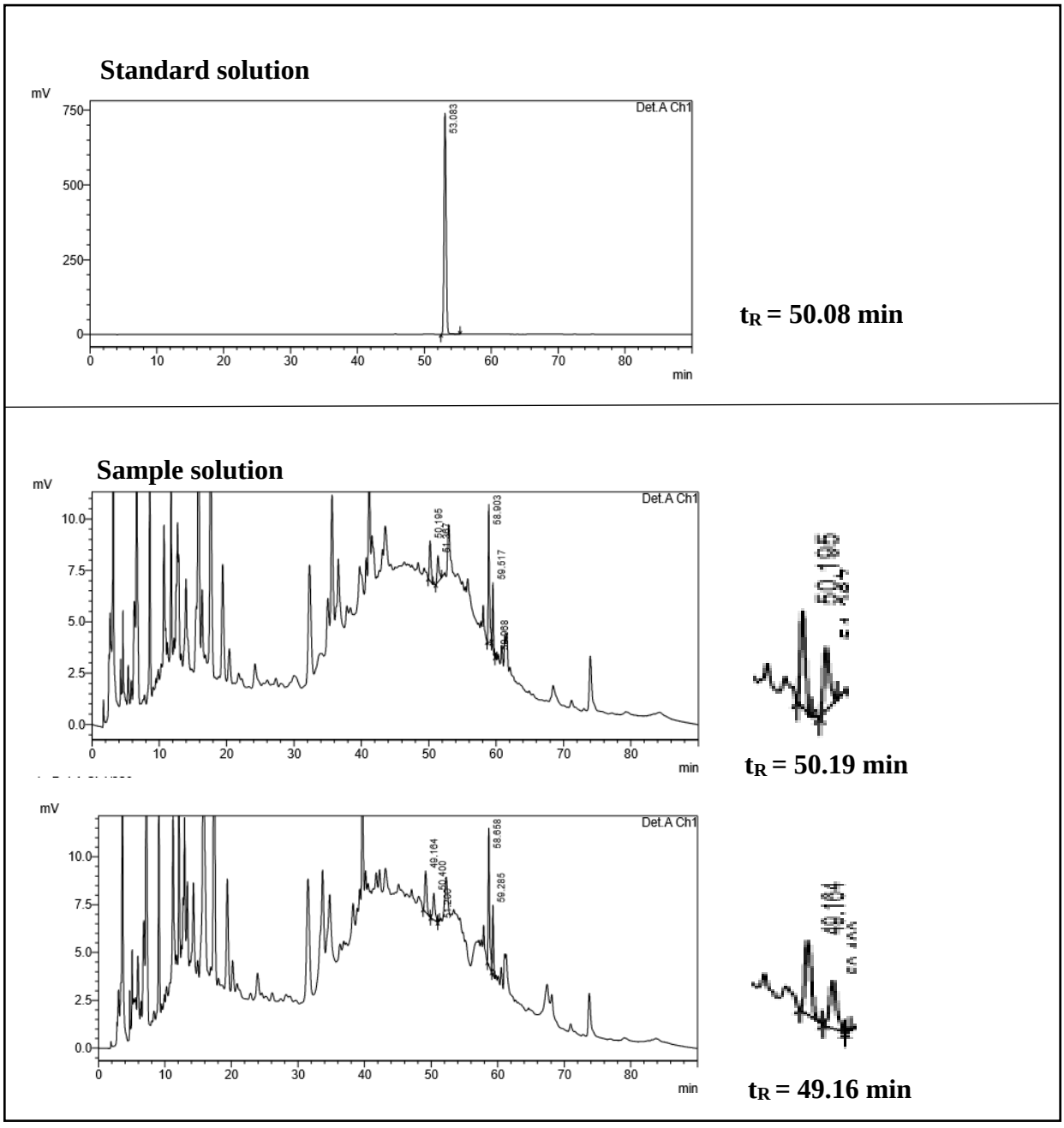

Figure 9 Chromatograms of standard and of "*Piedirosso"* grape pomace extract

The HPLC-UV method applied for the quantification of *trans*-resveratrol in the three GP extracts gave a bad to quite good separation in the chromatographic runs. In particular, the values of signal-to-noise ratio (S/N) in chromatograms of GP from *"Piedirosso"* and *"Aglianico del Vulture"* are very small (S/N << 3), intstead an acceptable values was obtained in chromatogram of GP from *"Yuko"* (SN ≈ 3). This means that the quantitative analysis of *trans*-resveratrol is not very precise and accurate, especially for GPs of *"Piedirosso"* and *"Aglianico del Vulture"*.

Nevertheless, this method, although it will need to be optimized, is the only one, among the many methods tested, to allow a preliminary quantitative evaluation of *trans*-resveratrol in the GP extracts.

For each experiment the peak area under curve were plotted and the concentration of *trans*-resveratrol was determined using the calibration curve. The results (table) was expressed as mg/Kg ± standard deviation (SD).

Table 4 Content of *trans*-resveratrol in grape pomace extracts

Samples	Content$_{trans\text{-resveratrol}}$ ± SD
Aglianico del Vulture	41.69 ± 0.82
Yuko	36.71 ± 0.09
Piedirosso	8.92 ± 1.21

As it can be seen in the chromatograms of GP from *"Piedirosso"* (Figure 12) a high and wide band partially covers the peak of *trans*-resveratrol, which is not much resolved. For this reason the content of *trans*-resveratrol analysed in these GP extracts is very low.

A better separation was obtained in the chromatographic runs of GP from *"Aglianico del Vulture"* (Figure 10) and the content of *trans*-resveratrol is quite in agreement with the results obtained in previous research on different red grape.

The better separation was obtained in the chromatographic runs of GP from *"Yuko"*, the peak of *trans*-resveratrol is quite resolved and the content is very high considering the methodology extraction used.

CHAPTER 2. SYNTHESIS OF 2,3-DIARYL-2,3-DIHYDROBENZOFURAN SYSTEMS

2.1 Introduction

2.1.1 Natural compounds with 2,3-dihydrobenzofuran core

The 2,3- dihydrobenzofuran (DHB), consisting of a benzene ring fused with a reduced furan, (Figure 10) is a key structural unit in a variety of biologically active natural products. With the presence of two substituents, R_1 and R_2 in position 2 and 3, there are two possible geometric isomers, *cis* (with R_1 and R_2 on the same side of the cyclic structure) and *trans* (with R_1 and R_2 on opposite faces of the cyclic structure). In general, most natural, such as alkaloids, isoflavonoids, lignans and neolignans, bear the *trans*-configuration which has favorable thermodynamic stability.

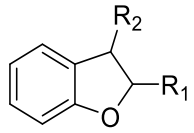

Figure 10 2,3-dihydrobenzofuran (DHB) structure

For example, (+)-Conocarpan (Figure 11), a benzofuran neolignan isolated from *Conocarpus erectus*[28], is a component in many medical plants and is known to have insecticidal, anti-fungal, anti-tubercolosis, photoprotective, antinociceptive and anti-inflammatory activities.[29]

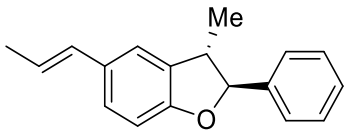

Figure 11 (+)-Conocarpan structure

The (2*R*,3*S*)-3′,4-di-O-Methylcedrusin (Figure 12), one of the minor components of the red latex called ‘dragon blood’ in traditional medicine, was isolated from the bark of various *Euforbiacee* species and has been shown to act as an inhibitor of cell proliferation.[30]

[28] Hayashi, T.; Thomson, R.H.; *Phytochemistry* **1975**, *14*, 1085–1087.

[29] Yang, G.; Ma, H.; Wu, Y.; Zhou, B.; Zhang, C.; Chai, C.; Cao, Z. *Food Chem. Toxicol.* **2019**, *129*, 281–290

[30] Pieters, L.; Van Dyck, S.; Gao, M.; Bai, R.; Hamel, E.; Vlietinck, A.; Lemiére, G. *J. Med. Chem.* **1999**, *42*, 5475-5481.

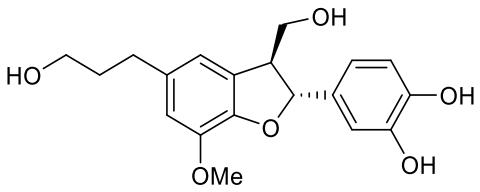

Figure 12 (2*R*,3*S*)-3′,4-di-O-Methylcedrusin structure

Different oligostilbenes having dihydrobenzofuran moiety were isolated from plant kingdom, in particular from five families: *Vitacee, Leguminose, Gnetaceae, Dipterocarpaceae,* and *Cyperaceae*. They are resveratrol oligomers characterized by the polymerization of two to eight, or even more resveratrol units. These so-called "viniferins" have been found in plants[31] as a result of infection or stress and are supposed to be formed by oxidative dimerization catalyzed by plant peroxidases and/or phenoloxidases. Among the different patterns found for stilbene oligomers, those containing dihydrobenzofuran moiety possess two monomeric units linked by a C–C and a C–O–C linkage.[32] Resveratrol oligomers have multiple beneficial properties, of which some are superior in activity, stability, and selectivity compared with resveratrol.

The first resveratrol oligomer ever characterized was hopeaphenol (Figure 13), a resveratrol tetramer isolated by Coggon et al.[33] Originally isolated in 1951 from the heartwood of *Hopea odorata* and *Balanocarpus heimii*, two members of the *Dipterocarpaceae* family, 15 years passed before the structure was elucidated. It has been demonstrated that this tetramer had more powerful antioxidant properties than resveratrol.[34] The activity of this compound is attributed to its complex structure, with many hydroxyl groups, which can donate hydrogen or electrons to free radicals, effecting neutralization. A recent study identified hopeaphenol and related stilbenoid analogues as potent and selective inhibitors of viral entry across multiple SARS-CoV-2 variants including those with increased infectivity and/or reduced susceptibility to existing vaccines.[35]

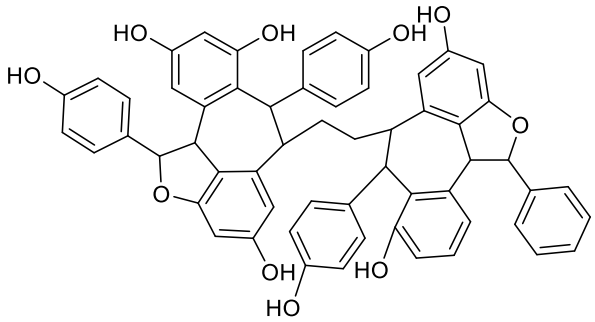

Figure 13 Hopeaphenol structure

[31] Cichewicz, R. H.; Kouzi, S. A.; *Stud. Nat. Prod. Chem.* **2002**, *26*, 507-579.

[32] T. Shen, X.-N. Wang, H.-X. Lou, *Nat. Prod. Rep.* **2009**, *26*, 916-935.

[33] Coggon, P.; Janes, N. F.; King, F. E.; King, T. J.; Molyneux, R. J.; Morgan, J. W. W.; Sellars, K. *J. Chem. Soc.* **1965**, 406−409.

[34] Subramanian, R.; Raj, V.; Manigandan, K.; Elangovan, N.; *J. Taibah Univ. Sci.* **2015**, *9*, 237-244.

[35] Tietjen, I.; Cassel, J.; Register, E. T.; Zhou, X. Y.; Messick, T. E.; Keeney, F.; Lu, D. L; Beattie, K. B.; Rali, T.; Ertl, H. C. J.; Salvino, J. M.; Davis, R. A.; Montaner, L. J. *Antimicrob. Agents Chemoter.* **2021**, *12*.

A decade later, the building block for hopeaphenol and nearly all higher-order oligomers, the dimer ε-Viniferin, was identified. ε-Viniferin (Figure 14) was first isolated from *Vitis vinifera* (Vitaceae) and showed antifungal, antibacterial, and antiviral activities.[36]

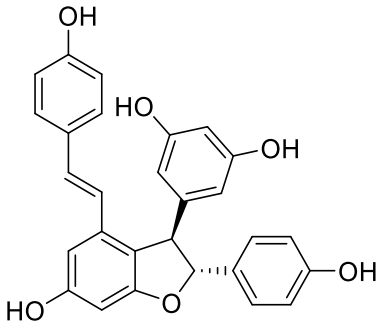

Figure 14 ε-Viniferin structure

To date, many studies of this dimer are about the antioxidant and anticancer activities. The antioxidant activity of ε-Viniferin is essential in the prevention of oxidative damage or chemical-induced cancer by inhibiting the initiation and progression of the disease. It was reported that ε-Viniferin showed the better antioxidant properties to radicals (IC_{50} value of 0.12 to 0.16 mM) than resveratrol (IC_{50} value of 0.92 to 0.98 mM) and could inhibit reactive oxygen species production.[37]

ε-Viniferin also showed the direct cytotoxicity to various cancer cells. It was reported that ε-Viniferin could kill C6, HepG2, HeLa, and MCF-7 cancer cell lines in a dose-dependent manner with IC_{50} values of 18.4, 74.3, 20.4, and 44.8 g/mL, respectively.[38] In contrast, resveratrol showed stronger cytotoxicity against C6 and HepG2 with IC_{50} values of 8.2 and 11.8 g/mL and weaker cytotoxicity against HeLa and MCF-7 with IC_{50} values of 20.4 and 44.8 g/mL, respectively.[39]

Moreover ε-Viniferin showed a better anti-inflammatory activity than resveratrol. It was reported that it could inhibit the transcription factor NF-kB[40] and the action of the enzyme 5 lipoxygenase (5 LOX), blocking the formation of leukotrienes from arachidonic acid.[41]

The condensation of ε-Viniferin and ascorbic acid provides the Levifonol (Figure 15), a oligostilbene isolated from the bark of *Vatica odorata*. This compound showed antibacterial

---

[36] a) Lee, S.; Mailar, K.; Kim, M.I.; Park, M.; Kim, J.; Min, D.H.; Heo, T.H.; Bae, S.K.; Choi, W.; Lee, C.; *Viruse*, **2019**, *11*, 890. b) Bala, A. E. A.; Kollmann, A.; Ducrot, P. H. et al., *J. Phytopathol.*, **2000**, *148*, 29–32.

[37] a) Privat, C.; Telo, J. P.; Bernardes-Genisson, V.; Vieira, A.; Souchard, J. P.; Nepveu, F. *J. Agric. Food Chem.*, **2002**, *50*, 1213–1217. b) Kim, H. J.; Chang, E. J.; Cho, S. H.; Chung, S. K.; Park, H. D.; Choi, S. W. *Biosci. Biotechnol. Biochem*. **2002**, *66*, 1990–1993.

[38] Mishima, S.; Matsumoto, K.; Futamura, Y. et al., *J. Exp. Ther. Oncol.*, **2003**, *3*, 283–288.

[39] Quiney, C.; Dauzonne, D.; Kern, C. et al. *Leuk. Res.*, **2004**, *28*, 851–861.

[40] Ha, D.T.; Long, P.T.; Hien, T.T.; Tuan, D. T.; An, N. T. T.; Khoi, N. M., Van Oanh, H.; Hung, T. M. *Chem. Cent. J.* **2018,** *12*, 14.

[41] Hartung, N.M.; Fischer, J.; Ostermann, A.I.; Willenberg, I., Rund, K.M.; Schebb, N.H.; Garscha, U. *Biochim Biophys Acta Mol Cell Biol Lipids* **2019**, *1864*, 1536-1544.

activity on gram-positive and negative bacteria and cytotoxic properties against P-388 murine leukemia cells.[42]

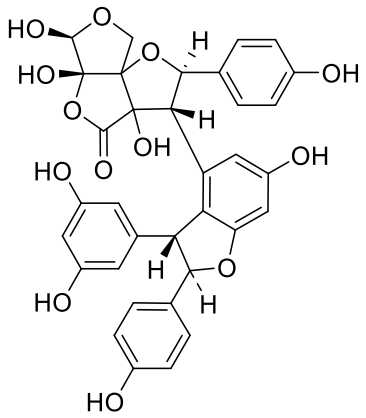

Figure 15 Levifonol structure

α-Viniferin (Figure 16) is a stilbene trimer isolated from *Caragana sinica, Caragana chamlagu,* and the stem bark of *Dryobalanops aromatic*. This compound displayed a striking growth inhibitory effect on various cancer cell lines. It showed marked cytotoxic activity against HL-60 and moderately cytotoxic activity against MCF-7, HepG2, A549, and murine leukemia P-388 cells.[43] In addition, α-Viniferin inhibited the proliferation in a concentration- and time-dependent manner by arresting cell cycle at the S phase but not inducing apoptosis of human colon cancer cells *in vitro*, including HCT-116, HT-29, and Caco-2 cell lines.[44]

Furthermore, compared to resveratrol, α-Viniferin showed 3- to 4-fold higher inhibition on cyclooxygenase activity.[45]

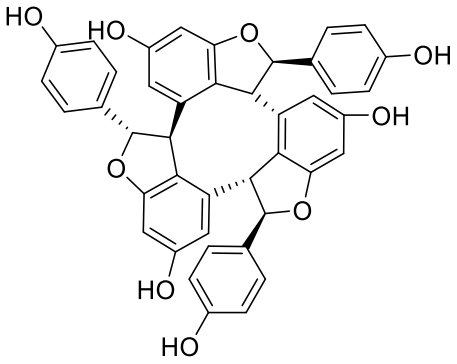

Figure 16 α-Viniferin structure

[42] Wan, Z.; Wan, M. Z.; Kamaruzaman, J. *World Appl. Sci. J*. **2010**, *8*, 1056-1059.

[43] Wibowo, A.; Ahmat, N.; Hamzah, A. S. et al. *Fitoterapia*, **2011**, *82*, 676–681.

[44] González-Sarrías, A.; Gromek, S.; Niesen, D.; Seeram, N P.; Henry, G. E. *J. Agric. Food Chem.*, **2011**, *59*, 8632–8638.

[45] Lee, S.-H.; Shin, N.-H.; Kang, S.-H. et al., *Planta Med.* **1998**, *64*, 204–207.

Another dimer of resveratrol is Gnetin C (Figure 17), isolated from several species of the Gnetaceae family and from *Rheum ilasaense.* The ethanol extracts from the fruits, leaves, and seeds of melinjo (*G. gnemon*), an edible plant native to Southeast Asia and the western Pacific islands, are rich in resveratrol and various stilbenes, including Gnetin C.[46] These melinjo derivatives (melinjo seed extract (MSE)) possess antioxidant and antimicrobial activities[46,47] and immunomodulatory effects.[48]

In literature it was reported that consumption of 750 mg/day for 8 weeks of MSE was well tolerated and decreased blood serum uric acid level. This decrease was related to the 50% inhibition (IC_{50}) of xanthine oxidase (XO) enzyme activity by Gnetin C[49] with a superior potency respect its parental *trans* resveratrol.

Gnetin C also showed an anti-inflammatory activity trough the negative reduction of pro-inflammatory chemokines production. Tanaka and coworkers[50] examined the effect of Gnetin C on the dsRNA-induced production of pro-inflammatory chemokines, CCL2 and CCL5, using cultured human astrocytoma and neuroblastoma cells, as models of human astrocytes and neurons, respectively. This study showed that Gnetin C suppressed the production of CCL2 and CCL5 in both cell types, so this dimer could potentially be used for controlling the progression of virus-mediated neuroinflammation.

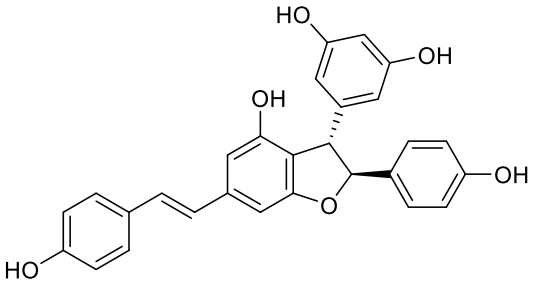

Figure 17 Gnetin C structure

Nevertheless, these resveratrol oligomers are present in very small quantities in plants and for this reason they have recently received significant attention from the scientific community in order to obtain them synthetically.

Along with the total synthesis of these compounds, the synthesis of 2,3-dihydrobenfuran 2,3-disubstituted systems, a key structural motif in resveratrol dimers, has also attracted considerable interest.

---

[46] Kato, E., Y. Tokunaga & F. Sakan. *J. Agric. Food Chem.* **2009**, *57*, 2544–2549.

[47] Sakagami, Y., A. Sawabe, S. Komemushi, et al. *Biocontrol Sci.* **2007**, *12*, 7–14.

[48] Kato, H., M. Samizo, R. Kawabata, et al. *Planta Med.* **2011**, *77*, 1027–1034.

[49] Saraswaty, V.; Adnyana, IK.; Pudjiraharti, S.; Rachmawati, H. *Rasayan J. Chem.* **2020**, *13*, 1363-1371.

[50] Yoshida, H.; Imaizumi, T.; Matsumiya, T.; Seya, K.; Kawaguchi, S.; Tanaka, H., *Biomed. Res.* **2018,** *39*, (5), 231–240.

2.1.2 Synthesis of 2,3-disubstituted 2,3-dihydrobenzofurans

The methods for the construction of compounds with 2,3-dihydrobenzofuran core are based on biomimetic approaches, intermolecular or intramolecular cyclization and transformation of benzofurans to dihydrobenzofurans.[3]
Although different synthetic approaches are known for the preparation of the 2,3-dihydrobenzofuran ring-system, few of them are efficient for the synthesis of 2,3-disubstituted dihydrobenzofurans.

2.1.2.1 Biomimetic coupling and cyclization

Resveratrol oligomerization appears to proceed *via* the coupling of oxidatively generated phenoxyl radicals, as originally proposed by Langcake and Price.[51] The dimerization, according to Keylor et al,[52] tipically occurs through three regioisomeric modes (Scheme 1):

1) 8-10’ coupling (ε-Viniferin and ampelosin F)
2) 8-8’ coupling (quadrangularin A and pallidol)
3) 3-8’ (δ-Viniferin)

Moreover, 8-12’ (Gnetin C) and 12-12’ coupling (amurensin M) have also been identified, but they are relatively uncommon.

[51] Langcake, P.; Price, R. *J. Phytochem.* **1977**, *16*, 1193-1196
[52] Keylor, M. H.; Matsuura, B. S.; Stephenson, R. J. *Chem. Rev.* **2015**, *115*, 8976−9027

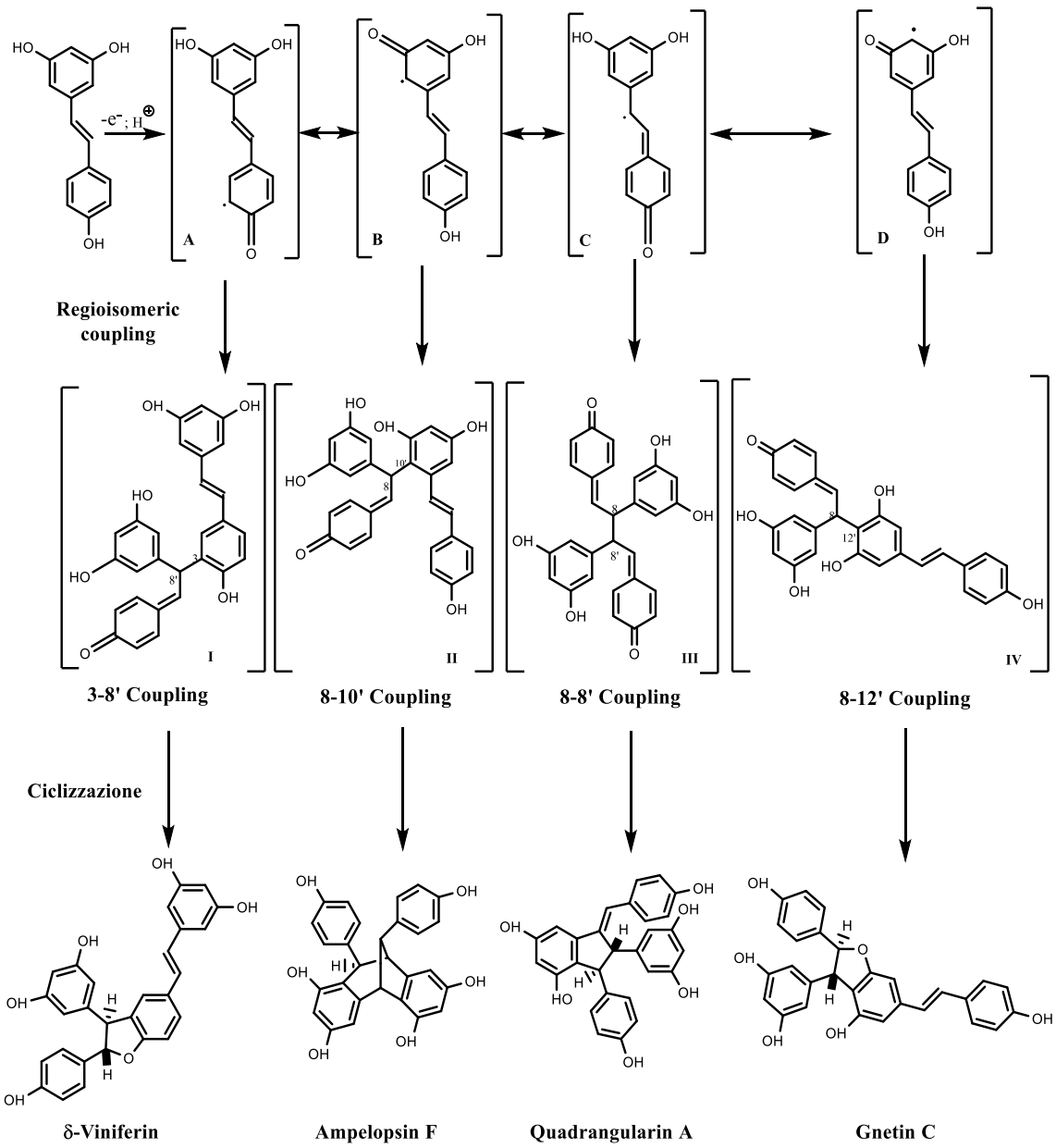

Scheme 1 Regioisomeric modes of resveratrol dimerization

The 8-10’ connectivity is by far the most prevalent found among resveratrol-derived oligomeric natural products (Scheme 2). Upon oxidation of resveratrol (**I**) and 8-10’ dimerization, hypothetical *para*-quinone methide intermediate (**II**) can follow divergent cyclization pathways to generate either ε-Viniferin or other dimers:

- oxa-conjugate addition (**IV**) (Scheme , path A)
- Friedel-Crafts reaction (path B) from which a second intramolecular cyclization yields the dimer ampelosin F (**VII**), while tautomerization yields the isomer ampelosin D (**VIII**). Oxidative cleavage of the olefin of this last dimer results in the formation of the natural product pauciflorol F (**IX**).

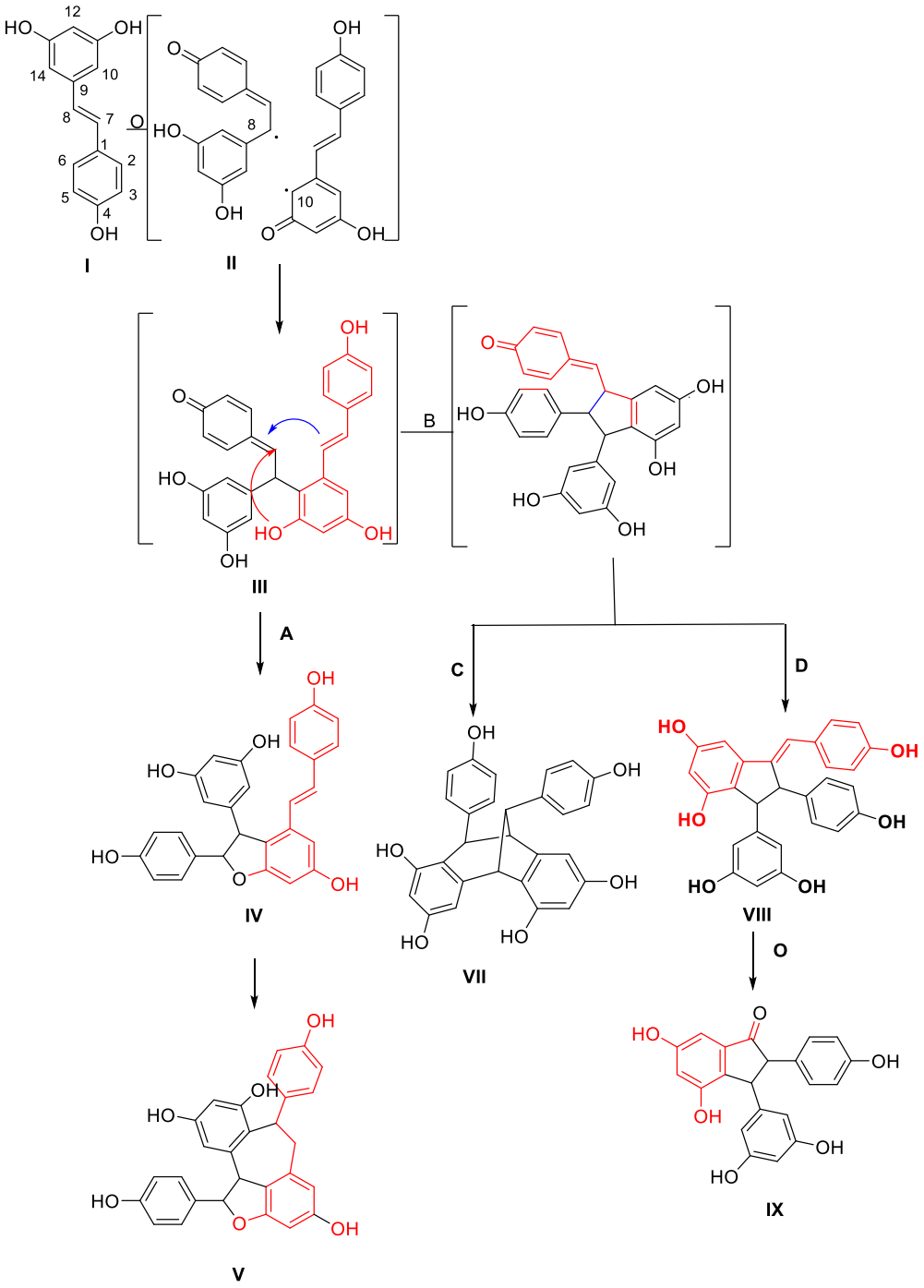

Scheme 2 Proposed biosynthesis of the 8-10’ dimers

The first biomimetic synthesis of a resveratrol dimer was described by Langcake and Pryce in 1977.[51] By subjecting resveratrol to oxidation condition by the horseradish peroxidase/H_2O_2 they isolated δ-Viniferin in 40% yield (Scheme 3).

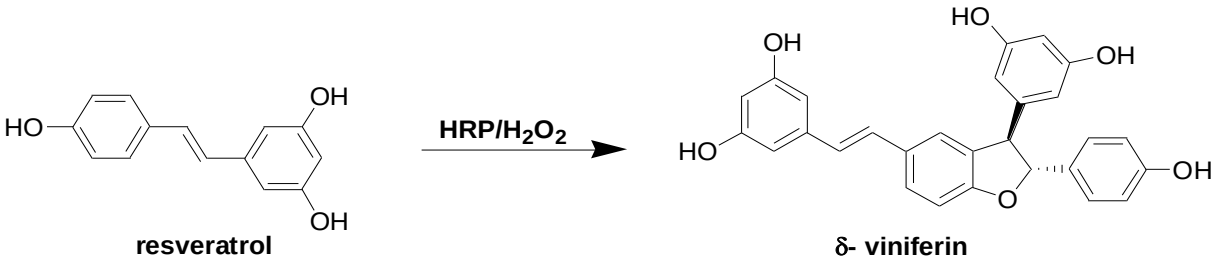

Scheme 3 First biomimetic synthesis of δ-Viniferin

Since this contribution, several groups have dimerized resveratrol using a variety of oxidation strategies, including organic,[53] inorganic,[54] enzymatic[55] and photochemical[56] oxidations.

In 2004, Iinuma *et al*. described a nonezymatic biomimetic method for the regioselective synthesis of (*E*)-dehydrodimer (*trans* δ-Viniferin) (Scheme 4).[54c] The resveratrol was treated with an equimolar amount of AgOAc in dry MeOH at 50°C for 1 h leading the final product in racemic form and in quantitative yield.
The formation of the dehydrodimer can be reasonably explained by virtue of a single-electron transfer from resveratrol to the cation Ag^+, a regioselective coupling of the phenoxyl radical (**A** and **A'**) generated by deprotonation of the 4-hydroxystilbene cation radical and subsequent intramolecular cyclization.

[53] a) Wang, M.; Jin, Y.; Ho, C.-T. *J. Agric. Food Chem.* **1999**, *47*, 3974−3977. b) Shang, Y.-J.; Qian, Y.-P.; Liu, X.-D.; Dai, F.; Shang, X.-L.; Jia, W.-Q.; Liu, Q.; Fang, J.-G.; Zhou, B. *J. Org. Chem.* **2009**, *74*, 5025−5031.

[54] a) Takaya, Y.; Terashima, K.; Ito, J.; He, Y.-H.; Tateoka, M.; Yamaguchi, N.; Niwa, M. *Tetrahedron* **2005**, *61*, 10285−10290. b) Fan, G.-J.; Liu, X.-D.; Qian, Y.-P.; Shang, Y.-J.; Li, X.-Z.; Dai, F.; Fang, J.-G.; Jin, X.-L.; Zhou, B. *Bioorg. Med. Chem.* **2009**, *17*, 2360−2365. c) Sako, M.; Hosokawa, H.; Ito, T.; Iinuma, M, *J. Org. Chem.* **2004**, *69*, 2598-2600. d) D'Orsi, R,; Morrongiello, F.; Laurita, T.; Funicello, M.; Lupattelli, P.; Chiummiento, L. *ChemistrySelect*, **2021**, *6*, 6863-6866.

[55] a) Nicotra, S.; Cramarossa, M. R.; Mucci, A.; Pagnoni, U. M.; Riva, S.; Forti, L. *Tetrahedron* **2004**, *60*, 595−600. b) Li, C.; Lu, J.; Xu, X.; Hu, R.; Pan, Y. *Green Chem*. **2012**, *14*, 3281−3284. c) Ponzoni, C.; Beneventi, E.; Cramarossa, M. R.; Raimondi, S.; Trevisi, G.; Pagnoni, U. M.; Riva, S.; Forti, L. *Adv. Synth. Catal*. **2007**, *349*, 1497−1506.

[56] Song, T.; Zhou, B.; Peng, G.-W.; Zhang, Q.-B.; Wu, L.-Z.; Liu, Q.; Wang, Y. *Chem. Eur. J.* **2014**, *20*, 678−682.

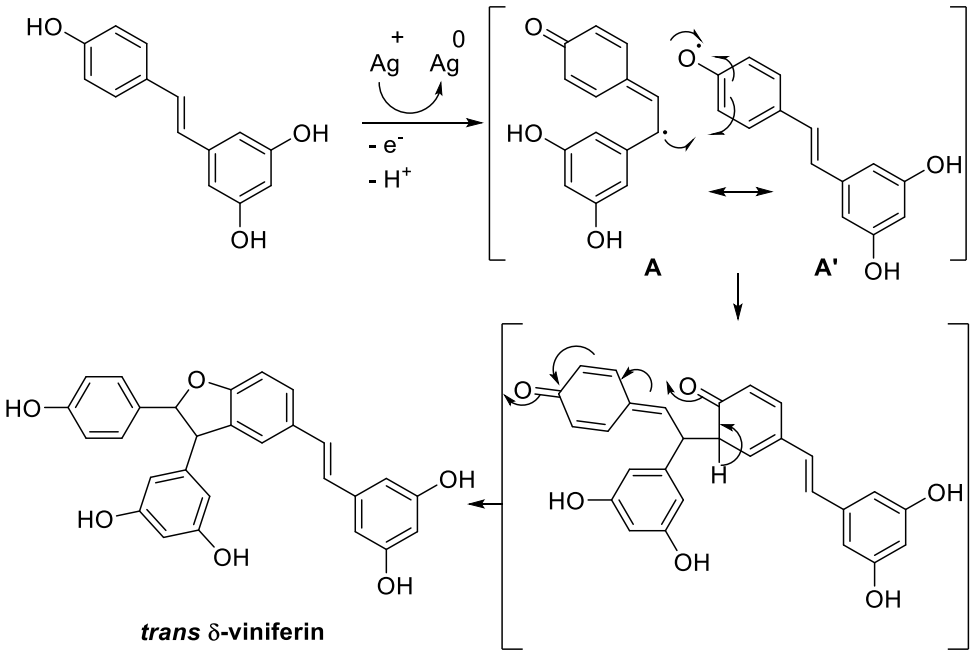

Scheme 4 A most plausible mechanism for the oxidative dimerization of resveratrol

Yang and co-workers, in 2012, reported the total synthesis of (±)-Ampelosin B.[57] Oxidative coupling of resveratrol (**I**) with $FeCl_3 \cdot 6H_2O$ yielded the natural product ε-Viniferin (**II**). Then the Friedel-Crafts intramolecular alkylation of (**II**) in the presence of 10 mol % Tf_2O as catalyst, directly provided the (±)-Ampelosin B (**III**) in 41 % yield (Scheme 5).
Despite the lower yield, this route has only two steps and omits the use of protecting groups.

[57] a) Wang, G. W.; Wang, H. L.; Capretto, D. A.; Han, Q.; Hu, R. B.; Yang, S. D. *Tetrahedron*, **2012**, *68*, 5216–5222. b) Yao, C.-S.; Lin, M.; Wang, Y.-H. *Chinese J. Chem.* **2004**, *22*, 1350-1355

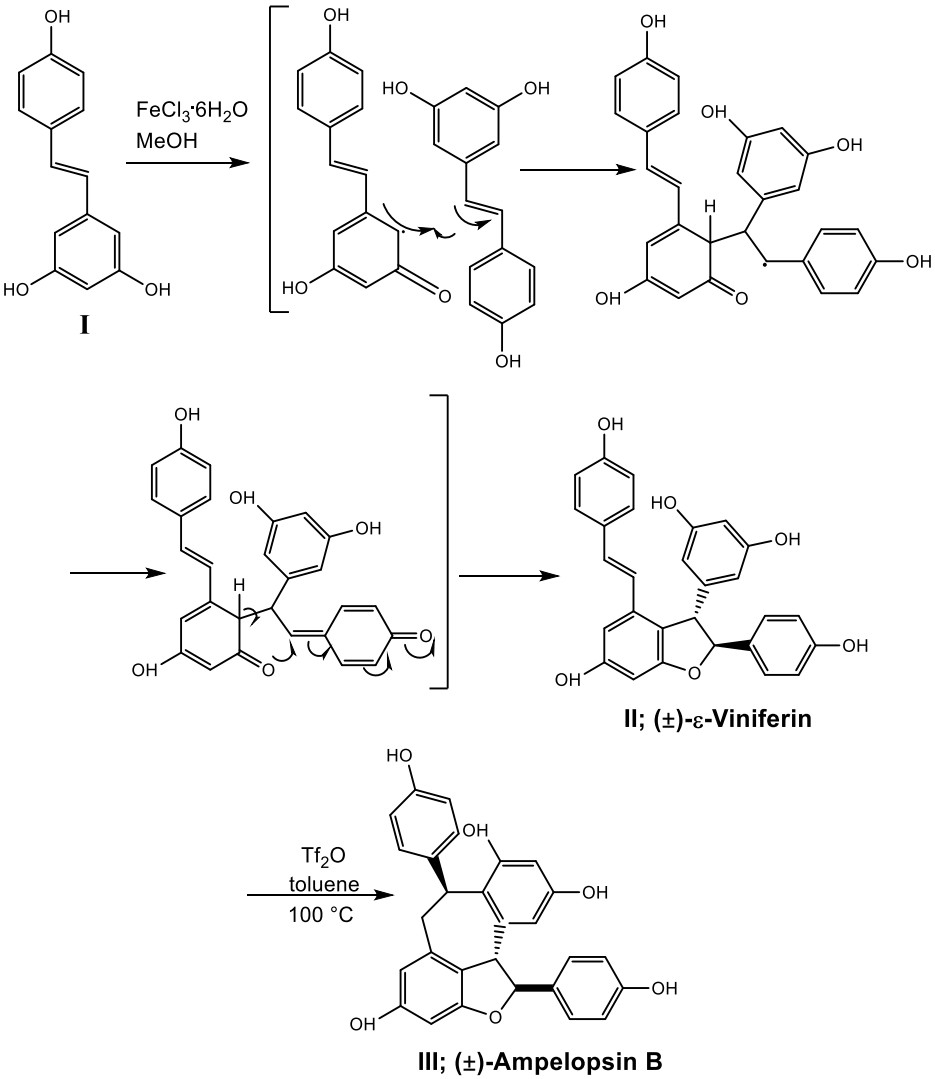

Scheme 5 Total synthesis of natural product by Friedel-Crafts alkylation

Recently (2021),[54d] our group disclosed a biomimetic synthesis of (±)-ε-Viniferin. The iodination of resveratrol by NIS afforded iodinated ε-Viniferin (**I**) (Scheme 6)[54d] *via* a radical pathway promoted by NIS. The *para*-phenol moiety of iodinated resveratrol was oxidized by NIS to form hypoiodite (RO-I), the C-O bond of RO-I is thermally or photochemically cleaved to generate alkoxy and iodine radicals. Then, coupling between two resonance form of a radical resveratrol (**A** and **B**) occurs. At last acetoxylation, dehalogenation and deacetoxylation of iodinated (±)-ε-Viniferin (**I**) provided the (±)-ε-Viniferin (**II**) in 20% of yield.

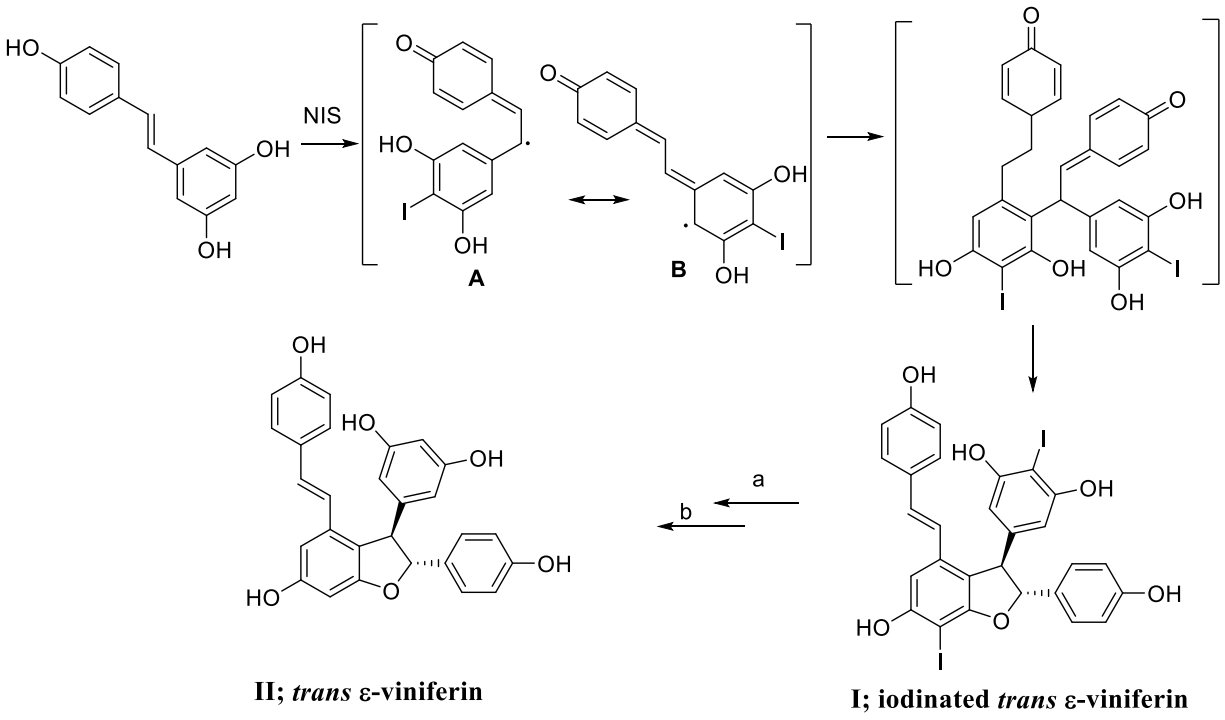

II; *trans* ε-viniferin **I; iodinated *trans* ε-viniferin**

Scheme 6 Biomimetic synthesis of (±)-ε-Viniferin by NIS. a) Ac_2O, DMSO, CH_2Cl_2, 0° to rt; b) Na, MeOH, rt.)

Chemoenzymatic approaches were also proposed for the synthesis of substituted dihydrobenzofurans by direct annulation reactions. In a work by Bassanini, Riva, and co-workers (2018),[58] laccase from *T. versicolor* was used for the oxidative (homo)coupling of (*E*)-4-styrylphenols in a versatile and selective chemoenzymatic synthesis of substituted *trans*-2,3-diaryl-5-[(*E*)-styryl]-dihydrobenzofurans (Scheme 7). The (*E*)-4-styrylphenols were prepared from commercially available phenylacetic acids and *p*-hydroxybenzaldehyde via a Perkin-like reaction. Thanks to this synthetic strategy, sixteen dihydrobenzofurans based potential allosteric activators of the heat shock protein 90 (Hsp90) were prepared.

[58] Bassanini, I.; D'Annessa, I.; Costa, M.; Monti, D.; Colombo, G.;Riva, S. *Org. Biomol. Chem.* **2018**, *16*, 3741.

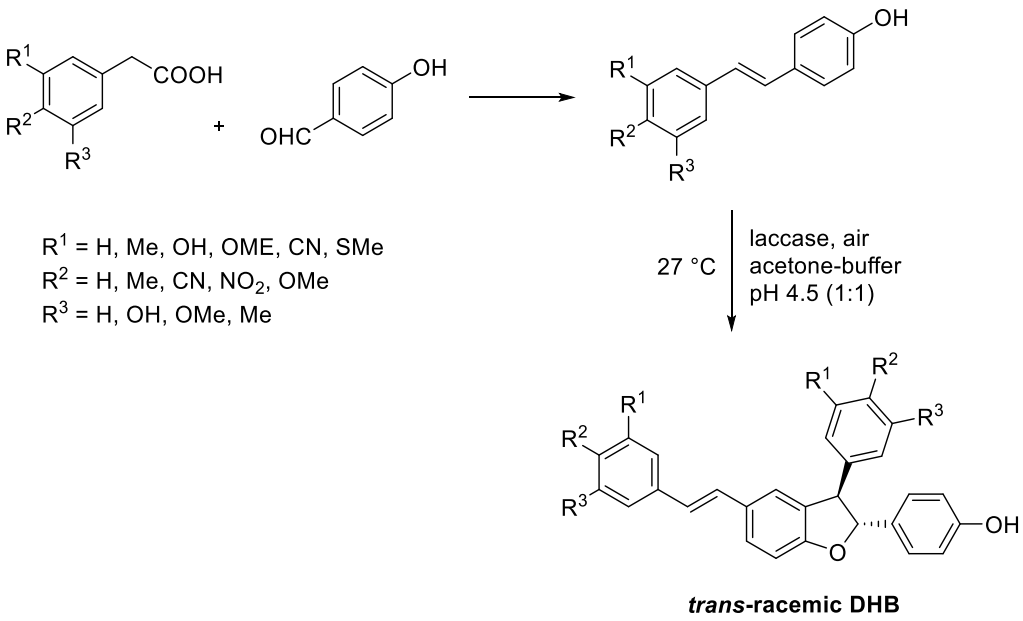

Scheme 7 Laccase-mediated (homo)coupling of (*E*)-4-styrylphenols

2.1.2.2 From Benzofuran to Dihydrobenzofuran

In the last years the direct hydrogenation of benzofurans to dihydrobenzofurans has been greatly enhanced and produced notable results, even in the synthesis of natural products. For example, in the total synthesis of resveratrol dimers (±)-ampelopsin B and (±)-ε-Viniferin, the furan ring (**I**) in an advanced intermediate was reduced by catalytic transfer hydrogenation to form the corresponding dihydrobenzofuran (**II**) in excellent yield (Scheme 8).[59] Deprotection reaction furnished a polyphenol (**III**), which, after elaboration of C4-moiety, was transformed into (±)-ε-Viniferin in 5 % overall yield.

Instead, the cyclopropylmethyl-protected *cis*-ε-Viniferin (**V**), prepared after elaboration of C4-moiety of (**II**), allowed an acid-promoted three-step/one-pot deprotection–epimerization–cyclization of an intermediate to give (±) ampelopsin B in 5 % overall yield. This was the first synthesis of ampelopsin B that did not involve a dimerization of resveratrol. A noteworthy advantage of this strategy was the possibility of synthesizing analogues of resveratrol oligomers to further investigate their chemistry and biology.

[59] Lindgren, A. E. G.; Oberg, C. T.; Hillgren, M. J.; Elofsson, M.; *Eur, J. Org. Chem.* **2016**, *3*, 426-429

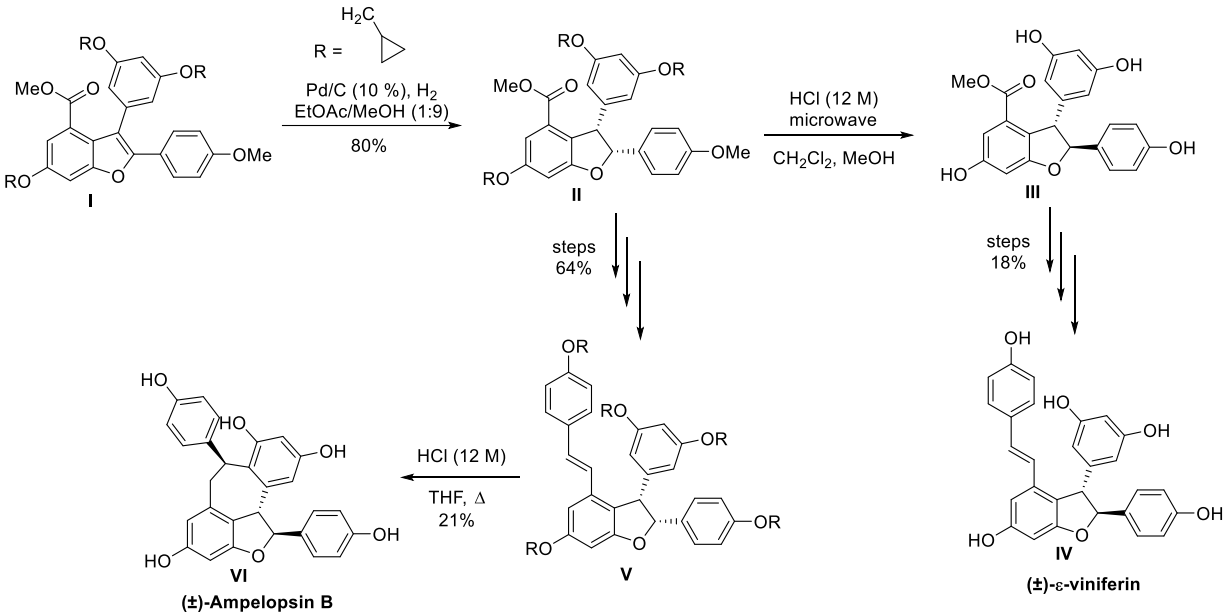

Scheme 8 Catalytic hydrogenation of benzofuran in the synthesis of (±)-ε-Viniferin and (±)-ampelopsin B

In 2016, Yao et al. described a facile and practical total synthesis to produce the permethylated (±)-ε-Viniferin and the natural (±)-ampelospin F (Scheme 9).[60] Triethylsilane-mediated reduction of advanced polymethoxylated 2,3-diarylbenzofuran (**I**) led to the corresponding *trans*-2,3-diaryl-dihydrobenzofuran (**II**) in almost quantitative yield. The subsequent incorporation of the final aryl moiety provided the permethylated (±)-ε-Viniferin (**III**) in 27% overall yield with 9 total steps. Then BBr3-mediated one-pot demethylation and cascade intramolecular cyclization reaction of permethylated Viniferin furnished (±)-ampelospin F in 39% yield.

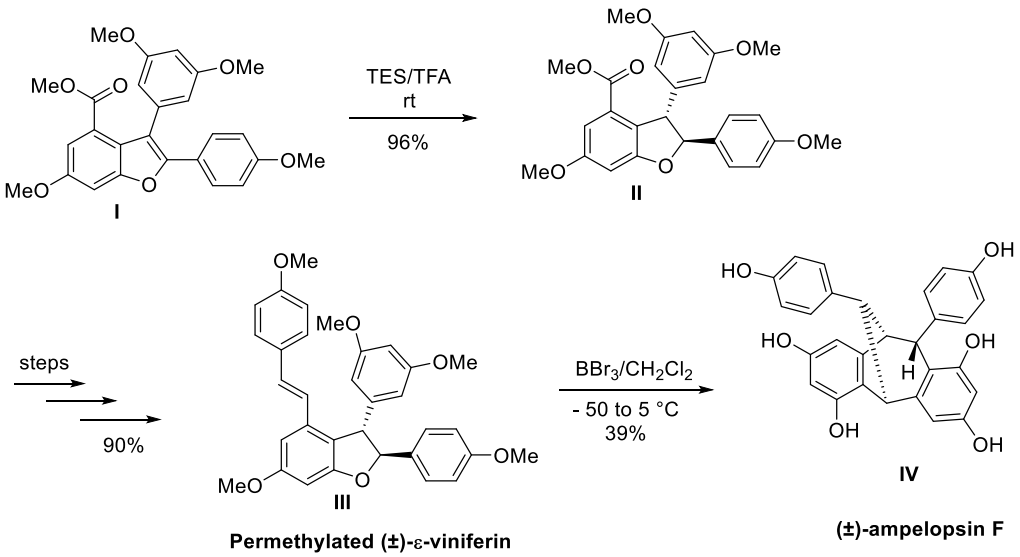

Scheme 9 Triethylsilane-mediated reduction of benzofuran in the synthesis of (±)-ε-Viniferin and (±)-ampelospin F

[60] Zhang, J.; Zhang, J.; Kang, Y.; Shi, J.; Yao, C. *Synlett* **2016**, *27*,1587.

2.1.2.3 Intermolecular approaches

The intermolecular approaches are subdivided according to the parent intermediate for the key reaction.

Zhou and co-workers reported a facile method for the stereoselective synthesis of 2,3-disubstituted dihydrobenzofurans using *ortho*-quinone methides as useful intermediates and suitable stabilized sulfur ylides, both of which were formed *in situ* from 2-(tosylalkyl)phenols and sulfonium salts, respectively under mild basic condition (Scheme 10).[61]

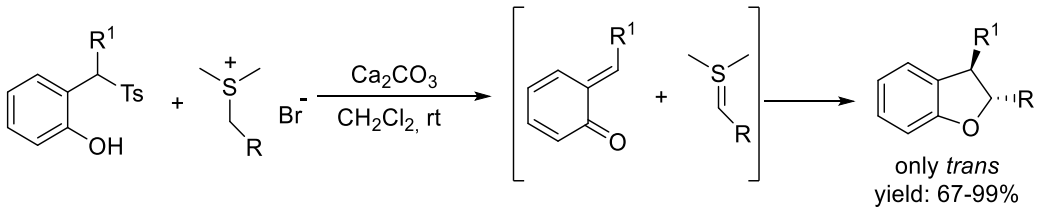

Scheme 10 Stereoselective synthesis via *o*-quinone methide

Alternatively, hydroxyl-containing *p*-quinone methides have also been indicated as powerful intermediate for formal [4+n] annulations. For example, Yao, Huang *et al.* in 2018 reported a formal 1,6-conjugate addition-mediated [4+1] annulation of *o*-hidroxyphenyl-substituted *p*-quinone with solfonium or ammonium bromides (Scheme 11).[62]

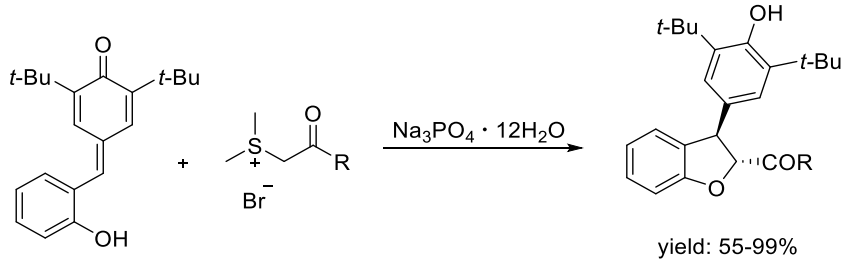

Scheme 11 Stereoselective synthesis *via p*-quinone methide

This domino-type process offered an efficient method for the synthesis of *trans* 3-aryl-2-substituted DHBs in good yields, exhibiting good functional group tolerance, scalability and high diastereostereoselectivity.

In 2019, Wang and co-workers disclosed the first catalytic enantioselective formal [4+1] annulation reaction between hydroxyl-substituted *p*-quinone and α-halogenated ketone by a dipeptide-based bifunctional phosphonium salt catalyst. This method represented a novel and complementary approach for the preparation of optically active 2,3-dihydrobenzofuran

[61] Chen, M.-W.; Cao, L.-L.; Ye, Z.-S.; Jiang, G.-F.; Zhou, Y.-G. *Chem. Commun.* **2013**, *49*, 1660.

[62] Liu, L.; Yuan, Z.; Pan, R.; Zeng, Y.; Lin, A.; Yao, H.; Huang, Y. *Org. Chem. Front.* **2018**, *5*, 623.

derivates in excellent diastereo- and enantioselectivities (Scheme 12).[63] Mechanistic study of the reaction intermediate and control experiments indicated that the annulation reaction underwent a cascade pathway including intermolecular nucleophilic substitution and subsequent intramolecular 1,6.addition.

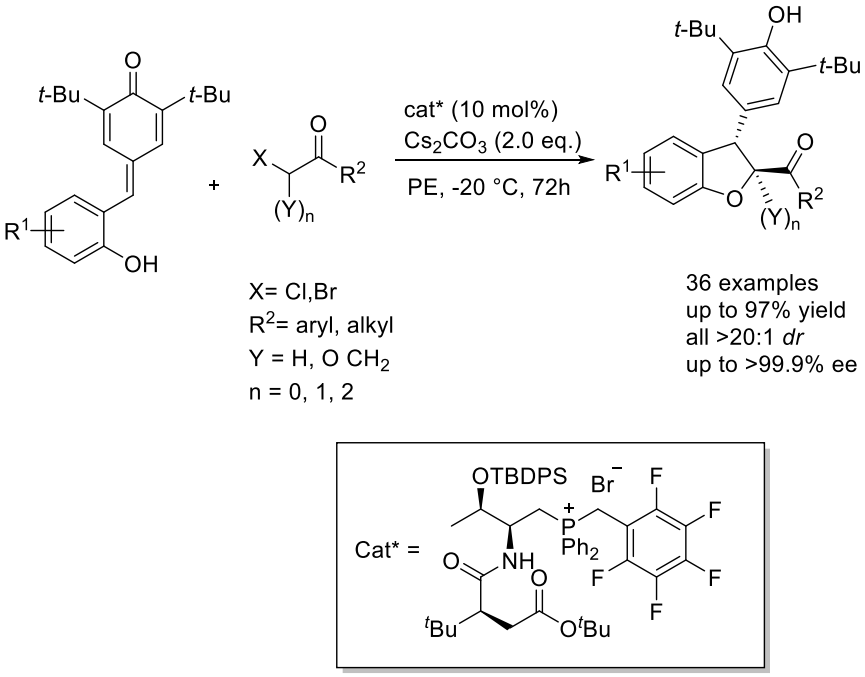

Scheme 12 Asymmetric construction of 2.3-dihydrobenzofurans via bifunctional phopsphonium salt-catalyzed

Nitrogen-containing phenols and quinones are also suitable building blocks for intermolecular coupling reaction. For example, Correia at al. described the first enantioselective oxy-Heck-Matsuda reaction using a variety of styrenic olefins and *o*-hydroxyarenediazonium salts to generate chiral dihydrobenzofurans (Scheme 13).[64] The reaction proceeds in moderate to good yields, with high *trans* diastereoselectivity (up to 20:1) in enantioselectivities up to 90:10 using the *N,N*-ligand pyrimidine-bisoxazoline.

[63] Tan, J.-P.; Yu, P.; Wu, J.-H.; Chen, Y.; Pan, J.; Jiang, C.; Ren, X.; Zhang, H.-S.; Wang, T. *Org. Lett.* **2019**, *21*, 7298.

[64] Silva, A. R.; Polo, E. C.; Martins, N. C.; Correia, C. R. D. *Adv. Synth. Catal.* **2018**, *360*, 346.

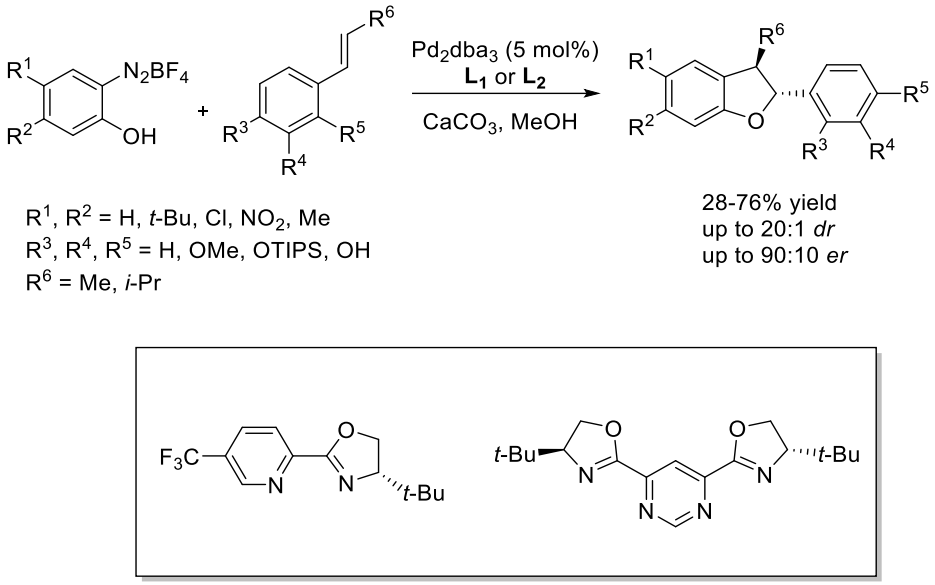

Scheme 13 Dihydrobenzofurans by enantioselective oxy-Heck-Matsuda reaction

2.1.2.4 Intramolecular approaches

The intramolecular approaches are subdivided by which bond is formed in the key reaction. Among these, the intramolecular alkylation of a phenol is a traditional method for the preparation of dihydrobenzofurans. For example in 2007, Pineschi et al.[65] reported a novel and simple method for the stereoselective synthesis of 2,3-disubstituted 2,3-dihydrobenzofurans by intramolecular cyclization of hydroxyphenols. The regio- and stereoselective ring-opening of aryl-epoxide with aryl-borate occured through an *ortho*-alkylation leading to the hydroxyphenol with *syn* stereoselectivity. These compounds could be cyclodehydrated to differently 3-aryl-2,3-dihydrobenzofurans. The treatment of hydroxyphenol **III** with catalytic amounts of *p*-TsOH in refluxing toluene gave an inseparable 68/32 mixture of diastereoisomers *cis*/*trans* **IV** and **V** . When the cyclodehydration was effected by means of an intramolecular Mitsunobu-type protocol (PPh_3, DEAD, THF, rt), the diastereoselectivity was improved up to synthetically useful levels (*dr* >95/5) and compound **IV** was isolated with 80% yield (Scheme 14).

[65] Bertolini, F.; Crotti, P.; Di Bussolo, V.; Macchia, F.; Pineschi, M. *J. Org. Chem.*, **2007**, *72*, 7761-7764.

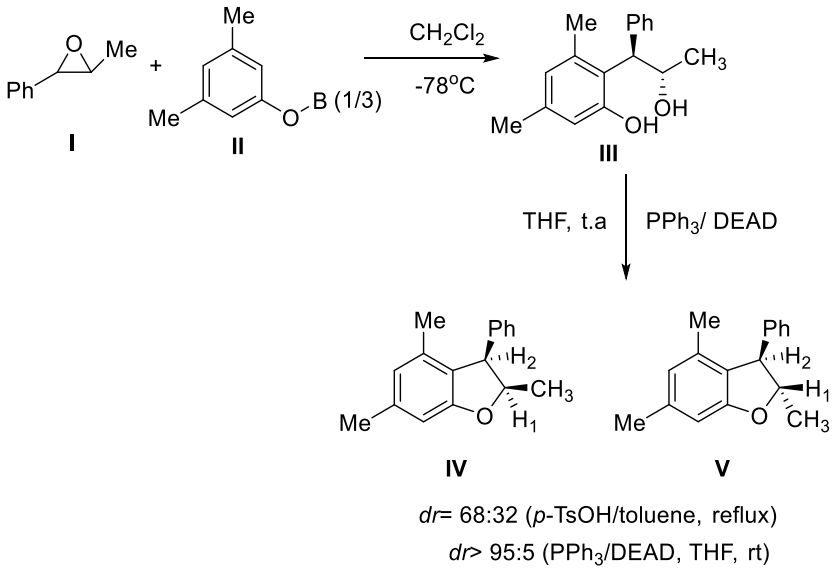

Scheme 14 Synthesis of 2,3-disubstituted-2,3-dihydrobenzofurans *via* intramolecular cyclodehydration

In 2014 Snyder and Wright,[66] in the total synthesis of reaveratrol trimer Caraphenol A, disclosed a different approach for the preparation of 2,3-diaryl-dihydrobenzofurans. Starting from a suitable diaryl ketone (Scheme 15), prepared in 3 steps from commercially available 3,5-dibenzylbenzyl alcohol, the dihydrobenzofuran ring system was obtained *via* four-pot/7-operation process involving Corey-Chaykovsky epoxidation, ZnI_2-mediated Meinwald rearrangement and Grignard addition to afford a triaryl alcohol. After benzyl ether cleavage, acid-catalyzed cyclization occurred, with silyl deprotection and phenol reprotection. These three final operations collectively provided the 2,3-diaryl-dihydrobenzofurans in 80% yield as 10:1 mixture of separable *trans*- and *cis*- isomers.

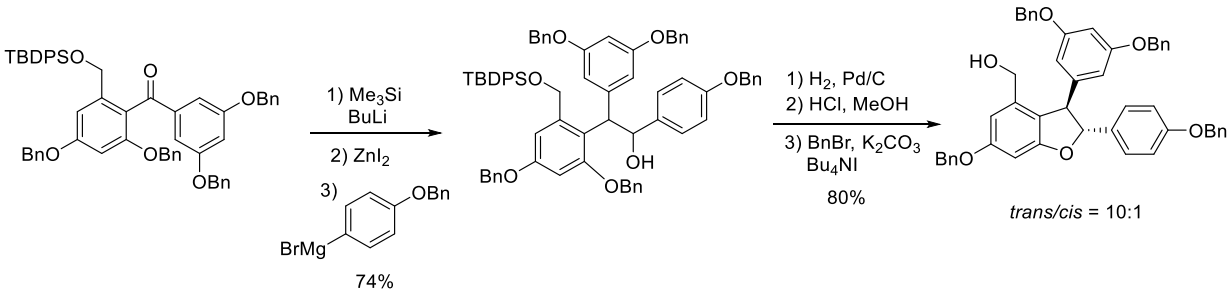

Scheme 15 Synthesis of 2,3-diaryl dihydrobenzofurans from diaryl ketone

An alternative intramolecular methodology is the transition-metal-catalyzed insertion into a saturated C-H bond for the construction of C-C bonds. For example, Che and co-workers described a ruthenium porphyrin-catalyzed stereoselective intramolecular carbenoid C-H insertion. Using [Ru^{II}(TTP)(CO)] as catalyst, aryltosylhydrazones were converted in 2,3-dihydrobenzofurans in good yield and remarkable *cis* selectivity (up to 99%). The reaction was

[66] Wright, N. E.; Snyder, S. A. *Angew. Chem. Int. Ed.* **2014**, *53*, 3409.

performed treating the sodium salt of tosylhydrazone with [Ru^{II}(TTP)(CO)] (1 mol %) and *n*-Bu$_4$NBr (10 mol %) as phase-transfer catalyst in toluene at 110 °C (Scheme 16).[67]

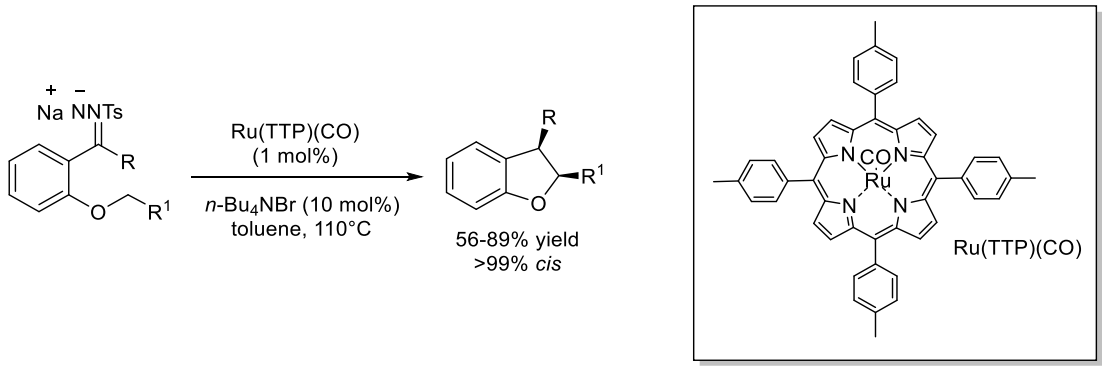

Scheme 16 Ru-catalyzed intramolecular carbenoid C-H insertion

Recently Elofsson and co-workers reported a library of forty-eight compounds based on 2,3-diaryl-2,3-dihydrobenzofuran scaffold for a screening of antibacterial activity.[68] These compounds were prepared by utilizing Pd-catalyzed one-pot multicomponent reactions and ruthenium-catalyzed intramolecular carbenoid C-H insertions, starting from salicylaldehydes, aryl iodides e benzyl halides. The key intermediate in this pathway were the 2-hydroxydiarylketones (**II**).

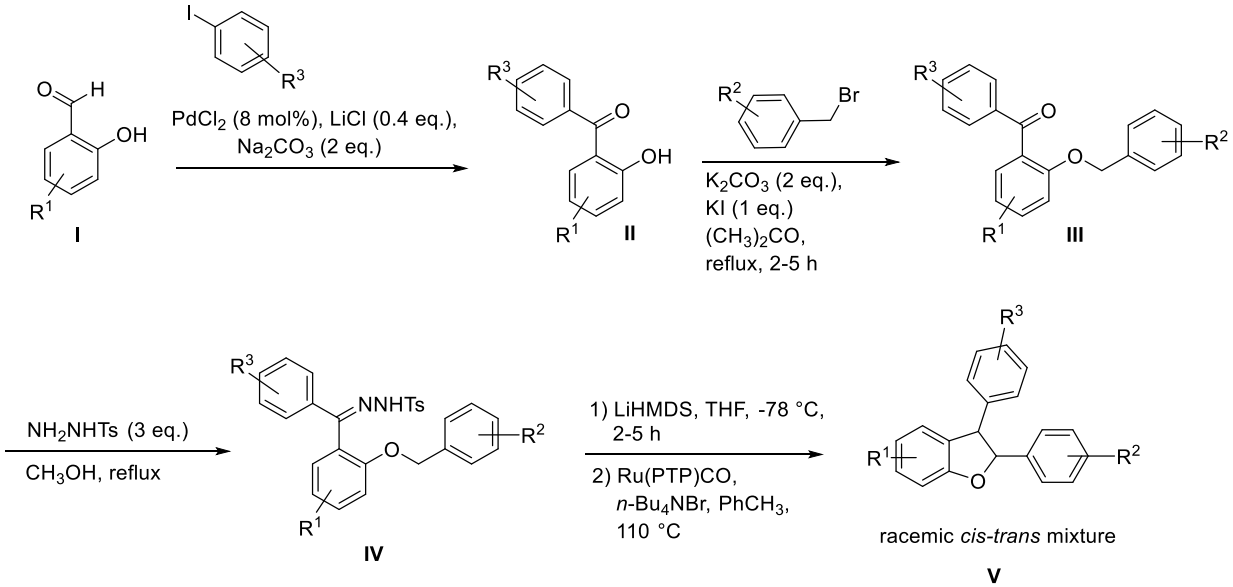

Scheme 17 Synthesis of a racemic *cis-trans* 2,3-diaryl-dihydrobenzofurans

[67] Cheung, W.-H.; Zheng, S.-L.; Yu, W.-Y.; Zhou, G.-C.; Che, C.-M. *Org. Lett.*, **2003**, *5*, 2535-2538.

[68] Saleeb, M.; Mojica, S.; Eriksson, A. U.; Andersson, C. D.; Gylfe, A.; Elofsson, M. *Eur. J. Med. Chem.*, **2018**, *143*, 1077-1089.

The salicylaldehydes were coupled to the aryl iodides using $PdCl_2$ to afford the corresponding 2-hydroxylarylketones in 40–93% yields (Scheme 17). Subsequently, those intermediates were *O*-alkylated with two different benzyl bromides to afford intermediates **III** in essentially quantitative yields. Aryl tosylhydrazones (**IV**) were prepared from the corresponding ketone in 70–99% yields by condensation with *p*-toluenesulfonylhydrazide and were, then, used as precursors for the carbenoid C-H insertion. Eventually, two-step one-pot ruthenium carbenoid intramolecular C-H insertion afforded a racemic *cis-trans* mixture of the dihydrobenzofurans (**V**) *via in situ* generation of diazo compounds. They used commercially available ruthenium porphyrin (Ru^{II}(TPP)CO), which yielded a racemic *cis-trans* mixture in a ratio ranging between 1:1 and 1:3 and 27–70% yields over two steps. This diastereomeric mixture was subsequently resolved by HPLC and the stereochemistry was verified on the ^{1}H NMR spectra by the *J* coupling constants.

In 2014,[69] Shaw et al. disclosed the first asymmetric C-H insertion reactions of rhodium donor-donor carbenoids for the synthesis of a broad range of *cis* 2,3-disubstituted-2,3-dihydrobenzofurans. The synthetic strategy involved the formation of the corresponding hydrazones through a nucleophilic addition between hydrazine and 2-hydroxybenzophenone. The hydrazones were oxidized with MnO_2 to the corresponding diaryl diazomethanes which, by the use of the chiral Rh_2(*R*-PTAD)$_4$, underwent intramolecular C-H insertions leading to various *cis* 2,3-disubstituted-2,3-dihydrobenzofurans with high diastereo- and enantioselectivity. (Scheme 18).

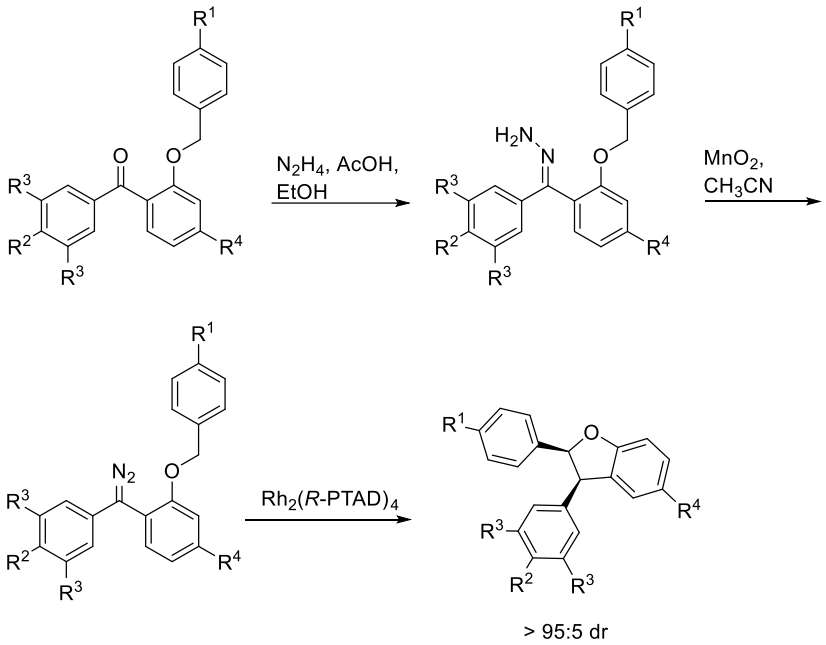

Scheme 18 Synthesis of *cis* 2,3-disubstituted-2,3-dihydrobenzofurans

[69] Soldi, C.; Lamb., K. N.; Squiteri, R. A.; onz lez-L pez, M.; Di Maso, M. J.; Shaw, J. T. *J. Am. Chem. Soc.* **2014**, *136*, 15142-15145.

This methodology was used, by the same authors, for the first enantioselective synthesis of (*E*)-δ-Viniferin. Benzophenone **I**, available in five steps from commercially available starting materials, was easily converted to the corresponding hydrazine, which underwent an intramolecular C-H insertion, using 1 mol% of Rh_2(*R*-PTAD)$_4$ as catalyst, affording the *cis* 2,3-disubstituted-2,3-dihydrobenzofuran **II** (Scheme 19). Subsequent demethylation and epimerization on carbon C2 gave the *trans* 2,3-disubstituted-2,3-dihydrobenzofuran **III** which after acetylation, Heck coupling with 3,5-diacetoxystyrene and deacetylation provided the (*E*)-δ-Viniferin. Control experiments confirmed that epimerization occurred with no loss of enantiomeric purity and that the optical rotation of the synthetic sample matched to the reported value. This was the first enantioselective synthesis of an oligoresveratrol natural product.

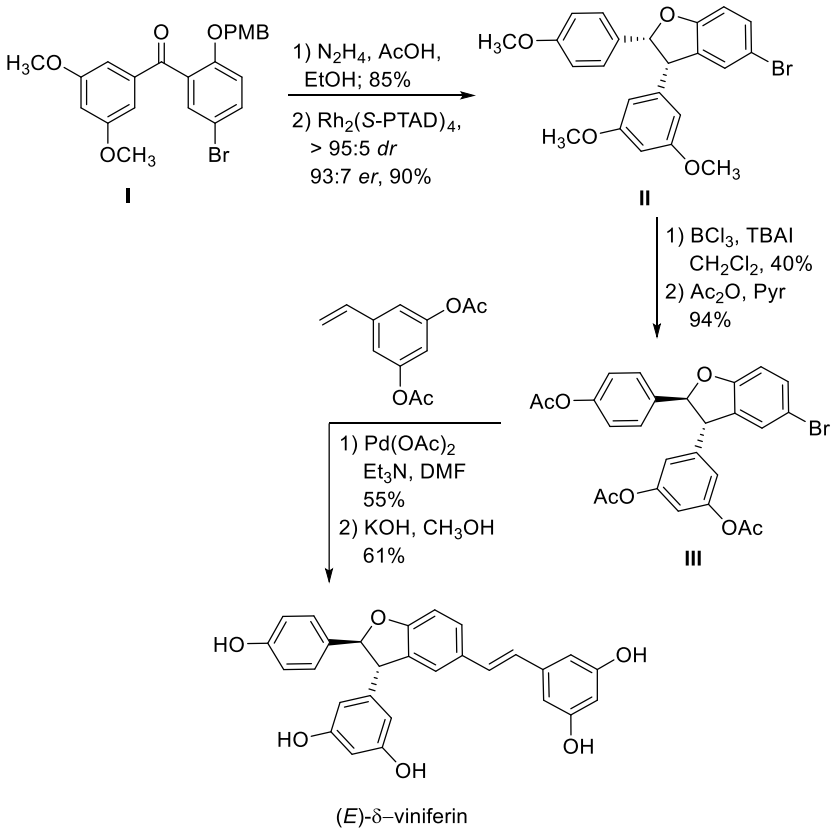

Scheme 19 Enantioselective synthesis of (*E*)-δ-Viniferin

Hashimoto and co-workers,[70] in 2015, reported a second asymmetric synthesis of (-)-(*E*)-δ-Viniferin by intramolecular C-H insertion of a suitable diaryldiazomethane using a chiral Rh (II) catalyst. Initially they prepared the model system *cis*-2,3-diphenyl-2,3-dihydrobenzofuran **III** (Scheme 20) by oxidation with MnO_2 of the hydrazone **I** to the model diaryldiazomethane **II**, which underwent intramolecular CH insertion using 1 mol % of Rh_2(*S*-PTTL)$_4$ in CH_2Cl_2 at 60°C, leading *cis*-2,3-diphenyl-2,3-dihydrobenzofuran **III** with 88% yield and high enantiomeric excess (97% *ee*).

[70] Natori, Y.; Ito, M.; Anada, M.; Nambu, H.; Hashimoto, S. *Tetr. Lett.*, **2015**, *56*, 4324-4327.

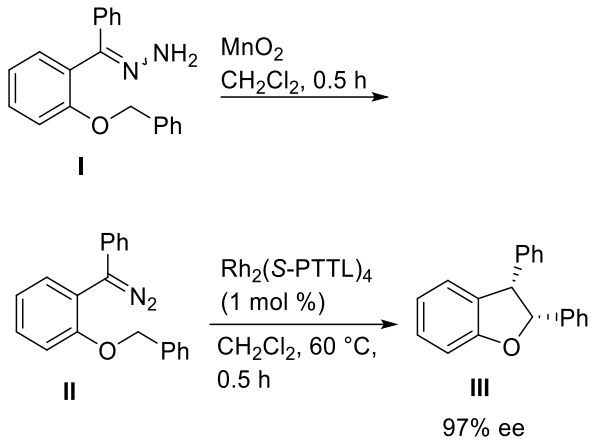

Scheme 20 Diastereo- and enantioselective synthesis of *cis*-2,3-diphenyl-2,3-dihydrobenzofuran

Encouraged by this result, they used the same strategy for the synthesis of (-)-δ-Viniferin, choosing the suitable starting substrates and using the key epimerization on C2 sterocenter in the very last step (Scheme 21). The oxidation of hydrazone **IV** with MnO_2 provided the diaryldiazomethane **V**, which, by intramolecular CH insertion using 1 mol % of Rh_2(*S*-PTTL)$_4$ led to *cis*-2,3-disubtituted-2,3-dihydrobenzofuran **VI**. Subsequently, Heck coupling with 3,5-diacetoxystyrene, epimerization and deprotection led to the (-)-δ-Viniferin with high enantiomeric excess.

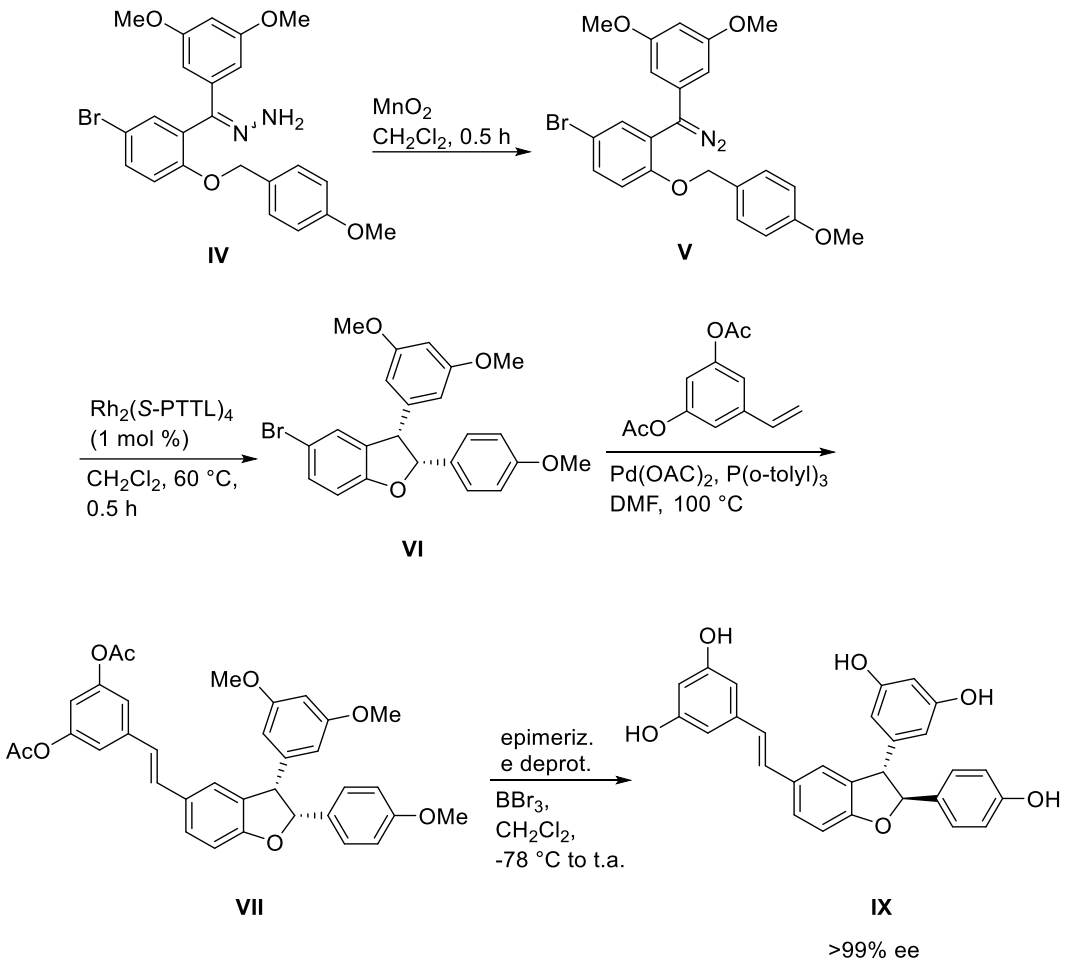

Scheme 21 Enantioselective synthesis of (-)-δ-Viniferin

The epimerization proceeded exclusively at the C2 sterocenter via the *p*-quinonemethide intermediate **VIII** generated by the Lewis acid BBr_3 (Scheme 22). Therefore, for the preparazion of (-)-(*E*)-δ-Viniferin **IX** the presence of *para*-hydroxyaryl group in position 2 is compulsory, because it allows the formation of the intermediate carbenium ion with the opening of the dihydrobenzofuran.

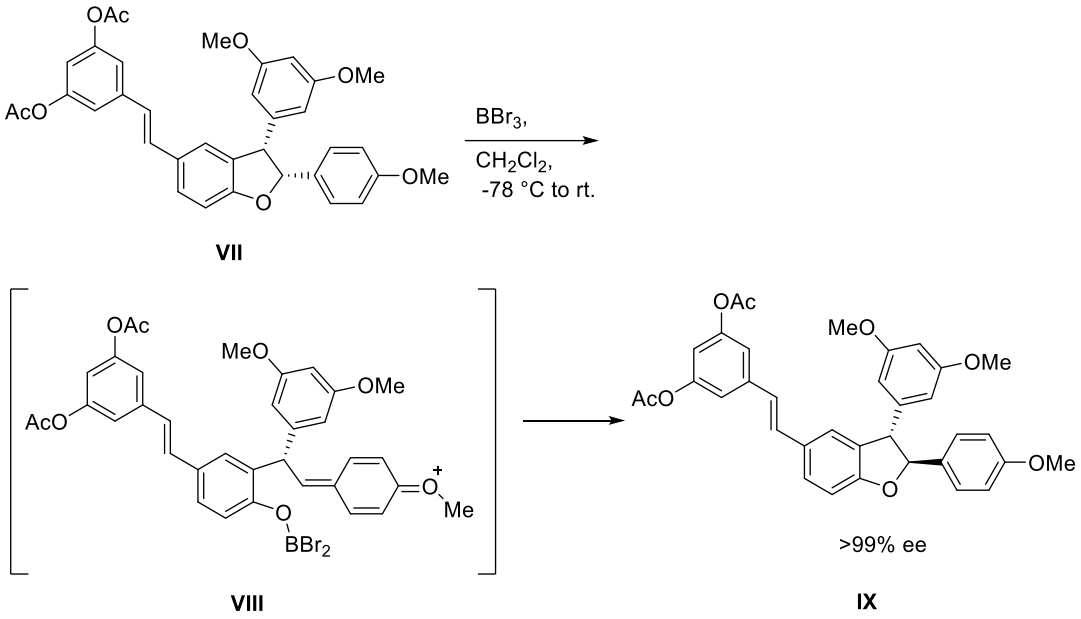

Scheme 22 Epimerization at the C2 stereocenter

Therefore this asymmetric method appears general only for the preparation of *cis* 2,3-diaryl-2,3-dihydrobenzofuras , while the isomerization key step to *trans* isomer is driven by the *p*-hydroxyl group on C2 ring.

2.2 Stereoselective access to *trans*-2,3-diphenyl-2,3-dihydrobenzofuran

In my previous work, during my master thesis at University of Basilicata, I developed a quite general method for a direct stereoselective access to *trans* 2,3-diphenyl-2,3-dihydrobenzofuran, from *trans* 2,3-diaryloxiranes **C**, whose retrosynthetic approach is depicted in Scheme 23.[71] In this strategy, the final dihydrobenzofuran **A** could be derived by a Mitsunobu-type cyclodehydration from the suitable hydroxyphenol **B**, which could be formed by a regio- and stereoselective ring opening reaction of *ortho* substituted diaryloxirane **C**. The diaryloxirane can be easily obtained by the Corey-Chaykovsky reaction between the suitable *o*-substituted aldehyde **D** and a benzylidene sulfur ylide **F**.

[71] Teresa Laurita, *Sintesi stereoselettiva di 2,3-difenil-2,3-diidrobenzofurani a partire da trans 2,3-diarilossirani omochirali*, Tesi di Laurea Magistrale in Scienze Chimiche, Università degli studi della Basilicata, a.a. 2017-2018.

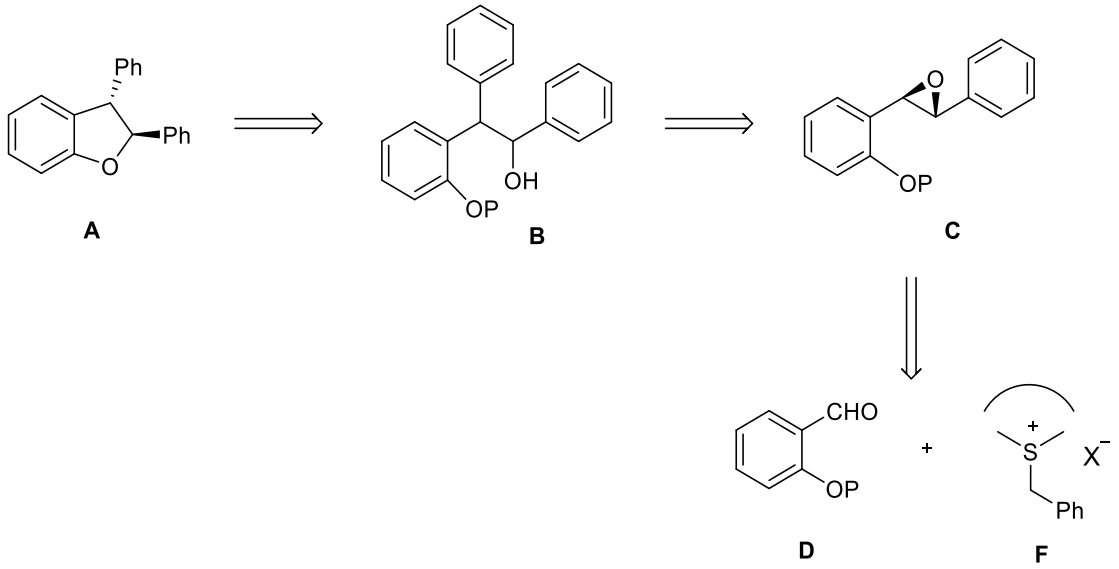

Scheme 23 Retrosynthetic approach to *trans* 2,3-diaryl-2,3-dihydrobenzofurans.

The key steps are the Corey-Chaykovsky epoxidation and the ring opening of diaryloxirane because their efficiency in terms of regio- and stereoselectivity can be critical for the success of the whole strategy.

2.2.1 The Corey-Chaykovsky epoxidation

The Corey–Chaykovsky reaction is a chemical reaction used in organic chemistry for the synthesis of epoxides, aziridines, and cyclopropanes. It was discovered in 1961 by A. William Johnson[72] and developed significantly by E. J. Corey and Michael Chaykovsky.[73]

The reaction mechanism provides the generation *in situ* of a sulfur ylide by deprotonation of the parent sulfonium salt with a base. The ylide initially acts as a nucleophile towards the carbonyl compound, generally an aldehyde, leading the betaine intermediate. The resulting oxygen anion which reacts as an intramolecular nucleophile toward the electrophilic ylide carbon, displacing the sulfide as a good leaving group (Scheme 24).

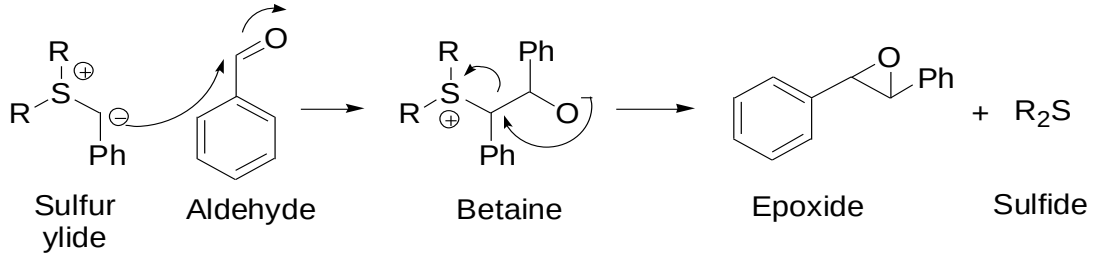

Scheme 24 Mechanism of the Corey-Chaykovsky epoxidation

[72] Johnson, A. W.; LaCount, R. B. J. *Am. Chem. Soc.* **1961**, *83*, 417-423.

[73] Corey, E. J.; Chaykovsky, M. J. *Am. Chem. Soc.* **1962**, *84*, 3782-3783.

The reaction is generally diastereoseletive towards *trans* epoxide. This diastereoselectivity is due to the fact that *anti* betaines undergo fast elimination to the ylide and aldehyde, whereas the corresponding *syn* diastereoisomers can decompose back to reactants (Scheme 25).[74] In other words, addition of the ylide to benzaldehyde is irreversible in the *anti* case, leading to *trans* epoxide, whereas in the *syn* case, the ensuing elimination of sulfide to *cis* epoxide is slow, resulting in competitive reversion to reactants.

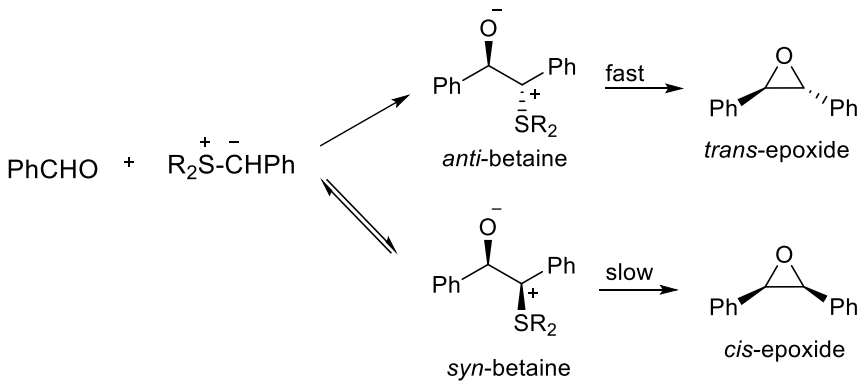

Scheme 25 Mechanism of epoxidation accounting for high *trans* selectivity

The factors that influence the stereoselectivity are: steric hindrance of the sulfide, ylide conformation, ylide face selectivity, type of aldehyde, reversibility of betaine formation and solvent. In the case of stabilized ylides,[75] having an electron releasing group that stabilizes the adjacent anion, the reaction provides exclusively *trans* epoxides, with both aromatic and aliphatic aldehydes. Studies of Aggarwal[76] showed that both *syn*- and *anti*-betaines were formed reversibly, but only the *anti* betaine evolved to the corresponding *trans* epoxide due to a lower torsional energy barrier compared to that of *syn* betaine, which would lead to the corresponding *cis* epoxide. In the case of semi-stabilized ylide, bearing weakly anion-stabilising groups such as substituted benzyl or allyl groups, the reaction with aldehydes is governed by more subtle effects. In reactions with benzaldehyde, the formation of *anti*-betaine is irreversible, while that of *syn* is reversible. DFT calculations revealed that the highest activation barriers along the route leading to either the *trans*- or *cis*- epoxides were C–C bond rotations of the intermediate betaines (Scheme 26).

[74] Aggarwal, V.K.; Calamai, S.; Ford, J.G. *J. Chem. Soc., Perkin Trans.* **1997**, *1*, 593.

[75] Aggarwal, V.K.; Harvey, J.N.; Richardson, J. *J. Am. Chem. Soc*. **2002**, *124*, 5747.

[76] Aggarwal, V.K.; Richardson, J. *J. Chem. Soc., Chem. Comm*. **2003**, 2644.

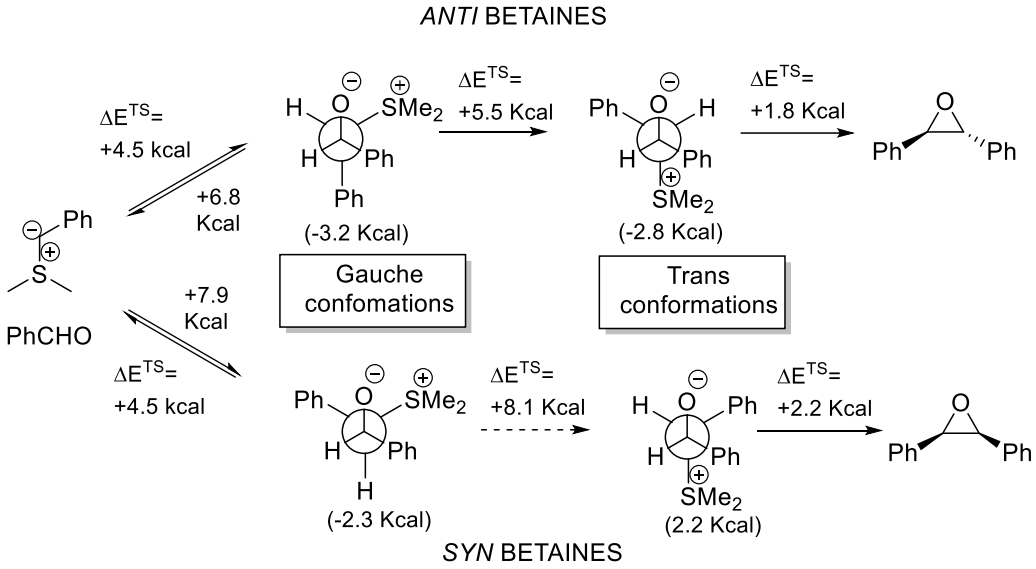

Scheme 26 Energetic profile (DFT calculations) of ylide reaction with benzaldehyde giving stilbene oxide.

In the case of the *syn*-betaine the barrier to bond-rotation was higher than reversal to starting materials whereas for the *anti*-betaine, the barrier to returning to starting materials was higher than bond rotation to the transoid conformation. In reactions involving different substrates, the diastereoselectivity can be low if *syn*-betaine formation is nonreversible or only partially reversible. Four factors contribute to reduced reversibility of the betaine back to the original starting materials, which in turn leads to reduced *trans* selectivity:

- Lower stability of the carbonyl group, which reduces the tendency for the betaine to revert back to the ylide and carbonyl group. For example, aliphatic aldehydes generally give considerably lower levels of diastereocontrol than aromatic and unsaturated aldehydes.
- Reduced stability of the ylide reduces reversibility of betaine formation. Electron-donating groups on the aromatic ring destabilise the ylide and therefore lead to lower diastereocontrol.
- Reduced steric hindrance of the ylide/aldehyde allows more facile bond rotation from the gauche to the *trans* conformation of the betaine and therefore reduces reversibility and thus diastereoselectivity. Low diastereocontrol was observed with acetylenic aldehydes. It follows then that more hindered substrates with respect to either the ylide or the electrophile will lead to increased barriers to bond rotation of the initially formed gauche conformers of the betaines and will result in increased reversibility, thus leading to increased *trans* diastereoselectivity.
- Increased solvation of charges of the betaine leads to a reduction in the barrier to bond rotation of the intermediate betaine. This results in reduced reversibility and a corresponding decrease in diastereoselectivity.

When a chiral sulfide is used, in addition to the diastereoselectivity of the reaction, enantioselectivity is also observed. To achieve high enantioselectivity it is necessary to:

- form a single diastereomeric sulfonium ylide
- achieve high levels of control in ylide conformation

- achieve high levels of control in facial selectivity of the ylide
- ensure that anti-betaine formation is non-reversible

The fourth criterion plays a vital role in the stereochemical outcome of a number of asymmetric reactions, while the nature of the electrophile is less important.

Aggarwal[77] and Solladiè-Cavallo[78] reported the synthesis of epoxies in good yields and high diastereo- and enantioselectivity using stoichiometric amounts of sulfonium salts deriving from chiral sulfide **1** and **2** (Figure 18).

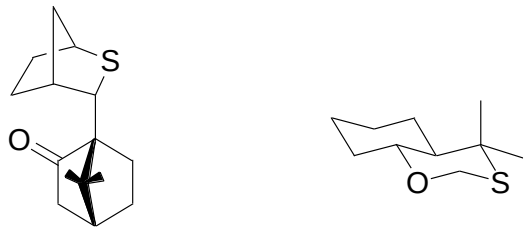

1 **2**

Figure 18 Structure of keto-sulfide **1** and Eliel's oxathiane **2**

The high diastereo- and enantioselectivity is due to the formation of only one diastereoisomer of ylide with both sulfides. This, in the case of sulfide **1**, is caused by the steric effects. In the case of the Eliel's oxathiane **2**, the diastereoselectivity is determined by the two methyl groups in α position respect to the sulfur. In fact, it can be noted that the steric interaction and the anomeric effect make the equatorial lone pair less nucleophilic than the axial one. For both sulfides, there are two important conformers of the ylide, **1A** / **B** and **2A** / **B** (Scheme 27).

[77] Aggarwal, V.K.; Charmant, J.; Dudin, L.; Porcelloni, M.; Richardson, J. *Proc. Nat. Acc. Sci*, **2004**, *10*, 5467.

[78] a) Solladié-Cavallo, A.; Diep-Vohuule, A.; Sunjic, V.; Vinkovic, V. A. *Tetrahedron: Asymmetry* **1996**, *7*, 1783-1788. b) Solladié-Cavallo, A.; Diep-Vohuule, A. *J. Org. Chem.* **1995**, *60*, 3494-3498. c) Solladié-Cavallo, A.; Adib, A. *Tetrahedron* **1992**, *48*, 2453-2464. d) Solladié-Cavallo, A.; Roje, M.; Isarno, T.; Sunjic, V.; Vinkovic, V. *J. Org. Chem.* **2000**, 1077-1080.

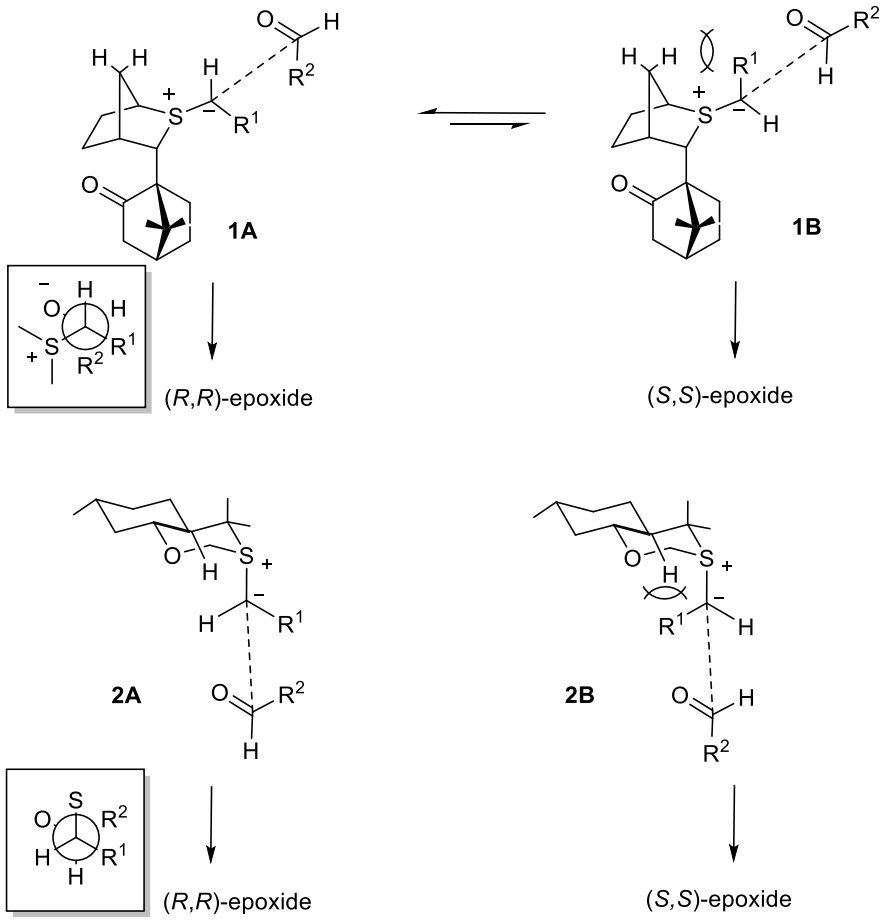

Scheme 27 Conformers of the ylide **1**

Conformers **1A** and **2A** are much more favored, due to the reduced steric interactions. In case of ylide **1A**, face selectivity is ensured by the presence of a bulky group (a camphoryl group) which makes accessible only the *Re* face of the ylide. Instead in the case of ylide **2A**, face selectivity is guaranteed from the steric hindrance of the two methyl groups which favors the *Re* face rather than the *Si* face. The direct asymmetric transformation of carbonyl compounds into epoxides using chiral sulfur ylides also offers a complementary and potentially advantageous method over the two-step protocol of Wittig olefination followed by asymmetric epoxidation.[79]

Initially, this sulfur ylide-mediated asymmetric epoxidation was not widely used due to two limitations:

- availability of sulfide: in fact, it has been shown that sulfides providing a high enantioselectivity require multi-step synthesis
- the starting material is commercially available only in one enantiomeric form, constituting a limit in the application of these sulfides.

[79] O. Illa, E. M. McGarrigle, V. K. Aggarwal In *Encyclopedia of Reagents for Organic Synthesis*; (Eds.: L. A. Paquette, D. Crich, P. L. Fuchs, G. A. Molander), eEROS John Wiley & Sons Ltd.: Hoboken, New Jersey, **2012**.

The limit of this strategy, in fact, concerns precisely the obtaining of the various epoxides only in one enantiomeric form and the need, for example, to prepare Eliel's oxathiane,[80] not commercialy available, through multistape-synthesis starting from (+)-*pulegone* (Scheme 28).

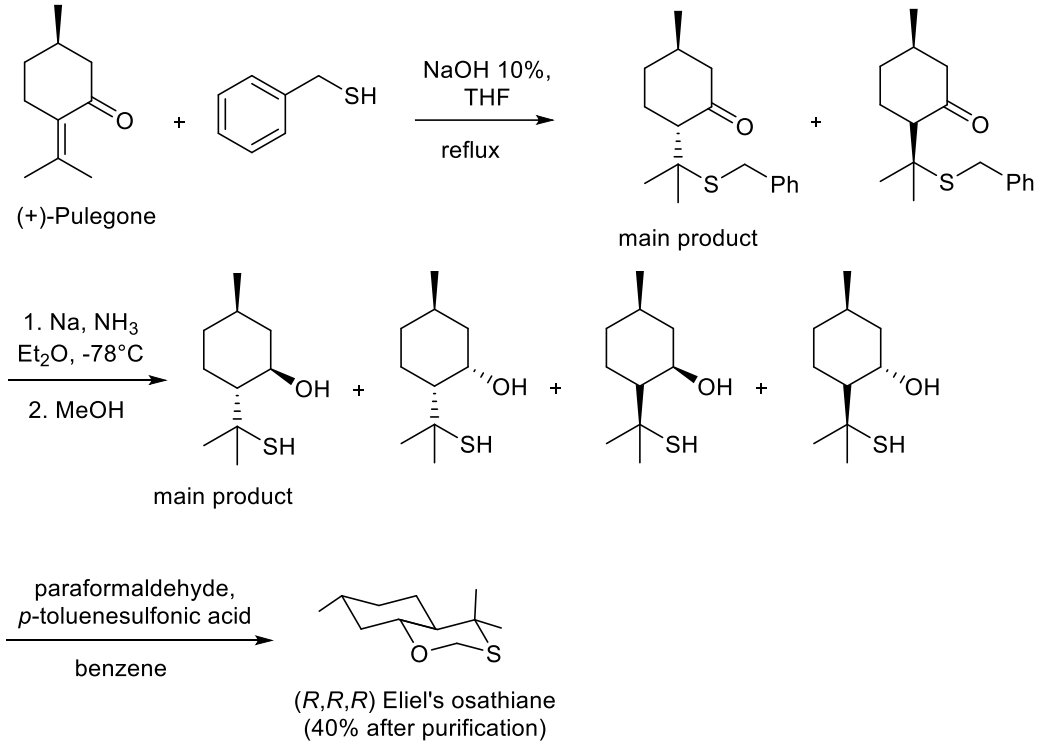

Scheme 28 Preparation of Eliel's oxathiane

Around ten years ago, Aggarwal reported the preparation and use of a chiral sulfide, isothiocineole, which simultaneously addressed both of these limitations.[81] The sulfide was easily prepared in one step from limonene and elemental sulfur and it was soon commercially available in both enantiomeric forms (Figure 19). Thus, enantiomeric epoxides could be prepared in good yields and high diastereo- and enantioselectivity.

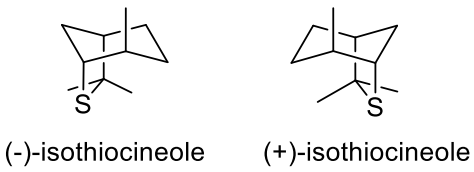

Figure 19 Structure of (-)-isothiocineole and (+)-isothiocineole

Isothiocineole **3** was investigated due to its well-defined rigid architecture and somewhat close resemblance to our previous successful sulfide **1** (Scheme 29).

---

[80] Eliel, E. L.; Lynch, J. E.; Kume, F.; Frye, S. V. *Org. Synth.* **1987**, *65*, 215-221.

[81] a) Illa, O.; Arshad, M.; Ros, A.; McGarrigle, E. M.; Aggarwal, V. A. *J. Am. Chem. Soc.* **2010**, *132*, 1828-1830; b) Illa, O.; Namutebi, M.; Saha, C.; Ostovar, M.; Chun Chen, C.; Haddow, M. F.;Nocquet-Thibault, S.; Lusi, M.; McGarrigle, E. M.; Aggarwal, V. K. *J. Am. Chem. Soc.* **2013**, *135*, 11951-11966.

The enantioselectivity is governed, as usual, by three main factors:

- ylide conformation
- facial selectivity of the ylide
- degree of reversibility in the betaine formation

The complete facial selectivity can be expected as a result of the Me group blocking reaction from one face. The salt is closely related to the ylide intermediate and shows that one face is essentially completely blocked, whereas the other face is open and therefore accessible to substrates.

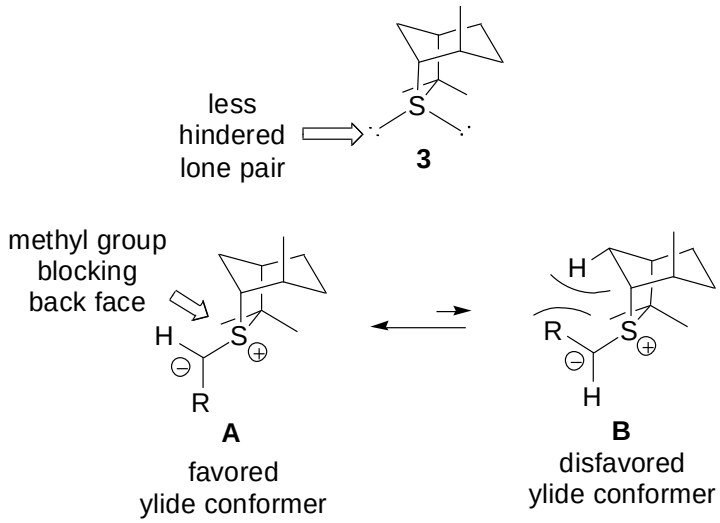

Scheme 29 Design features of isothiocineole for enantioselectivity in asymmetric epoxidation

Semi-stabilized sulfonium ylide gave general high enantioselectivity with different aldehydes. This suggests that the dominant factor responsible for enantioselectivity with all of these substrates is ylide conformation (**A**: **B** ratio), rather than the difference in reactivity of the two ylide conformers. As stated above (Scheme 30), the ylide can adopt conformations **A** or **B**, but **A** should be strongly favored as **B** suffers from nonbonded 1,4 steric interactions.

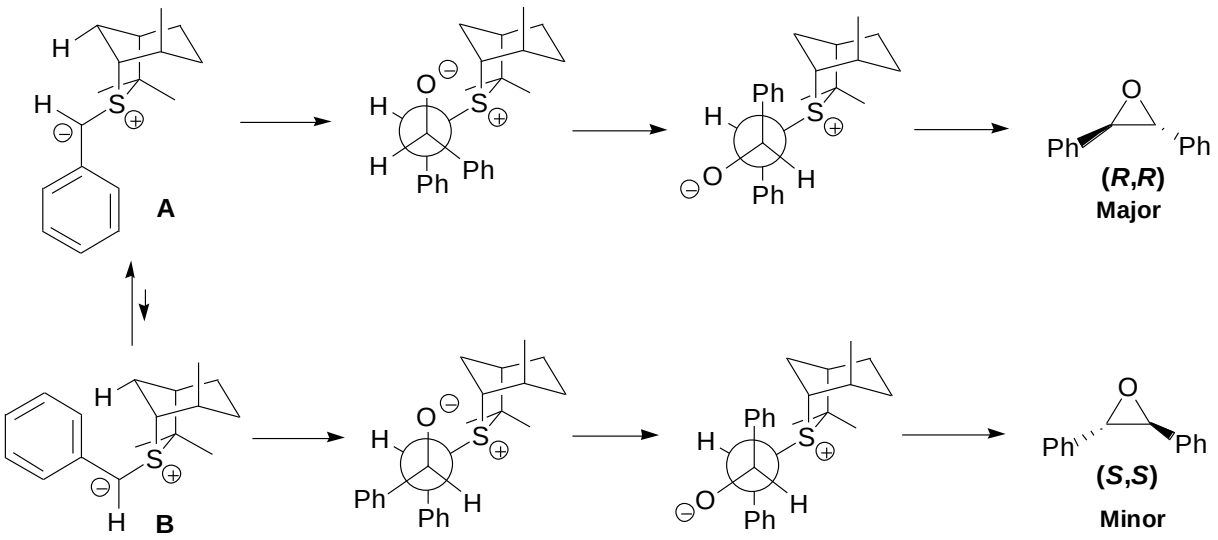

Scheme 30 Origin of Enantioselectivity for Epoxidation with Sulfur Ylide

In terms of preparation, Weitkamp had reported a one-step synthesis of isothiocineole **3** from simple and cheap reagents, elemental sulfur and limonene.[82] Heating the two components followed by distillation and separation of isothiocineole from by-products by co-crystallization gave the target molecule in 20% yield and 94:6 enantiomeric ratio (*er*). Aggarwal et al. noted that the conversion of limonene into isothiocineole **3** requires the overall addition of sulfur and two hydrogens, but the generation of the two hydrogens from limonene need high temperature and thus results in significant formation of the unsaturated sulfide.[81a] Therefore, a more efficient source of the two hydrogens was chosen, the γ-terpinene, allowing the reaction to run at lower temperatures. The synthesis was initially conducted at 125 °C, adding γ-terpinene to the sulfur and limonene, furnishing pure isothiocineole in much improved yield (36%) and, more important, without racemization (99:1 *er*). Subsequently, sulfur and γ-terpinene were added at 125 °C in two portions, leading to isothiocineole with 61% yield in 24 h (Scheme 31).

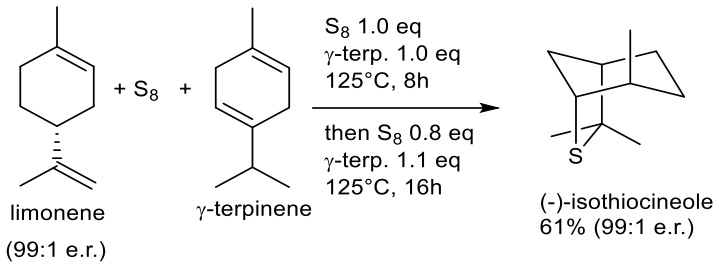

Scheme 31 Synthesis (-) isothiocineole

In recent years, our research group took advantage of this chiral auxiliary preparing a series of new enantioenriched 2-aryl-3-phenyloxiranes by asymmetric sulfur ylide mediated epoxidation of aldehydes,.[83] Reactions of the corresponding benzyl sulfonium salt with aromatic aldehydes in presence of KOH as a base, in either H_2O/ CH_3CN or *t*-BuOH/CH_3CN solvent mixtures, worked smoothly well in all cases, furnishing good yields and very high levels of diastereo- and enantioselectivity (Table 5).

Table 5 Preparation of enantioenriched *trans* 2-aryl-3-phenyloxiranes

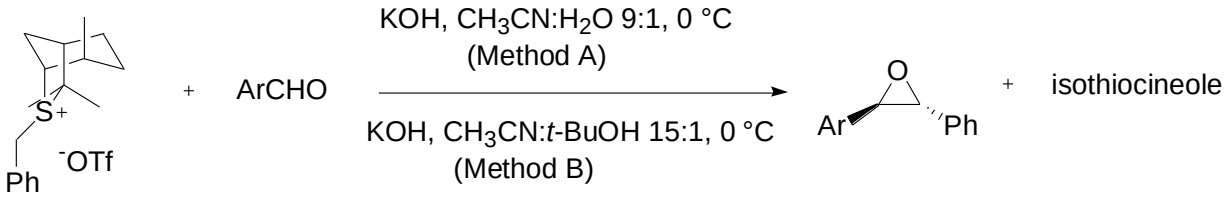

[82] Weitkamp, A. W. *J. Am. Chem. Soc.* **1959**, *81*, 3430-3434.

[83] Lupattelli, P.; Chiummiento, L.; Funicello, M.; Tramutola, F.; Marmo, A.; Gliubizzi, N.; Tofani, D. *Tetrahedron* **2015**, *71*, 5662-5668.

Entry	Ar	Method	Yield %	*d.r* (*trans*/*cis*)	*e.r.* (*trans*)
1	*o*-Br-C_6H_4	B	60	95/5	97/3
2	*o*-Cl-C_6H_4	B	60	95/5	96/4
3	*o*-NO_2-C_6H_4	A	80	only *trans*	>99/1
4	*o*-CH_3O-C_6H_4	B	88	only *trans*	>99/1
5	*o*-TsO-C_6H_4	B	68	only *trans*	95/5
6	*o*-TIPSO-C_6H_4	B	65	only *trans*	>99/1
7	*o*-BnO-C_6H_4	B	80	only *trans*	>99/1
8	3',5'-di-CH_3O-C_6H_3	A	70	only *trans*	95/5
9	*p*-NO_2-C_6H_4	A	78	only *trans*	95/5

In the recent years, the racemic version of Corey-Chaykovsky reaction has been also the subject of several studies and optimizations. In 2013, Graham and co-workers[84] reported a very efficient procedure for the preparation of *trans* stilbene oxide from benzaldehyde and benzylidene tetrahydrothienyl ylide, using guanidine and amidina bases, such as 1,5,7-Triazabicyclo[4.4.0]dec-1-ene (TBD), 7-methyl-1,5,7-triazabicyclo[4.4.0]dec-1-ene (MTBD) and 1,8-diazabycyl [5.4.0] undec-7-ene (DBU), with high yield and excellent stereoselectivity (Table 6).

Table 6 Preparation of achiral *trans*-diaryloxiranes

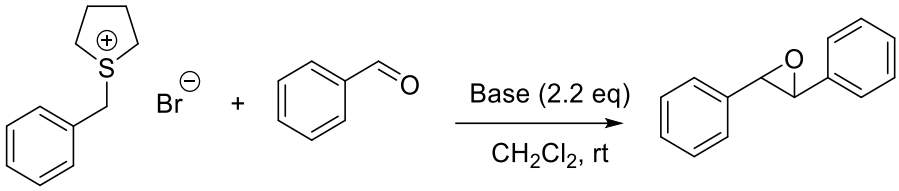

Entry	Time	Base	Conversion (%)	*d.r.* (*trans:cis*)
1	24 h	Et_3N	0	-
2	24 h	DBU	71	95:5
3	10 min	TBD	100	92:8
4	10 min	MTBD	100	94:6

Considering these good results, as will see later, it was decided to use the Corey-Chaykovsky reaction for the preparation of the suitable *ortho*- substituted 2,3-diaryloxiranes, key intermediates of the synthetic strategy.

2.2.2 The nucleophilic ring-opening of diaryloxirane

2,3-Diaryloxiranes can be considered non-conventional epoxides in terms of their synthesis and their reactivity. If compared to alkyl ones, they usually show lower reactivity towards nucleophiles and they need some activation by Lewis acids. The particular chemical behavior

[84] Phillips, D.J.; Kean, J. L.; Graham, E.A. *Tetrahedron*, **2013,** 69, 6196-6202.

of benzyl type carbons in neutral or acidic medium makes them challenging substrates, due to the little differences in reactivity of the two oxiranyl carbons and the possible side reactions such as eliminations or rearrangements.[85]

During the last twenty years, our research group has been studying non conventional reactivity of 2,3-diaryloxiranes, starting from nucleophilic ring-opening reactions with metal halides, such as $MgBr_2$ and LiX (X = I, Br, Cl) under different reaction conditions.[86] In particular the results obtained on substituted diaryloxiranes with LiBr/Amberlyst 15 system showed a dramatic effect of substituent electronic properties on the regioselectivity of the reaction. Reacting oxiranes with one phenyl ring bearing a strong EWG (NO_2, CF_3) in *para*- or in *ortho*- position, only one regioisomer was detected, which derived from the opening at the β-carbon with respect to the substituted phenyl ring. On the other hand, in the presence of a strong ERG (OCH_3) only the regioisomer derived from an α-opening was observed (Scheme 32).[87] Theoretical calculation confirmed the hypothesis of an acyclic cationic intermediate, suggesting a general chemical behavior of such substrates, no matter the nucleophile used. In addition, the extremely high stereoselectivity toward *syn* product obtained with *ortho*-substituted substrates, indicated a likely stereo-orienting effect of the substituent on the cationic intermediate, which led to the product with retention of configuration.

[85] a) Jamalian, A.; Rathman, B.; Borosky, G. L.; Laali, K. K. *Appl. Catal. A* **2014**, *486*, 1–11; b) Bonini, C.; Lupattelli, P. *ARKIVOC* **2008**, *7i*, 150–182.

[86] a) Solladiè-Cavallo, A.; Lupattelli, P.; Marsol, C; Isarno, T.; Bonini, C.; Caruso, L.; Maiorella, A. *Eur. J. Org. Chem.* **2002**, 1439-1444. b) Lupattelli, P.; Bonini, C.; Caruso, L.; Gambacorta, A. *J. Org. Chem.* **2003**, *68*, 3360-3362

[87] Solladiè-Cavallo, A.; Lupattelli, P.; Bonini, C. *J. Org. Chem*, **2005**, *70*, 1605-1611.

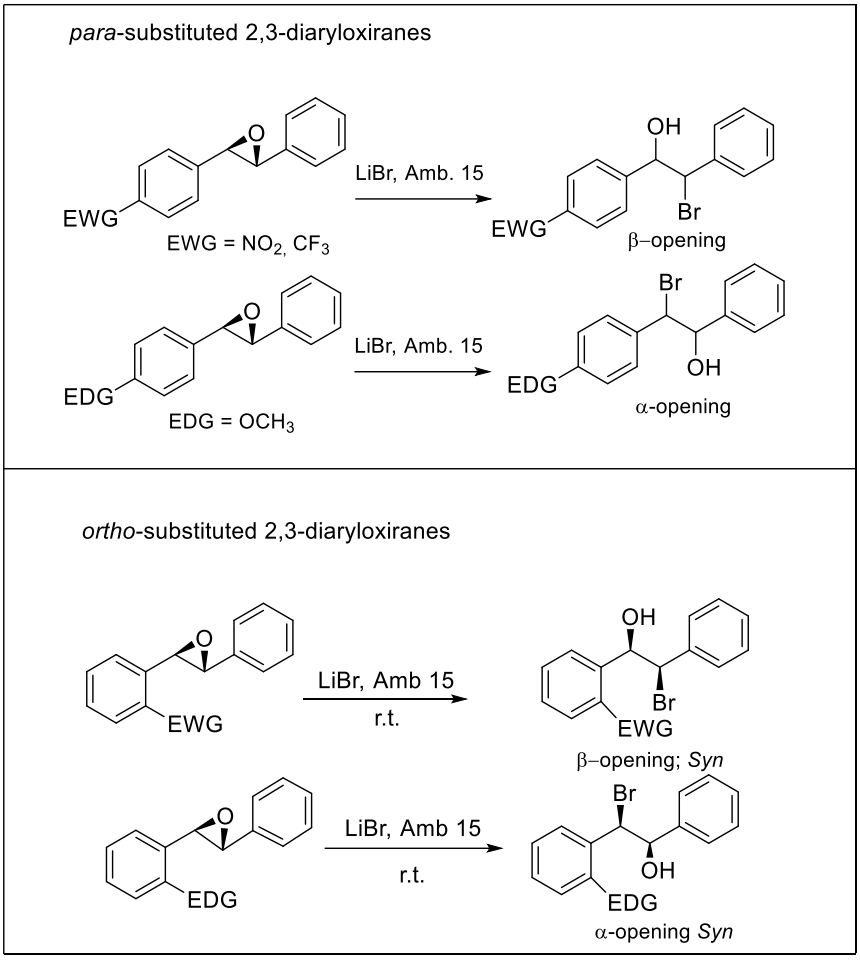

Scheme 32 Ring-opening reaction of *para*- and *ortho*-substituted-2,3-diaryloxiranes

This behavior prompted us to investigate on regio- and stereoselective phenylation of *trans* 2-*ortho*-oxosubstituted phenyl-3-phenyloxiranes **C**, to obtain the corresponding monoprotected hydroxyphenols **B**. Such substrate should retain the regio- and stereoselectivity of the model substrates, undergoing *syn* α-opening. After the cleavage of protecting group, the desired model *trans* 2,3-diphenyl-2,3-dihydroxybenzofuran **A** could be afforded by cyclodehydration under Mitsunobu conditions (Scheme 34).

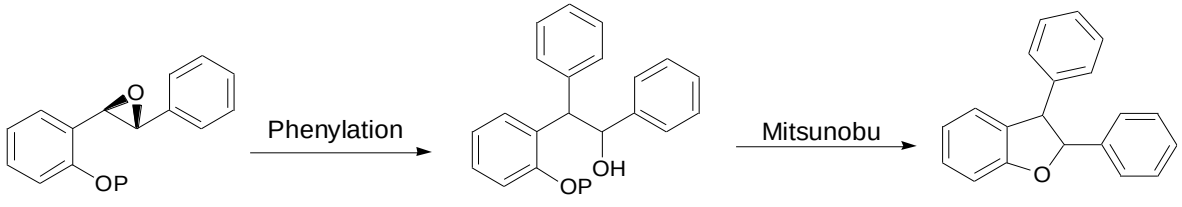

C **B (*syn*)** **A (*trans*)**

Scheme 34 Synthetic route to *trans* 2,3-diphenyl-2,3-dihydrobenzofuran

2.2.3 Results

Different epoxides were prepared taking advantage of the Corey-Chaykovsky reaction between the suitable *ortho*-oxosubstituted benzaldehyde and a benzilidene sulfur ylide. Racemic *trans ortho*-oxosubstituted diaryloxiranes ***rac*-6** were prepared in good yield and high

stereoselectivity from the parent aldehyde **4** using S-benzyltetrahydrothiophenium bromide **5** as ylide source and K_2CO_3 in acetonitrile, as a modification of Graham procedure[84] (Table 7).

Table 7 Synthesis of racemic *trans ortho*-oxosubstituted 2,3-diaryloxiranes

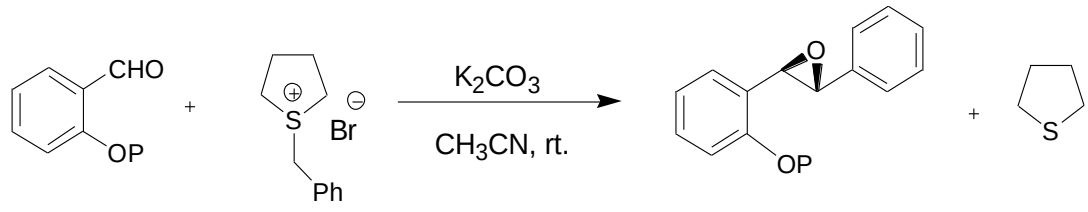

4 **5** ***rac*-6**

Exp.	Aldehyde.	P	Yield (%)	*d.r.* *(trans:cis)*
1	**4a**	Me	80 (**6a**)	80/20
2	**4b**	EOM	90 (**6b**)	83/17
3	**4c**	(iPr)$_3$Si	75 (**6c**)	*trans* only
4	**4d**	Bn	78 (**6d**)	*trans* only

The availability of isothiocineol **3** in both enantiomeric forms, either commercial or easily prepared, allowed us to prepare also *ortho*-substituted diaryloxiranes **(+)-6/ (-)-6** in high yield and excellent *ee* by first *in situ* deprotonation of benzylsulfonium salt **7** of isothiocineol with KOH and subsequent reaction of the ylide with the suitable *ortho* substituted benzaldehyde (Scheme 35). The yield was from discrete to excellent and the *ee* was high in all cases.

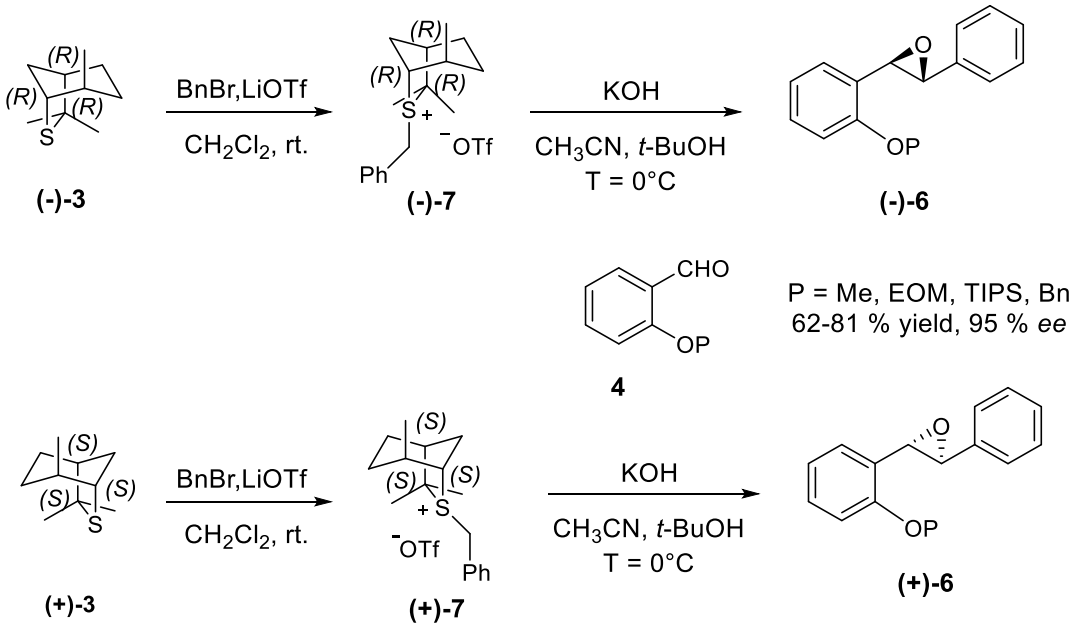

Scheme 35 Preparation of enantiopure ortho-oxosubstituted-2,3-diaryloxiranes.

Regio-and stereoselective ring-opening reactions using carbon nucleophiles have been traditionally limited to the use of stabilized carbanions, strong organometallic reagents and π-

rich aromatics.[88] Treatment of terminal epoxides, even enantiomerically pure, with alkyl-, alkenyl-, or aryl-Grignard reagents in the presence of catalytic amounts of a copper salt, or corresponding cuprates, provides a general route to substituted alcohols as building blocks in multistep syntheses.[89] On the other hand, in the case of internal epoxides, with substituents exerting similar steric and electronic effects, the examples are few, showing that this issue represents a great challenge for organic chemists, in particular for substrates which lack an efficient directing group, as 2,3-epoxy alcohols. Moreover, asymmetric catalytic versions of such transformations are difficult because few carbon-centered nucleophiles possess sufficient reactivity to open epoxides without effecting decomposition of the chiral metal catalyst.[90]

The lack of a systematic study on ring-opening reactions of 2,3-diaryloxiranes with aryl nucleophiles prompted us to test some traditional organometallic systems with the *ortho* benzyloxy substituted epoxide ***rac*-6d** as model substrate.

Treating ***rac*-6d** with either PhMgBr or PhLi at room temperature we noted a completely lack of reactivity, at least for the first three hours. The use of CuI/PhMgBr system[91] furnished a complex reaction mixture. On the other hand, by activation of the epoxide with either Amberlyst 15 or BF_3[92] the reaction with PhLi resulted in a mixture of products, in which the main one was diarylacetaldehyde **8**. Again, $PhBF_3K$ in presence of trifluoroacetic anhydride, which had been successfully used on phenyl glycidates,[93] afforded diarylacetaldehyde **8** as the only reaction product. Such aldehyde represents a typical product of the so-called "Meinwald rearrangement", which is usually promoted by inorganic and organometallic Lewis acids and is often the favored reaction in the case of diaryloxiranes[94] (Scheme 36).

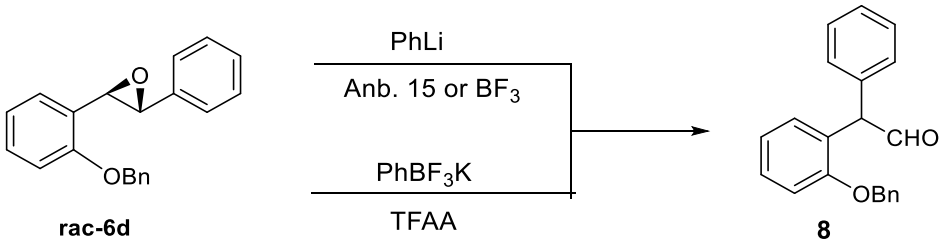

Scheme 36 Meinwald rearrangement of **rac-6d**

Using the $PhB(OH)_2/Et_2Zn$ system, which was recently described in regio- and diastereoselective C-arylation of sugar epoxides,[95] good results were obtained with different *o*-oxosubstituted epoxides (Table 8). The phenylzinc reagent was generated from phenyl boronic acid and diethylzinc *via* a facile B–Zn exchange process. The subsequent addition of epoxides

[88] M. Pineschi, *Eur. J. Org. Chem.* **2006**, 4979–4988.

[89] P. Crotti, M. Pineschi In *Aziridines and Epoxides in Organic Synthesis* (Ed.:Andrei K. Yudin), Wiley-VCH, Weinheim, **2006**, p. 271.

[90] a) N. Oguni, Y. Miyagi, K. Itoh, *Tetrahedron Lett.* **1998**, *39*, 9023–9026; b) A. Alexakis, E. Vrancken, P. Mangeney, *Synlett* **1998**, 1165–1167.

[91] Qiao, C.-J.; Wang, X.-K.; Zhong, W.; Li, S. *Molecules* **2015**, *20*, 22272–22285.

[92] Mizuno, M.; Kanai, M.; Iida, A.; Tomioka, K. *Tetrahedron: Asymmetry* **1996**, *7*, 2483–2484.

[93] Roscales, S.; Csàky, G. *Chem. Commun.* **2014**, *50*, 454–456.

[94] a) Robinson, M. W. C.; Pillinger, K. S.; Mabbett, I.; Timms, D. A.; Graham, E. *Tetrahedron* **2010**, *66*, 8377–8382; b) Ertürk, E.; Göllü, M.; Demir, A. S. *Tetrahedron* **2010**, *66*, 2373–2377 and references cited therein.

[95] Tatina, M. B.; Kusunuru, A. K.; Mukherjee D. *Org. Lett.* **2015**, *17*, 4624 − 4627.

***rac*-6a–d** resulted in the alcohols **10** as principal product in good yield and 15–20 % amount of the corresponding aryl-phenylacetaldehyde as byproduct.
The reaction was completely regioselective in all cases, being the nucleophilic attack only at the α-carbon with respect to the substituted phenyl ring. These results confirmed the our previous hypothesis of the general chemical behaviour of such epoxides, driven by the electronic characteristics of the substituents on the phenyl rings.

Table 8 Diethylzinc promoted one-pot phenylation of *trans* diaryloxiranes with phenylboronic acid

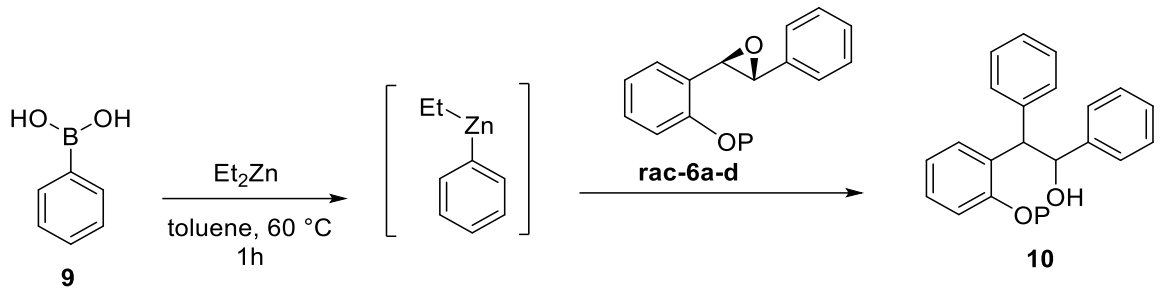

Exp.	P	$PhB(OH)_2$	Et_2Zn	Yield (%)	*syn/anti*[a]
1	Me (**rac-6a**)	3.0 eq.	10 eq.	62 (**10a**)	100/0
2	EOM (**rac-6b**)	3.0 eq.	10 eq.	65 (**10b**)	100/0
3	$(i\text{Pr})_3\text{Si}$ (**rac-6c**)	1.5 eq.	4.5 eq.	65 (**10c**)	70/30
4	Bn (**rac-6d**)	1.5 eq.	4.5 eq.	65 (**10d**)	100/0

[a] The notation *syn*/*anti* refers to the relative stereochemistry of the incoming phenyl nucleophile and the OH group.

Moreover, the stereochemical outcome confirmed the trend for a ring-opening reaction with retention of configuration at the electrophilic carbon, as the favorable pathway. Indeed, the *syn*/*anti* ratio ranged from 7/3, in the case of silyl ether derivative **10c**, to complete stereoselectivity toward *syn* compound, in all other cases.

The structure **10**, as a single regioisomer, was confirmed for all the products obtained, by careful $^{1}H/^{13}C$ NMR analysis: once carbons and hydrogens at the side chain have been assigned by direct $^{1}H/^{13}C$ correlation experiments, a long-range $^{1}H/^{13}C$ correlation between the C2 carbon and the proton at C7 was observed for all the products obtained. No correlation was observed between C2 and the proton at C8, which had been assigned to C*H*(OH) (Figure 20).

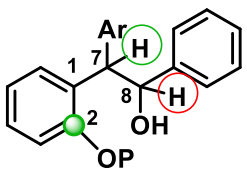

Figure 20 Diagnostic correlations between 1H and 13C NMR signals of structures **10**

With the desired regioisomers in hand different deprotection reactions were investigated, to afford the suitable hydroxyphenols for the last Mitsunobu type cyclodehydration reaction. The

reactions were run with all the products obtained, since they were also useful for the identification of the relative stereochemistry of compounds **10**.

The demethylation reaction of **10a** with BCl_3 or $BF_3{\cdot}Et_2O$ resulted in a complex reaction mixture.

The benzyloxy derivative **10d** appeared unexpectedly inert toward the most common deprotection procedures. After numerous unsuccessful attempts using H_2/Pd,C (10 %) in different reaction mediums, 10%Pd,C /$HCOONH_4$ [96] or $NiCl_4/NaBH_4$ [97] systems, the substrate was successfully reacted with H_2, 10% Pd/C 50%$Pd(OH)_2$/C system in THF/*i*-PrOH (3:1).[98] Unfortunately hydroxyphenol **11**, derived by a cleavage of both benzyl and phenyl groups on C2 at the side chain, was the only product observed (Scheme 37).

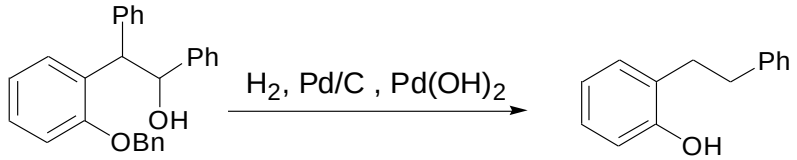

10d **11**

Scheme 37 Attempt of deprotection of **10d**

On the other hand, **10b** was treated with 10% TFA/THF mixture at 0°C and the corresponding hydroxyphenol **12a** was obtained in good yield (Scheme 38).

The trisopropylsilyl derivates ***syn*-10c** and ***anti*-10c** were transformed into the corresponding *syn* and *anti* hydroxyphenols **12a** and **12b** in good yield, using either *n*-Bu_4F in THF[99] or the CsF/18-Crown-6 system[100] (Scheme 38).

[96] Ranu, B. C.; Sakkar, A.; Sankar, K. G.; Ghosh, K. J. *J. Indian Chem. Soc.* **1998**, *75*, 690–694.
[97] Chouhan, M.; Kumar, K.; Sharma, R.; Grover, V.; Nair, V. A. *Tetrahedron Lett.* **2013**, *54*, 4540–4543.
[98] Li, Y.; Manickam, G.; Ghoshal, A.; Subramaniam, P. *Synt. Commun.* **2006**, *36*, 925–928.
[99] Corey, E. J.; Wu, L. I. *J. Am. Chem. Soc.* **1993**, *115*, 9327–9328.
[100] Farr, R. N.; Kwok, D.-I.; Daves Jr., G.-D. *J. Org. Chem.* **1992**, *57*, 2093–2100.

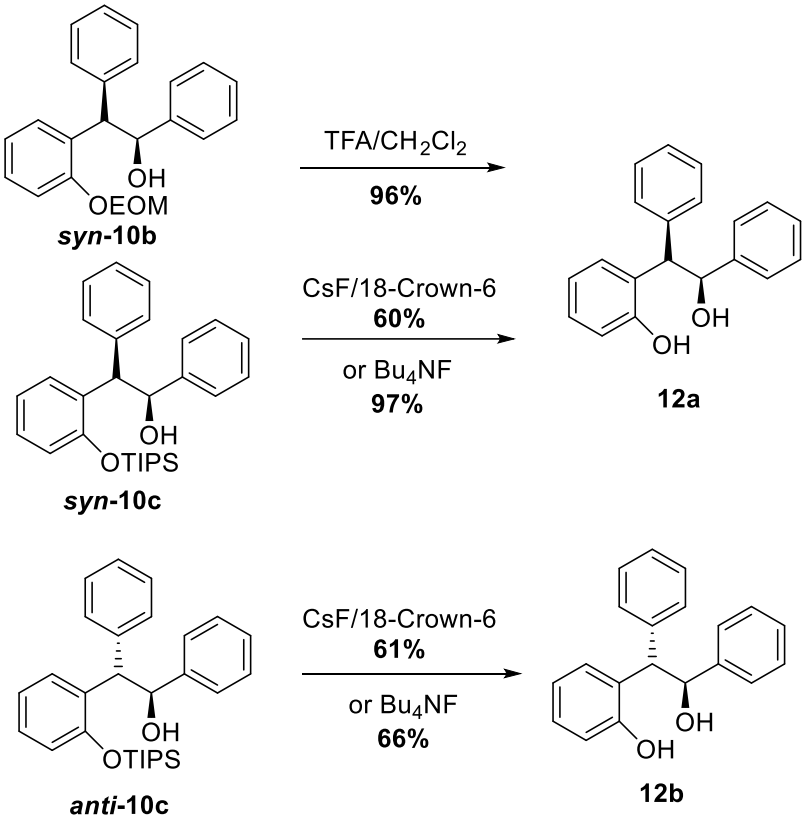

Scheme 38 Deprotection reactions of **10b** and **10c**

The hydroxyphenols **12a** and **12b** were finally submitted to Ph_3P/DEAD in THF[65] affording the corresponding *trans* and *cis* 2,3-diphenyl-2,3-dihydrobenzofurans **13a** and **13b**, respectively, in high yield (Scheme 39).

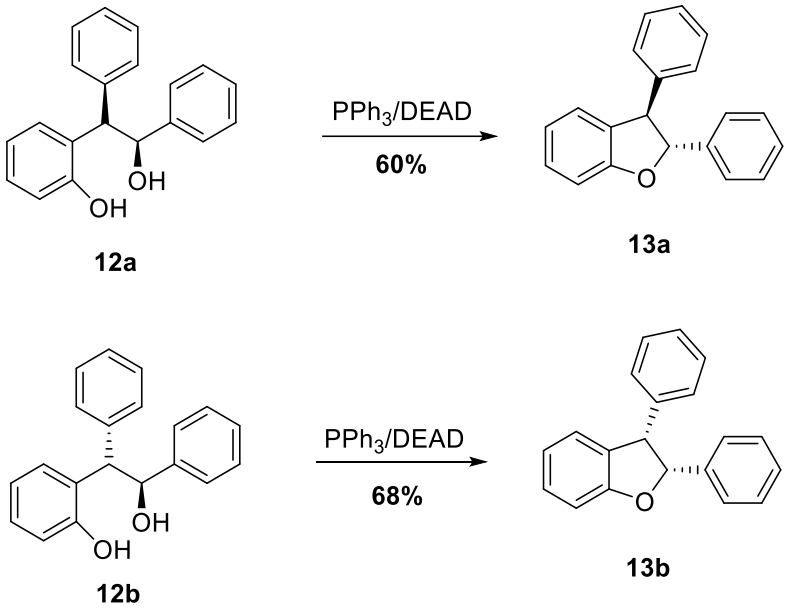

Scheme 39 Access to *trans* and *cis* 2,3-diphenyl-2,3-dihydrobenzofuran **13a** and **13b**

The NMR spectra of the products were compared with those described in literature[68] and confirmed the stereochemistry of both compounds. Thus, the relative stereochemistry of all the intermediates **10b**, **10c**, **12a** and **12b** was indirectly confirmed as well.
The synthetic pathway was successfully repeated for homochiral epoxides **(-)-6b** and **(-)-6c** affording the corresponding homochiral *trans* and *cis* 2,3-diphenyl-2,3-dihydrobenzofurans **(2*R*,3*R*)-13a** and **(2*R*,3*S*)-13b** (Scheme 40).
The comparison of HPLC analysis with chiral phase and optical activity of **13b** with those described in literature confirmed its absolute configuration as well as those of the other intermediates and final products **10a**, 1**0b**, and **13a**.
Moreover, the initial *ee* of the starting epoxides was retained in the final products and in the intermediates throughout the synthesis.

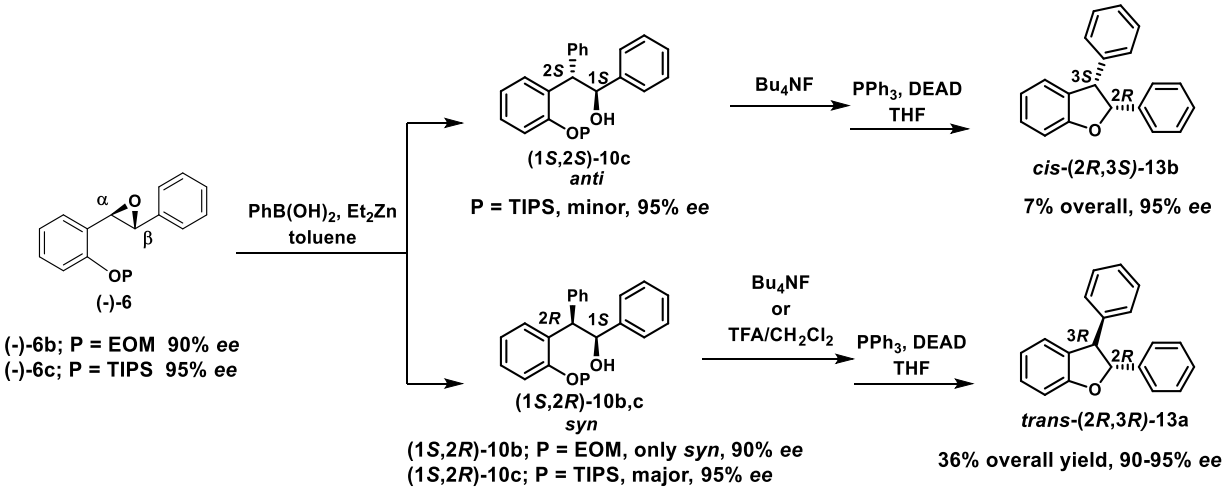

Scheme 40 Access to *cis*-(2*R*,3*S*) *trans* (2*R*,3*R*)-2,3-diphenyl-2,3-dihydrobenzofurans.

2.3 Goal of the work

The preliminary good results obtained in regio- and stereoselective phenylation of *ortho*-oxo substituted *trans* 2,3-diaryloxiranes by phenylzinc reagent, which allowed a high yielding access to *trans* 2,3-diphenyl-2,3-dihydrobenzofuran, even in enantioenriched form, motivated us towards the following goals:

- Investigate the scope in terms of regio- and stereoselectivity of the key nucleophilic ring opening reaction of *ortho*-oxo substituted 2,3-diaryloxiranes using various aryl boronic acid.

- Apply the same synthetic approach to preparation of polyfunctionalized 2,3-diaryl-2,3 dihydrobenzofurans of type **A** (Figure 21), with different degree of substitution, different isomerism and chirality, looking for insights on a possible effect of these parameters on anti-inflammatory activity.

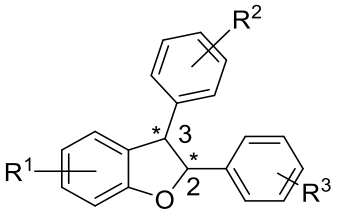

A

Figure 21 General structure of polyfunctionalized 2,3-diaryl-2,3-dihydrobenzofuran

2.4 Ring-opening reaction of epoxide with different arylboronic acids

The regio- and diastereoselective ring opening reaction that already showed a good results with different *ortho*-substituted diaryloxiranes using $PhB(OH)_2/Et_2Zn$, was chosen for a methodological study.

The opening reaction was tested using various aryl boronic acids as nucleophilic source and the *trans* 2-(2-Ethoxymethoxy-phenyl)-3-phenyl-oxirane **6b** as electrophilic acceptor, in different reaction conditions. The results are given in Table 9.

Table 9 Substrate scope of arylboronic acids for ring-opening reaction of *trans* 2-(2-ethoxymethoxyphenyl)-3-phenyloxirane **6b**.

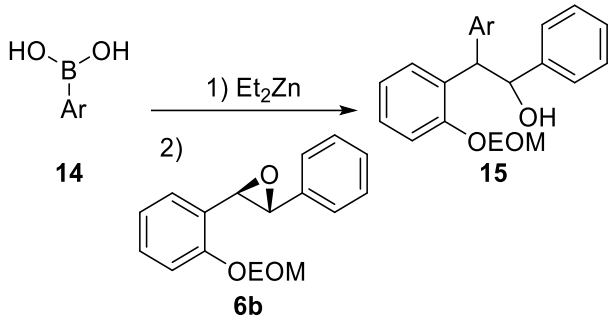

Exp.	Ar	$ArB(OH)_2$	Et_2Zn	T (°C)	Time	Yield %	*syn/ anti* [a]
1	3,5-di-OMePh (**14a**)	1.1 eq.	3 eq.	60 to rt.	0.5 h	-	-
2	3-CF_3Ph (**14b**)	1.1 eq.	3 eq.	60 to rt.	1.30 h	10	*syn*
3	2,4-di-OMePh (**14c**)	1.1 eq.	3 eq.	60 to rt.	3 h	-	-
4	3-FPh (**14d**)	1.1 eq.	3 eq.	60° to rt.	1.30 h	15	*syn*
5	3-FPh (**14d**)	2.2 eq.	6 eq.	60	1.30 h	20	*syn*
6	3-CF_3Ph (**14b**)	2.2 eq.	6 eq.	60	18 h	20	*syn*
7	4-BrPh (**14e**)	3eq.	10 eq.	60	2 h	65[b]	*syn*
8	3-Benzothienyl (**14f**)	3eq.	10 eq.	60	18 h	60	*syn*
9	3-CF_3Ph (**14b**)	3eq.	10 eq.	60	2 h	55[b]	*syn*
10	3-FPh (**14d**)	3eq.	10 eq.	60	0.5 h	50[b]	80/ 20[d]

11	4-OMePh (**14g**)	3eq.	10 eq.	60	2 h	60	mix. [c]
12	3-OMe (**14h**)	3eq.	10 eq.	60	2 h	62	35/31 (34) [d,e]

[a] The notation *syn*/*anti* refers to the relative stereochemistry of the incoming aryl nucleophile and the OH group. [b] 15–20 % amount of the corresponding aryl-phenylacetaldehyde was detected. [c] Equimolar mixture of the four possible products was obtained. [d] Diasteroisomeric ratio determined from ^{1}H NMR of the purified mixture. [e] Equimolar quantity of the other regioisomer (probably *syn*) was detected in the NMR spectra of the mixture

Initially the opening reactions were performed by generating the arylethyl zinc at 60 °C under argon, then adding the epoxide and carrying out the reaction at room temperature. Under these conditions, the desired product was obtained only in the case of 3-CF_3PhB$(OH)_2$ (**14b**) and 3-FPhB$(OH)_2$ (**14d**), although in very low yield (exp 1-4), while using 3,5-di-OMePhB$(OH)_2$ (**14a**) and 2,4-di-OMePhB$(OH)_2$ (**14c**) only degradation products were obtained.

Therefore, we decided to perform the opening reaction at 60 °C under argon, after adding the epoxide at room temperature. Furthermore, the overall reagents/epoxide molar ratio was increased, from Ar$B(OH)_2$/Et_2Zn/epoxide = 1.1/3.0/1.0 to 2.2/6.0/1.0 (exp. 5-6). These modifications led to an improvement in yield in the case of 3-CF_3PhB$(OH)_2$ (**14b**) and 3-FPhB$(OH)_2$ (**14d**) even if remaining below synthetically useful values.

A decisive improvement was obtained by using a high excess of reagents, bringing the overall molar ratio Ar$B(OH)_2$/Et_2Zn/epoxide = 3.0/10.0/1.0 (exp. 7-13). As it can be seen in the Table, the reaction appeared almost general affording the corresponding *syn* aryl alcohols **15** exclusively, in acceptable yield in the case of 4-BrPhB$(OH)_2$ (**14e**), 3-CF_3PhB$(OH)_2$ (**14b**) and benzothienyl-B$(OH)_2$ (exp 7-8-9). In the case of 3-FPhB$(OH)_2$ (**14d**) the corresponding product **15d** was obtained in a promising 80:20 *syn*/*anti* mixture (entry 10). Only in the case of 4-methoxyphenylboronic acid **14g** the regio- and stereoselectivity of the reaction dropped dramatically, affording an equimolar mixture of the four possible ring opening products. Better results were achieved using 3-MeOPhB$(OH)_2$ **14f**, the reaction affording almost equimolar mixture of *syn*/*anti* **15e** and the other regioisomer (probably *syn*). This last result appeared quite unexpected suggesting, for the first time, an effect of the nucleophilic character of the incoming reagent on the selectivity of the reaction.

Nevertheless, the procedure appeared almost general in terms of regio- and stereoselectivity and therefore we decided to investigate the reactivity of polyfunctionalised epoxides in order to prepare polyfunctionalised dihydrobenzofurans.

2.4.1 Characterization of the aryl alcohols

The structure **15**, as a single regioisomer, was confirmed for all the products obtained, by careful ^{1}H/^{13}C two-dimensional (2D) NMR analysis: heteronuclear single quantum correlation (HSQC) and heteronuclear multiple bond correlation (HMBC).

Usually HSQC is used to correlate the chemical shift of protons (displayed on the F1 axis) to the ^{13}C chemical shift (on the "indirect" F2 axis) of their directly attached carbons via the $^{1}J_{CH}$ coupling constants (typically 100-300 Hertz). Instead, the HMBC experiment reveals correlations between carbons and protons that are separated by two, three, and, sometimes in conjugated systems, four bonds via $^{2}J_{CH}$ and $^{3}J_{CH}$ coupling constants (typically 2-25 Hertz).
For all the structures **15** once carbons and hydrogens at the side chain have been assigned with HSQC and with HMBC experiments the correlation between the C2 carbon and the proton at C7 was observed. No correlation was observed between C2 and the proton at C8, which had been assigned to C*H*(OH) (Figure 22).

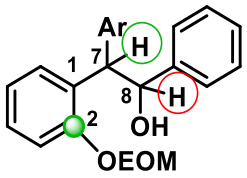

15

Figure 22 Diagnostic correlations between ^{1}H and ^{13}C NMR signals of structures **15**

By way of example, HSQC (Figure 23) and the HMBC (Figure 24) analysis performed for the characterization of aryl alcohol **15b** are reported.

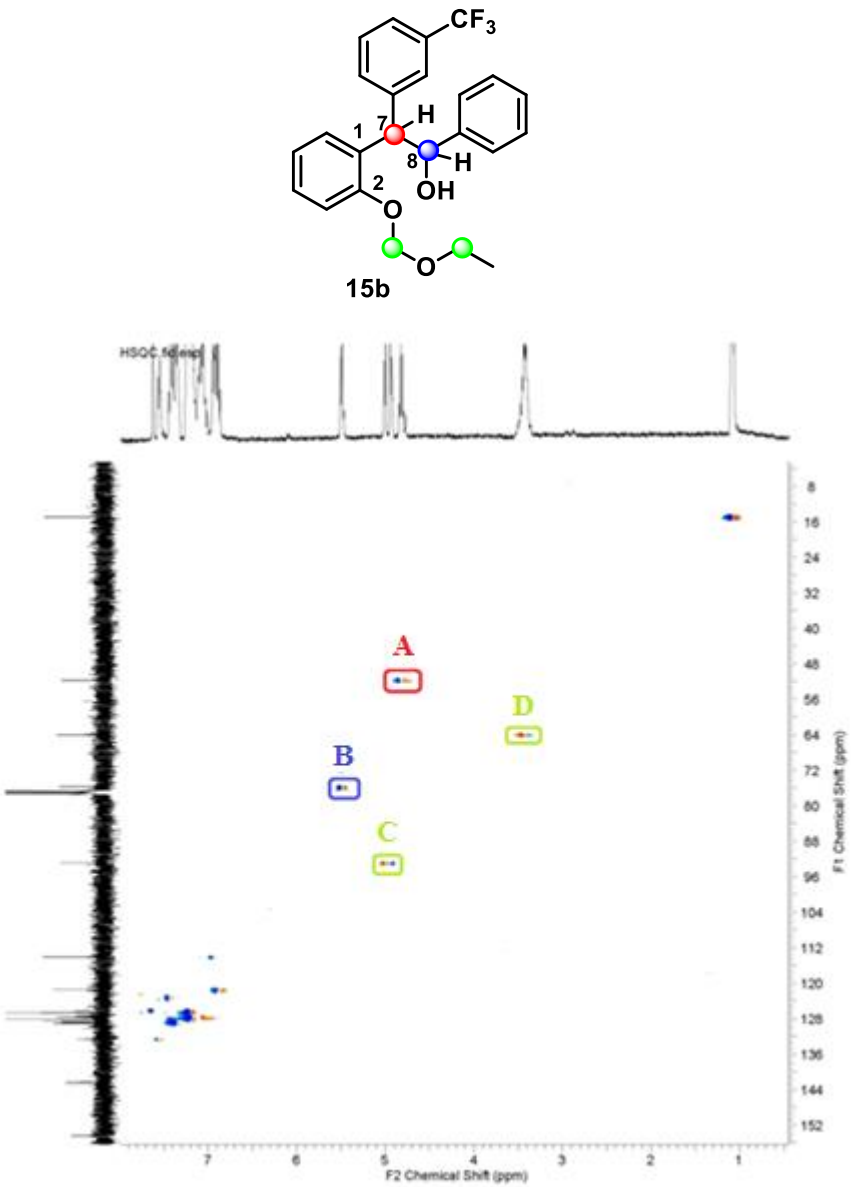

Figure 23 HSQC of **15b**

The HSQC allowed to assigned the carbons and the hydrogens on the chain. From the graph (Figure 23) the following correlations can be seen:

- **A**: proton at 4.81 ppm with the carbon at 51.74 ppm (C_7-H).
- **B**: proton at 5.49 ppm with the carbon at 75.76 ppm (C_8-H).
- **C**: the AB system of the CH_2 at 4.93-5.00 ppm with the carbon at 92.85 ppm.
- **D**: proton at 3.42 ppm with the carbon at 64.04 ppm.

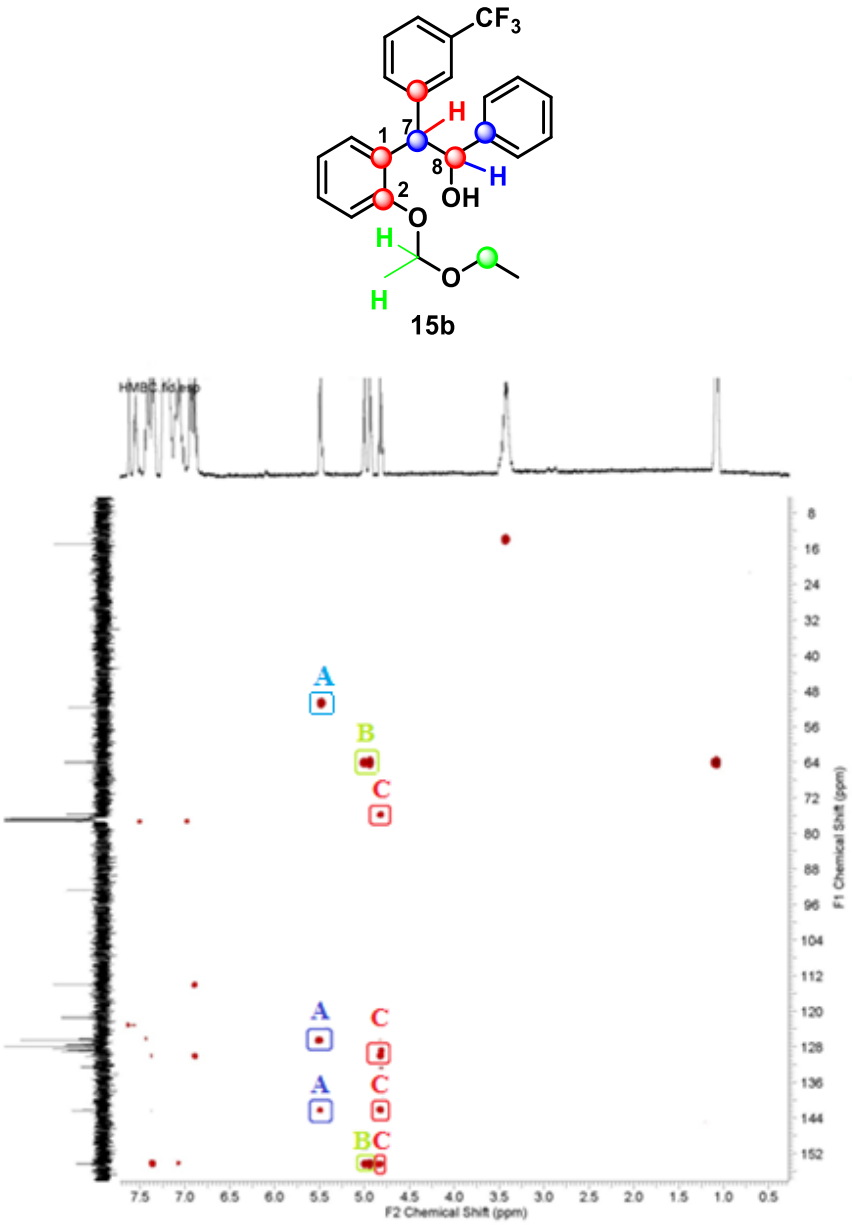

Figure 24 HMBC of **15b**

From the graph of HMBC (Figure 24) the following correlations can be seen:

- **A:** proton at 5.49 ppm (C_8-H) with the quaternary carbons at 142.41 ppm and 130.18 ppm.

- **B:** protons of O-CH_2-O group at 4.93-5.00 ppm with the quaternary carbon at 154.39 ppm and the carbon at 64.04 ppm.

- **C:** proton at 4.81 ppm (C_7-H) with the carbon at 75.76 ppm (C-OH) and the quaternary carbons at 154.39 ppm, 142.41 ppm and 130.18 ppm.

The correlation between the quaternary carbon at 154.39 ppm (C_2) with the proton at 4.81 ppm (C_8) confirms that it was obtained the regioisomer which derived from the opening on the α-carbon with respect to the substituted phenyl ring.

The stereoselectivity of the aryl alcohols **15** was identified by comparing ^{1}H-NMR data with structural analogues that we had previously characterized, in particular through the coupling constants $^{3}J_{HH}$ between the protons on C1 and C2 carbons. It was observed that the ***syn*-10** isomer had a constant around 8.0 Herz, while the ***anti*-10** isomer had around 9.0 Hertz (Figure 25).

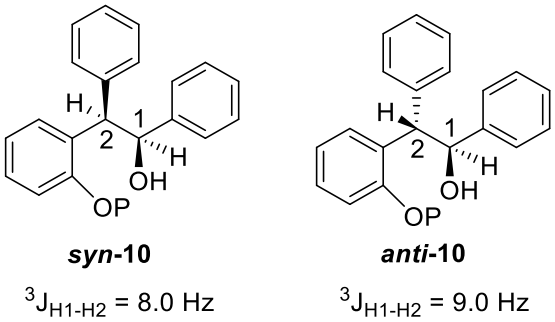

Figure 25 $^{3}J_{H1-H2}$ constants in *syn* and *trans* isomers

2.4.2 Plausible mechanism for the formation of aryl alcohols

The mechanism for the formation of the aryl alcohols may be explained on the basis of that proposed for the formation of α-aryl-glycoside, reported by Mukherjee and co-workers.[95]
They suggested *in situ* formation of the phenylethyl zinc **II** by a facile B-Zn exchange process between phenylboronic acid **I** and diethylzinc. This reagent, thanks to its Lewis acid character, activates the epoxide ring **III**, and thereby assists oxocarbonium ion **V** formation. The intramolecular attack of aryl substituent on the anomeric carbon occurs *syn* with respect to the oxygen deriving from the epoxide, leading the α-aryl-glycoside **VII** formation with high diastereoselectivity (Scheme 41).

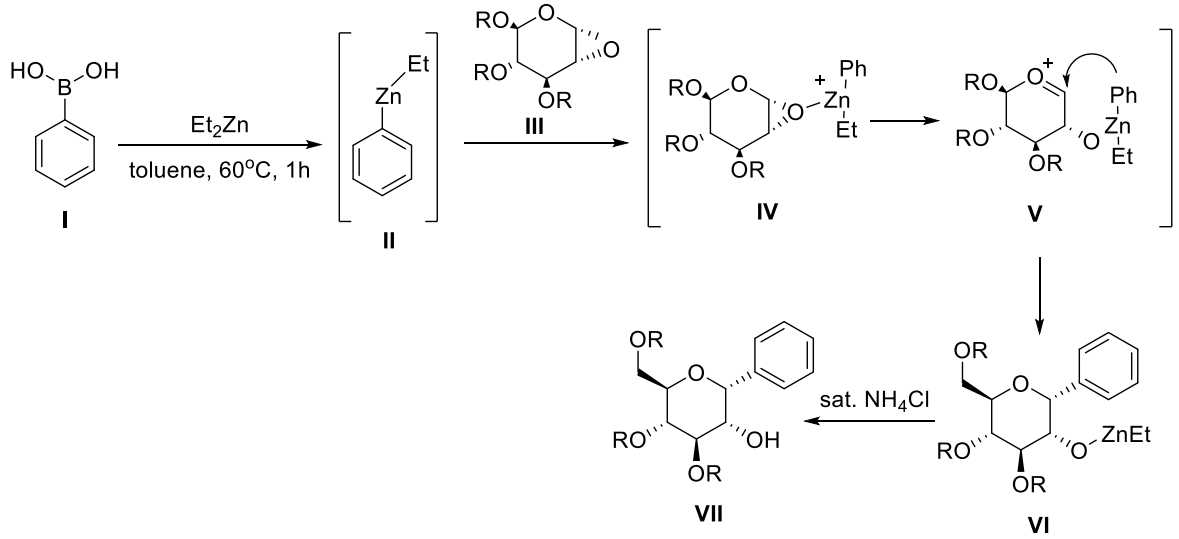

Scheme 41 Mechanism for the formation of α-aryl glycoside

In our case, we assume that the Lewis acidic character of *in situ* generated arylethyl zinc activates the epoxide ring **I** and subsequently assists the formation of the cationic species **III** stabilized by the mesomeric effect of the oxygenated substituent in *ortho*-position. The intramolecular delivery of the aryl substituent on the same side of O-Zn substituent leads to the *syn*-arylalcohols **15** with retention of configuration (Scheme 42).

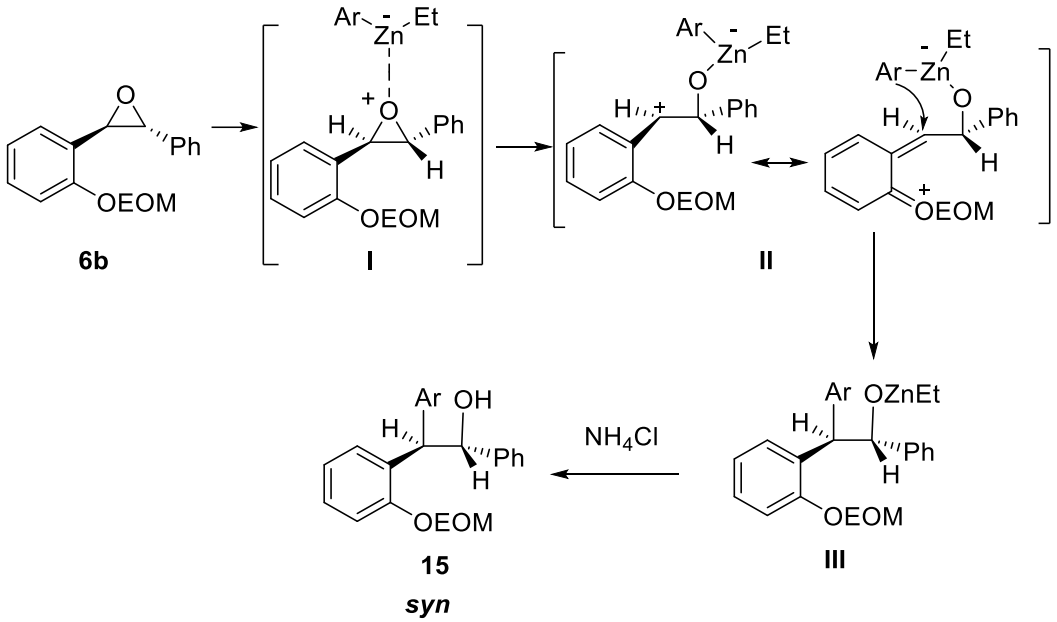

Scheme 42 Plausible mechanism for the formation of *syn*-arylalcohols

2.5 Stereoselective acces to polyfuncionalized 2,3-dihydrobenzofurans

The preliminary good results obtained for the synthesis of 2,3-diphenyl-2,3-dihyrobenzofuran[71] prompted us to exploit the applicability of the same methodology to the preparation of polyfunctionalized 2,3-diarylbenzofurans of type **A**, whose retrosynthetic approach is described in Scheme 43.

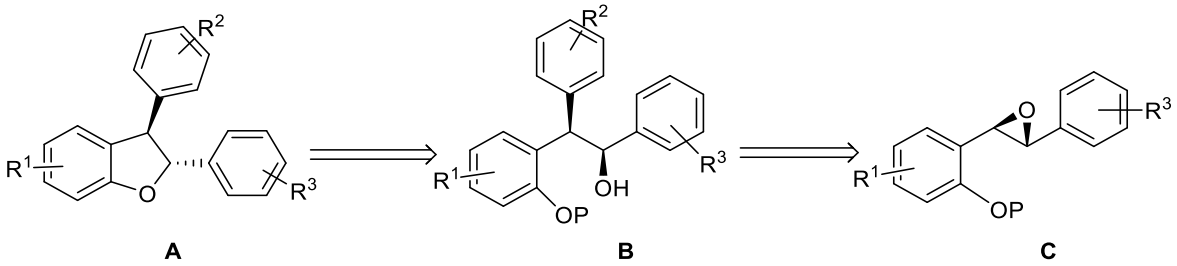

Scheme 43 Retrosynthetic approach to polyfunctionalized 2,3-diaryl-2,3-dihydrobenzofurans

In this approach the key steps are again the stereoselective access to *trans ortho*-oxo substituted 2,3-diaryloxiranes **C** and the regio- and stereoselective *syn* arylation to obtain **B**.

While 2,3-diaryloxiranes can be easily obtained by previously described Corey-Chaykovsky reaction between the suitable *o*-substituted aldehyde and a benzylidene sulfur ylide, the oxiranyl ring opening reaction needs for further confirmations, in particular with polyfunctionalised epoxides.

Initially we was focused on the preparation of methoxy-bromo derivatives of *trans*-2,3-diaryl-2,3-dihydrobenzofuran and then we extended the methodology on the preparation of polyfunctionalized intermediates bearing 2,3-diaryl-2,3-dihydrobenzofuran structure towards the synthesis of Gnetin C and ε-Viniferin.

2.5.1 Synthesis of methoxy-bromo derivatives of trans-2,3-diaryl-2,3-dihydrobenzofuran

The synthesis of methoxy-bromo derivatives of *trans*-2,3-diaryl-2,3-dihydrobenzofuran were made starting from the difunctionalized epoxides **16** and **17** (Figure 26).[101]

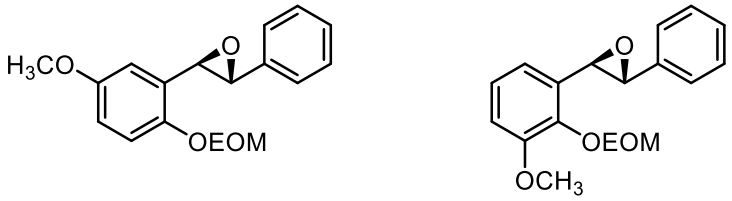

16 **17**

Figure 26 Structure of 2-(2-Ethoxymethoxy-5-methoxy-phenyl)-3-phenyl-oxirane **16** and 2-(2-Ethoxymethoxy-3-methoxy-phenyl)-3-phenyl-oxirane **17**

These epoxides were prepared taking advantage of the Corey-Chaykovsky reaction between the suitable *ortho*-substituted benzaldehyde and a benzylidene sulfur ylide.

The ethoxymethoxy group (EOM = $CH_2OCH_2CH_3$) was chosen as the protecting group because it had showed to be stable in the different reaction conditions, it did not interfere in subsequent reactions and was easily removable in suitable conditions, releasing the phenolic OH (hydroxy) group.

The commercially available 2-hydroxy-3-methoxybenzaldehyde **18** and 2-hydroxy-5-methoxybenzaldehyde **19** have been protected to lead to the corresponding 2-(ethoxymethoxy)-3-methoxybenaldehyde **20** and 2-(ethoxymethoxy)-5-methoxybenaldehyde **21** (Scheme 44).

[101] Laurita, T.; Pappalardo, I.; Chiummiento, L.; D'Orsi, R.; Santarsiero, A:; Marsico, M.; Infantino, V.; Todisco, S.; Lupattelli, P. *Bioorg. Med. Chem. Lett.*; **2021**, *49*, 128264.

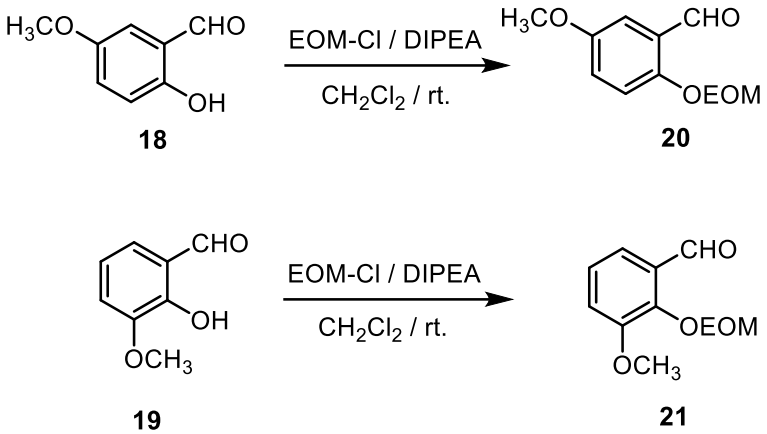

Scheme 44 Protection of aldehydes **18** and **19**

Racemic 2-(2-Ethoxymethoxy-5-methoxy-phenyl)-3-phenyl-oxirane **16** and 2-(2-Ethoxymethoxy-3-methoxy-phenyl)-3-phenyl-oxirane **17** were prepared in good yield and high stereoselectivity from the parent aldehydes **20** and **21** using *S*-benzyltetrahydrothiophenium bromide **4** as ylide source and K_2CO_3 in acetonitrile (Scheme 45).

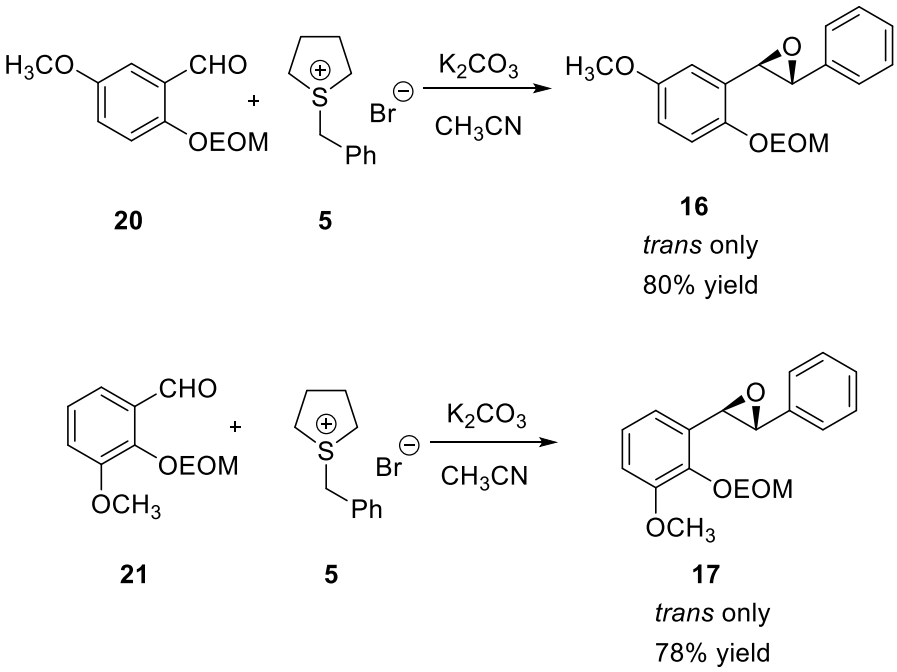

Scheme 45 Synthesis of epoxide **16** and **17**

Thus methoxy substituted *trans* diaryloxiranes **16** and **17**, were tested in opening reactions using different arylboronic acids as nucleophile precursors. The results are given in Table 10.

Table 10 Ring-opening reaction of *trans* methoxy substituted 2-(2-ethoxymethoxyphenyl)-3-phenyloxiranes.

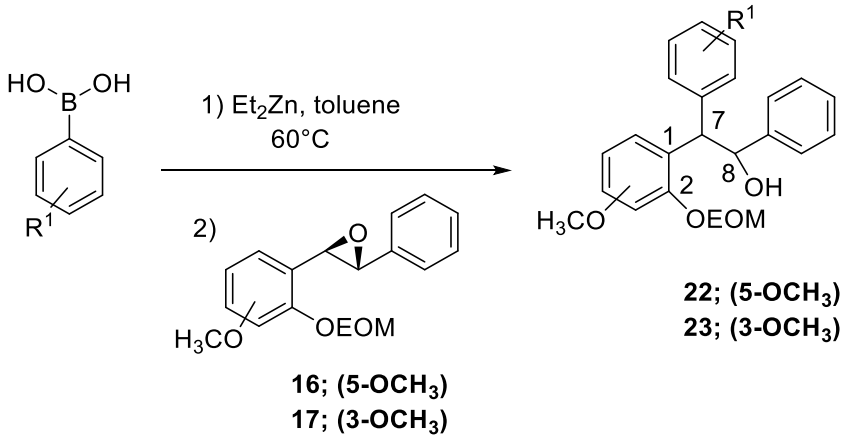

Exp.	Epoxide	$ArB(OH)_2$	Time (h)	Prod.	Yield (%)	*syn/anti*
1	**16;** (5-OCH_3)	$PhB(OH)_2$	3	**22a**	61	only *syn*
2	**16;** (5-OCH_3)	4-$BrPhB(OH)_2$	2	**22b**	65	5:1
3	**16;** (5-OCH_3)	3,5-di-$BrPhB(OH)_2$	3	**22c**	50	only *syn*
4	**17;** (3-OCH_3)	$PhB(OH)_2$	1	**23a**	74	only *syn*
5	**17;** (3-OCH_3)	4-$BrPhB(OH)_2$	1	**23b**	65	3:1

The opening reactions were performed by generating of arylethyl zinc at 60 °C under argon, then adding the epoxide at room temperature and carrying out the reaction at 60°C. The overall reagents/epoxide molar ratio was $ArB(OH)_2/Et_2Zn$/epoxide = 1.1/3.0/1.0. The reaction appeared completely regioselective for both epoxides, using either unsubstituted or brominated aryl boronic acids as nucleophile precursors, giving rise to products **22** and **23** respectively in moderate to good yield. Stereoselectivity was also complete toward *syn* products, with the exception of **22b** and **23b**, which were obtained as 5:1 and 3:1 *syn*/*anti* mixture, respectively.
As usual, characterization of new compounds **22** and **23** as single regioisomers was confirmed by direct (HSQC) and long-range (HMBC) correlation $^{1}H/^{13}C$ NMR experiments. The long-range correlation between the *C*2 carbon and the proton at C7 was diagnostic and no correlation was observed between *C*2 and the proton at C8.

With the desired regioisomers in hand we tried to deprotect phenolic OH group by the already used TFA/CH_2Cl_2 system. Unfortunately the reaction was generally poor in terms of yield and selectivity, so we were prompted to investigate milder procedures. After a screening of different acid catalysts, we took advantage from the use of Amberlyst 15, an acidic ion exchange resin. The reaction was made with Amberlyst 15/substrate = 400 mg/mmol ratio in CH_3OH at 60 °C, which gave good results in all cases (Table 11).

Table 11 Deprotection reactions of **22** and **23** using Amberlyst 15

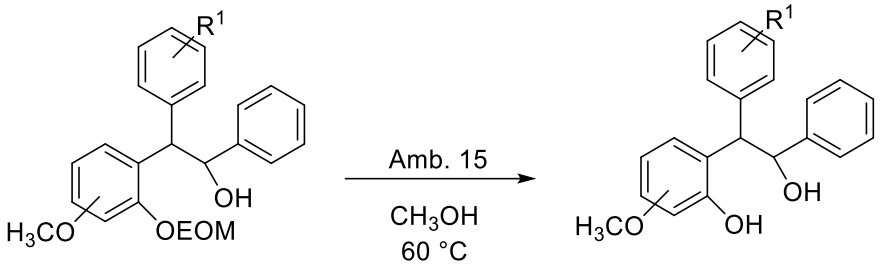

22; (5-OCH_3)
23; (3-OCH_3)

24; (5-OCH_3)
25; (3-OCH_3)

Exp.	Substrate	R^1	Time (h)	Prod.	Yield (%)
1	***syn*-22a**	H	2	***syn*-24a**	100
2	***syn*-22b**	4-Br	7	***syn*-24b**	100
3	***anti*-22b**	4-Br	6	***anti*-24b**	100
4	***syn*-22c**	3,5-di-Br	22	***syn*-24c**	60
5	***syn*-23a**	H	2	***syn*-25a**	75
6	***syn*- *anti*-23b** (3:1)	4-Br	2	***syn*- *anti*-25b** (3:1)	65

The last Mitsunobu type cyclodehydration was performed submitting hydroxyphenols **24** and **25** to PPh_3/DEAD system in THF and afforded the corresponding 2,3-diaryl-2,3-dihydrobenzofurans stereospecifically in good yield (Table 12).

Table 12 Access to polyfunctionalized 2,3-dihydrobenzofurans

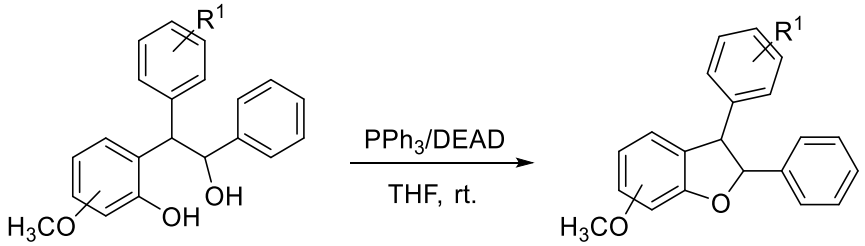

24; (5-OCH_3)
25; (3-OCH_3)

26; (5-OCH_3)
27; (3-OCH_3)

Exp.	Substrate	R^1	Time (h)	Prod.	Yield (%)
1	***syn*-24a**	H	2	***trans* 26a**	100
2	***syn*-24b**	4-Br	7	***trans* 26b**	100
3	***anti*-24b**	4-Br	6	***cis* 26b**	100
4	***syn*-24c**	3,5-di-Br	22	***trans* 26c**	60
5	***syn*-25a**	H	2	***trans* 27a**	75
6	***syn*- *anti*-25b** (3:1)	4-Br	2	***trans*/cis 27b** (3:1)	65

The *trans* 5-Methoxy-2,3-diphenyl-2,3-dihydrobenzofuran **26a** was prepared also in enantioenriched form starting from (2*R*,3*R*)-2-(2-Ethoxymethoxy-5-methoxy-phenyl)-3-phenyl-oxirane **16a**. This epoxide was prepared in good yield and *ee* by first *in situ* deprotonation of benzylsulfonium salt **7** of chiral isothiocineol **(-)-3** with KOH and subsequent reaction of the ylide with 2-ethoxymethoxy-5-methoxy-benzaldehyde **20** (Scheme 46).

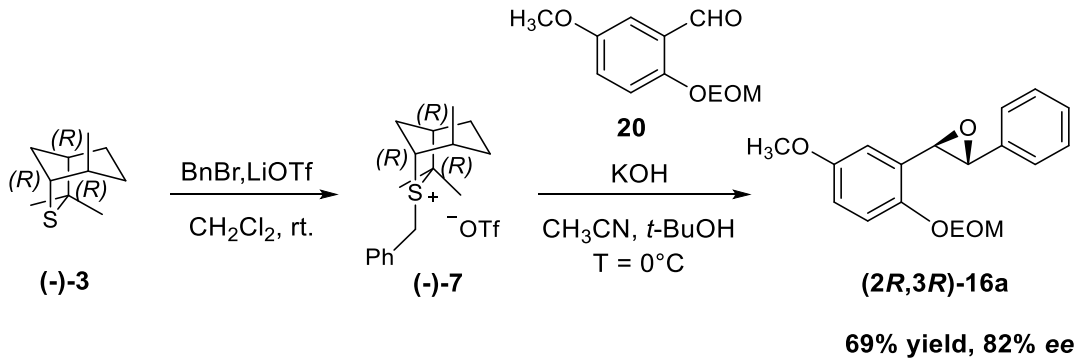

Scheme 46 Preparation of enantioenriched epoxide **(2*R*,3*R*)-16**

The synthetic pathway was successfully repeated, using $PhB(OH)_2$ as nucleophile precursor, affording the final *trans* (2*R*,3*R*)-2,3-diphenyl-2,3-dihydrobenzofuran **26a** in excellent overall yield and in enantioenriched form, although with slightly lower enantiomeric excess if compared with that of the starting epoxide (Scheme 47).

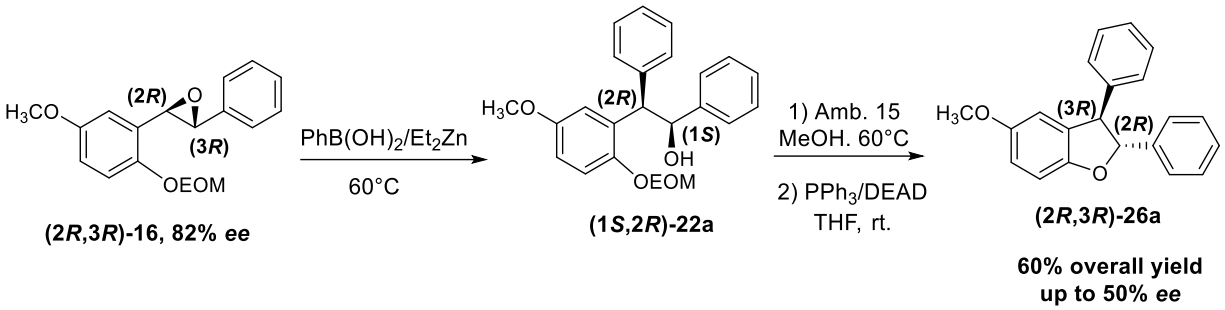

Scheme 47 Acces of enantioenriched 2,3-diphenyl-2,3-dihydrobenzofuran **(2*R*,3*R*)-26a**

This somewhat puzzling result can be explained by the occurring of Meinwald rearrangement of the starting epoxide which competes, to some extent, with the established oxiranyl opening reaction. By this competitive route, diarylacetaldehyde **27** can be formed, with a loss of a chiral centre and possible epimerization of the other. Subsequently it can react with PhZnEt affording ***syn*-22a**, with, in principle, lower *ee* (Scheme 48).

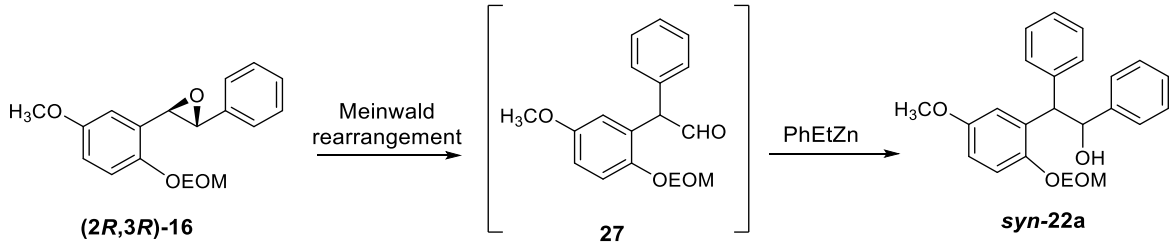

Scheme 48 Competitive route to ***syn*-22a**

2.5.2 Synthesis of polyfunctionalized intermediates bearing 2,3-diaryl-2,3-dihydrobenzofuran structure towards the synthesis of Gnetin C and ε-Viniferin.

The synthesis of polyfunctionalized intermediates bearing 2,3-diaryl-2,3-dihydrobenzofuran structure towards the synthesis of Gnetin C and ε-Viniferin was performed starting from the difunctionalized epoxides **28** and **29** respectively, which have the Br and OCH_3 groups on the appropriate position to access the intermediates of the two natural products (Figure 27).

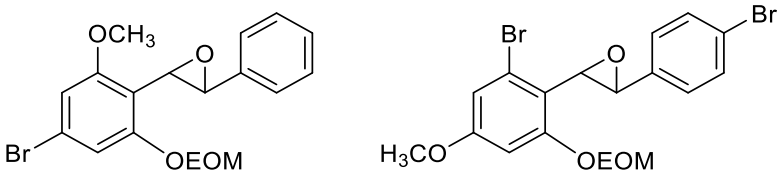

28 **29**

Figure 27 Structure of 2-(4-bromo-2-(ethoxymethoxy)-6-methoxyphenyl)-3-phenyloxirane **28** and 2-(2-bromo-6-(ethoxymethoxy)-4-methoxyphenyl)-3-(4-bromophenyl)-oxirane **29**

As usual, these epoxides were prepared taking advantage of the Corey-Chaykovsky reaction between the suitable *ortho*-ethoxymethoxy substituted benzaldehyde and a benzylidene sulfur ylide.

For the preparation of the starting aldheydes a formylation reaction[102] on commercially available 1-bromo-3,5-dimethoxybenzene **30** was performed, with dichloromethyl-methyl(Cl_2CHOCH_3)/Titanium tetrachloride ($TiCl_4$) = 1.2/2.4 ratio in CH_2Cl_2 anhydrous at room temperature.The reaction resulted in a 1:4 mixture of 4-bromo-2,6-dimethoxybenzaldehyde **31a** and 2-bromo-4,6-dimethoxybenzaldehyde **31b**. After chromatographic purification on silica gel **31a** (20% yield) and **31b (**67% yield) were obtained as pure products (Scheme 49).

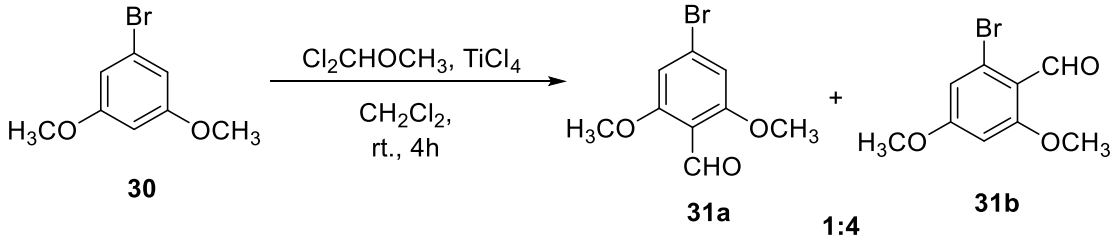

30 **31a** **1:4** **31b**

Scheme 49 Formylation reaction of **30**

Since 4-bromo-2,6-dimethoxybenzaldehyde **31a** was only obtained as by product, with very low yield, we were prompted to investigate an alternative procedure. From the cheap commercially available 4-bromo-2,6-difluorobenzaldehyde **32**, methoxydefluorination reactions by potassium hydroxide (KOH) in methanol (MeOH) were performed.[103] The first methoxydefluorination gave4-bromo-2-fluoro-6-methoxybenzaldehyde **33** in 38% yield, which was again methoxylated under the same conditions leading to the formation of 4-bromo-2,6-

[102] Jones, G.; Stanforth, S. P. *Org. React.*, **1997**, *49*, 1.

[103] Scott, J. S. *et al. J. Med. Chem.* **2019**, *62*, 1593-1608

dimethoxybenzalide **31a** in quantitative yield. Thus, we obtained the aldehyde **31a** in two steps, starting from **32** in 38% overall yield (Scheme 50), showing the procedure more advantageous with respect to that starting from 1-bromo-3,5-dimethoxybenzene **30**.

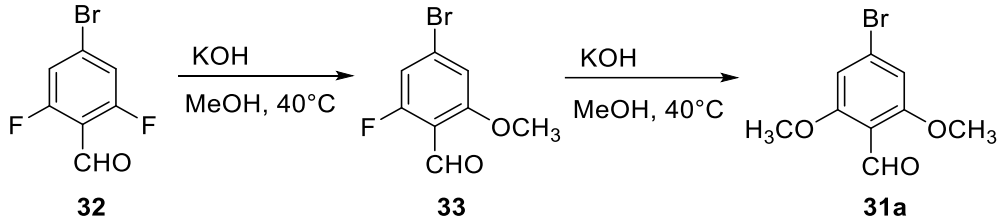

32 **33** **31a**

Scheme 50 Methoxidefluorination reaction of **32**

Subsequently, monodemethylation[104] reaction of aldehydes **31a** and **31b** with aluminum chloride ($AlCl_3$) and sodium iodide (NaI) in CH_2Cl_2/CH_3CN 1:1 afforded the corresponding 4-bromo-6-methoxysalicylaldehyde **34a** 2-bromo-4-methoxysalicylaldehyde **34b** in good yield (Scheme 51). Then these aldehydes were protected as ethoxymethyl ether by reaction with EOM-Cl and *N*,*N*-diisopropylethyleamine (DIPEA) in anhydrous CH_2Cl_2 at room temperature, affording the final 2-bromo-6-(ethoxymethoxy)-4-methoxybenzaldehyde **35a** and 4-bromo-2-(ethoxymethoxy)-6-methoxybenzaldehyde **35b** in excellent yield (Scheme 51).

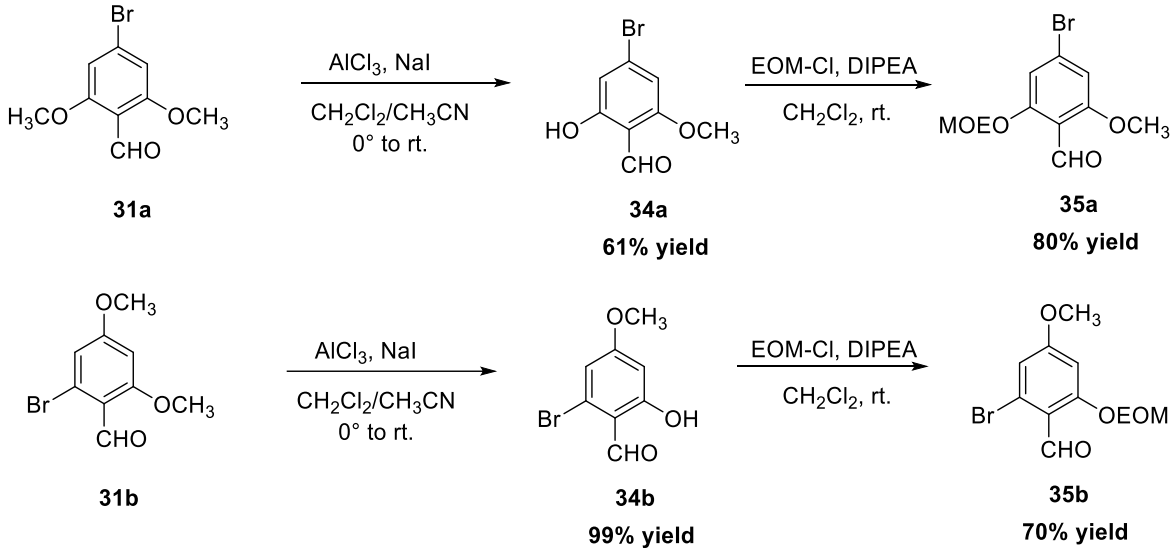

31a **34a** **61% yield** **35a** **80% yield**

31b **34b** **99% yield** **35b** **70% yield**

Scheme 51 Methoxydemethylation and protection reactions

As usual, the racemic *trans* 2-(2-bromo-6-(ethoxymethoxy)-4-methoxyphenyl)-3-(4-bromophenyl)-oxirane ***rac*-28** was prepared in good yield and high stereoselectivity from the parent aldehyde **35a** using *S*-benzyltetrahydrothiophenium bromide **5** as ylide source and K_2CO_3 in acetonitrile. The enantioenriched **(2*S*,3*S*)-28** was prepared in good yield and *ee* by first *in situ* deprotonation of benzylsulfonium salt **(+)-7** of chiral isothiocineol **(+)-3** with KOH and subsequent reaction of the ylide with the same aldehyde **35a** (Scheme 52).

[104] Black, J.; Scutt, J. N.; Whalley, L.; Willets, N. J. *PCT Int. Appl.*, **2014**.

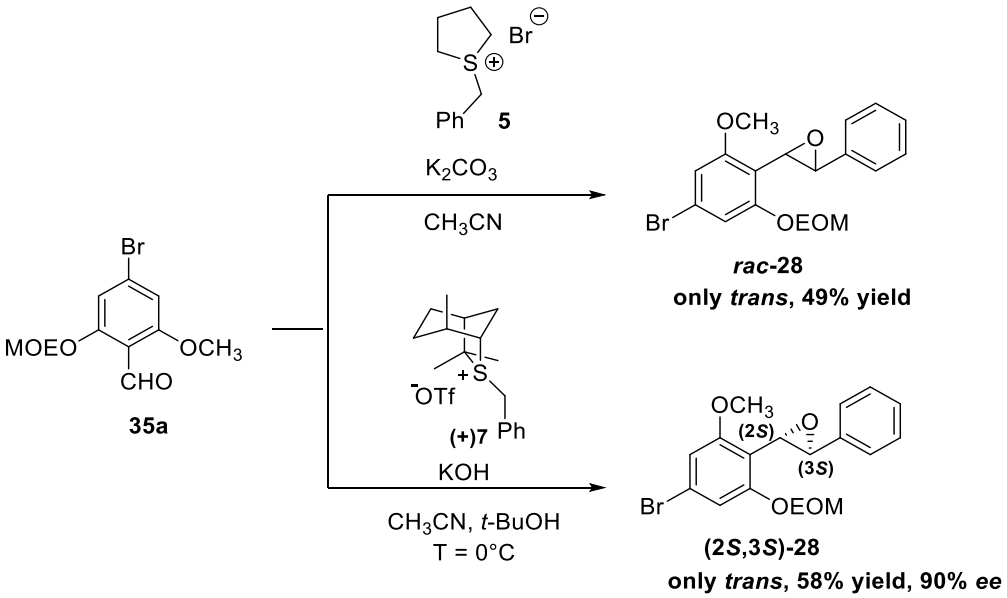

Scheme 52 Preparation of epoxides ***rac*-36** and **(2*S*,3*S*)-36**

Also the racemic 2-(4-bromo-2-(ethoxymethoxy)-6-methoxyphenyl)-3-phenyloxirane ***rac*-29** was prepared by classical procedure in good yield and high stereoselectivity from the parent aldehyde **35b** using 1-(4-Bromobenzyl)-tetrahydrothiophenium bromide **38** as ylide source and K_2CO_3 in acetonitrile (Scheme 53).

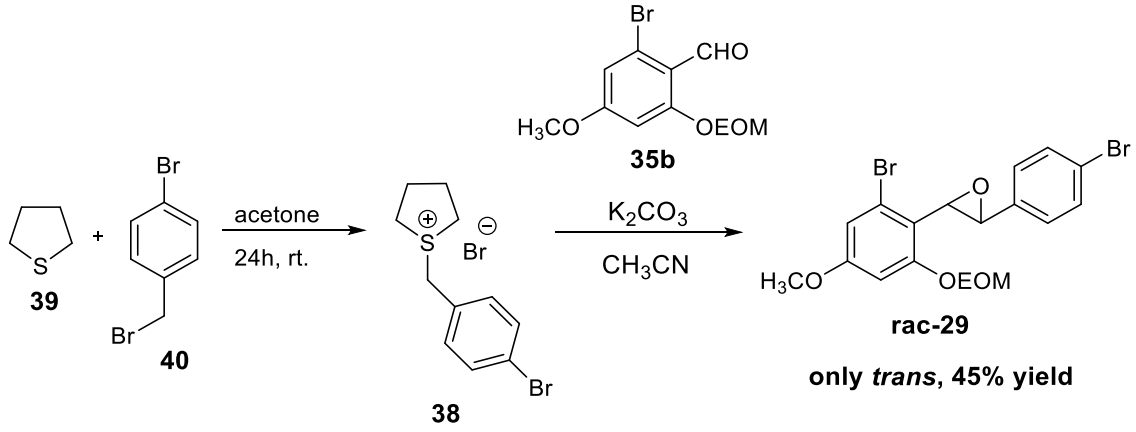

Scheme 53 Preparation of epoxide ***rac*-37**

On the other hand, the classical procedure for the preparation of enantioenriched **(2*S*,3*S*)-29** from the parent aldehyde **35b** with the arylsulfonium salt **(+)-41** of chiral isothiocineol **(+)-3** and KOH did not work, so we were prompted to make some modifications. We decided to use a stronger base, the 1,5,7-Triazabiciclo [4.4.0] dec-1-ene (TBD) for *in situ* formation of ylide in CH_2Cl_2 at -30 °C. The epoxidation was run at -30°C as well and after only 1.5h the desired product was obtained with good yield and high *ee* (Table 13).

Table 13 Epoxidation reactions of **(2*S*,3*S*)-37**

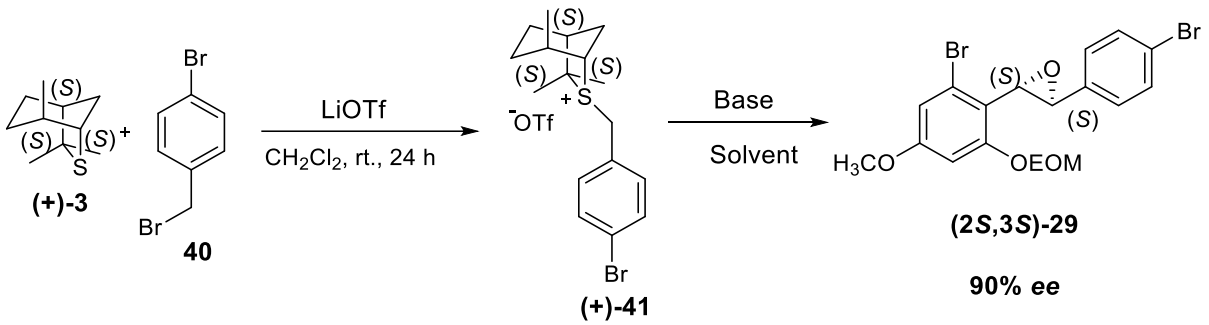

Entry	Ald.	Salt	Base	Solvent	T (°C)	Yield (%)
1	2 eq.	1	1.1 eq KOH	CH_3CN- *t*-BuOH	0	-
2	2 eq.	2 eq.	2.2 eq TBD	CH_2Cl_2	-30	60 (*trans* only)

Thus, polyfunctionalized *trans* diaryloxiranes ***rac*-28**, **(2*S*,3*S*)-28** and **(2*S*,3*S*)-29** were tested in opening reactions using phenylboronic acid, while ***rac*-29** was tested both using phenylboronic acid and 3,5-di-bromophenylboronic acid. The results are given in Table 14.

Table 14 Ring opening reactions of polyfunctionalized epoxides

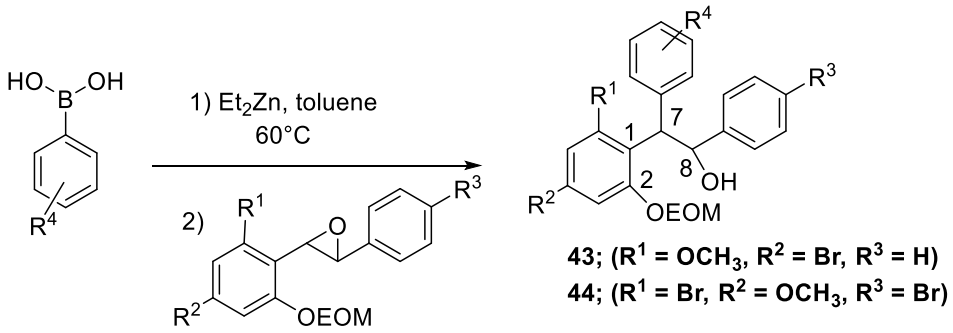

***rac*-28, (2*S*,3*S*)-36; (R^1 = OCH_3, R^2 = Br, R^3 = H)**
***rac*-29, (2*S*,3*S*)-37; (R^1 = Br, R^2 = OCH_3, R^3 = Br)**

Entry	Epox.	R^4	Prod.	Yield (%)
1	***rac*-28**	H	***rac syn*-43**	75
2	**(2*S*,3*S*)-28**	H	***syn*-(1*R*,2*S*)-43**	48
3	***rac*-29**	H	***rac syn*-44a**	82
4	**(2*S*,3*S*)-29**	H	***syn*-(1*R*,2*S*)-44a**	80
5	***rac*-29**	3,5-di-Br	***rac syn*-44b**	25

The ring opening reaction appeared completely regioselective and stereoselective also with this polyfunctionalized epoxides, using either unsubstituted or brominated aryl boronic acids as nucleophile precursors, giving the products in moderate to good yield. As usual, characterization of new compounds as single regioisomers was confirmed by direct (HSQC) and long-range (HMBC) correlation $^1H/^{13}C$ NMR experiments.

With the desired regioisomers in hand we performed the deprotection reaction using Amberlyst 15 in CH_3OH at 60°C. As shown in the Table 15 ***rac syn*-43**, ***syn*-(1*R*,2*S*)-43** and ***rac syn*-44b** gave the expected product along with the corresponding dihydrobenzofuran by *in situ* cyclodehydration; ***rac syn*-46a** gave only the corresponding hydroxyphenol while ***rac trans*-48a** gave the corresponding DHB as the only product.

The formation of acid-catalyzed DHB was unexpected and it is difficult to rationalize the reason why in some cases it occurred and in others not, but when it occurred the reaction run stereospecifically, providing only the *trans* isomer. Moreover, the initial *ee* of the starting epoxides **(2*S*,3*S*)-36** and **(2*S*,3*S*)-37** were retained in the final ***trans*-(2*S*,3*S*)-47** and ***trans*-(2*S*-3*S*)-48a**.

Table 15 Deprotection reactions

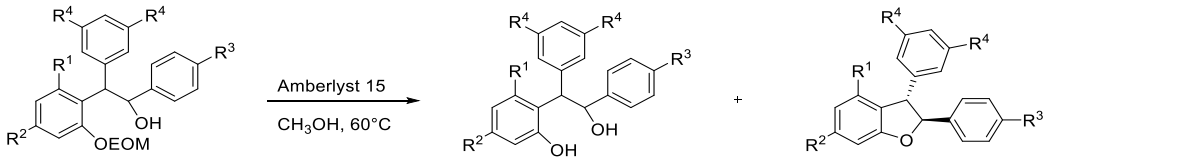

43; (R^1 = OCH_3, R^2 = Br, R^3 = H, R^4 = H)
44a; (R^1 = Br, R^2 = OCH_3, R^3 = Br, R^4 = H)
44b; (R^1 = Br, R^2 = OCH_3, R^3 = Br, R^4 = Br)

45; (R^1 = OCH_3, R^2 = Br, R^3 = H, R^4 = H)
46a; (R^1 = Br, R^2 = OCH_3, R^3 = Br, R^4 = H)
46b; (R^1 = Br, R^2 = OCH_3, R^3 = Br, R^4 = Br)

47; (R^1 = OCH_3, R^2 = Br, R^3 = H, R^4 = H)
48a; (R^1 = Br, R^2 = OCH_3, R^3 = Br, R^4 = H)
48b; (R^1 = Br, R^2 = OCH_3, R^3 = Br, R^4 = Br)

Entry	Substrate	Time (h)	Hydroxyphenol (Yield %)	DHB (Yield %)	*ee* (%)
1	***rac syn*-43**	5	***rac syn*-45 (67%)**	***rac trans*-47 (31%)**	-
2	***syn*-(1*R*,2*S*)-43**	2	***syn*-(1*R*,2*S*)-45 (46%)**	***trans*-(2*S*,3*S*)-47 (54%)**	90
3	***rac syn*-44a**	3	***rac syn*-46a (90%)**	-	-
4	***syn*-(1*R*,2*S*)-44a**	2	-	***trans*-(2*S*-3*S*)-48a (62%)**	90
5	***rac syn*-44b**	4	***rac syn*-46b (49%)**	***rac trans*-48b (41%)**	-

On the hydroxyphenols ***rac syn*-45** and ***rac syn*-46a** the Mitsunobu type cyclodehydration with PPh_3/DEAD system in THF was performed, affording the corresponding *trans*-DHB in good yield (Table 16).

Table 16 Mitsunobu type cyclodehydration of ***rac syn*-45** and ***rac syn*-46a**

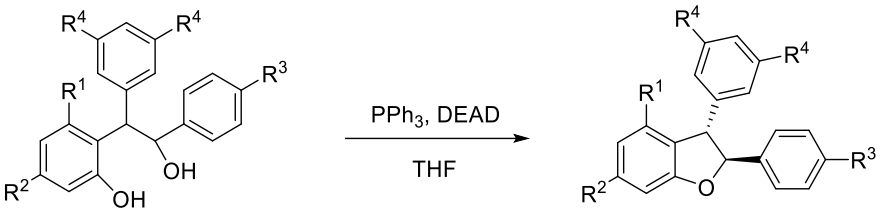

***rac syn*-45**; ($R^1 = OCH_3$, R^2 = Br, R^3 = H, R^4 = H)
***rac syn*-46a**; (R^1 = Br, $R^2 = OCH_3$, R^3 = Br, R^4 = H)

47; ($R^1 = OCH_3$, R^2 = Br, R^3 = H, R^4 = H)
48a; (R^1 = Br, $R^2 = OCH_3$, R^3 = Br, R^4 = H)

Entry	Hydroxyalcohol	Time (h)	DHB	Yield (%)
1	***rac syn*-45**	1	***rac trans*-47**	42
2	***rac syn*-46a**	4	***rac trans*-48a**	55

2.5.3 Attempt to access to bromo-methoxy derivative of Gnetin C

Preliminary interesting results were obtained in the synthetic approach to a bromo-methoxy derivative of Gnetin C (Figure 28). This product can be envisaged as a late intermediate of Gnetin C, which can be achieved by methoxydebromination and subsequent demethylation reactions.

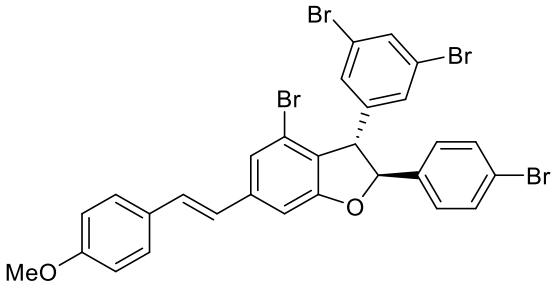

Figure 28 Structure of bromo-methoxy derivative of Gnetin C

The 4-bromo-2,6-dimethoxybenzaldheyde **31a** could provide the (*E*)-2,6-dimethoxy-4-(4-methoxystyryl)benzaldehyde **49** by Heck reaction with *p*-methoxystyrene (Figure 29).

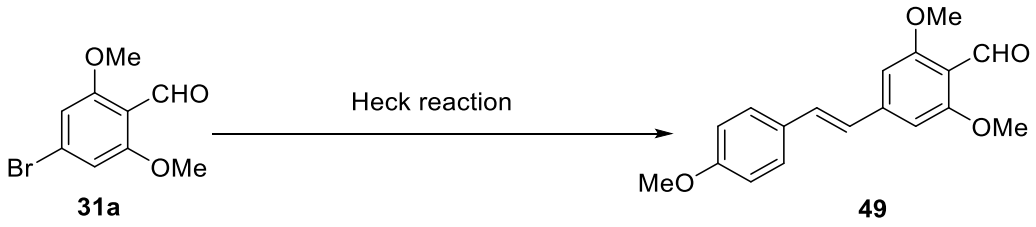

31a **49**

Figure 29 Access to compound **49** by Heck reaction

After various unsuccessful attempts under various conditions we obtained the desired product **49** in good yield (60%) using sodium carbonate and tris(dibenzylideneacetone)dipalladium(0) and tri(*o*-tolyl)-phosphine in DMF at 120°C for 24 h.[105]
Subsequently, monodemethylation[102] reaction of **49** with aluminum chloride ($AlCl_3$) and sodium iodide (NaI) in CH_2Cl_2/CH_3CN 1:1 afforded (*E*)-2-hydroxy-6-methoxy-4-(4-methoxystyryl)benzaldehyde **50** in very good yield (Scheme 54). Then this substituted salicylaldehyde was protected as ethoxymethyl ether by EOM-Cl and *N*,*N*-diisopropylethyleamine (DIPEA) in CH_2Cl_2 anhydrous at room temperature, affording the (*E*)-2-(ethoxymethoxy)-6-methoxy-4-(4-methoxystyryl)benzaldehyde **51** in good yield (Scheme 54).

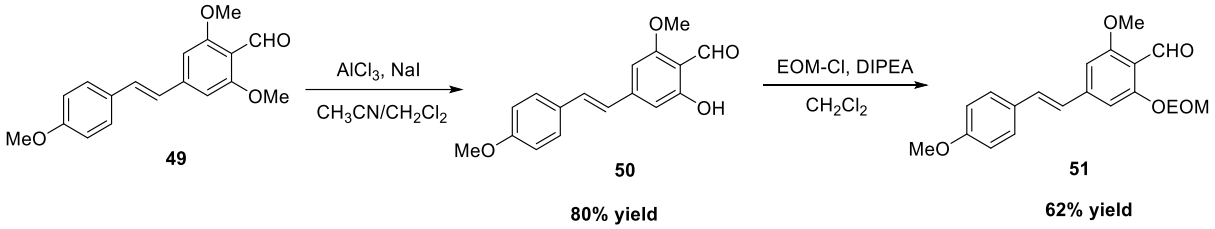

Scheme 54 Access to protected aldehyde **51**

The racemic (*E*)-2-(4-bromophenyl)-3-(2-(ethoxymethoxy)-6-methoxy-4-(4-methoxystyryl)-phenyloxirane **52** was prepared in moderate yield and high stereoselectivity from the parent aldehyde **51** using 1-(4-Bromobenzyl)-tetrahydrothiophenium bromide **38** as ylide source and 1,5,7-Triazabiciclo [4.4.0] dec-1-ene (TBD) as base in CH_2Cl_2 at room temperature (Scheme 55).

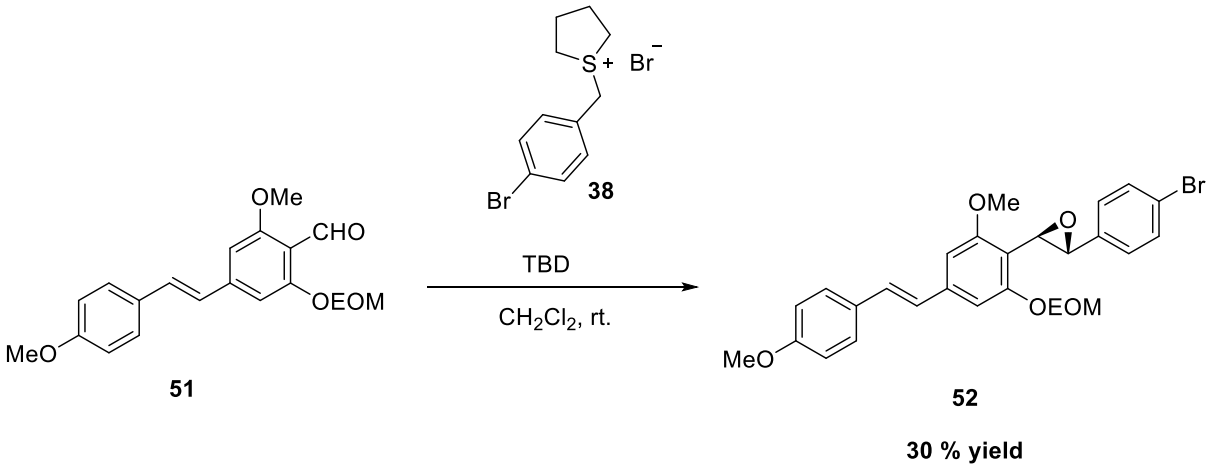

Scheme 55 Preparation of epoxide **52**

The diaryloxirane **52** was tested in opening reactions using 3,5-dibromophenylboronic acid as nucleophile precursor. In this case the direct (HSQC) and the long range (HMBC) correlation

[105] Jongcharoenkamol J.; Chuathong, P.; Amako, Y.; Kono, M.; Poonswat, K.; Ruchirawat, S.; Ploypradith, P. *J. Org. Chem.* **2018**, *83*, 13184-13210.

between ^{1}H and ^{13}C were different than the usual trend, in particular regarding the correlations between carbons and hydrogens at the side chain, in a way that we could not be able to understand whether we obtained the desired regioisomer **53** or the undesired regioisomer **54** (Scheme 56).

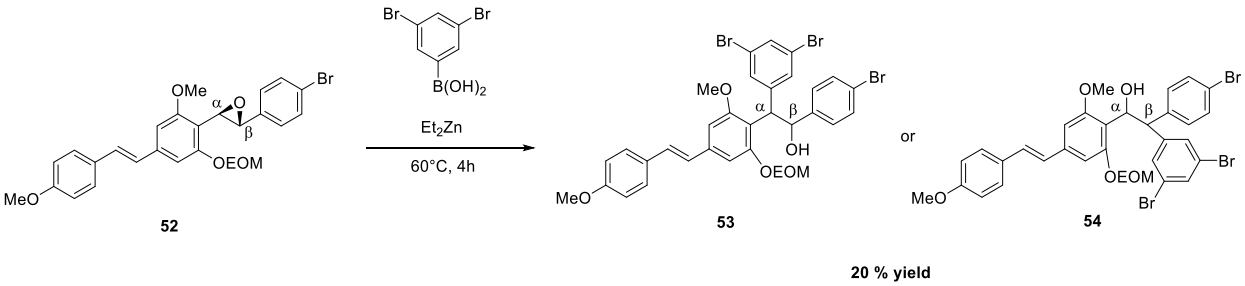

Scheme 56 Ring opening reaction of epoxide **52** with 3,5-dibromophenilboronic acid

The only way to understand which regioisomer had been obtained was to carry out the deprotection and the subsequent cyclohydration; only from the regioisomer **53** the final dihydrobenzofuran could be afforded by Mitsunobu type cyclodehydration.

After deprotection with Amberlyst 15 we isolated a compound that on TLC had an characteristic R_f of the dihydrobenzofuran (not very polar) and not of the hydroxyphenol (very polar) but unfortunately the isolated quantity was so low that we were unable to perform the characterization of the product.

In any case, this first attempt provided very preliminary interesting results which, following various modifications, opened a way to the possibility to obtain polyfunctionalized derivatives of natural Gnetin C.

2.6 Evaluation of anti-inflammatory activity

Inflammation is a defence mechanism underlying various physiological and pathological processes that usually occurs in the presence of noxious stimuli and conditions, such as infections and tissue injuries. Pathways of systemic inflammation have been recognized as an essential component in the pathogenesis of different multifactorial diseases encompassing chronic inflammatory rheumatic disorders, as well as a wide variety of conditions including type 2 diabetes, cardiovascular and neurodegenerative diseases, cancer, obesity, asthma, and ageing.

Lipopolysaccharide (LPS) or classically activated - also called M1 - macrophages acquire an inflammatory phenotype. During this shift from resting to activated status, plenty of metabolic changes occur to cope with the energetic needs of cells and in turn to achieve their own specific function. The rate of glycolysis and pentose phosphate pathways increases; OXPHOS (oxidative phosphorylation) is downregulated, and inflammatory mediators, such as nitric oxide (NO), reactive oxygen species (ROS), prostaglandin E_2 (PGE_2), IL-1**β** and other pro-inflammatory

cytokines, are produced. Inflammation is commonly treated with non-steroidal anti-inflammatory drugs and corticosteroids. However, these drugs are relatively old and have multiple serious side effects and often limited efficacy, so there is a continuing demand for new anti-inflammatory agents.

As already mentioned in the introduction of this chapter, natural oligostilbenes of resveratrol with dihydrobenzofuran moiety are increasingly attracting interest for their biological properties including anti-inflammatory activity.

Therefore, we decided to test the potential anti-inflammatory activity of some synthesized dihydrobenzofurans (Figure 30).[101]

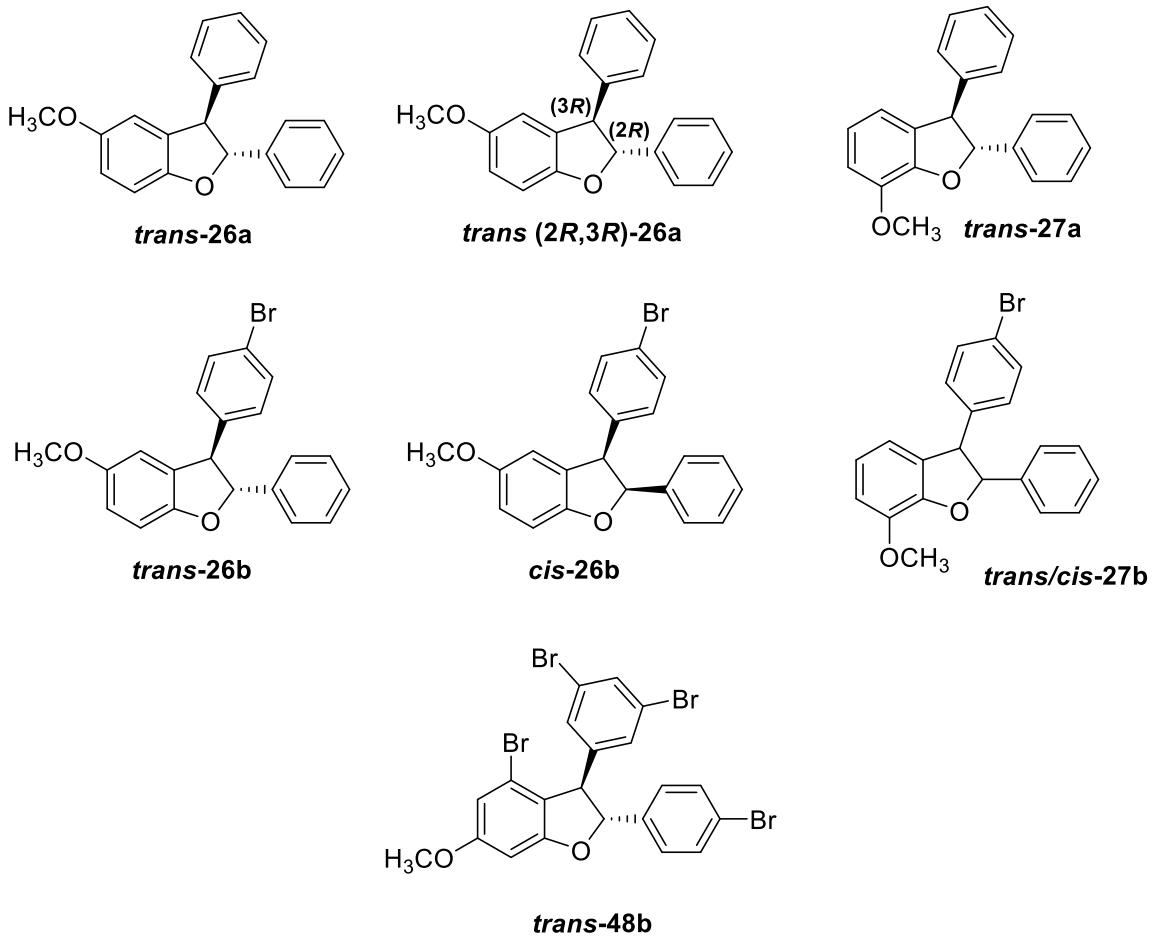

Figure 30 2,3-diaryl-2,3-dihydrobenzofurans tested as anti-inflammatory

We first verified that they were not toxic to U937 cells (a pro-monocytic, human myeloid leukaemia cell line that was isolated from the histiocytic lymphoma of a 37 year old male)[106] The experimental data showed that cell viability was not altered at the lowest concentration (0.01 μM) after 72 h of treatment with all compounds, except ***trans*/*cis*-27b** which was toxic at all concentrations tested (Figure 31). Therefore, the compounds were used at the lowest concentration (0.01 μM) for all subsequent experiments on U937 cells.

[106] Sundstrom, C.; Nilsson, K. *Int. J. Cancer*, **1976**, *17*,565–577.

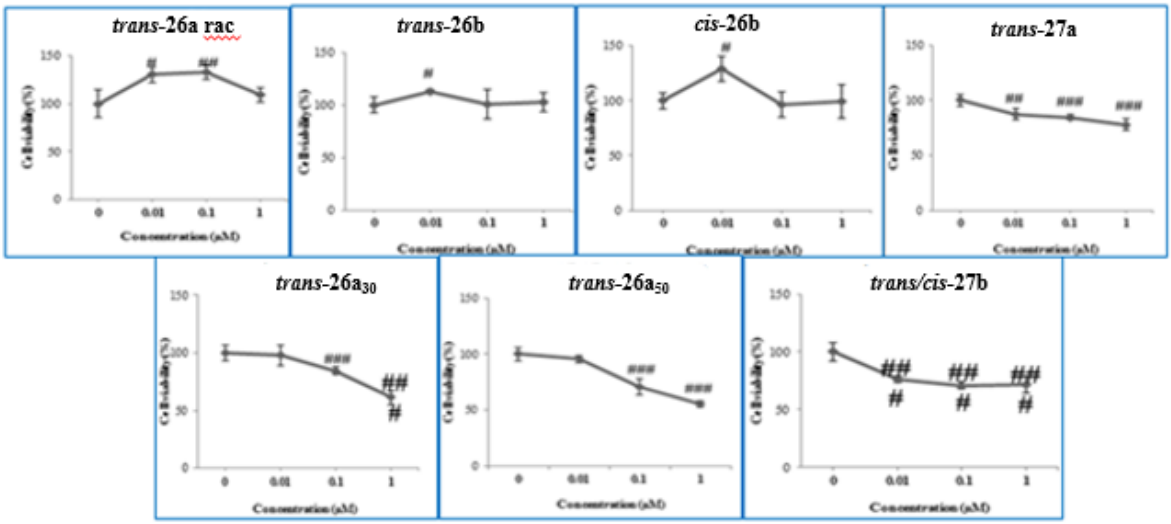

Figure 31 Effect of DHBs on U937 cells viability: U937 cells were treated with DMSO (0), 0.01, 0.1, 1 μM ***trans*-26a rac**, ***trans*-26b**, ***cis*-26b**, ***trans*-27a**, ***trans/cis*-27b**, ***trans*-26a$_{30}$** and ***trans*-26a$_{50}$** as indicated for 72 h. Cell viability was measured using a Millipore Scepter™ handheld automated cell counter. Results are presented as means ± SD from three independent experiments. # $p < 0.05$,## $p < 0.01$,### $p < 0.001$, # *vs*. control (one-way analysis of variance, ANOVA followed by Student's t-test for multiple comparisons).

The effect of these compounds on the inflammatory mediator NF-κB was investigated. The p65/p50 heterodimers and the p65/p65 homodimers are the most abundant forms of NF-κB, while other complexes have specific roles in some cell types. Generally, NF-κB dimers are kept inactive by binding to an inhibitory molecule of the IκB family, with IκBα being the most important. NF-κB can be activated by a wide variety of distinct stimuli, including LPS, inflammatory cytokines such as interleukin-1 or TNFα, but also physical stress such as γ irradiation or UV, reactive oxygen intermediates, as well as virus-derived dsDNA or RNA.[107] Activation of NF-kB involves its translocation from the cytosol to the nucleus and is controlled by targeted phosphorylation and subsequent degradation of IκB. NF-κB dimers in the nucleus bind to target DNA elements and activate the transcription of genes coding for proteins involved in immune or inflammatory responses.[108] Interestingly, the DHBs were able to resolve LPS-induced inflammation by reducing NF-κB levels. In detail, U937 cells were preincubated for 1 h with 0.01 μM of ***trans*-26a**, ***trans*-26b**, ***cis*-26b**, ***trans*-27a** and ***trans*-(2*R*,3*R*)-26a** (**26a$_{30}$** in 30% *ee* and **26a$_{50}$** in 50% *ee*) and subsequently activated with LPS for 3 h at 37 °C. LPS induced marked activation of the p65 NF-κB subunit, while in the presence of different compounds, the p65 NF-κB subunit does not show overexpression. Therefore, all the tested compounds reverted the increased p65 expression triggered by LPS treatment (Figure 32).

[107] Oeckinghaus, A.; Ghosh, S. *Cold Spring Harb. Perspect Biol.* **2009**, 1:a000034.

[108] Infantino V, Pierri CL, Iacobazzi V. *Curr. Med. Chem*. **2019**, *26*(40), 7104–7116.

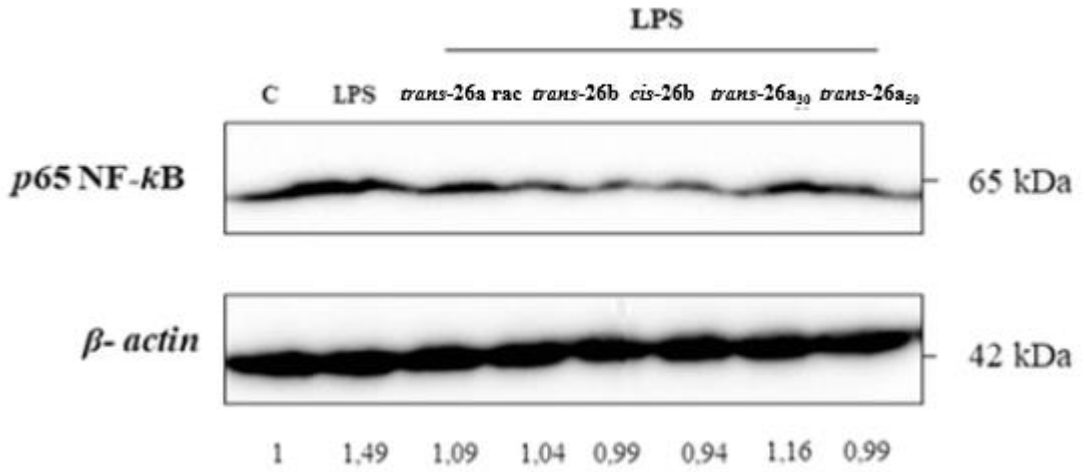

Figure 32 E**ffect of DHBs on p65/NF-kB expression level.** U937 cells were treated with or 200 ng/ml LPS alone (LPS) or LPS plus 0.01 μM ***trans*-26a**, ***trans*-26b**, ***cis*-26b**, ***trans*-27a**, ***trans*-26a$_{30}$** and ***trans*-26a$_{50}$**. By using specific antibodies, the expression levels of p65 and β-actin were detected. Levels of p65 protein were quantified using optical density versus β-actin and normalized cells versus control cells (C) are shown under the western blot image.

Immunocytochemistry was applied for examining the effect of the compounds on nuclear translocation of p65, the NF-kB subunit. After 3 h of treatment with only LPS, by means of FLoid™ Cell Imaging Station, we observed the translocation of NF-kB into the nucleus, while in cells co-treated with LPS and different compounds (0.01 μM), a major cytosolic localization of NF-κB was evident (Figure 33). Since the more enriched enantiomeric form ***trans*-26a$_{50}$** seemed somewhat more effective than the less enriched enantiomeric form ***trans*-26a$_{30}$** in blocking NF-κB signaling, only ***trans*-26a$_{50}$** was considered in subsequent investigations.

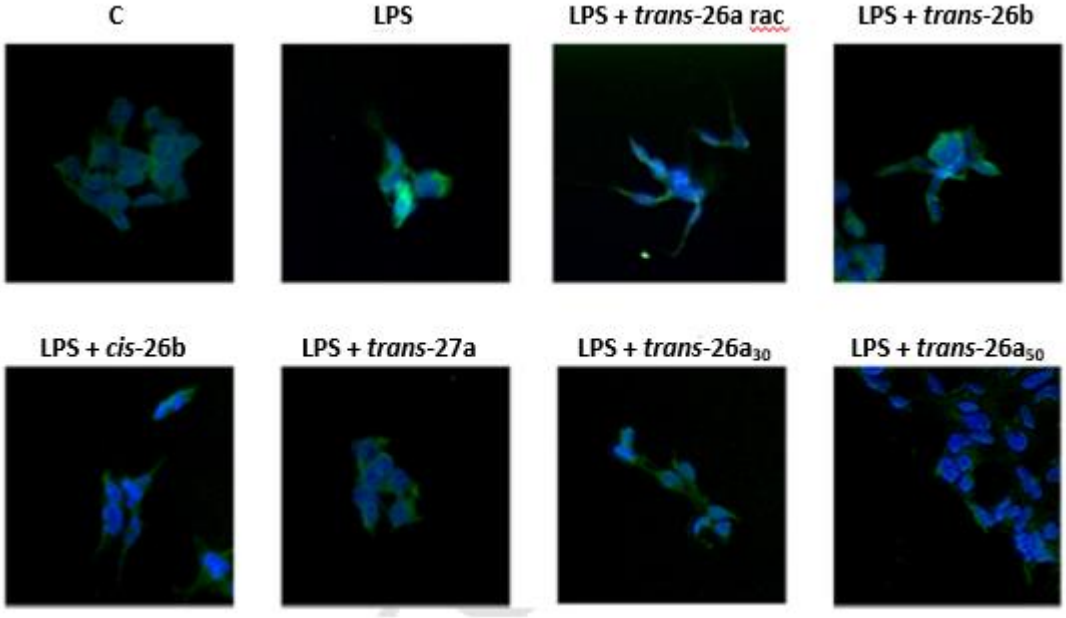

Figure 33 E**ffect of DHBs on p65/NF-kB traslocation.** HEK293 cells were treated with or 200 ng/ml LPS alone (LPS) or LPS plus 0.01 μM ***trans*-26a**, ***trans*-26b**, ***cis*-26b**, ***trans*-27a**, ***trans*-26a$_{30}$** and ***trans*-26a$_{50}$**. Immunocytochemistry (ICC) of p65/NF-kB on HEK293 cells: representative images of p65/NF-kB translocation following treatment with DHBs.

Therefore, from our data, it is clear that all compounds under examination play a significant role in inhibiting the NF-κB pathway.

To further explore their anti-inflammatory activity ***trans*-26a**, ***cis*-26b**, ***trans*-27a**, and ***trans*-26a$_{50}$**.were evaluated in their inhibitory action on the levels of inflammatory mediators such as ROS and NO (Figure 34).

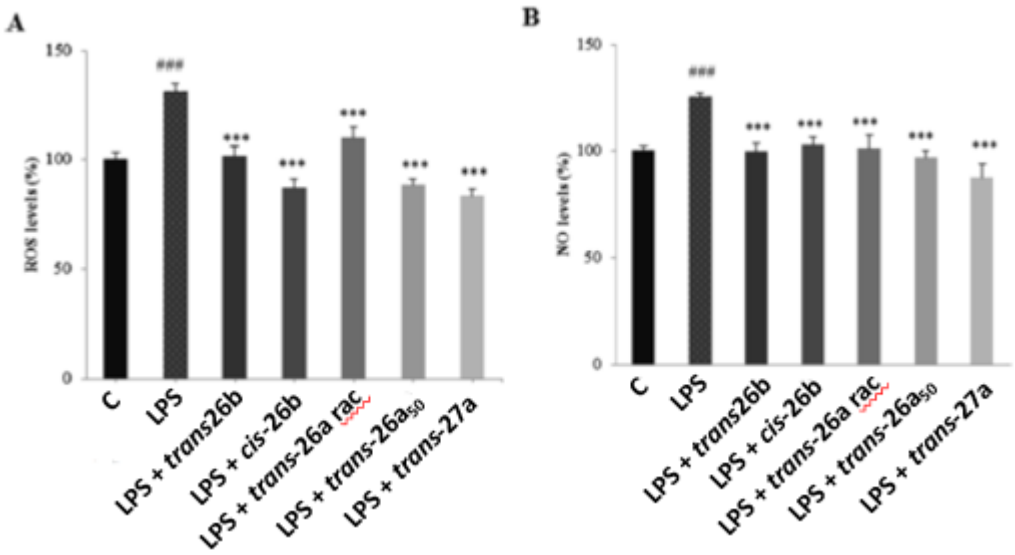

Figure 34 Effect of DHBs on ROS (A) and NO (B) production. U937 cells were treated with or 200 ng/ml LPS alone (LPS) or LPS plus 0.01 μM, ***trans*-26b**, ***cis*-26b**, ***trans*-26a rac**, ***trans*-26a$_{50}$**, and ***trans*-27b**. NO and ROS concentrations were measured after 24 h of LPS treatment. Means ± S.D. of four triplicate independent experiments are shown. In (**A**) and (**B**), activities are shown as the mean ± S.D. of three experiments. Statistical significance of differences was evaluated by one-way ANOVA followed by Student's *t*-test for multiple comparisons (###, ∗∗∗p < 0.001, # *vs*. C, * *vs*. LPS).

When U937 cells were activated with LPS we found a strong increase in ROS and NO levels compared with untreated cells (Figure 34; **LPS** *vs*. **C**, ### p < 0.001). All new synthesized derivatives were able to restore normal levels of reactive oxygen and nitric oxide species at the tested concentration (Figure 34; compounds *vs*. **LPS**, *** p < 0.001). Interestingly, between the tested compounds the enantioenriched ***trans*-26a$_{50}$** significantly reduces ROS levels compared to its racemic form **7a *rac*** (Figure 34 A, **LPS + *trans*-26a rac** *vs*. **LPS + *trans*-26a$_{50}$**, ***p < 0.001), showing possible enantioselective protective effect. To investigate this possibility, we focused on the different behaviour of the two compounds.

For this reason, we decided to study the effect of the ***trans*-26a rac** and ***trans*-26a$_{50}$** on ATP Citrate Lyase activity (ACLY) and PGE_2 secretion (Figure 35).

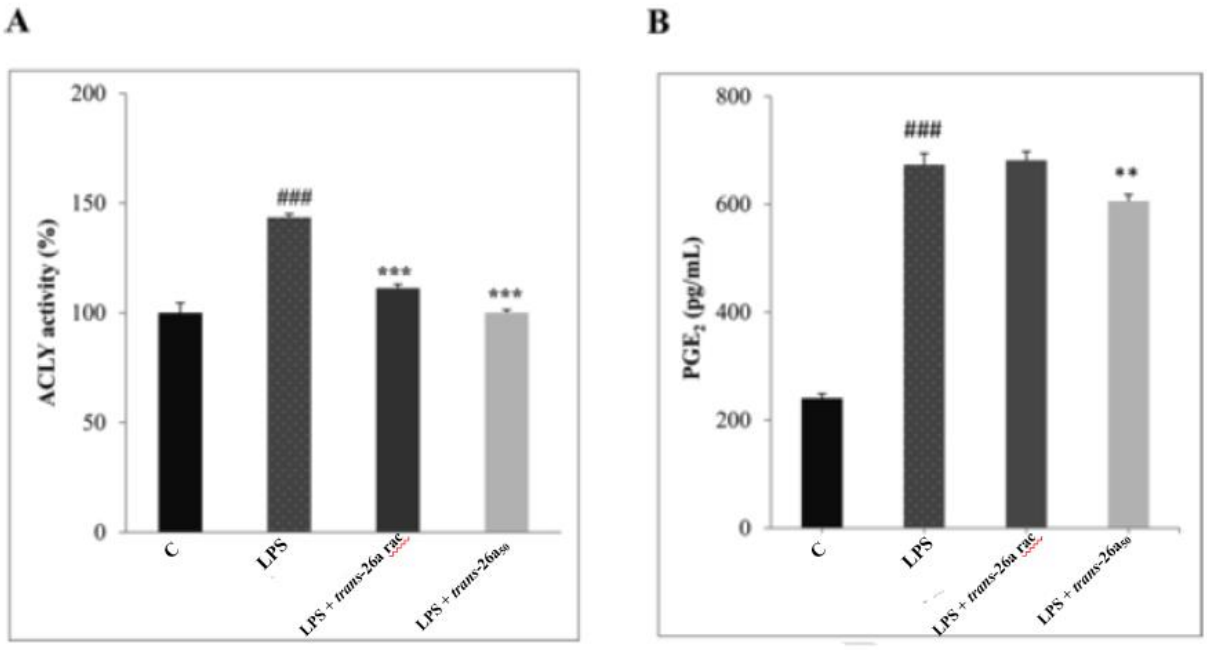

Figure 35 Effect of *trans*-26a rac and *trans*-26a$_{50}$ on ATP citrate lyase and PGE$_2$ production. U937 cells were treated with or 200 ng/ml LPS alone (LPS) or LPS plus 0.01 μM ***trans*-26a rac** and ***trans*-26a$_{50}$**. **A)** ACLY enzymatic activity were evaluated **B)** PGE$_2$ concentration was measured after 48 h of LPS treatment. Means ± S.D. of four triplicate independent experiments are shown. In (**A**) and (**B**), activities are shown as the mean ± S.D. of three experiments. Statistical significance of differences was evaluated by one-way ANOVA followed by Student's *t*-test for multiple comparisons (###, ***p < 0.001, ** p < 0.01, # *vs*. C, * *vs*. LPS).

ACLY is a component of citrate pathway which was demonstrated activated in inflammatory processes. Notably, ACLY is upregulated in Behçet's syndrome,[109] and in Down syndrome,[110] a genetic disease marked by inflammatory phenotypic aspects. ACLY is up-regulated very early in macrophages activated by LPS or by TNFα and/or IFNγ as well as in inflammatory conditions and its upregulation is related to NF-kB activation.[111] As it can be seen in Figure 35 **A**, LPS induced a 43% rise in ACLY activity. When ***trans*-26a rac** and ***trans*-26a$_{50}$** were added to LPS, both were able to abolish LPS induction. ***trans*-26a rac** reduced ACLY levels by approximately 32% and ***trans*-26a$_{50}$** by 43% compared to LPS. Noteworthy, while in the presence of ***trans*-26a rac** a slight increase, also if no significant, was observed compared to control in ACLY activity (about 11%), in the presence of ***trans*-26a$_{50}$** no differences were observed compared to control. Following LPS activation, the inhibition of ACLY leads to a reduction in inflammatory mediators.[112] Therefore, prostaglandin E2 levels were monitored both in the presence and in the absence of ***trans*-26a rac** and ***trans*-26a$_{50}$**. When U937 cells were activated with LPS there was an increase in PGE$_2$ secretion compared to untreated cells (Figure 35 **B**). Interestingly, the racemic form ***trans*-26a rac** slightly increased PGE$_2$ levels compared to LPSstimulated cells

[109] Santarsiero, A.; Leccese, P.; Convertini, P.; Padula, A.; Abriola, P.; D'Angelo, S.; Bisaccia, F.; Infantino, V. *Mediat Inflamm*. **2018**;8.

[110] Convertini, P.; Menga, A.; Andria, G.; Scala, I.; Santarsiero, A.; Castigione Morelli, M. A.; Iacobazzi, V.; Infantino, V. *Immunology*. **2016**; *149*(4); 423–431.

[111] Infantino V, Iacobazzi V, Palmieri F, Menga A. *Biochem Biophys Res Commun*. **2013**; *440*(1); 105–111.

[112] Vassallo, A.; Santoro, V.; Pappalardo, I.; Santarsiero, A.; Convertini, P.; De Luca, M.; Martelli, G.; Infantino, V.; Caddeo, C. *Nanomaterials*. **2020**; *10*; 2080.

(about 3%), while the enantioenriched ***trans*-26a$_{50}$** significantly reduced the levels of this critical inflammatory mediator (about 28%). All together, these results suggest a stereoselective interaction somewhere in the production of prostaglandin E_2 and a potential role of ***trans*-(2*R*,3*R*)-26a** as an anti-inflammatory drug.

2.7 Experimental procedures

2.7.1 General chemical experimental

All commercial reagents were purchased from Sigma-Aldrich, Alfa-Aesar, TCI Chemicals and directly used without further purification. Dry solvents were obtained through distillation over conventional drying agents. (THF, dioxane and toluene were distilled over sodium/benzophenone, dichloromethane were distilled over calcium hydride). Unless otherwise noted, all organic solvents were evaporated under reduced pressure using rotary evaporation at a temperature range of 25-45 °C. IR data were collected on a Perkin Elmer Model 2000 FTIR spectrometer and. ^{1}H NMR spectra were recorded on a high field NMR spectrometer at 500 or 400 MHz and are reported relative to $CDCl_3$ signal (7.26 ppm for ^{1}H NMR, 77.00 ppm for ^{13}C NMR). Thin layer chromatography (TLC) was carried out using pre-coated silica gel sheets (Merck 60 F254). Visual detection was performed using UV light at 254 nm and phosphomolybdic acid. Column chromatography was carried out on Merck silica gel (0.063-0.200 mm particle size) by progressive elution with suitable solvent mixtures. MS spectra were recorded on a gas-chromatograph equipped with with the Hewlett Packard GC / MS 6890-5973 spectrometer with EI (Electronic Impact) ion source. Enantiomeric excess was determined by HPLC analysis performed on a JASCO PU-1580 pump with a Varian 2550 UV detector and Daicel CHIRALCEL® and CHIRALPAK® columns (internal diameter 4.6 mm, column length 250 mm, particle size 10 µm). The optical rotation was evaluated by using a JASCO Mod Dip-370 polarimeter.

2.7.1.1 Formilation reaction

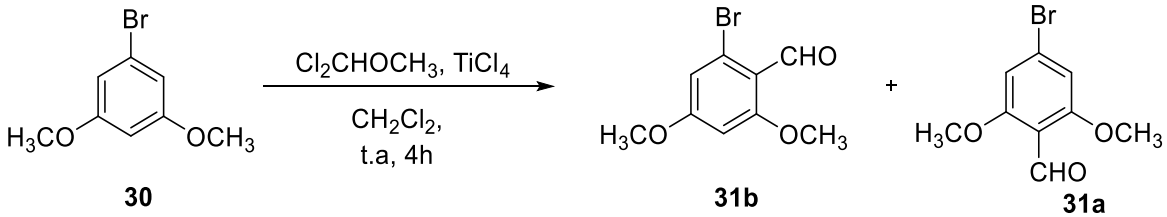

MW = 245 g/mol

A magnetically stirred solution of dichloromethyl methyl ether (2 eq., 9,22 mmol, 1.059 g, d =1.271 g/mL, 0.8 mL) and titanium tetrachloride (2.4 eq., 11.2 mmol, 2.09 g, d =1.73 g/mL) in anhyd CH_2Cl_2 (20 mL) was treated with a solution of commercially available 1-bromo-3,5-dimethoxybenzene **30** (1 eq., 4.6 mmol, 1.000 g) in anhyd CH_2Cl_2 (2.5 mL) at 0 °C. The reaction mixture was stirred at room temperature for 4 h. After the addition of cold 5% aq. HCl (2 mL)

at 0 °C, the stirring was continued for 15 min. The organic layer was then separated and the aqueous solution was extracted with CH_2Cl_2 (3 × 20 mL). The combined extracts were washed with 5% aq. NaHCO3 (20 mL) and brine (20 mL), dried with Na_2SO_4, and concentrated under reduced pressure. The crude was purify by chromatography on silica gel at atmospheric pressure to get the 2-bromo-4,6-dimethoxybenzaldheyde **31b** (755 mg, 67%) and 4-bromo-2,6-dimethoxybenzaldheyde **31a** (223 mg, 20%).
R_f = 0.4 (50% Et_2O/Hexane).

^{1}H NMR (400 MHz, $CDCl_3$); δ (ppm) 3.87 (s, 3H), 3.90 (s, 3H), 6.43 (brs, 1H), 6.78 (brs, 1H), 10.32 (s, 1H).

2.7.1.2 Methoxidefluorination reaction

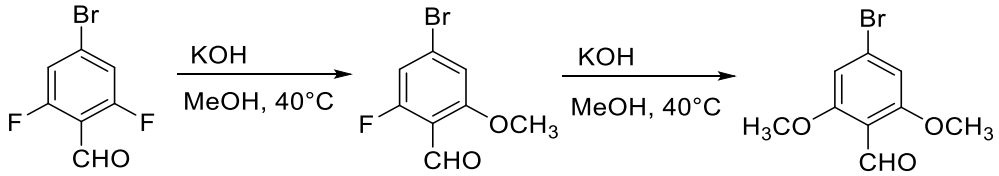

32 **33** **31a**

MW = 233 g/mol MW = 245 g/mol

To a solution of 4-bromo-2,6-difluorobenzaldehyde (1 g, 4.52 mmol) in MeOH (10 mL) was added potassium hydroxide (300 mg in 3 mL of MeOH) at 40°C and was stirred for 24 hours. At the end of the reaction, the solvent was removed under reduced pressure and the mixture was washed with a saturated aqueous solution of NH_4Cl and extracted with EtOAc. The organic phase was dried with anhydrous Na_2SO_4 and the solvent removed under reduced pressure. The crude was purified by column chromatography on a silica gel (10% Et_2O/Hexane) to get the 4-bromo-2-fluoro-6-methoxybenzaldehyde **33** (401 mg, 1.7 mmol, 38%).

Rf = 0.20 (10% Et_2O/Hexane)
^{1}H NMR (400 MHz, $CDCl_3$); *δ* (ppm) 3.96 (s, 3H), 6.96 (brs, 1H), 7.27 (s, 1H), 10.37 (s, 1H).

To a solution of 4-bromo-6-fluoro-2-methoxybenzaldehyde **33** (400 mg, 1.7 mmol) in MeOH (5 mL) was added potassium hydroxide (120 mg in 2 mL of MeOH) at 40 ° C and stirred for 15h. At the end of the reaction, the solvent was removed under reduced pressure and the reaction mixture washed with a saturated aqueous solution of NH_4Cl and extracted with EtOAc. The solvent was removed under reduced pressure to get 4-bromo-2,6-dimethoxybenzaldehyde **31a** with a quantitative yield (416 mg).

R_f = 0.40 (50% Et_2O/Hexane)
^{1}H NMR (400 MHz, $CDCl_3$); *δ* (ppm) 3.90 (s, 6H), 6.75 (s, 2H), 10.42 (s, 1H).

2.7.1.3 Heck reaction

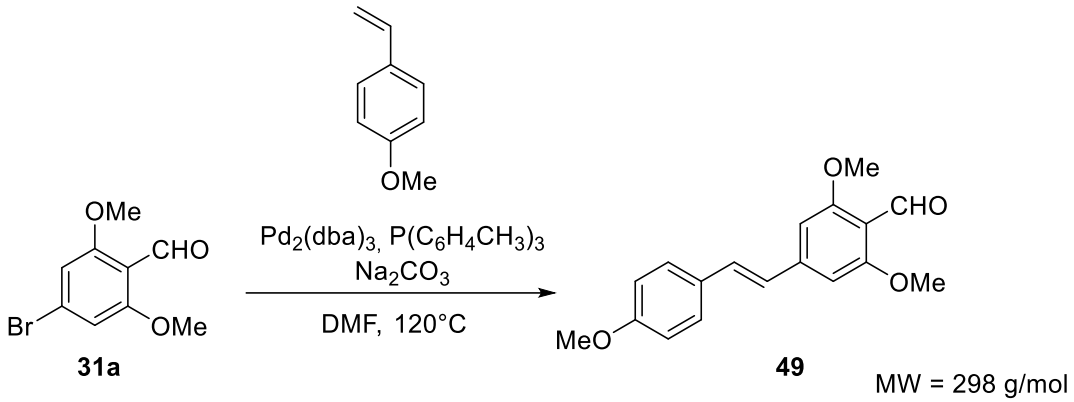

To a stirred solution 4-bromo-2,6-dimethoxybenzaldehyde **31a** (500 mg, 1 eq., 2 mmol) in N,N-dimethylformamide (DMF) were added 4-methoxystyrene (536 mg, d = 1.009 g/mL, 532 µL, 2 eq., 4 mmol), sodium carbonate (Na_2CO_3, 423 mg, 2 eq., 2 mmol), and tris(dibenzylideneacetone)dipalladium(0) ($Pd_2(dba)_3$, 183 mg, 0.1 eq, 0.2 mmol) with tri(o-tolyl)-phosphine ($P(C_6H_4CH_3)_3$, 61 mg, 0.1 eq., 0.2 mmol). The reaction mixture was heated to 120 °C for 24 h. Then, the reaction was allowed to cool to room emperature. The palladium was removed through Celite followed by he addition of water and ethyl acetate (EtOAc); the two phases were separated. The aqueous layer was extracted twice with EtOAc. The combined organic layer was washed with brine, dried over Na_2SO_4, filtered, and concentrated under reduced pressure to give the crude product, which was further purified by column chromatography on silica (40% EtOAc/hexanes) to furnish the (*E*)-2,6-dimethoxy-4-(4-methoxystyryl)benzaldehyde **49** (475 mg, 1.6 mmol, 62%).

R_f = 0.3 (30% EtOAc/Hexane)
^{1}H NMR (400 MHz, $CDCl_3$); δ (ppm) 3.85 (s, 3H), 3.96 (s, 6H), 6.68 (m, 2H), 6.93 (d, J = 8.4 Hz, 2H), 6.93 (d, J = 15.6 Hz, 1H), 7.17 (d, J = 15.6 Hz, 1H), 7.50 (d, J = 8.4 Hz, 2H), 10.48 (s, 1H). ^{13}C NMR (100 MHz, $CDCl_3$); δ (ppm) 55.3, 56.0, 101.6, 114.2, 125.6, 128.2, 131.7, 145.3, 160.0, 162.4, 188.6.

2.7.1.4 Demethylation

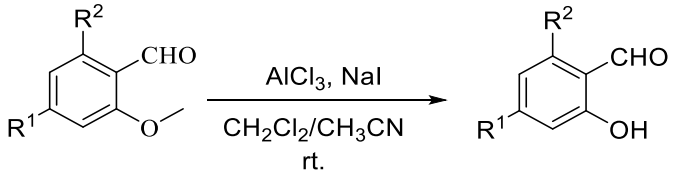

To a solution of suitable aldehyde (1 eq.) in CH_2Cl_2/CH_3CN 1:1 was added $AlCl_3$ (1.5 or 3.0 eq.) and NaI (1 or 2 eq.) at 0°C. The reaction was stirred at room temperature and was checked on TLC. The reaction mixture was then poured into cold water and extracted CH_2Cl_2. The combined organic layer was washed with brine and dried with Na_2SO_4. Products were purified by chromatography on silica gel at atmospheric pressure.

4-bromo-6-methoxysalicylaldehyde (34a) was obtained (199 mg, 0.86 mmol, 61%) using a ratio of reagents $AlCl_3$/NaI = 1.5:1 from commercial available 4-bromo-2,5-dimethoxybenzaldehyde **31a** (342 mg, 1.4 mmol).
R_f = 0.7 (40 % Et_2O/Hexane).
^{1}H NMR (400 MHz, $CDCl_3$); δ (ppm) 3.91 (s, 3H), 6.56 (s, 1H), 6.76 (s, 1H), 10.27 (s, 1H), 12.09 (s, 1H).

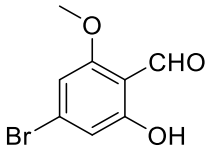

34a

2-bromo-4-methoxysalicylaldehyde (34b) was obtained (702 mg, 3.04 mmol, 99%) using a ratio of reagents $AlCl_3$/NaI = 1.5:1 from 2-bromo-4,6-dimethoxybenzaldheyde **31b** (752 mg, 3.07 mmol) without purification.
R_f = 0.3 (40 % Et_2O/Hexane).
^{1}H NMR (400 MHz, $CDCl_3$); δ (ppm) 3.73 (s, 3H), 6.21 (brs, 1H), 6.57 (brs, 1H), 9.93 (s, 1H), 12.33 (s, 1H).

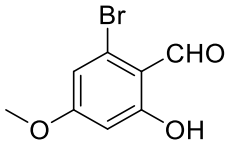

34b

(*E*)-6-methoxy-4-(4-methoxystyryl)salicylaldehyde 50 (MW = 284 g/mol) was obtained (225 mg, 0.8 mmol, 80%) using a ratio of reagents $AlCl_3$/NaI = 3:2 from (*E*)-2,6-dimethoxy-4-(4-methoxystyryl)benzaldehyde **49** (306 mg, 1 mmol).

R_f = 0.3 (40 % EtOAc/Hexane).
^{1}H NMR (400 MHz, $CDCl_3$); δ (ppm) 3.85 (s, 1H), 3.96 (s, 3H), 6.48 (s, 1H), 6.64 (s, 1H), 6.87 (d, J = 15.6 Hz, 2H), 6.92 (d, J = 8.4 Hz, 1H), 7.18 (d, J = 15.6 Hz, 1H), 7.48 (d, J = 8.4 Hz, 2H), 10.26(s, 1H), 12.01 (s, 1H). ^{13}C NMR (100 MHz, $CDCl_3$); δ (ppm) 55.3, 55.7, 98.8, 107.7, 109.9, 114.2, 125.4, 128.9, 132.5, 147.7, 160.1, 162.4, 163.8, 193.0.
.

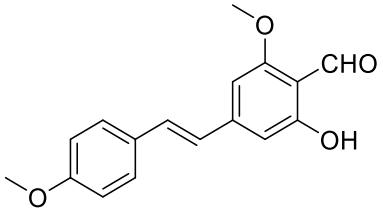

50

2.7.1.5 Protection of salicylaldehydes

General procedure

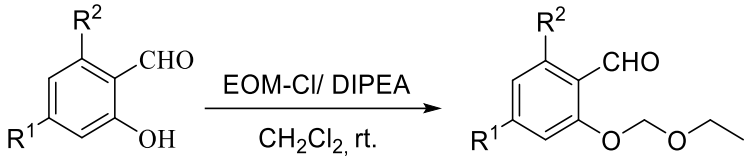

A mixture of a suitable salicylaldehydes (1 eq.), chloromethyl ethyl ether and *N*,*N*-diisopropylethyleamine (the ratio of reagents was different for each starting aldehyde) in dichloromethane was stirred at room temperature. The progress of the reaction was checked on TLC (Hexane / Et2O 6: 4) until complete conversion of substrate. The reaction was quenched with saturated NH_4Cl solution and extracted three times with dichloromethane. The combined extracts were dried with sodium sulfate and the solvent removed under reduced pressure. Products were purified by chromatography on silica gel at atmospheric pressure.

2-(ethoxymethoxy)benaldehyde (4b) (MW = 180 g/mol) was obtained (662 mg, 3.7 mmol, 90%) using the ratio of reagents EOM-Cl/DIPEA = 1.2eq/2eq. from commercial salicylaldehyde (500 mg, 4.09 mmol) as a oil.

R_f =0.6 (20% EtOAc/EP)

^{1}H NMR (400 MHz, $CDCl_3$): δ (ppm) 1.22 (t, 3H, CH_3, J = 6.8 Hz), 3.76 (q, 2H, CH_2, J = 6.8 Hz), 5.34 (s, 2H, CH_2), 7.06 (dd, 1H, $J_1 = J_2$ = 7.6 Hz), 7.23 (d, 1H, J = 8.4 Hz), 7.52 (dd, 1H, $J_1 = J_2$ = 7.6 Hz), 7.82 (d, 1H, J = 8.0 Hz) 10.48 (s, 1H, CHO).

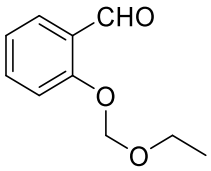

4b

2-(ethoxymethoxy)-5-methoxybenaldehyde (20) (MW = 210 g/mol) was obtained (721 mg, 3.4 mmol, 89%) using the ratio of reagents EOM-Cl/DIPEA = 1.2eq/2eq. from commercial 5-methoxysalicylaldehyde **18** (584 mg, 3.84 mmol) as a oil, after purification by column chromatography at atmospheric pressure.

R_f = 0.5 (10% Et_2O/EP).

^{1}H NMR (400 MHz, $CDCl_3$): δ (ppm) 1.25 (t, J = 7.2 Hz, 3H), 3.77 (q, J = 7.2 Hz, 2H), 3.83 (s, 3H), 5.30 (s, 2H), 7.14 (dd, $J_1 = J_2$ = 3.2 Hz, 1H), 10.46 (s, 1H).

^{13}C NMR (100 MHz, $CDCl_3$): δ (ppm) 15.1, 55.8, 64.8, 94.1, 109.9, 117.3, 123.6, 125.9, 154.4, 154.6, 189.6.

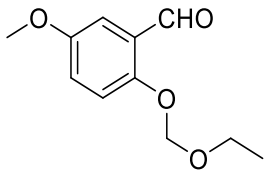

20

2-(ethoxymethoxy)-3-methoxybenaldehyde (21) (MW = 210 g/mol) was obtained (1.14 g, 5,4 mmol, 82%) using the ratio of reagents EOM-Cl/DIPEA = 1.2eq/2eq. from commercial 3-methoxysalicylaldehyde **19** (1.00 g, 6.57 mmol) as a oil, after purification by column chromatography at atmospheric pressure.

R_f = 0.5 (20% Et_2O/EP)

^{1}H NMR (400 MHz, $CDCl_3$): δ (ppm) 1.25 (3H, t, J = 7.0 Hz), 3.53 (2H, q, J = 7.0 Hz), 3.80 (3H, s), 5.01 (2H, s), 6.58-6.66 (2H, 6.63 (dd, J = 8.6, 2.7 Hz), 6.62 (dd, J = 8.6, 2.7 Hz)), 7.25 (1H, t, J = 8.6 Hz).

^{13}C NMR (100 MHz, $CDCl_3$): δ (ppm) 15.2, 56.2, 63.5, 93.3, 107.7, 107.7, 123.6, 137.6, 148.40, 155.3.

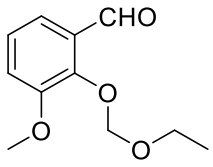

21

4-bromo-2-(ethoxymethoxy)-6-methoxybenaldehyde (35a) (MW = 289 g/mol)was obtained (329 mg, 1.13 mmol, 80%) using the ratio of reagents EOM-Cl/DIPEA = 6eq/10eq. from 4-bromo-6-methoxysalicylaldehyde **34a** (199 mg, 0.86 mmol) as a oil, after purification by column chromatography at atmospheric pressure.

Rf = 0.40 (40% Et_2O/Hexane)

^{1}H NMR (400 MHz, $CDCl_3$); δ (ppm) 1.23 (t, J = 7.2 Hz, 3H), 3.74 (q, J = 7.2 Hz, 2H), 3.89 (s, 3H), 5.29 (s, 2H), 6.78 (brs, 1H), 7.02 (brs, 1H), 10.42 (s, 1H).

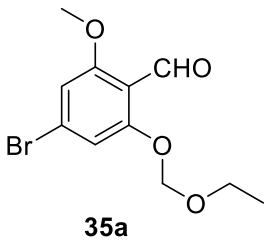

35a

2-bromo-6-(ethoxymethoxy)-4-methoxybenaldehyde (35b) (MW = 289 g/mol) was obtained (744 mg, 2.57 mmol, 71%) using the ratio of reagents EOM-Cl/DIPEA = 2eq/2eq. from 2-bromo-4-methoxysalicylaldehyde **34b** (838 mg, 3.63 mmol) as a oil without purification.
R_f =0.3 (40% Et_2O/Hexane).

^{1}H NMR (400 MHz, $CDCl_3$); δ (ppm) 1.20 (t, *J* = 7.2 Hz, 3H), 3.71 (q, *J* = 7.2 Hz, 2H), 3.83 (s, 3H), 6.72 (d, *J* = 2.0 Hz, 1H), 6.82 (d, *J* = 2.0 Hz, 1H), 10.30 (s, 1H)

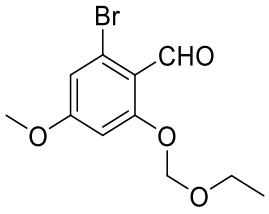

35b

(*E*)-2-(ethoxymethoxy)-6-methoxy-4-(4-methoxystyryl)benzaldehyde 51(MW = 342 g/mol) was obtained (212 mg, 0.62 mmol, 62%) using the ratio of reagents EOM-Cl/DIPEA = 1.8eq/3eq. from (*E*)-6-methoxy-4-(4-methoxystyryl)salicylaldehyde **50** (225 mg, 0.8 mmol) as a oil, after purification by column chromatography at atmospheric pressure.

R_f = 0.6 (30% EtOAc/EP)

^{1}H NMR (400 MHz, $CDCl_3$); δ (ppm) 1.25 (t, *J* = 6.8 Hz, 3H), 3.79 (q, *J* = 6.8 Hz, 2H), 3.84 (s, 1H), 3.96 (s, 3H), 5.26 (s, *2*H), 6.72 (s, 1H), 6.92 (m, 4H), 7.16 (d, *J* = 15.6 Hz), 7.49 (d, *J* = 8.4 Hz), 10.47 (s, 1H). ^{13}C NMR (100 MHz, $CDCl_3$); δ (ppm) 15.1, 55.3, 56.0, 64.8, 93.4, 102.3, 105.2, 114.2, 125.5, 128.2, 129.0, 131.7, 159.9, 160.4, 161.9, 188.8.

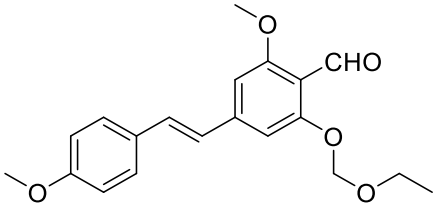

51

2.7.1.6 Preparation of achiral sulfonium salts

Benzyltetrahydrothiophenium bromide (5)

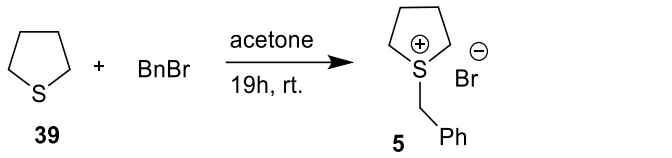

39 **5**

MW = 258 g/mol

A mixture of tetrahydrothiophene **39** (1 eq., 3.57 g, 40.6 mmol) and benzyl bromide (1 eq., 6.94 g, 40.6 mmol) in acetone (20 mL) was stirred for 19h at room temperature. At this time, the resultant solid was collected by filtration and washed with additional acetone (2 × 50 mL) to give benzyltetrahydrothiophenium bromide **5** (7.51 g, 29.1 mmol, 72%) as a white solid.

^{1}H NMR (400 MHz, $CDCl_3$): δ (ppm) 2.06-2.27 (m, 4H), 3.21-3.46 (m, 4H) 4.41 (s, 2H), 7.31-7.47 (m, 5H).

1-(4-Bromobenzyl)-tetrahydrothiophenium bromide (38)

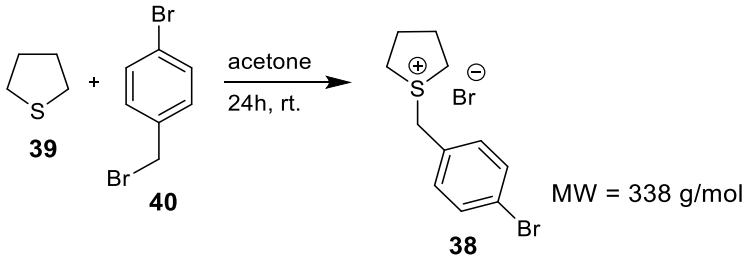

39 **40** **38**

MW = 338 g/mol

A mixture of tetrahydrothiophene **39** (1 eq., 2.5 g, 10 mmol) and 4-bromobenzyl bromide **40** (1.5 eq., 1.32 g, 15 mmol) in acetone (5 mL) was stirred for 24h at room temperature. At this time, the resultant solid was collected by filtration and washed with additional acetone (2 × 50 mL) to give 1-(4-Bromobenzyl)-tetrahydrothiophenium bromide **38** (3.19 g, 9.4 mmol, 94%) as a white solid.

^{1}H NMR (400 MHz, $CDCl_3$); δ (ppm) 2.12 (m, 4H), 3.28 (m, 4H), 4.33 (s, 2H), 7.47 (d, J = 8.0 Hz, 2H) 7.53 (d, J = 8.0 Hz, 2H).

2.7.1.7 Preparation of chiral sulfonium salts

General procedure

Sulfide (1 eq.) was dissolved in dichloromethane (1 ml for each 2.4 mmol of sulfide) and then the appropriate bromide (2 eq) and a solution of lithium triflate (5 eq.) in water (1 ml for each 5 mmol of LiOTf) were added. The resulting biphasic mixture was stirred at r.t. for 1 day. Water (same amount as starting volume) and dichloromethane (same amount as starting volume) were added and the layers were separated. The aqueous organic layer was extracted with dichloromethane (3 × half the amount of starting volume). The combined organic layers were dried over Na_2SO_4 and the solvent was removed under reduced pressure. The crude product was dissolved in the minimum amount of dichloromethane and added drop-wise to rapidly stirred diethyl ether (at least 10 times the volume of dichloromethane used to dissolve the crude). The precipitate was filtered and washed several times with diethyl ether (same amount as used to precipitate the salt).

(*1R,4R,5R,6R*)-6-Benzyl-4,7,7-trimethyl-6-thioniabicyclo[3.2.1]octane trifluoromethanesulfonate ((-)-7)

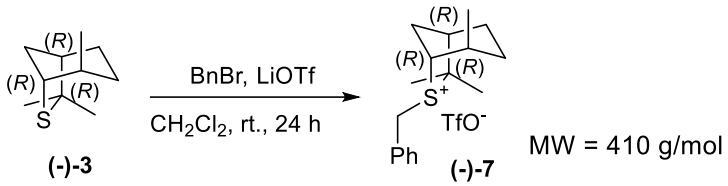

Using general procedure, (-)-isothiocineole **(-)-3** (1 eq., 10 mmol, 1.7 g, d = 1.00 g/mL, 1.78 mL), yielded sulfonium salt **(-)-7** as a white solid (3.20 g, 7.80 mmol, 72%).

$[\alpha]_D^{25}$ -144 (*c* 1.00, $CHCl_3$)

^{1}H NMR (400 MHz, $CDCl_3$): δ (ppm) 1.08 (d, 1H, *J* = 7.2 Hz), 1.50-1.80 (m, 4H, 2 x CH_2), 1.76 (s, 3H, CH_3), 1.80 (s, 3H, CH_3), 2.10 (m, 1H, C*H*Me), 2.39 (m, 2H, C*H*CS e C*H*H del ciclo), 2.72-2.76 (m, 1H, CH*H* del ciclo), 3.86 (m, 1H, C*H*S), 4.57 (d, 1H, *J* = 12.8 Hz, SC*H*H), 4.90 (d, 1H, *J* = 12.8 Hz, SCH*H*), 7.36 (m, 3H, ArH), 7.55-7-56 (m, 2H, ArH).

^{13}C-NMR (100 MHz, CDCl3): δ (ppm) 17.8 (CH3), 22.2 (CH2), 23.2 (CH3), 25.2 (CH2), 25.5 (CH3), 31.7 (CH2), 32.1 (CH), 42.2 (CH2), 50.5 (CH), 63.9 (CH), 72.5 (C), 120.9 (q, *J* = 321, CF3), 129.1 (C), 129.7 (CH), 129.8 (CH), 130.6 (CH).

(*1S,4S,5S,6S*)-6-Benzyl-4,7,7-trimethyl-6-thioniabicyclo[3.2.1]octane trifluoromethanesulfonate ((+)-7)

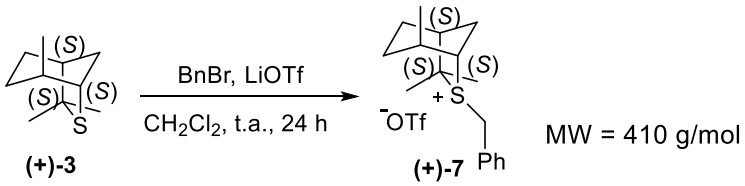

Using general procedure, (+)-isothiocineole **(+)-3** (1 eq., 4.1 mmol, 0.7 g, d = 1.00 g/mL, 0.74 mL), yielded sulfonium salt **(+)-7** as a white solid (1.58 g, 3.80 mmol, 94%).

$[\alpha]_D^{25}$ +140 (*c* 1.00, $CHCl_3$)

^{1}H NMR (400 MHz, $CDCl_3$): δ (ppm) 1.10 (d, 1H, *J* = 8.0 Hz), 1.50-1.72 (m, 4H, 2 x CH_2), 1.77 (s, 3H, CH_3), 1.80 (s, 3H, CH_3), 2.11 (m, 1H, C*H*Me), 2.38 (m, 2H, C*H*CS e C*H*H del ciclo), 2.73-2.77 (m, 1H, CH*H* del ciclo), 3.90 (m, 1H, CHS), 4.57 (d, 1H, *J* = 12.8 Hz, SC*H*H), 4.90 (d, 1H, *J* = 12.8 Hz, SCH*H*), 7.36 (m, 3H, ArH), 7.54-7-56 (m, 2H, ArH).

^{13}C-NMR (100 MHz, CDCl3): δ (ppm) 17.8 (CH3), 22.2 (CH2), 23.2 (CH3), 25.2 (CH2), 25.5 (CH3), 31.7 (CH2), 32.1 (CH), 42.2 (CH2), 50.5 (CH), 63.9 (CH), 72.5 (C), 120.9 (q, *J* = 321, CF3), 129.1 (C), 129.7 (CH), 129.8 (CH), 130.6 (CH).

(*1S,4S,5S,6S*)-6-(4-Bromobenzyl)-4,7,7-trimethyl-6-thioniabicyclo[3.2.1]octane trifluoromethanesulfonate ((+)-41)

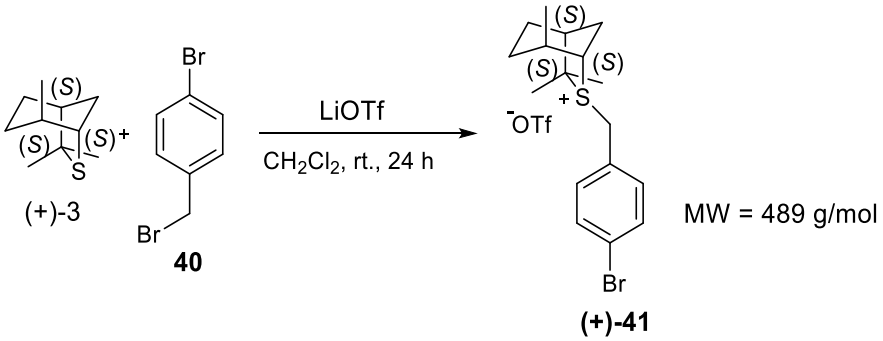

Using general procedure, (+)-isothiocineole **(+)-3** (1 eq, 5.72 mmol, 1.43 g, d = 1.00 g/mL, 1.43 mL), yielded sulfonium salt **(+)-41** as a white solid (1.47 g, 3.00 mmol, 52%).

^{1}H NMR (400 MHz, $CDCl_3$); δ (ppm) 1.10 (d, *J* = 7.0 Hz, 3H), 1.70-1.80 (m, 4H), 1.76 (s, 3H), 1.80 (s, 3H), 2.08 (brs, 1H), 2.38 (m, 2H), 2.76 (m, 1H), 3.76 (m, 1H), 4.55 (d, *J* = 12.5 Hz, 1H), 4.89 (d, *J* = 12.5 Hz, 1H), 7.43 (m, 4H).

2.7.1.8 Preparation of diaryloxiranes

General procedures

Method A: Sulfonium salt (1 eq.) was dissolved in a mixture of CH_3CN/*tert*-ButOH 15:1 (2 ml for every 0.37 mmol of sulfonium salt). Then the aldehyde (2 eq.) was added. The solution was then placed in a 0 °C bath and freshly ground KOH (1.1 eq.) was added. The solution was stirred at 0 °C overnight. CH_3CN/*tert*-ButOH was then evaporated under reduced pressure and CH_2Cl_2 (5 ml) and H_2O (5 ml) were added. The organic layer was separated and the aqueous layer was extracted with CH_2Cl_2 (2 × 5 ml). The organic phases were then combined, dried with Na_2SO_4 and the solvent evaporated under reduced pressure. Products were purified by column chromatography on silica gel at atmospheric pressure.

Method B: Sulfonium salt (2 eq.) was dissolved in CH_3CN. Then the aldehyde (1 eq.) was added. The solution was then placed in a 0 °C bath and K_2CO_3 (4 eq.) was added. The solution was stirred for 24-48h at room temperature. Then, the reaction mixture was evaporated under reduced pressure, dichloromethane (40 mL) was added and the resulted mixture was washed with water (3×20 mL). The organic layer was dried over sodium sulfate and the solvent removed to give a colourless oil, which was purified by column chromatography.

Method C: Sulfonium salt (2 eq.) was dissolved in CH_2Cl_2. Then the aldehyde (1 eq.) was added. The solution was then placed in a -30 °C bath and the 1,5,7-Triazabiciclo [4.4.0] dec-1-ene (TBD) (2.2 eq.) was added dropwise. The reaction was stopped with H_2O (2 x 20 mL) and extracted with CH_2Cl_2 (3 x 20 mL). The organic phases were then combined, dried with Na_2SO_4 and the solvent evaporated under reduced pressure. Products were purified by column chromatography on silica gel at atmospheric pressure.

***Trans rac* 2-(2-Ethoxymethoxy-phenyl)-3-phenyl-oxirane (rac-6b)** (MW = 270 g/mol) was obtained (202 mg, 0.75 mmol, 75%) by **method B** using **a** as sulfonium salt from 2-ethoxymethoxy benzaldehyde **5b** (210 mg, 1.0 mmol), as a pale yellow oil after purification by column chromatography at atmospheric pressure (5% Et_2O/EP).

R_f = 0.6 (5% Et_2O/EP).
^{1}H NMR (400 MHz, $CDCl_3$): δ (ppm) 1.17 (t, J = 6.8 Hz, 3H), 3.67 (q, J = 6.8 Hz, 2H), 3.80 (brs, 1H), 4.25 (brs, 1H), 5.23 (brs, 2H), 7.04 (dd, J_1 = $J2$ = 7.6 Hz, 1H), 7.15 (d, J = 8.0 Hz, 1H) 7.27 (dd, J_1 = J_2 = 7.6 Hz, 2H), 7.37 (m, 5H). ^{13}C NMR (100 MHz, $CDCl_3$): δ (ppm) 15.0, 58.2, 62.2, 64.3, 93.2, 114.0, 121.8, 124.9, 125.5, 126.3, 128.1, 128.4, 128.8, 137.3, 155.9. MS (m/z, %): 270.10 [M+] (0.3), 91.10 (100). IR (CCl_4, cm^{-1}), 2990, 2978, 2861, 1486, 1452, 701, 695.

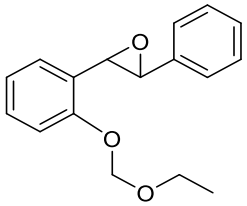

***trans* rac-6b**

***Cis rac* 2-(2-Ethoxymethoxy-phenyl)-3-phenyl-oxirane (rac-6b)** (MW = 270 g/mol) was obtained (41 mg, 0.15 mmol, 15%) by **method B** using **5** as sulfonium salt from 2-ethoxymethoxy benzaldehyde **5b** (210 mg, 1.0 mmol), as a pale yellow oil after purification by column chromatography at atmospheric pressure (5% Et_2O/EP).

R_f = 0.5 (5% Et_2O/EP).
^{1}H NMR (400 MHz, $CDCl_3$): δ (ppm) 1.15 (t, J = 6.8 Hz, 3H), 3.51 (q, J = 6.8 Hz, 2H), 4.40 (A of AB system, J_{AB} = 4.0 Hz, 1H), 4.45 (B of AB system, J_{AB} = 4.0 Hz, 1H), 5.03 (A of AB system, J_{AB} = 7.2 Hz, 1H), 5.17 (B of AB system, J_{AB} = 7.2 Hz, 1H), 6.89 (dd, $J_1 = J_2$ = 7.2 Hz, 1H), 6.96 (d, J = 8.4 Hz, 1H), 7.14 (m, 6H), 7.32 (d, J = 7.2 Hz, 1H). ^{13}C NMR (100 MHz, $CDCl_3$): δ (ppm) 15.0, 57.6, 59.3, 64.0, 92.8, 113.2, 120.8, 123.5, 126.5, 127.3, 127.4, 128.3, 128.5, 134.8, 155.2.

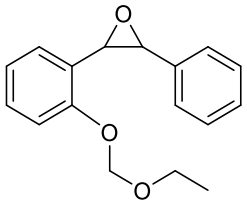

cis rac-6b

***Trans rac* 2-(2-Ethoxymethoxy-5-methoxy-phenyl)-3-phenyl-oxirane (rac-16)** (MW = 300 g/mol) was obtained (240 mg, 0.8 mmol, 80%) by **method B** using **5** as sulfonium salt, from 2-ethoxymethoxy-5-methoxybenzaldehyde **20** (289 mg, 1.0 mmol) as oil after column chromatography at atmospheric pressure (5% EtOAc/PE).

R_f = 0.4 (5% EtOAc/PE)

^{1}H NMR (400 MHz, $CDCl_3$): δ (ppm) 1.17 (t, J = 7.1 Hz, 3H), 3.66 (q, J = 7.1Hz, 2H), 3.79 (d, J = 2.0 Hz, 1H), 3.81 (s, 3H), 4.24 (d, J = 2.0 Hz, 1H), 5.15 (A of AB system, J_{AB} = 6.7 Hz, 1H), 5.16 (B of AB system, J_{AB} = 6.7 Hz, 1H), 6.83 (m, 2H), 7.09 (d, J = 8.5 Hz, 1H), 7.38 (m, 5H). ^{13}C NMR (100 MHz, $CDCl_3$): δ (ppm) 15.0, 55.6, 58.3, 62.4, 64.2, 94.2, 110.0, 114.2, 116.2, 125.6, 127.8, 128.2, 128.4, 137.2, 150.0, 154.9.

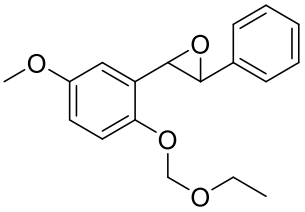

rac-16

***Trans* (2*R*,3*R*)-16** was obtained (204 mg, 0.68 mmol, 68% yield) by **method A** using **(-)-7** as sulfonium salt (410 mg, 1.0 mmol).
$[\alpha]_D^{25}$ -92 (c 1.00 CH_2Cl_2) 90% *ee*. HPLC conditions: Chiralpak IA column, 10% *i*PrOH/n-hexane, 1 mL/min; t_R = 5.60 min.

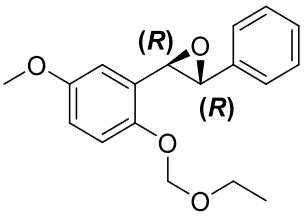

(2*R*,3*R*)-16

***Trans rac* 2-(2-Ethoxymethoxy-3-methoxy-phenyl)-3-phenyl-oxirane (rac-17)** (MW = 300 g/mol) was obtained (234 mg, 0.78 mmol, 78%) by **method B** using **5** as sulfonium salt, from 2-ethoxymethoxy-3-methoxybenzaldehyde **21** (289 mg, 1.0 mmol) as oil after column chromatography at atmospheric pressure (30% Et_2O/EP).

R_f = 0.6 (30% Et_2O/EP).

^{1}H NMR (400 MHz, $CDCl_3$): δ (ppm) 0.95 (t, *J* = 7.1 Hz, 3H), 3.55 (m, 2H), 3.82 (d, *J* = 1.9 Hz, 1H), 3.85 (s, 3H), 4.33 (d, *J* = 1.9 Hz, 1H), 5.13 (m, 2H), 6.90 (m, 2H), 7.20 (m, 6H). ^{13}C NMR (100 MHz, $CDCl_3$): δ(ppm) 14.7, 55.7, 58.7, 62.3, 65.4, 97.5, 111.8, 116.5, 124.6, 125.5, 126.8, 128.2, 128.4, 131.5, 137.1, 151.9.

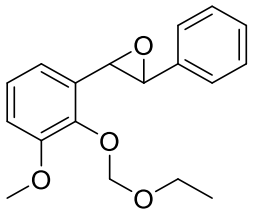

rac-17

***Trans rac* 2-(2-bromo-6-(ethoxymethoxy)-4-methoxyphenyl)-3-(4-bromophenyl)-oxirane (rac-29)** (MW = 458 g/mol) was obtained (278 mg, 0.61 mmol, 45%) by **method B** using **38** as sulfonium salt, from 2-bromo-6-(ethoxymethoxy)-4-methoxybenaldehyde **35b** (390 mg, 1.35 mmol) as oil after column chromatography at atmospheric pressure (30 % Et_2O/Hexane).

R_f = 0.45 (30 % Et_2O/Hexane).

^{1}H NMR (400 MHz, $CDCl_3$): δ (ppm) 1.22 (t, J = 7.2 Hz, 3H), 3.77 (m, 6H), 4.06 (brs, 1H), 5.27 (brs, 2H), 6.71 (brs, 1H), 6.78 (brs, 1H), 7.31 (brd, J = 6.1 Hz, 2H), 7.50 (brd, J = 6.1 Hz, 2H). ^{13}C NMR (100 MHz, $CDCl_3$); δ (ppm) 15.0, 55.5, 59.5, 60.1, 64.6, 93.5, 101.3, 110.8, 118.1, 121.9, 124.7, 127.3, 131.5, 136.5, 157.9, 160.6.

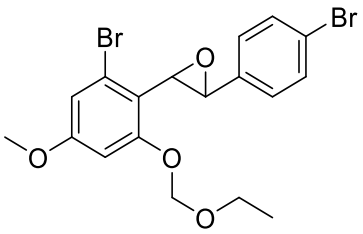

rac-29

***Trans* (2*S*,3*S*)-29** was obtained (165 mg, 0.36 mmol, 60% yield) by **method C** using **(+)-41** as sulfonium salt from 2-bromo-6-(ethoxymethoxy)-4-methoxybenaldehyde **35b** (174 mg, 0.6 mmol).

$[\alpha]_D^{25}$ = +105 (c 1.2, CH_2Cl_2). 90% *ee*, HPLC conditions: Chiralpak IA column, 5% *i*PrOH/Esano. 1.0 mL/min, t_R

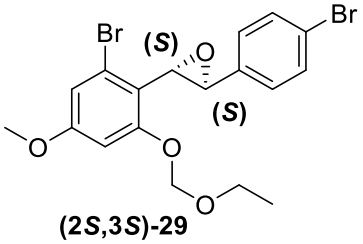

(2*S*,3*S*)-29

***Trans rac* 2-(4-bromo-2-(ethoxymethoxy)-6-methoxyphenyl)-3-phenyloxirane (rac-28)** (MW = 379 g/mol) was obtained (164 mg, 0.43 mmol, 58%) by **method B** using **5** as sulfonium salt, from 4-bromo-2-(ethoxymethoxy)-6-methoxybenaldehyde **35a** (221 mg, 0.76 mmol) as oil after column chromatography at atmospheric pressure (40% Et_2O/EP).

R_f = 0.6 (40% Et_2O/EP).

^{1}H NMR (400 MHz, $CDCl_3$); δ (ppm) 1.16 (t, J = 7.2 Hz, 3H), 3.08 (s, 3H), 3.29 (m, 1H), 3.43 (m, 1H), 4.07 (d, J = 2.0 Hz, 1H), 4.45 (d, J = 2.0 Hz, 1H), 6.59 (brs, 1H), 7.20 (brs, 5H), 7.47 (brs, 1H). ^{13}C NMR (100 MHz, $CDCl_3$); δ (ppm) 15.5, 55.9, 57.3, 59.4, 65.2, 94.1, 109.3 (2C), 112.1, 123.8, 126.4, 128.6, 129.2, 139.6, 159.0, 160.9.

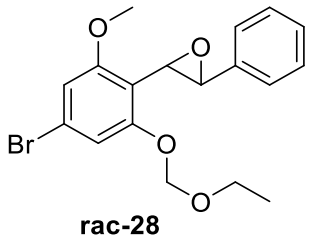

rac-28

***Trans* (2*S*,3*S*)-28** was obtained (50 mg, 0.13 mmol, 49% yield) by **method A** using **(+)-7** as sulfonium salt (90 mg, 0.22 mmol).

$[\alpha]_D^{25}$ = +95 (c 1.2, CH2Cl2). 90% *ee*, HPLC conditions: Chiralpak IA column, 5% *i*PrOH/Esano. 1.0 mL/min, t_R

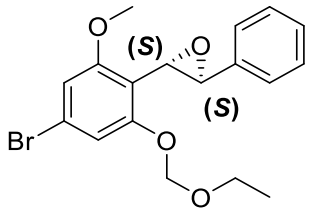

(2*S*,3*S*)-28

***Trans* (*E*)-2-(4-bromophenyl)-3-(2-(ethoxymethoxy)-6-methoxy-4-(4-methoxystyryl)-phenyloxirane 52** (MW = 511 g/mol) was obtained (33 mg, 0.06 mmol, 26% yield) by **method C** using **38** as sulfonium salt from (*E*)-2-(ethoxymethoxy)-6-methoxy-4-(4-methoxystyryl)benzaldehyde **51** (96 mg, 0.25 mmol), as oil after column chromatography at atmospheric pressure (40% EtOAc/EP).

R_f = 0.44 (40% EtOAc/EP).

^{1}H NMR (400 MHz, $CDCl_3$); δ (ppm) 1.20 (t, *J* = 4 Hz, 3H), 3.47 (m, 2H), 3.7 (s, 3H), 3.84 (s, 3H) 4.15 (m, 1 H), 4.89 (m, 2H), 4.93 (m, 1H), 6.67 (s, 1H), 6.83 (s, 1H), 6.89 (d, *J* = 24 Hz, 1H), 6.90 (s, 1H), 7.0 (s, 1H), 7.02 (d, *J* = 24 Hz, 1H), 7.29 (d, *J* = 8.0 Hz, 2H), 7.45 (d, *J* = 8.0 Hz, 2H). ^{13}C NMR (100 MHz, $CDCl_3$) δ (ppm) 15.1, 55.3, 55.5, 73.1, 93.3, 102.2, 105.6, 114.2, 123.0, 127.8, 128.7, 129.0, 129.6, 130.4, 139.3, 156.1, 158.0, 159.5.

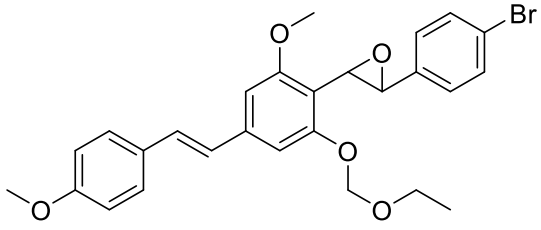

52

2.7.1.9 Ring opening arylation of trans 2,3-diaryloxiranes

General procedures

Method A: 1.0 mol.L^{-1} solution of Et_2Zn (3 eq,) was slowly added to a solution of arylboronic acid (1.1 eq.) in dry toluene under inert atmosphere. The mixture was stirred at 60 °C for 1 h and cooled to room temperature. Then, a solution of the diaryloxirane (1 eq.) in toluene (5 mL) was added and the reaction was stirred at room temperature for 30 min-3 h. The reaction was quenched with 5 mL of saturated NH_4Cl solution and extracted with ethyl acetate (2×30 mL). The combined extracts were washed with brine, dried with Na_2SO_4 and evaporated under reduced pressure. The product was purified by column chromatography on silica gel at atmospheric pressure.

Method B: 1.0 mol.L^{-1} solution of Et_2Zn (6 eq.) was slowly added to a solution of arylboronic acid (2.2 eq.) in dry toluene under inert atmosphere. The mixture was stirred at 60 °C for 1 h and cooled to room temperature. Then, a solution of the diaryloxirane (1 eq.) in toluene (5 mL) was added and the reaction was stirred at 60 °C for 3 h. The reaction was quenched with 5 mL of saturated NH_4Cl solution and extracted with ethyl acetate (2×30 mL). The combined extracts were washed with brine, dried with Na_2SO_4 and evaporated under reduced pressure. The product was purified by column chromatography.

Method C: 1.0 mol.L^{-1} solution of Et_2Zn (10 eq.) was slowly added to a solution of arylboronic acid (3 eq.) in dry toluene under inert atmosphere. The mixture was stirred at 60 °C for 1 h and cooled to room temperature. Then, a solution of the diaryloxirane (1 eq.) in toluene (5 mL) was added and the reaction was stirred at 60 °C for 3 h. The reaction was quenched with 5 mL of saturated NH_4Cl solution and extracted with ethyl acetate (2×30 mL). The combined extracts were washed with brine, dried with Na_2SO_4 and evaporated under reduced pressure. The product was purified by column chromatography.

***Syn* 2-(2-ethoxymethoxy-phenyl)-1-phenyl-2-(3-trifluoromethyl-phenyl)-ethanol (*syn*-15b)**

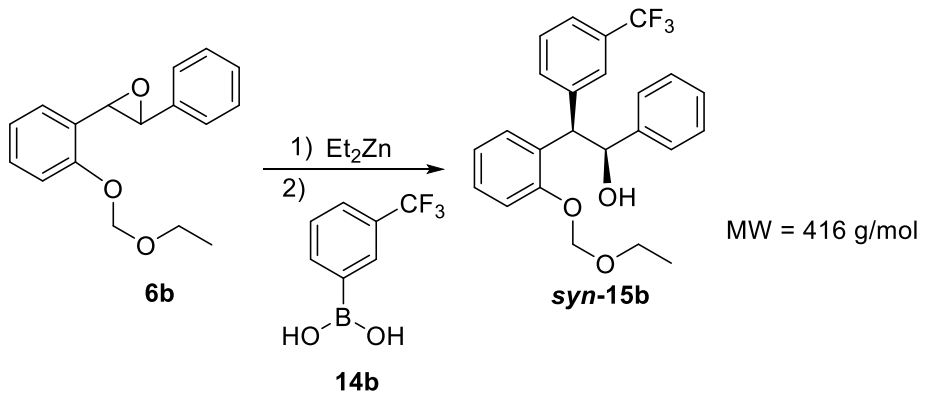

Method A: product **15 b** was obtained (15 mg, 0.04 mmol, 10%) from 3-trifluorophenyl bornic acid **14b** and *trans rac* 2-(2-Ethoxymethoxy-phenyl)-3-phenyl-oxirane **6b** (100 mg, 0.37 mmol).

Method B: product **15 b** was obtained (25 mg, 0.06 mmol, 20%) from 3-trifluorophenyl bornic acid **14b** and *trans rac* 2-(2-Ethoxymethoxy-phenyl)-3-phenyl-oxirane **6b** (80 mg, 0.30 mmol).

Method C: product **15 b** was obtained (73 mg, 0.18 mmol, 55%) from 3-trifluorophenyl bornic acid **14b** and *trans rac* 2-(2-Ethoxymethoxy-phenyl)-3-phenyl-oxirane **6b** (87 mg, 0.32 mmol).

R_f = 0.57 (20% EtOAc/EP)
^{1}H NMR (400 MHz, $CDCl_3$): δ (ppm) 1.23 (t, J = 7.1 Hz, 3H), 1.60 (brs, 1H), 3.42 (m, 2H), 4.81 (d, J = 8.0 Hz, 1H), 4.93 (A of AB system, J_{AB} = 6.9 Hz, 1H), 5.00 (B of AB system, J_{AB} = 6.9 Hz, 1H), 5.49 (d, J = 8.0 Hz, 1H), 6.92 (m, 2H), 7.07 (m, 2H), 7.21 (m, 4H), 7.37 (m, 3H), 7.55 (m, 1H), 7.62 (m, 1H). ^{13}C NMR (100 MHz, $CDCl_3$): δ (ppm) 14.9, 51.7, 64.0, 75.8, 92.8, 114.1, 121.5, 123.2, 126.2, 126.6, 127.6, 127.7 (q, $^1J_{C\text{-}F}$ = 270 Hz), 127.9, 128.0, 128.5, 128.8, 128.9 (q, $^2J_{C\text{-}F}$ = 31 Hz), 130.2, 132.6, 142.1, 142.4, 154.4. MS (m/z, %): 398 (6), 310 (7), 309 (9), 265 (11), 251 (16), 249 (11), 107 (100). IR (CCl_4, cm^{-1}), 3604, 2961, 2930, 1739, 1330, 1269, 1126, 1161, 1009, 700.

HSQC

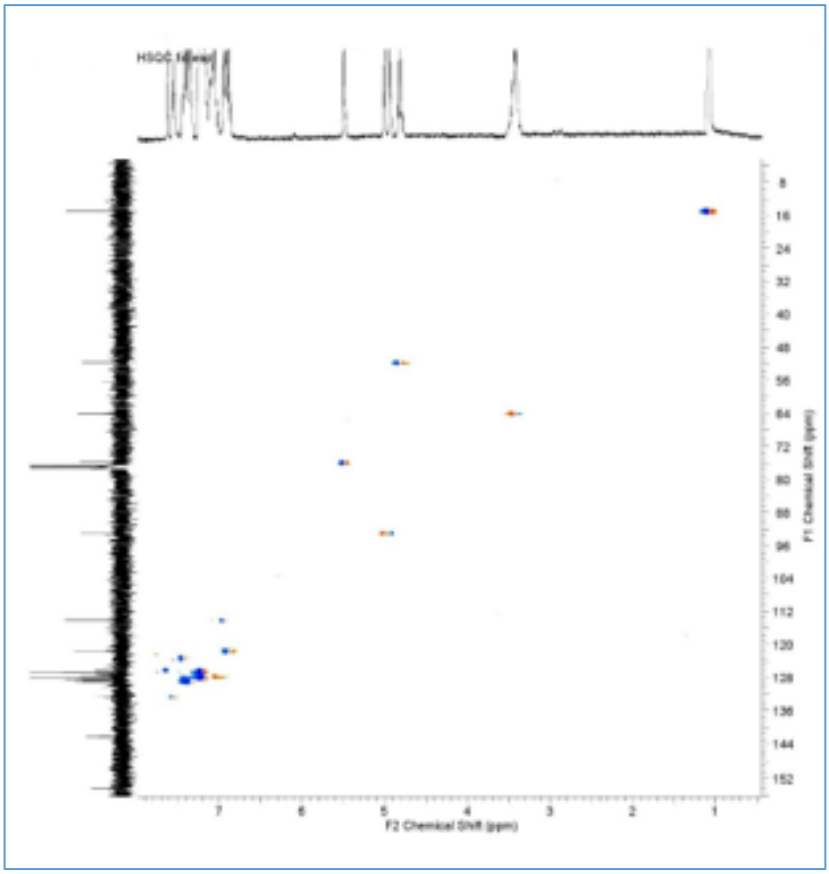
F2 Chemical Shift (ppm)
F1 Chemical Shift (ppm)

HMBC

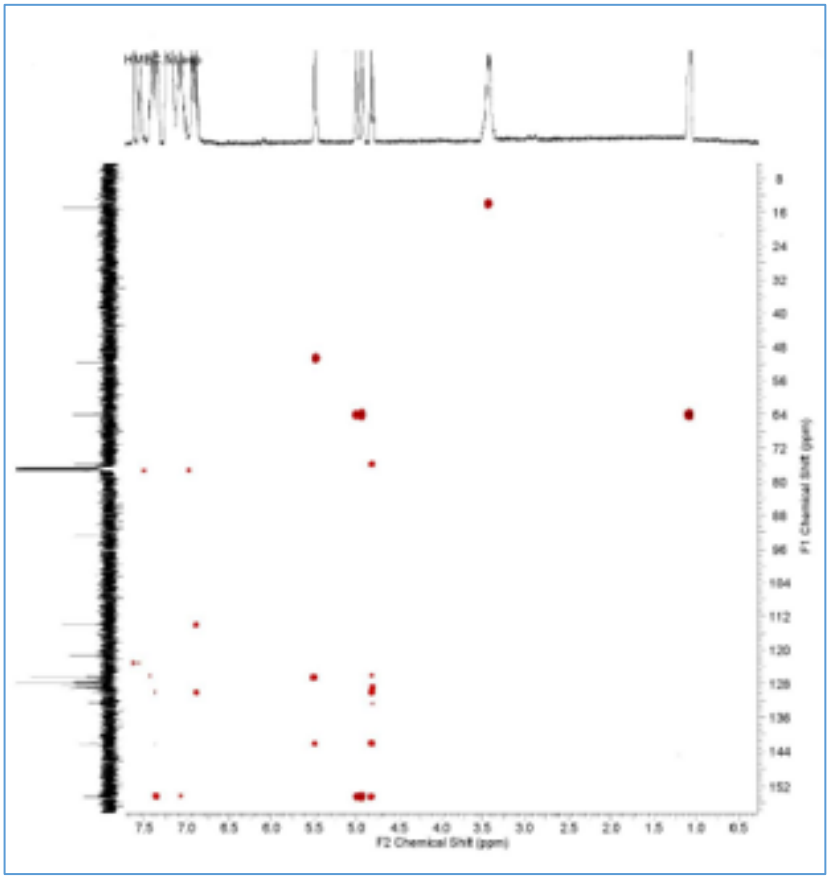
F2 Chemical Shift (ppm)
F1 Chemical Shift (ppm)

***Syn* and *anti* 2-(2-ethoxymethoxy-phenyl)-2-(3-fluorophenyl)-1-phenyl--ethanol (15d)**

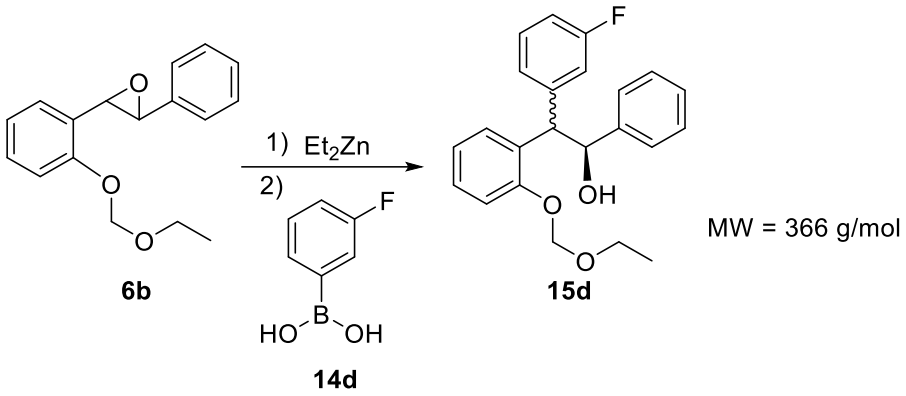

Method A: product ***syn*-15d** was obtained (20 mg, 0.05 mmol, 15%) from 3-fluorophenyl bornic acid **14d** and *trans rac* 2-(2-Ethoxymethoxy-phenyl)-3-phenyl-oxirane **6b** (100 mg, 0.37 mmol).

Method B: product ***syn*-15d** was obtained (27 mg, 0.07 mmol, 20%) from 3-fluorophenyl bornic acid **14d** and *trans rac* 2-(2-Ethoxymethoxy-phenyl)-3-phenyl-oxirane **6b** (100 mg, 0.37 mmol).

Method C: ***syn*-** and ***anti*-15d** as a mixture (80:20) was obtained (49 mg, 0.14 mmol, 50%) from 3-fluorophenyl bornic acid **14d** and *trans rac* 2-(2-Ethoxymethoxy-phenyl)-3-phenyl-oxirane **6b** (70 mg, 0.26 mmol).

R_f =0.3 (30% Et_2O/EP)
^{1}H NMR (400 MHz, $CDCl_3$): δ (ppm) 1.09 (t, J = 7.1 Hz, 3H), 1.70 (brs, 1H), 3.45 (m, 2H), 4.66 (d, J = 9.39 Hz, 1H, *anti* minor) 4.79 (d, J = 8.2 Hz, 1H, *syn* major), 4.89 (A of AB system, J_{AB} = 7.0 Hz, 1H, *syn* major), 4.98 (B of AB system, J_{AB} = 7.0 Hz, 1H, *syn* major), 5.03 (A of AB system, J_{AB} = 6.6 Hz, 1H, *anti* minor) 5.09 (B, of AB system, J_{AB} = 6.6 Hz, 1H, *anti* minor) 5.41 (brd, J = 8.2 Hz, 1H, *syn* major and 1H, *anti* minor overlapped), 6.90 (m, 2H), 7.15 (m, 10H), 7.36 (m, 1H). ^{13}C NMR (100 MHz, $CDCl_3$): δ (ppm) 14.1 (*syn*), 15.0 (*anti*), 51.4 (*syn*), 51.6 (*anti*), 64.0 (*syn*), 64.1 (*anti*), 75.5 (*anti*), 76.0 (*syn*), 92.9 (*anti*), 93.0 (*syn*), 113.4 (d, $^2J_{C\text{-}F}$ = 21.2 Hz) (*syn*), 113.7 (d, $^2J_{C\text{-}F}$ = 21.2 Hz) (*anti*), 114.16 (d, $^2J_{C\text{-}F}$ = 21.2 Hz) (*anti*), 114.17 (*syn*), 114.8 (*anti*), 116.2 (d, $^2J_{C\text{-}F}$ = 21.2 Hz) (*syn*), 121.4 (*syn*), 121.8 (*anti*), 122.6 (d, $^4J_{C\text{-}F}$ = 2.3 Hz) (*anti*), 124.9 (d, $^4J_{C\text{-}F}$ = 2.3 Hz) (*syn*), 126.3 (*anti*), 126.7 (*syn*), 126.8 (*anti*), 127.5 (*anti*), 127.9 (*syn*), 128.6 (*syn*), 128.91 (d, $^3J_{C\text{-}F}$ = 9.0 Hz) (*anti*), 128.97 (*syn*), 129.1 (*syn*), 129.6 (d, $^3J_{C\text{-}F}$ = 8.4 Hz) (*syn*), 130.40 (*syn*), 130.47 (*anti*), 140.5 (*anti*), 142.4 (*syn*), 143.8 (d, $^3J_{C\text{-}F}$ = 6.8 Hz) (*syn*), 143.8 (d, $^3J_{C\text{-}F}$ = 6.9 Hz) (*anti*), 154.4 (*syn*), 155.4 (*anti*), 162.5 (d, $^1J_{C\text{-}F}$ = 244.2 Hz) (*anti*), 162.8 (d, $^1J_{C\text{-}F}$ = 244.2 Hz) (*syn*).

HSQC

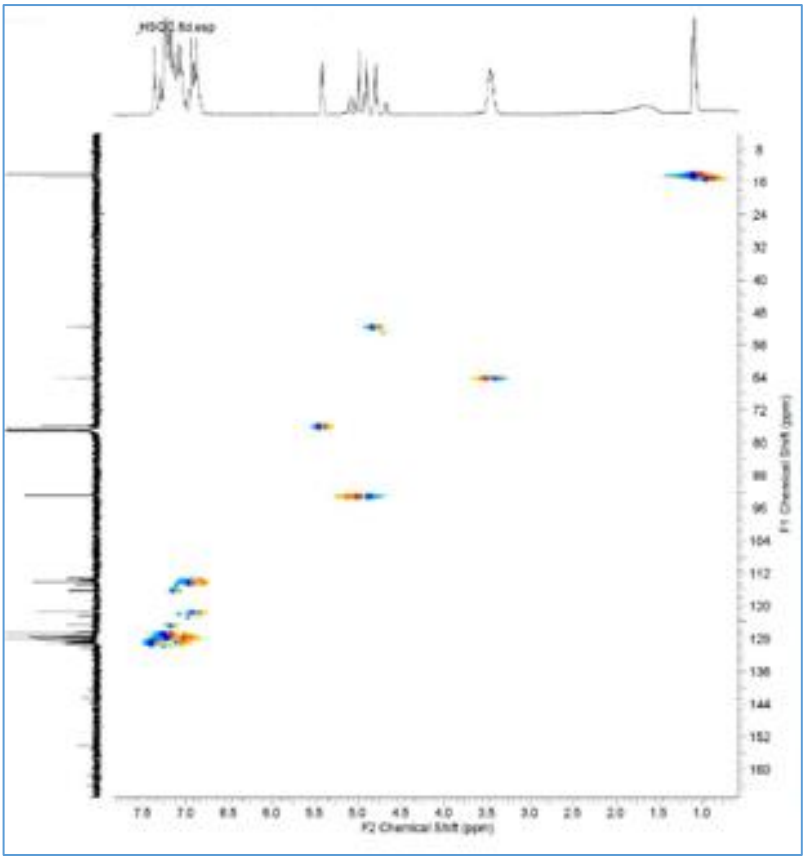

HMBC

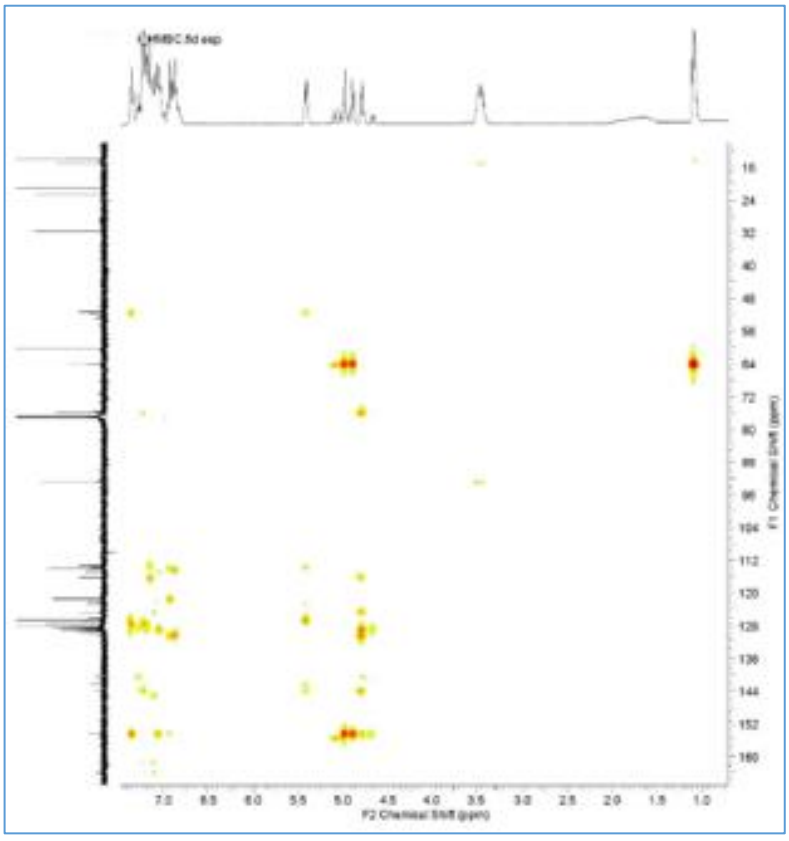

***Syn* 2-(4-Bromo-phenyl)-2-(2-ethoxymethoxy-phenyl)-1-phenyl-ethanol (*syn*-15e)**

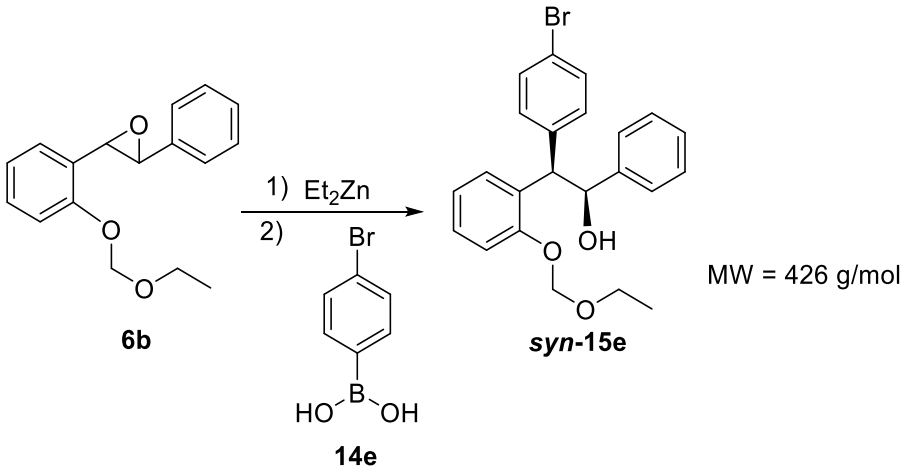

Product **15e** was obtained (277 mg, 0.65 mmol, 65%) by **method C** from 4-bromophenyl boronic acid **14e** and *trans rac* 2-(2-Ethoxymethoxy-phenyl)-3-phenyl-oxirane **6b** (270 mg, 1.0 mmol).

R_f = 0.2 (20% Et_2O/EP)
^{1}H NMR (400 MHz, $CDCl_3$): δ (ppm) 1.13 (t, J = 7.1 Hz, 3H), 3.47 (m, 2H), 4.78 (d, J = 7.8 Hz, 1H), 4.93 (A of AB system, J_{AB} = 7.0 Hz, 1H), 5.00 (B of AB system, J_{AB} = 7.0 Hz, 1H), 5.44 (d, J = 7.8 Hz, 1H), 6.92 (dd, *J1* = *J2* = 7.4 Hz, 1H), 6.96 (d, J = 8.4 Hz, 1H), 7.10 (dd, J_1 = J_2 = 7.4 Hz, 1H), 7.24 (m, 8H), 7.40 (m, 2H). ^{13}C NMR (100 MHz, $CDCl_3$): δ (ppm) 15.0, 51.0, 64.0, 75.8, 92.9, 114.1, 120.3, 121.4, 126.6, 127.5, 127.7, 127.9, 128.9, 130.5, 131.0, 131.2, 140.0, 142.4, 154.4. MS (m/z, %): 410 (3), 408 (3), 353 (4), 351 (4), 277 (7), 275 (7), 263 (8), 261 (8), 107 (100). IR (CCl_4, cm^{-1}), 3609, 3452, 2978, 2873, 1739, 1491, 1452, 1217, 987, 691.

HSQC

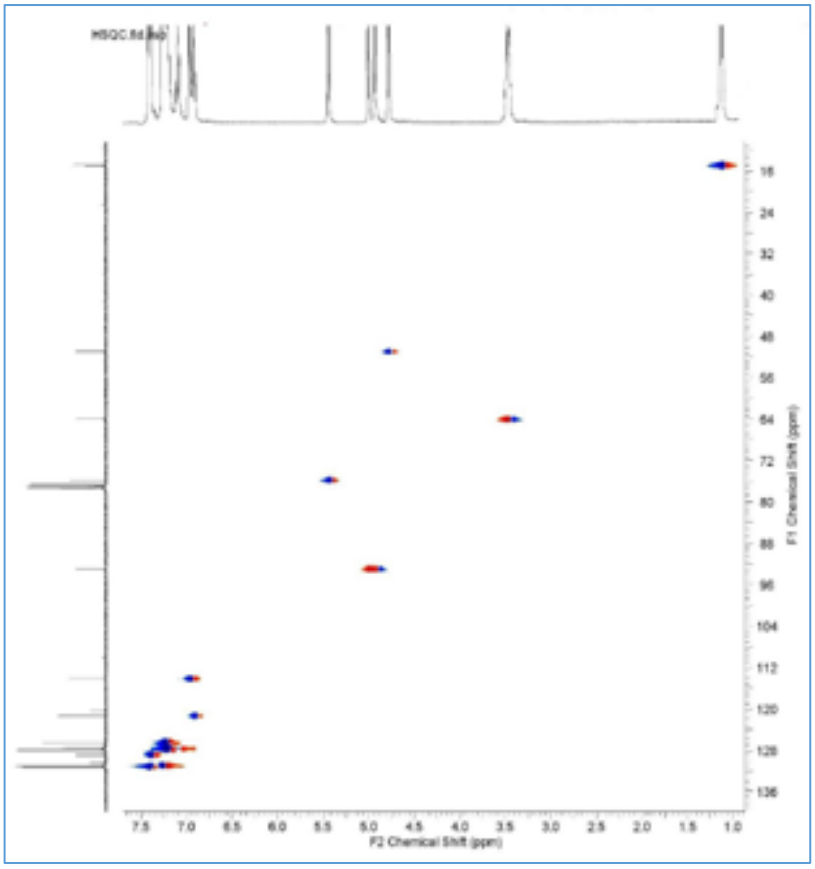
F2 Chemical Shift (ppm)
F1 Chemical Shift (ppm)

HMBC

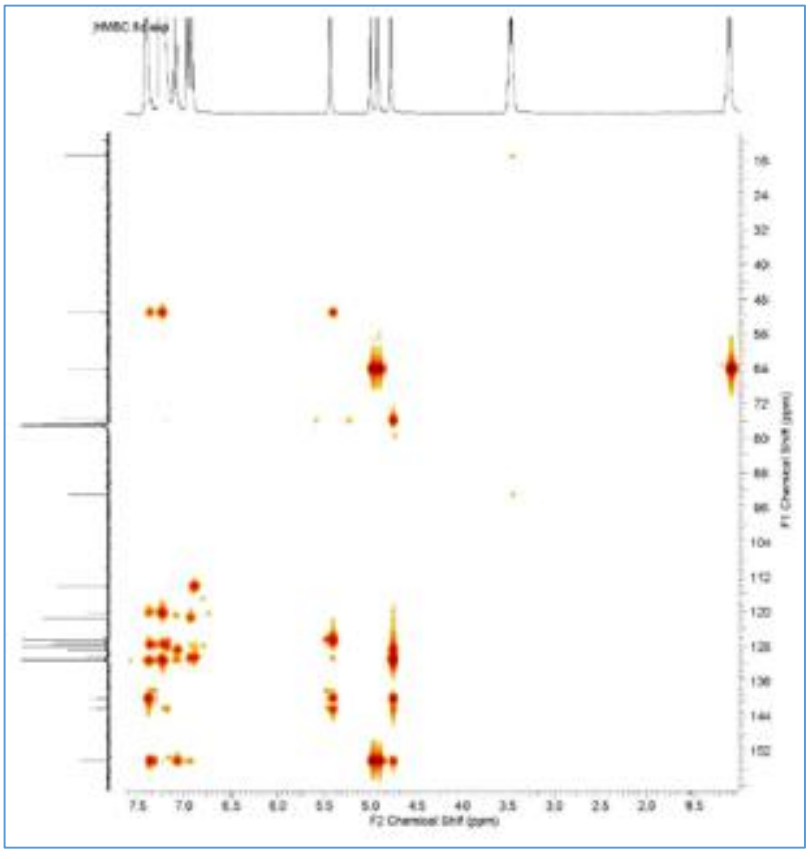
F2 Chemical Shift (ppm)
F1 Chemical Shift (ppm)

***Syn* 2-Benzo[*b*]thiophen-3-yl-2-(2-ethoxymethoxy-phenyl)-1-phenyl-ethanol (*syn*-15f)**

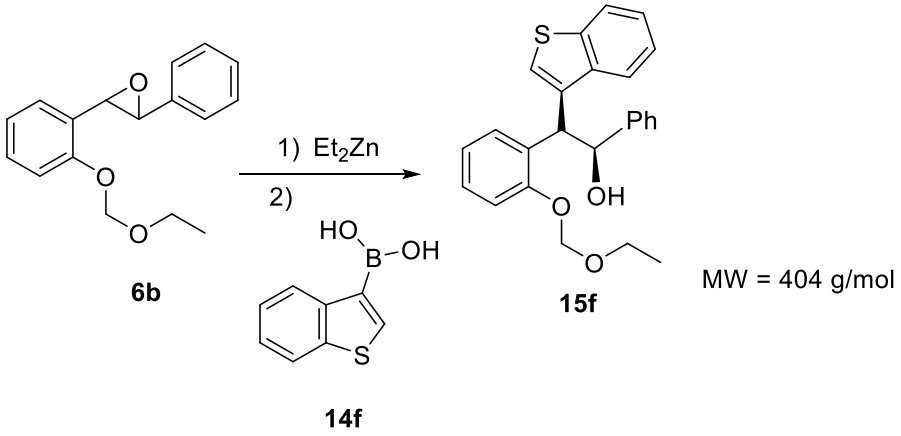

Products **15f** was obtained (242 mg, 60%) by **method C** from 3-benzothienyl boronic acid **14f** and *trans rac* 2-(2-Ethoxymethoxy-phenyl)-3-phenyl-oxirane **6b** (270 mg, 1.0 mmol).

R_f = 0.3 (20% Et_2O/EP).
^{1}H NMR (400 MHz, $CDCl_3$): δ (ppm) 1.20 (t, J = 7.0 Hz, 3H), 3.55 (m, 1H), 3.69 (m, 1H), 4.83 (A of AB system, J_{AB} = 7.0 Hz, 1H), 5.02 (B of AB system, J_{AB} = 7.0 Hz, 1H), 5.30 (d, J = 7.9 Hz, 1H), 5.41 (d, J = 7.9 Hz, 1H), 6.84 (dd, J_1 = J_2 = 7.4 Hz, 1H), 6.99 (d, J = 7.8 Hz, 1H), 7.06 (m, 2H), 7.20 (m, 7H), 7.64 (d, J = 7.8 Hz, 1H), 7.72 (s, 1H), 7.81 (d, J = 7.4 Hz, 1H). ^{13}C NMR (100 MHz, $CDCl_3$): δ (ppm) 15.1, 45.2, 64.1, 76.7, 93.5, 114.1, 121.5, 122.0, 122.5, 122.6, 124.2, 126.5, 127.2, 127.6, 127.9, 129.0, 129.4, 135.5, 139.5, 140.0, 142.1, 154.8.

Syn and ***anti*** **2-(2-Ethoxymethoxy-phenyl)-2-(3-methoxy-phenyl)-1-phenyl-ethanol 15h and 1-(2-Ethoxymethoxy-phenyl)-2-(3-methoxy-phenyl)-2-phenyl-ethanol**

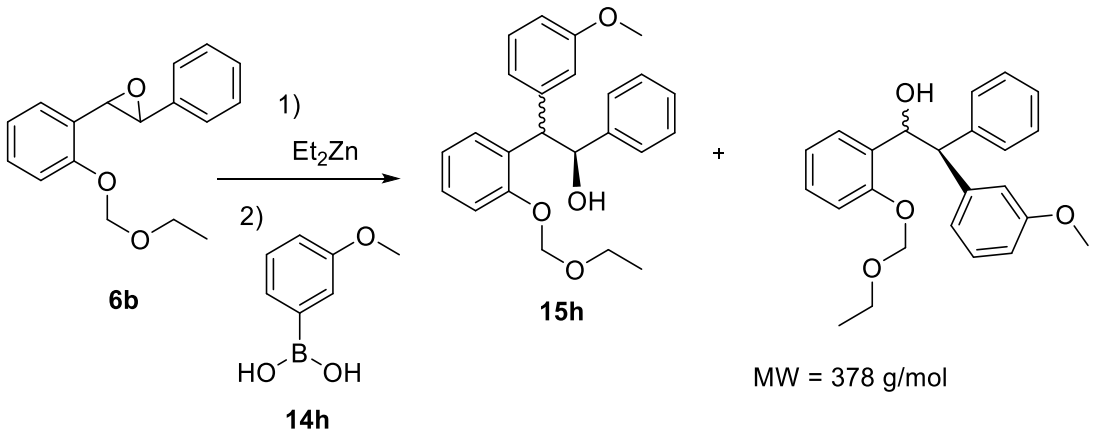

Products ***syn*-** and ***anti*-15h** and the regioisomer were obtained (230 mg, 61%) by **method C** from 3-methoxyphenyl boronic acid **14h** and *trans rac* 2-(2-Ethoxymethoxy-phenyl)-3-phenyl-oxirane **6b** (270 mg, 1.0 mmol), as oil mixture.

^{1}H NMR (400 MHz, $CDCl_3$): δ (ppm) 1.12 (m, 3H), 2.08 (brs, 1H), 3.49 (m, 2H), 3.69 (s, 3H), 3,70 (s, 3H), 3.78 (s, 3H), 4.73 (d, J = 9.1 Hz, 1H, *anti*), 4.83 (d, J = 8.2 Hz, 1H, *syn*, overlapped to d, J = 8.2 Hz, 1H, regioisomer), 4.87 (A of AB system, J_{AB} = 6.7 Hz, 1H, regioisomer), 4.92 (A of AB system, J_{AB} = 7.1 Hz, 1H, *syn*), 4.98 (B of AB system, J_{AB} = 7.1 Hz, 1H, *syn*), 5.00 (B of AB system, J_{AB} = 6.7 Hz, 1H, regioisomer), 5.05 (A of AB system, J_{AB} = 6.9 Hz, 1H, *anti*), 5.12 (B of AB system, J_{AB} = 6.9 Hz, 1H, *anti*), 5.43 (m, 1H, overlapping of *syn*, *anti* and regioisomer), 6.76 (m, 2H), 6.93 (m, 2H), 7.08 (m, 3H), 7.22 (m, 3H), 7.31 (m, 1H), 7.42 (m, 2H). ^{13}C NMR (100 MHz, $CDCl_3$): characteristic signals δ (ppm) 14.96, 14.99, 15.2 (3x*C*H_3CH_2), 51.6 (CH-Ar, *syn*), 52.6 (CH-Ar *anti*), 55.09, 55.11, 55.2 (3xOCH3), 64.0 (O*C*H_2CH_3, *syn*), 64.1 (O*C*H2CH3, *anti*), 65.8 (O*C*H_2CH_3, regioisomer), 76.0, 76.1, 76.3 (3xCHOH), 92.96, 92.99, 93.0 (3xOCH2O), 130.0, 130.7, 131.0, 140.9, 141.4, 142.3, 142.6, 144.1, 144.2 (9xCq), 154.46, 154.49, 155.4 (3x*C*ArOCH_2O), 159.16, 159.18, 159.6 (3x*C*ArOCH_3).

HSQC

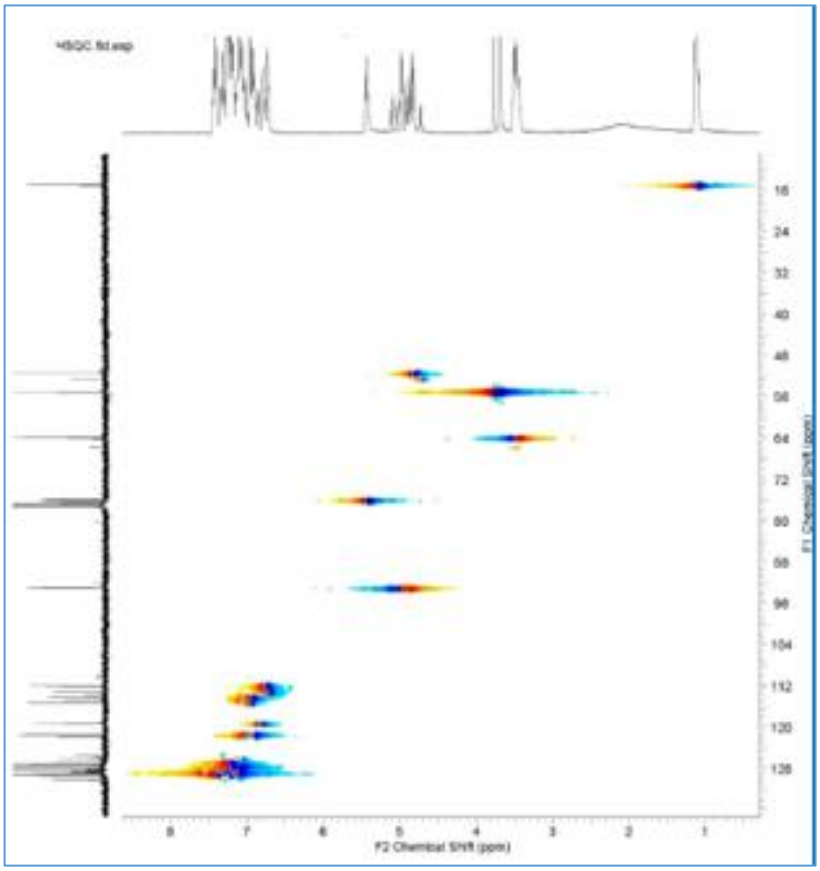

HMBC

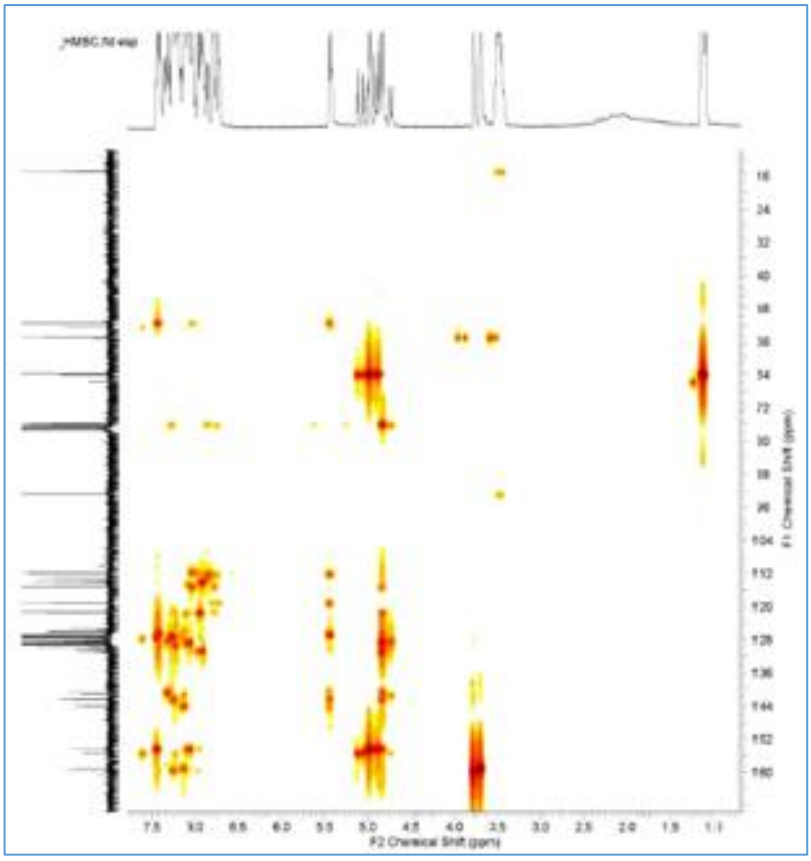

***Syn* 2-(2-ethoxymethoxy-5-methoxy-phenyl)-1,2-diphenylethanol (*syn*-22a)**

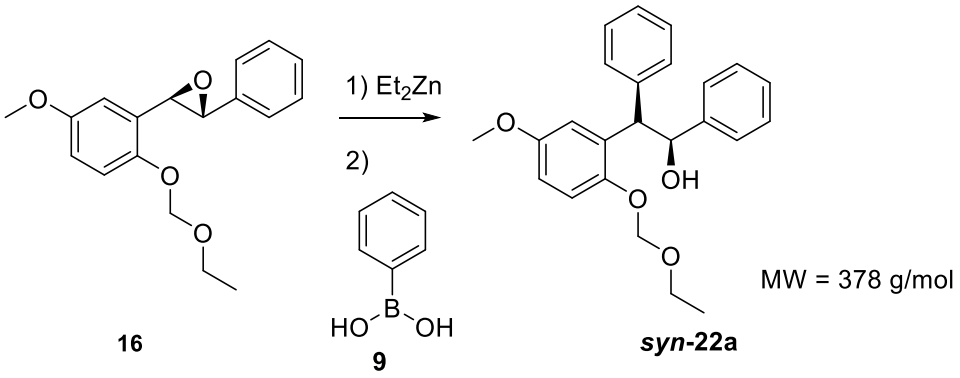

Product **rac *syn*-22a** was obtained (302 mg, 80% yield) by **method C** from phenylboronic acid **9** and *trans* 2-(2-Ethoxymethoxy-5-methoxy-phenyl)-3-phenyl-oxirane **rac-16** (300 mg, 1.0 mmol).

R_f = 0.5 (40% Et_2O/EP).

^{1}H NMR (400 MHz, $CDCl_3$): δ (ppm) 1.14 (t, J = 7.1 Hz, 3H), 2.29 (brs, 1H), 3.50 (q, J = 7.2 Hz, 2H), 4.73 (A part of AB system, J_{AB} = 7.1 Hz, 1H), 4.82 (d, J = 8.5 Hz, 1H), 4.86 (B part of AB system, J_{AB}, 7.1 Hz, 1H), 5.42 (d, J = 8.5 Hz, 1H), 6.59 (dd, J_1 = 8.6 Hz, J_2 = 2.5 Hz, 1H), 6.90 (d, J = 8.6 Hz, 1H), 7.03 (brs, 1H),7.18-7.33 (m, 8H), 7.42 (m, 2H). ^{13}C NMR (100 MHz, $CDCl_3$): δ (ppm) 15.0, 51.7, 55.6, 63.8, 76.2, 93.9, 111.4, 115.5, 115.7, 126.7, 126.8, 127.4, 127.9, 128.5, 129.1, 132.4, 140.7, 142.4, 148,9, 154.1.

***Syn*-(1*S*,2*R*)-2-(2-ethoxymethoxy-5-methoxy-phenyl)-1,2-diphenylethanol, ((1*S*,2*R*)-22a)** was obtained (306 mg, 81%) from phenylboronic acid and **(2*R*,3*R*)-16** (300mg, 1.0 mmol).

$[\alpha]_D^{25}$ + 8 (c 0.5 CH_2Cl_2).

HSQC

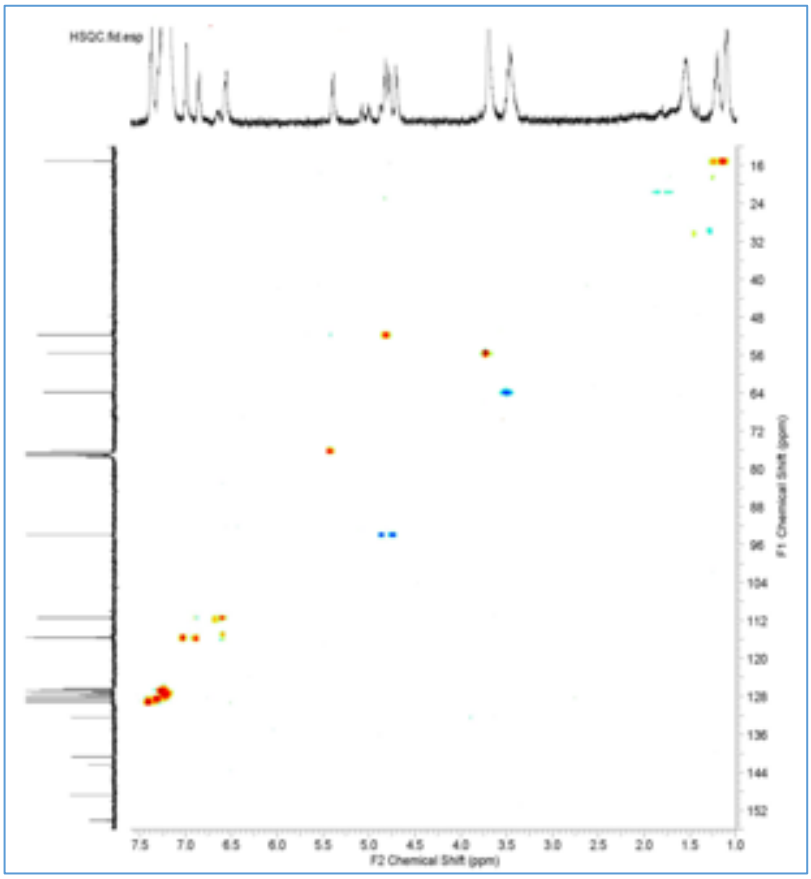

HMBC

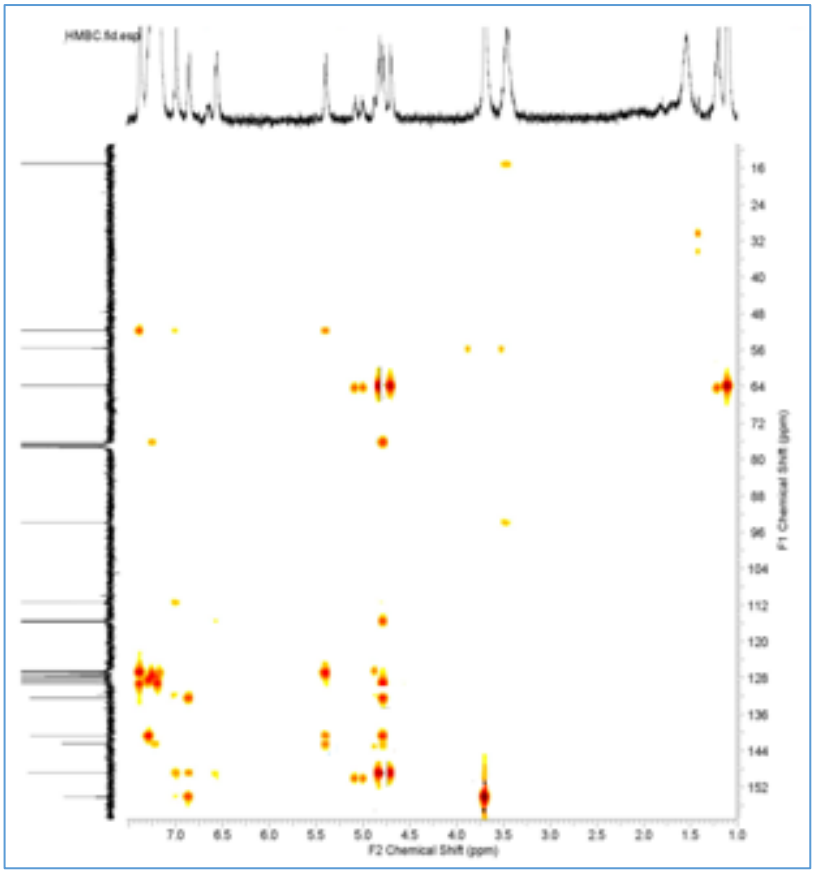

***Syn*- and *anti*-2-(4-Bromo-phenyl)-2-(2-ethoxymethoxy-5-methoxy-phenyl)-1-phenyl-ethanol (22b)**

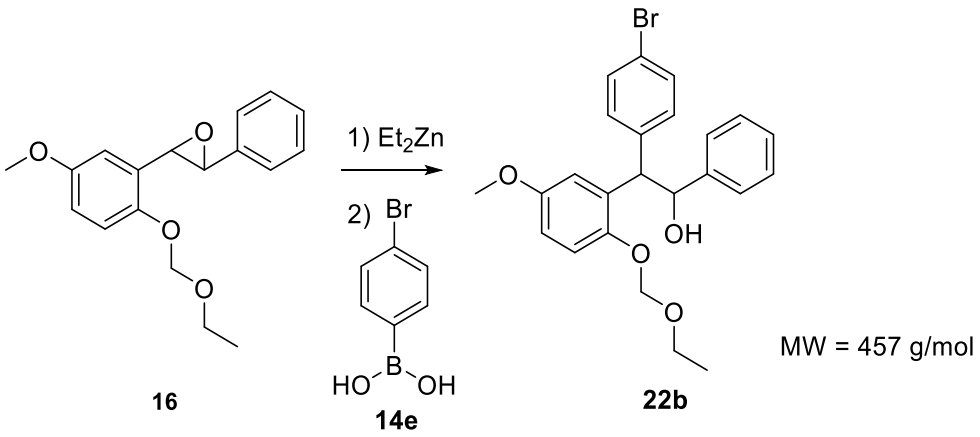

16 14e 22b

***Syn* 2-(4-Bromo-phenyl)-2-(2-ethoxymethoxy-5-methoxy-phenyl)-1-phenyl-ethanol (*syn*-22b)** was obtained (247 mg, 54%) by **method C** from 4-bromophenylboronic acid **14e** and *trans* 2-(2-Ethoxymethoxy-5-methoxy-phenyl)-3-phenyl-oxirane **16** (300 mg, 1.0 mmol).

R_f = 0.4 (40% Et_2O/EP)

^{1}H NMR (400 MHz, $CDCl_3$): δ (ppm) 1.15 (t, J = 7.0 Hz, 3H), 2.24 (brs, 1H), 3.50 (m, 2H), 3.72 (s, 3H), 4.75 (d, J = 8.0 Hz, 1H), 4.79 (A of AB system, J_{AB} = 7.0 Hz, 1H), 4.89 (B of AB system, J_{AB} = 7.0 Hz, 1H), 5.38 (d, J = 8.0 Hz, 1H), 6.62 (m, 1H), 6.91 (d, J = 8.9 Hz, 1H), 6.98 (m, 1H), 7.24 (m, 7H), 7.41 (d, J = 8.1 Hz, 2H). ^{13}C NMR (100 MHz, $CDCl_3$): δ (ppm) 15.0, 51.1, 55.6, 63.9, 75.9, 93.8, 111.5, 115.6, 115.6, 120.5, 126.7, 127.6, 128.0, 130.9, 131.0, 131.3, 139.8, 142.5, 148.7, 154.1.

***Anti* 2-(4-Bromo-phenyl)-2-(2-ethoxymethoxy-5-methoxy-phenyl)-1-phenyl-ethanol (*syn*-22b)** was obtained (50 mg, 11%) by **method C** from 4-bromophenylboronic acid **14e** and *trans* 2-(2-Ethoxymethoxy-5-methoxy-phenyl)-3-phenyl-oxirane **16** (300 mg, 1.0 mmol).

R_f = 0.35 (40% Et_2O/EP)
^{1}H NMR (400 MHz, $CDCl_3$): δ (ppm) 1.14 (t, J = 7.0 Hz, 3H), 3.53 (m, 2H), 3.81 (s, 3H), 4.66 (d, J = 9.0 Hz, 1H), 4.96 (A of AB system, J_{AB} = 7.0 Hz, 1H), 5.04 (B of AB system, J_{AB} = 7.0 Hz, 1H), 5.37 (d, J = 9.0 Hz, 1H), 6.76 (brd, J = 8.7 Hz, 1H), 6.98 (m, 1H), 7.14 (m, 7H), 7.25 (m, 3H), 7.34, (d, J = 8.1 Hz, 2H). ^{13}C NMR (100 MHz, $CDCl_3$): δ (ppm) 15.0, 52.9, 55.6, 64.1, 75.8, 93.9, 111.9, 115.1, 116.4, 121.1, 126.3, 128.1, 128.6, 128.7, 131.0, 131.2, 140.8, 141.5, 149.6, 154.5.

HSQC

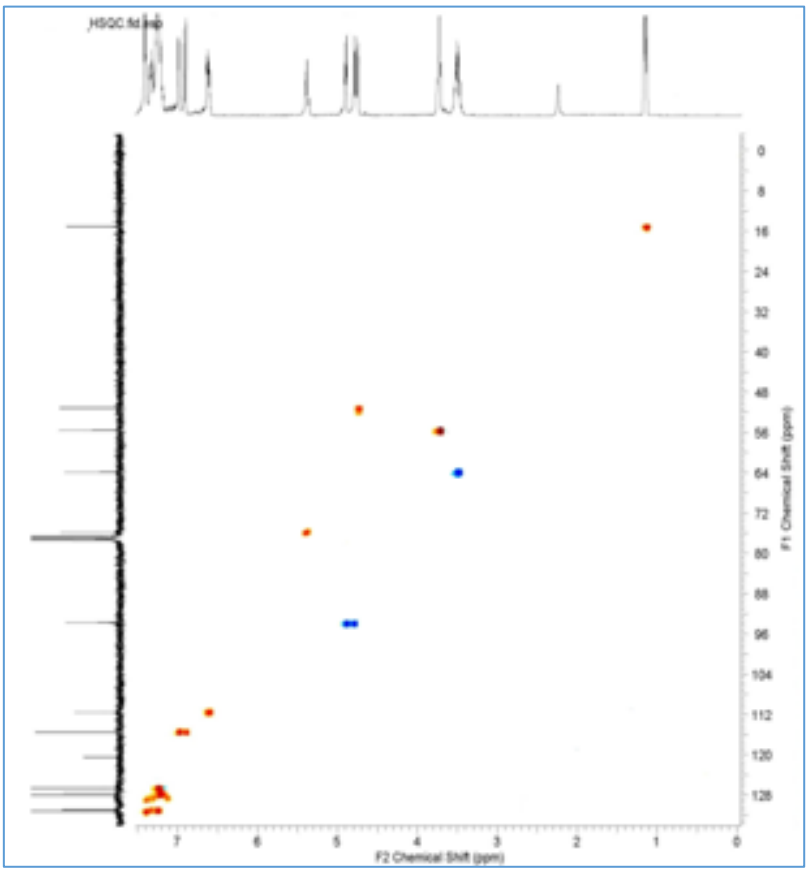

HMBC

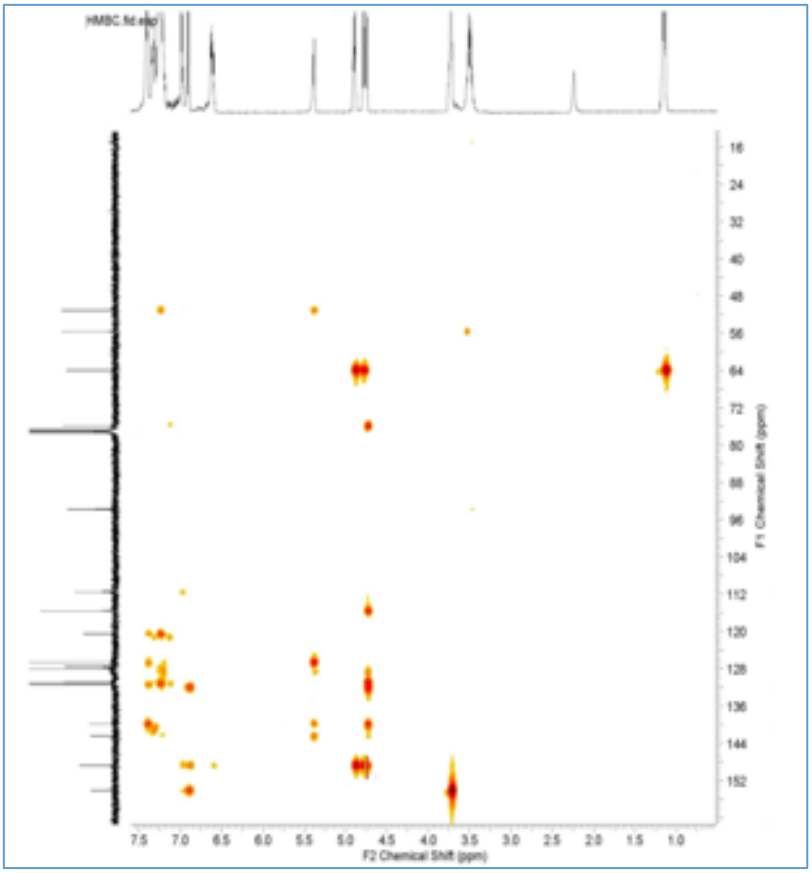

***Syn* 2-(3,5-Dibromo-phenyl)-2-(2-ethoxymethoxy-5-methoxy-phenyl)-1-phenyl-ethanol (*syn*-22c)**

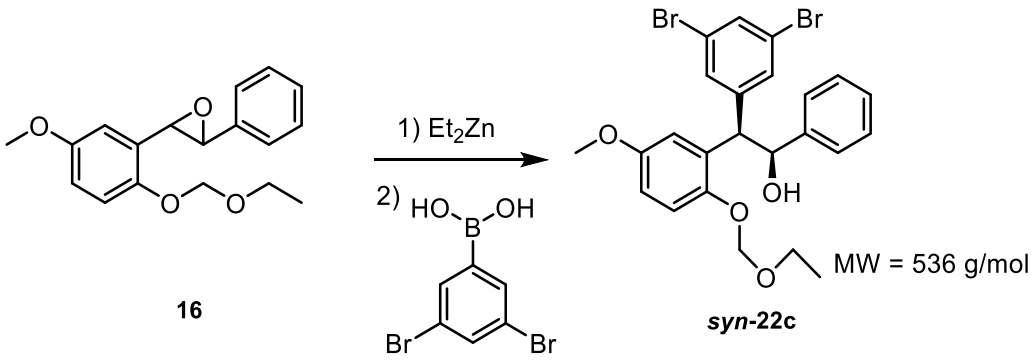

16 **14i** ***syn*-22c**

Product ***syn*-22c** was obtained (268 mg, 50%) as oil from 3,5-dibromophenyl boronic acid **14i** and *trans* 2-(2-Ethoxymethoxy-5-methoxy-phenyl)-3-phenyl-oxirane **16** (300 mg, 1.0 mmol).

R_f = 0.5 (20% Et_2O/EP).

^{1}H NMR (400 MHz, $CDCl_3$): δ (ppm) 1.11 (t, J = 7.2 Hz, 3H), 2.70 (brs, 1H), 3.48 (m, 2H), 3.77 (s, 3H), 4.56 (d, J = 8.4 Hz, 1H), 4.91 (A of AB system, J_{AB} = 6.8 Hz, 1H), 4.99 (B of AB

system, J_{AB} = 6.8 Hz, 1H), 5.30 (d, *J* = 8.0 Hz, 1H), 6.55 (s, 1H), 6.64 (d, *J* = 8.8 Hz, 1H) 6.72 (d, *J* = 8.8 Hz, 1H), 7.01- 7.23 (m, 7H), 7.44 (s, 1H). ^{13}C NMR (100 MHz, $CDCl_3$): δ (ppm), 15.0, 52.9, 55.7, 64.1, 75.3, 94.0, 112.2, 122.3, 126.4, 126.7, 127.7, 128.3, 128.7, 128.7, 130.43, 132.8, 140,3, 146.6, 149.6, 154.5.

Syn 2-(2-ethoxymethoxy-3-methoxy-phenyl)-1,2-diphenylethanol (_syn_-23a)

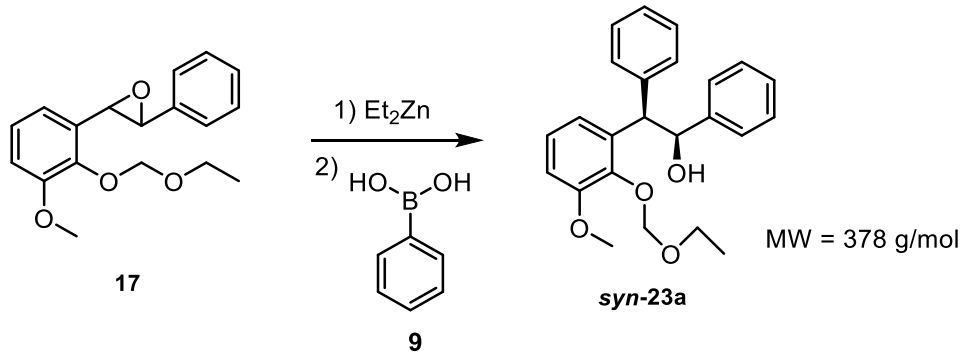

17 9 ***syn*-23a**

Product ***syn*-23a** was obtained (279 mg. 74%) by **method C** from phenylboronic acid **9** and *trans rac* 2-(2-Ethoxymethoxy-3-methoxy-phenyl)-3-phenyl-oxirane **17** (300 mg, 1.0 mmol).

Rf = 0.50 (30% Et_2O/EP).

^{1}H NMR (400 MHz, $CDCl_3$): δ 1.26 (3H, t, *J* = 7.0 Hz), 3.54 (2H, q, *J* = 7.0 Hz), 3.73 (3H, s), 4.94 (1H, d, *J* = 4.5 Hz), 5.05 (2H, brs), 5.41 (1H, d, *J* = 4.5 Hz), 6.65 (1H, dd, J_1 = 8.6, J_2 = 2.6 Hz), 6.76 (1H, dd, J_1 = 8.0, J_2 = 2.6 Hz), 7.20 (4H, m), 7.30 (3H, m), 7.44 (2H, m), 7.81 (2H, m). ^{13}C NMR (100 MHz, $CDCl_3$): *δ* (ppm) 15.2, 39.5, 51.5, 54.9, 56.2, 65.4, 76.2, 97.7, 113.0, 126.6, 126.8, 128.5, 128.6, 128.8, 128.9, 129.1, 129.4, 140.3, 143.6, 152.0.

HSQC

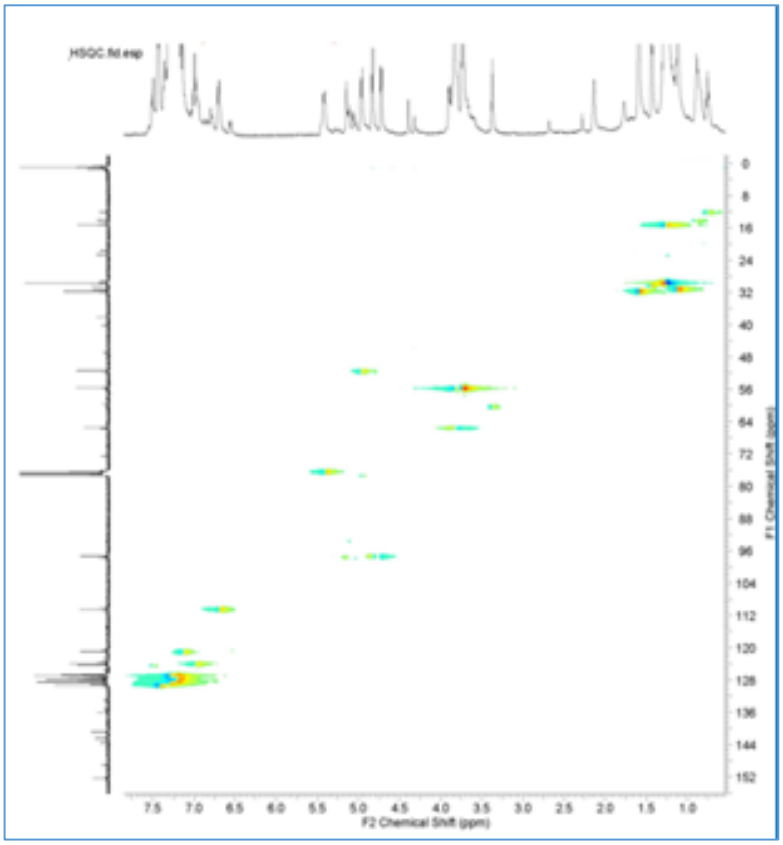
HSQC fid.esp
F2 Chemical Shift (ppm)
F1 Chemical Shift (ppm)

HMBC

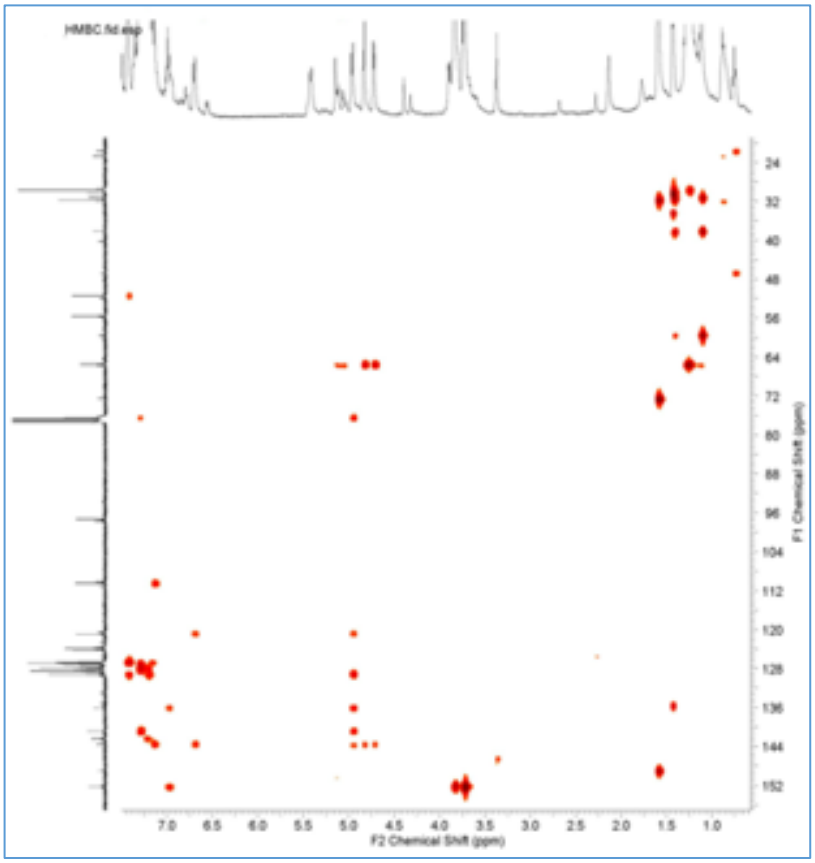
HMBC fid.esp
F2 Chemical Shift (ppm)
F1 Chemical Shift (ppm)

***Syn* and *anti* 2-(4-Bromo-phenyl)-2-(2-ethoxymethoxy-3-methoxy-phenyl)-1-phenyl-ethanol (*syn/anti*-23b)**

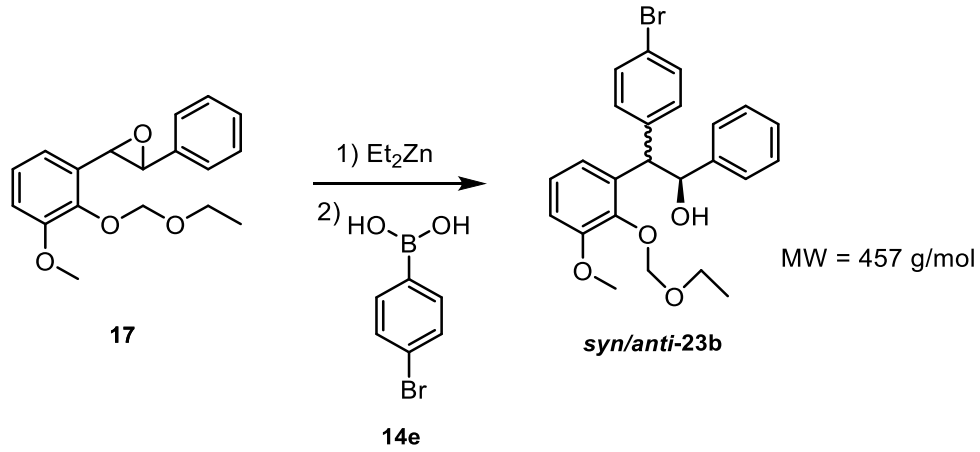

17 **14e** ***syn/anti*-23b**

Product ***syn/anti*-23b** were obtained (297 mg, 65%) as 3:1 *syn*/*anti* mixture by **method C** from 4-bromophenyl boronic acid **14e** and *trans* 2-(2-Ethoxymethoxy-3-methoxy-phenyl)-3-phenyl-oxirane (300 mg, 1.0 mmol).

R_f = 0.2 (30% Et_2O/EP).

^{1}H NMR (400 MHz, $CDCl_3$): *δ* (ppm) 1.24 (m, 3H, *syn* + *anti*), 3.70 (brs, 3H, *syn* + *anti*), 3.79 (m, 2H, *syn* + *anti*), 4.77 (m, 1H, *syn* + *anti*), 4.85 (m, 1H, *syn* + *anti*), 4.90 (m, 1H, *syn* + *anti*), 5.33 (d, *J* = 8.5 Hz, 1H, *anti*), 5.35 (d, *J* = 7.7 Hz, 1H, *syn*), 6.67 (m, 2H, *syn* + *anti*), 6.96 (m, 1H, *syn* + *anti*), 7.05 (m, 1H, *syn* + *anti*), 7.15-7.41 (m, 8H). ^{13}C NMR (100 MHz, $CDCl_3$): δ (ppm) 15.1 (*syn* + *anti*), 50.5 (*syn*), 51.1 (*anti*), 55.5 (*syn* + *anti*), 65.5 (*syn* + *anti*), 75.8 (*anti*), 76.1 (*syn*), 97.3 (*syn* + *anti*), 110.6 (*syn*), 112.0 (*anti*), 117.2 (*syn* + *anti*), 120.4 (*anti*), 120.8 (*syn*), 123.9 (*anti*), 124.0 (*syn*), 126.7 (*syn*), 127.4 (*anti*), 128.0 (*syn*), 128.5 (*anti*), 128.7 (*anti*), 129.1 (*anti*), 130.95 (*anti*), 131.01 (*syn*), 131.3 (*syn*), 132.2 (*syn*), 135.5 (*anti*), 135.6 (*syn*), 140.0 (*syn*), 140.4 (*anti*), 141.3 (*anti*), 142.3 (*syn*), 143.52 (*syn*), 143.56 (*anti*), 152.16 (*syn*), 152.20 (*anti*), 155.3 (*syn* + *anti*).

HSQC

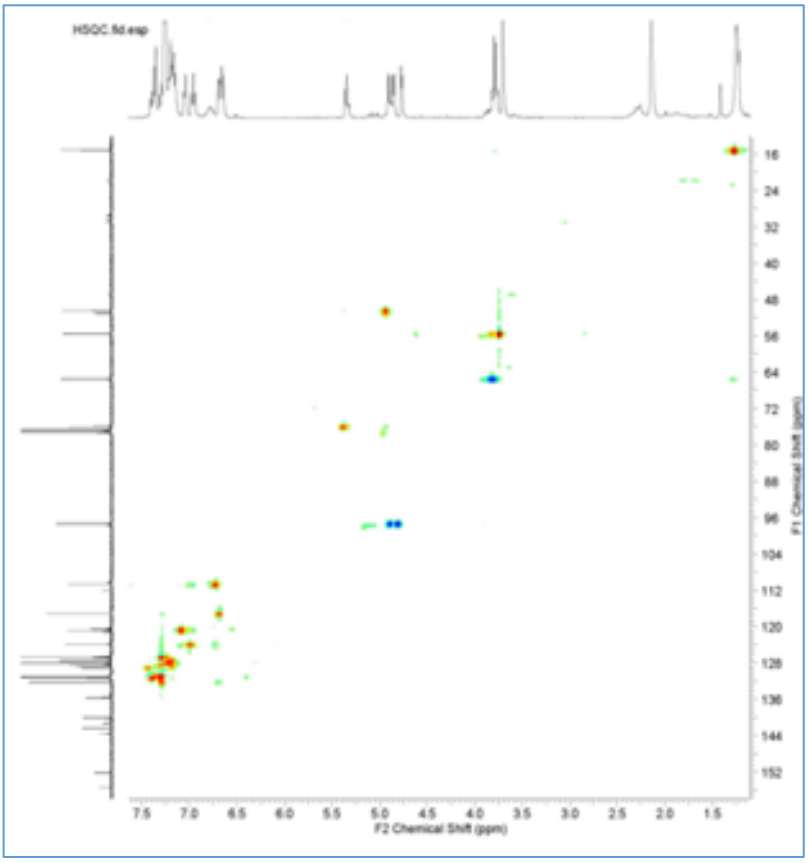
HSQC.fid.esp
F2 Chemical Shift (ppm)
F1 Chemical Shift (ppm)

HMBC

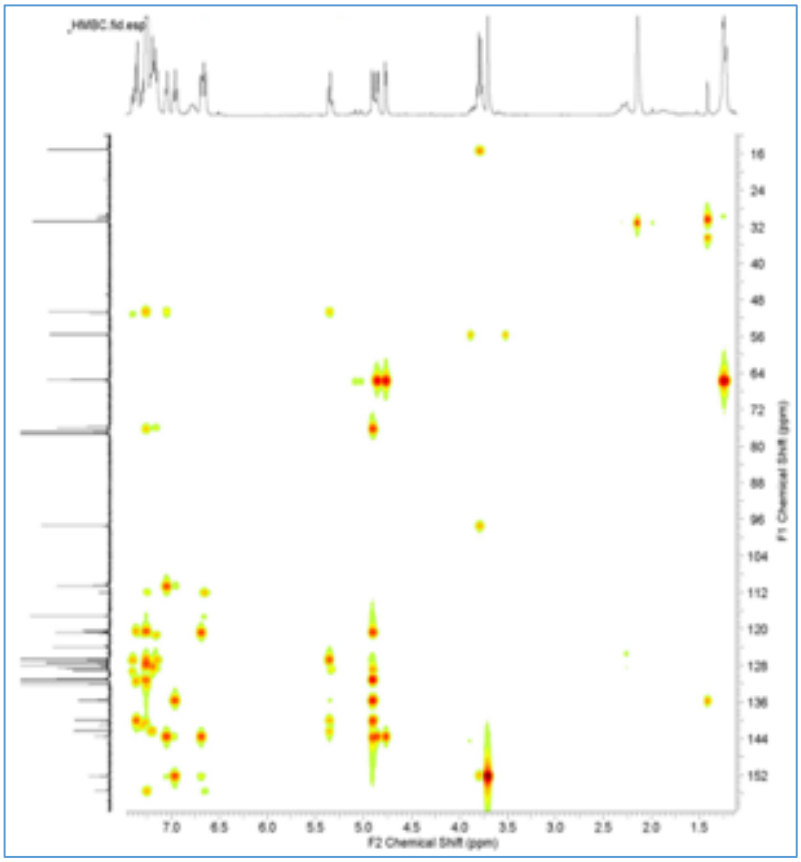
HMBC.fid.esp
F2 Chemical Shift (ppm)
F1 Chemical Shift (ppm)

***Syn* 2- (4-bromo-2- (ethoxymethoxy) -6-methoxyphenyl) -1,2-diphenylethanol (*syn*-43)**

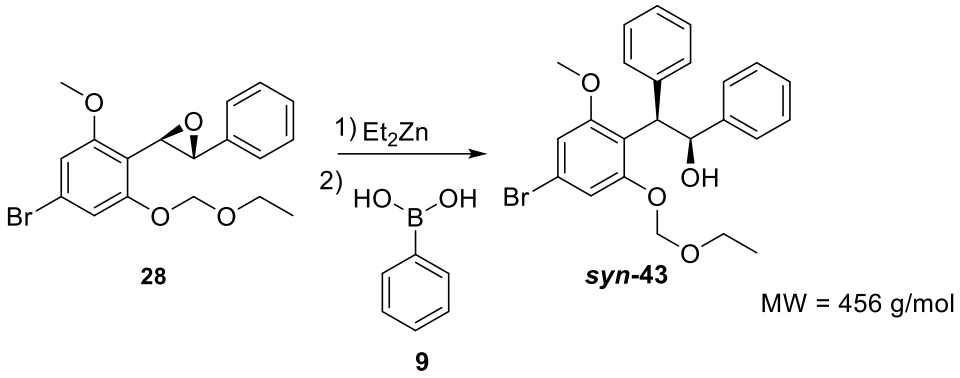

Product **rac *syn*-43** was obtained (41 mg, 0.09 mmol, 75%) by **method C** from phenylboronic acid **9** and *trans rac* 2-(4-bromo-2-(ethoxymethoxy)-6-methoxyphenyl)-3-phenyloxirane **rac-28** (46 mg, 0.12 mmol).

***Syn*-(1*R*,2*S*)-43** was obtained (11 mg, 0.02 mmol, 48%) by **method C** from phenylboronic acid **9** and **(2*S*,3*S*)-28** (19 mg, 0.05 mmol).

Rf = 0,22 (30% Et_2O/Hexane)

^{1}H NMR (400 MHz, $CDCl_3$); δ (ppm) 1.18 (m, 3H), 3.49 (m, 2H), 3.72 (s, 3H), 4.99 (A of AB system, J_{AB} = 7.1 Hz, 1H), 5.05 (d, J = 9.1 Hz, 1H), 5.11 (B of AB system, J_{AB} = 7.1 Hz, 1H), 5.88 (d, J = 9.1 Hz, 1H), 6.51 (brs, 1H), 6.77 (brs, 1H), 7.20 (m, 3H), 7.31 (m, 5H), 7.56 (m, 2H). ^{13}C NMR (100 MHz, $CDCl_3$); δ (ppm) 15.3, 29.7, 64.3, 65.8, 73.8, 93.3, 108.7, 110.8, 120.6, 126.3, 126.6, 127.5, 127.8, 128.1, 128.9, 131.3, 134.7, 141.4, 142.7, 158.1.

***Syn*-2-(2-bromo-6-(ethoxymethoxy)-4-methoxyphenyl)-1-(4-bromophenyl)-2-phenylethanol (*syn*-44a)**

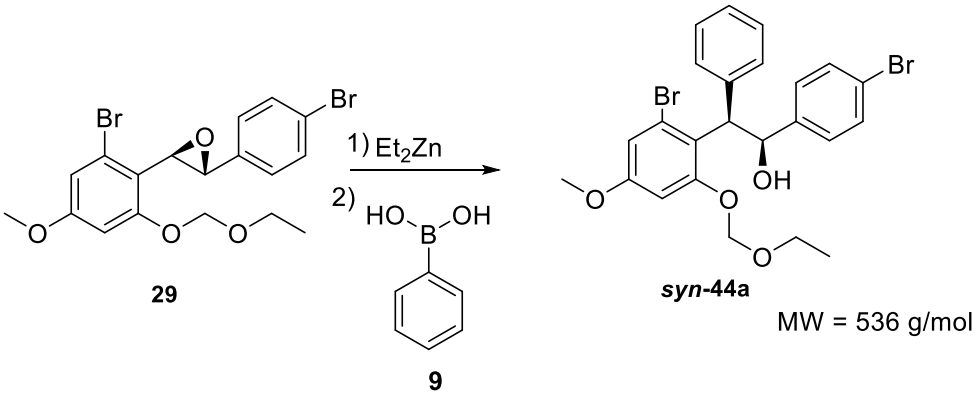

Product **rac *syn*-44a** was obtained (81 mg, 0.15 mmol, 84%) by **method C** from phenylboronic acid **9** and *trans rac* 2-(2-bromo-6-(ethoxymethoxy)-4-methoxyphenyl)-3-(4-bromophenyl)-oxirane **rac-29** (83, 0.18 mmol).

***Syn*-(1*R*,2*S*)-44** was obtained (92 mg, 0.13 mmol, 60%) by **method C** from phenylboronic acid and **(2*S*,3*S*)-29** (100 mg, 0.22 mmol).

R_f = 0.2 (30% Et_2O/Hexane)
^{1}H NMR (400 MHz, C_6D_6): δ (ppm) 1.27 (m, 3H), 2.12 (brs, 1H), 2.94 (s, 3H), 3.07 (m, 1H), 3.27 (m, 1H), 4.54 (A of AB system, J_{AB} = 7.2 Hz, 1H), 4.72 (B of AB system, *J*AB = 7.2 Hz, 1H), 5.28 (brd, *J* = 9.0 Hz, 1H), 5.83 (brd, *J* = 9.0 Hz, 1H), 6.52 (brs, 1H), 6.64 (brs, 1H), 7.11 (m, 1H), 7.24 (m, 8H), 7.68 (d, *J* = 7.7 Hz, 2H). ^{13}C NMR (100 MHz, C_6D_6); δ (ppm) 15.5, 55.1, 64.9, 73.8, 76.5, 93.5, 102.7, 111,2, 122.1, 124.4, 128.7, 129.1, 129.5, 129.6, 131.6, 131.7 142.3, 143.2, 144.4, 157.4.

Syn-2-(2-bromo-6-(ethoxymethoxy)-4-methoxyphenyl)-1-(4-bromophenyl)-2-(3,5-dibromophenyl) ethanol

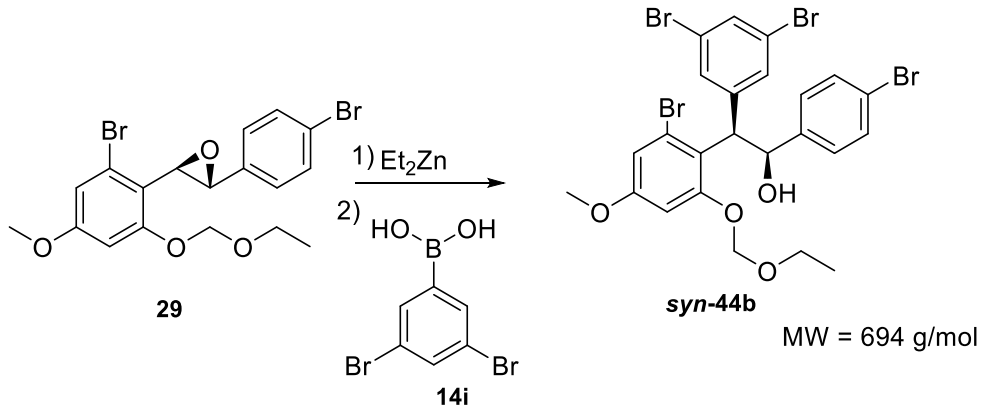

Product **rac *syn*-44b** was obtained (99 mg, 0.14 mmol, 65%) by **method C** from phenylboronic acid **9** and *trans rac* 2-(2-bromo-6-(ethoxymethoxy)-4-methoxyphenyl)-3-(4-bromophenyl)-oxirane **rac-29** (100 mg, 0.22 mmol).

R_f = 0.5 (Et_2O/Hexane)
^{1}H NMR (400 MHz, $CDCl_3$): δ (ppm) 1.13 (m, 3H), 2.43 (brs, 1H), 3.37 (m, 1H), 3.54 (m, 1H), 3.64 (s, 3H), 4.97 (A of AB system, J_{AB} = 7.5 Hz, 1H), 5.03 (brd, *J* = 8.5 Hz, 1H), 5.10 (B of AB system, J_{AB} = 7.5 Hz, 1H), 5.86 (brd, *J* = 8.5 Hz, 1H), 6.52 (d, *J* = 2.1 Hz, 1H), 6.58 (d, *J* = 2.1 Hz, 1H), 7.20 (m, 3H), 7.30 (m, 4H), 7.54 (d, *J* = 7.4 Hz, 2H). ^{13}C NMR (100 MHz, $CDCl_3$); δ (ppm) 15.0, 55.4, 64.5, 73.3, 80.6, 93.2, 101.6, 110.7, 121.3, 120.0, 126.4, 128.1, 128.4, 128.6, 131.0, 134.7, 140.6, 141.4, 156.5, 159.1.

HSQC

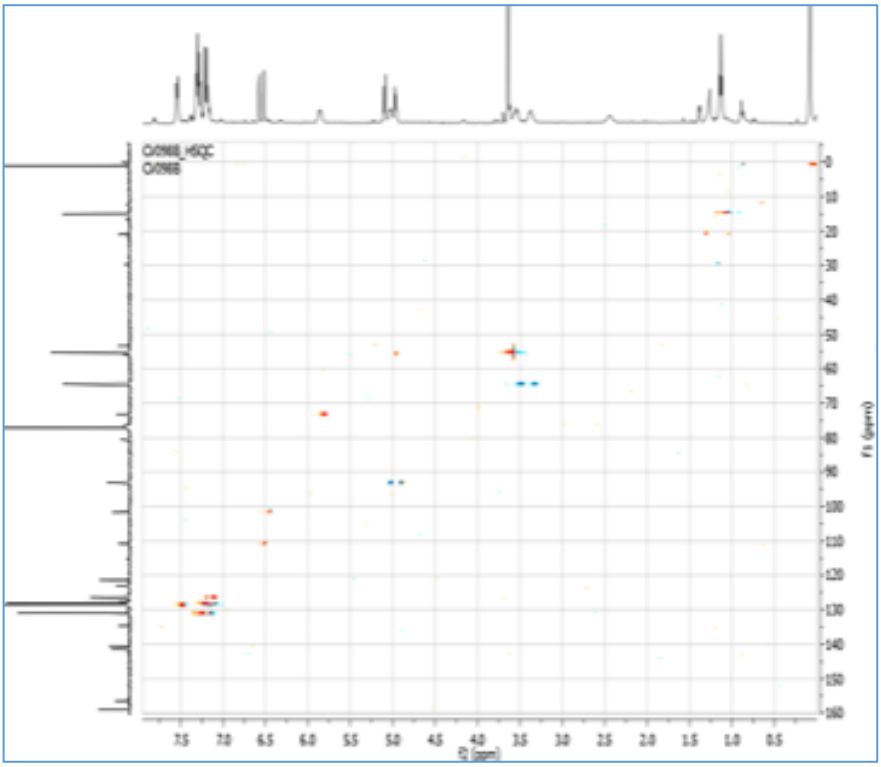

HMBC

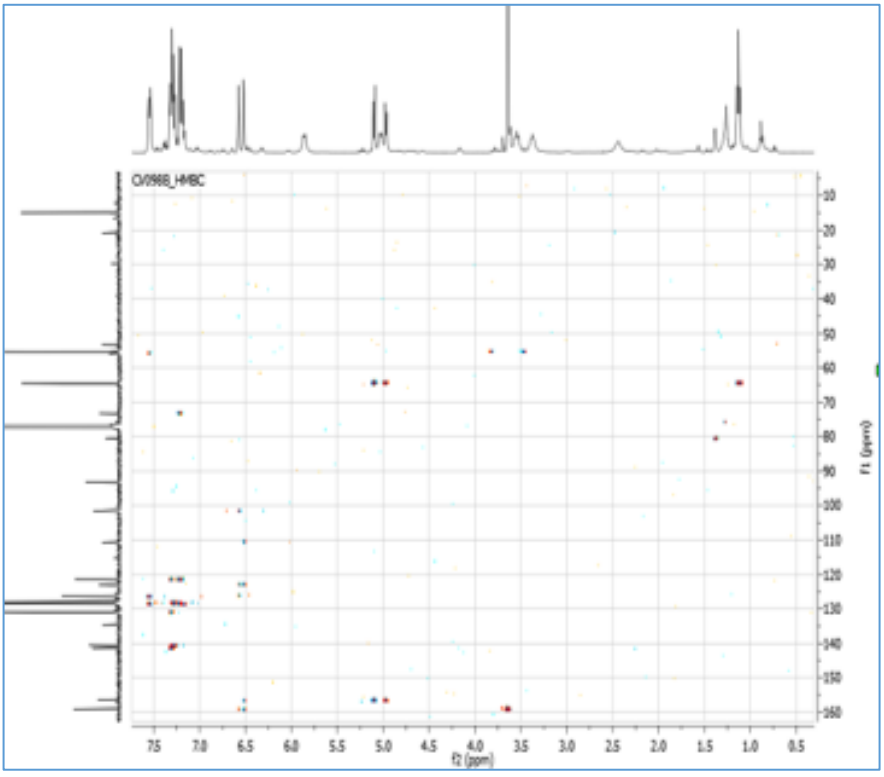

(*E*)-1-(4-bromophenyl)-2-(3,5-dibromophenyl)-2-(2-(ethoxymethoxy)-6-methoxy-4-(4-methoxystyryl)phenyl)ethanol 53 was obtained (11 mg, 0.015 mmol, 17%) by **method C** from 3,5-dibromo-phenylboronic acid **14i** and *trans* (*E*)-2-(4-bromophenyl)-3-(2-(ethoxymethoxy)-6-methoxy-4-(4-methoxystyryl)-phenyloxirane **52** (43 mg, 0.084 mmol).

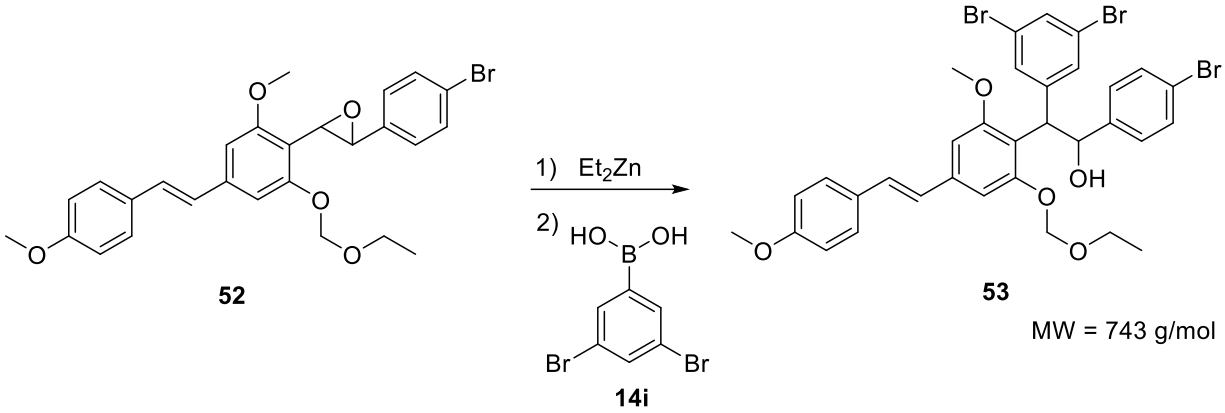

52 **14i** **53**

MW = 743 g/mol

R_f = 0.6 (50% EtOAc/EP)

^{1}H NMR (400 MHz, $CDCl_3$): δ (ppm) 1.14 (t, J = 6.8 Hz, 3H), 3.54 (m, 2H), 5.22 (m, 2H), 5.58 (d, J = 7.2 Hz, 1H), 5.94 (d, J = 7.2 Hz, 1H), 6.78 (s, 1H), 6.94 (m, 4H), 7.09 (d, J = 16.4 Hz, 1H), 7.26 (m, 3H), 7.51 (m, 4H), 7.81 (s, 1H), 7.99 (s, 1H). ^{13}C NMR (100 MHz, $CDCl_3$); δ (ppm) 15.0, 55.3, 55.9, 64.5, 78.7, 83.4, 102.7, 105.2, 114.2, 121.7, 122.9, 126.1, 126.9, 127.7, 129.4, 131.7, 136.1, 136.7, 140.3, 141.0, 156.7, 158.9, 159.5.

HSQC

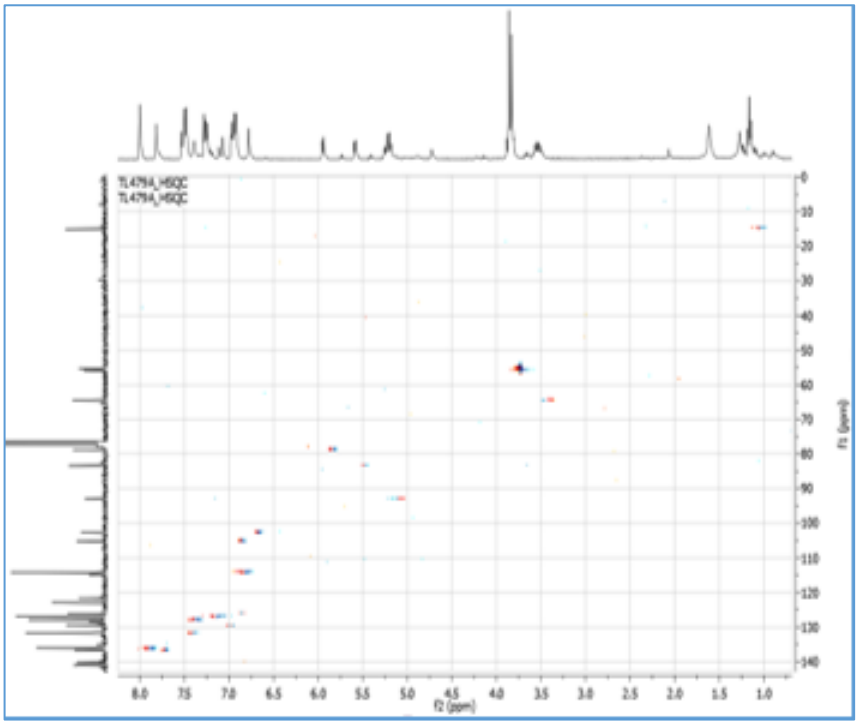
TL4764_HSQC
TL4764_HSQC
F2 (ppm)
F1 (ppm)

HMBC

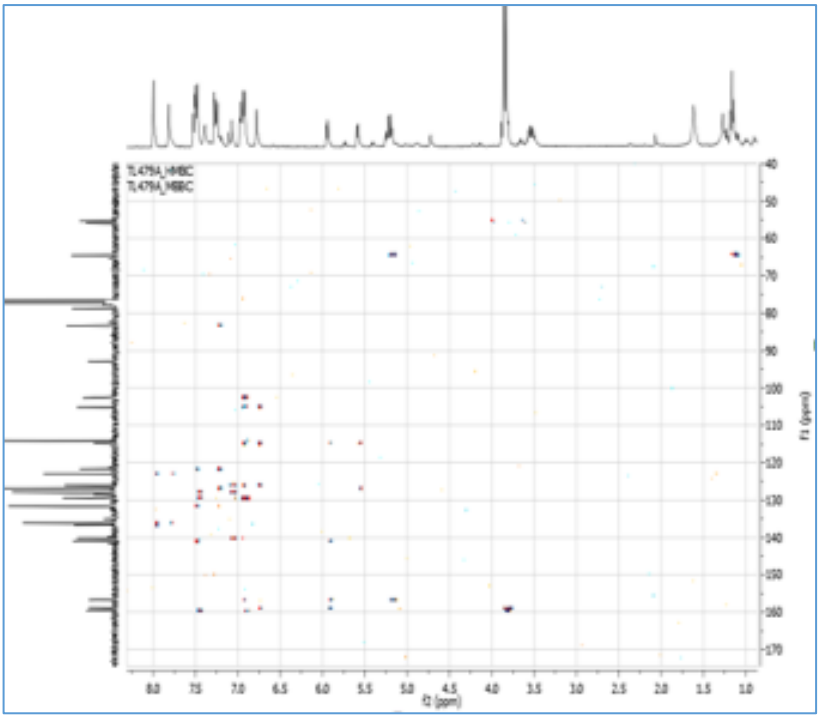
TL4764_HMBC
TL4764_HMBC
F2 (ppm)
F1 (ppm)

2.7.1.10 Deprotection reaction

General procedure

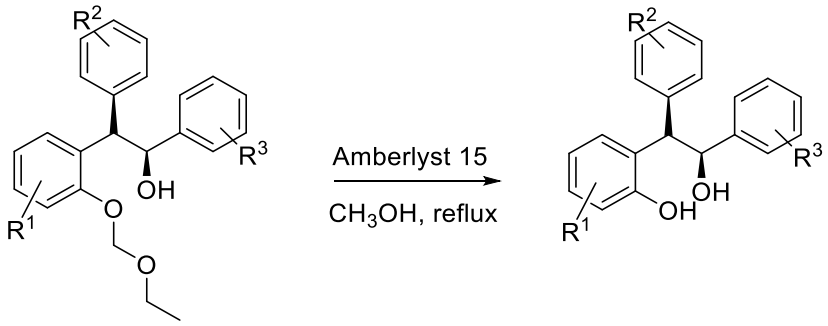

The suitable EOM-protected substrate (1 eq.) was dissolved in CH_3OH and 400 mg of Amberlyst 15 (400 mg/mmol of substrate) were added. The mixture was reacted at 60°C for the appropriate time. Then the mixture was cooled to room temperature, solid $NaHCO_3$ were added, the mixture was filtered and the filtrate evaporated under reduced pressure. The product was purified by column chromatography on silica gel at atmospheric pressure.

***Syn* 2- (2-hydroxy-5-methoxyphenyl) -1,2-diphenylethanol (rac *syn*-24a)** (MW = 320 g/mol) was obtained (96 mg, 0.3 mmol, quantitative yield) from **(rac *syn*-22a)** (113 mg, 0.3 mmol) after 2h reaction time.

R_f = 0.33 (40% Et_2O/EP)

^{1}H NMR (400 MHz, $CDCl_3$): δ (ppm) 3.66 (s, 3H), 4.57 (d, J = 6.0 Hz, 1H), 5.45 (d, J = 6.0 Hz, 1H), 6.57 (A of AB system, J_{AB} = 8.4 Hz, 1H), 6.64 (B of AB system, J_{AB} = 8.4 Hz, 1H), 6.79 (brs, 1H), 7.23 (m, 10H). ^{13}C NMR (100 MHz, $CDCl_3$): δ (ppm) 54.5, 55.7, 76.2, 112.7, 116.2, 117.6, 126.6, 127.1, 127.8, 128.2, 128.5, 129.5, 139.0, 142.1, 147.7, 153.4.

***Syn*-(1*S*,2*R*)-2-(2-Hydroxy-1,2-diphenyl-ethyl)-4-methoxy-phenol, (*Syn*-(1*R*,2*S*)-24a)** was obtained (291 mg, 91%) from **((1*S*,2*R*)-3a)** after 2h reaction time.

$[\alpha]_D^{25}$ - 14 (c = 0.9 CH_2Cl_2).

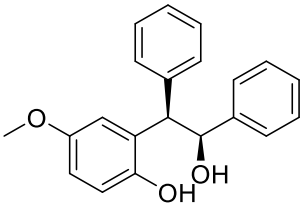

***syn*-24a**

***Syn* 2-[1-(4-Bromo-phenyl)-2-hydroxy-2-phenyl-ethyl]-4-methoxy-phenol (sy-24b)** (MW = 398) was obtained (399 mg, 1.0 mmol, quantitative yield) from ***syn*-22b** (457 mg, 1.0 mmol) after 7h reaction time and column chromatography (30% Et_2O/EP).

Rf = 0.5 (30% Et_2O/EP).

^1H NMR (400 MHz, $CDCl_3$): δ (ppm) 3.69 (s, 3H), 4.51 (d, J = 5.6 Hz, 1H), 5.46 (d, J = 5.6 Hz, 1H), 6.62-6.91 (m, 3H), 7.11 (d, J = 8.4 Hz, 2H), 7.24-7.30 (m, 5H), 7.37 (d, J = 8.4 Hz, 2H). ^{13}C NMR (100 MHz, $CDCl_3$): δ (ppm) 54.0, 55.7, 76.1, 112.8, 116.2, 117.5, 120.9, 126.5, 127.9, 128.2, 131.1, 131.3, 131.3, 138.2, 141.9, 147.5, 153.4.

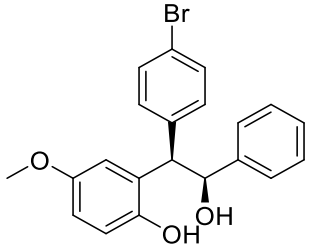

***syn*-24b**

***Anti* 2-[1-(4-Bromo-phenyl)-2-hydroxy-2-phenyl-ethyl]-4-methoxy-phenol (*anti*-24b)** (MW = 398) was obtained (399 mg, 1.0 mmol, quantitative yield) from ***anti*-22b** (457 mg, 1 mmol) after 6h reaction time and column chromatography (40% Et_2O/EP).

Rf = 0.2 (40% Et_2O/EP).

^1H NMR (400 MHz, $CDCl_3$): δ (ppm) 3.66 (s, 3H), 4.43 (d, J = 6.4 Hz, 1H), 5.44 (d, J = 6.4 Hz, 1H), 6.56 (brs, 1H), 6.67 (d, J = 8.4 Hz, 1H), 6.79 (d, J = 8.4 Hz, 1H), 7.10 (d, J = 8.4 Hz, 2H), 7.23 (m, 5H), 7.33 (d, J = 8.4 Hz, 2H). ^{13}C NMR (100 MHz, $CDCl_3$): δ (ppm) 55.3, 55.6, 77.0, 113.0, 116.9, 118.1, 121.5, 126.8, 128.1, 128.5, 128.6, 130.3, 131.3, 139.7, 140.8, 148.6, 153.4.

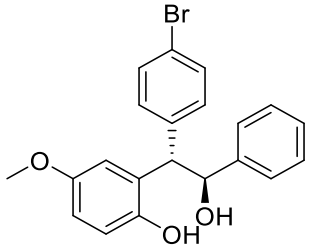

***anti*-24b**

***Syn* 2-[1-(3,5-Dibromo-phenyl)-2-hydroxy-2-phenyl-ethyl]-4-methoxy-phenol (*syn*24c)** (MW = 478 g/mol) was obtained (287 mg, 0.6 mmol, 60%) from ***syn*-22c** (536 mg, 1.0 mmol) after 22h reaction time and column chromatography (40% Et_2O/EP).

Rf = 0.4 (40% Et_2O/EP).

^1H NMR (400 MHz, $CDCl_3$): δ (ppm) 1.61 (brs, 1H), 3.70 (s, 3H), 4.42 (d, J = 7.6 Hz, 1H), 5.41 (d, J = 7.6 Hz, 1H), 6.69 (m, 2H), 6.80 (d, J = 8.8 Hz, 1H), 7.28 (m, 7H), 7.47 (brs, 1H). ^{13}C NMR (100 MHz, $CDCl_3$): δ (ppm) 55.1, 55.8, 76.3, 113.4, 116.6, 118.1, 122.7, 127.08, 127.14, 128.5, 128.6, 128.7, 133.3, 139.3, 145.8, 148.4, 153.7.

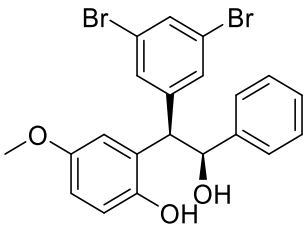

***syn*-24c**

***Syn* 2-(2-Hydroxy-1,2-diphenyl-ethyl)-6-methoxy-phenol (*syn*-25a)** (MW = 320 g/mol) was obtained (240 mg, 0.75 mmol, 75%) from ***syn*-23a** (378 mg, 1.0 mmol) after 2h reaction time and column chromatography (30% Et_2O/EP).

R_f = 0.3 (30% Et_2O/EP).

^{1}H NMR (400 MHz, $CDCl_3$): δ (ppm) 2.13 (brs, 1H), 3.78 (s, 3H), 4.76 (d, J = 8.5 Hz, 1H), 5.54 (d, J = 8.5 Hz, 1H), 5.74 (brs, 1H), 6.63 (d, J = 8.2 Hz, 1H), 6.72 (dd, $J_1 = J_2$ = 8.2 Hz, 1H), 6.99 (d, J = 8.2 Hz, 1H), 7.18-7.35 (m, 8H), 7.46 (d, J = 7.5 Hz, 2H) ^{13}C NMR (100 MHz, $CDCl_3$): δ (ppm) 52.5, 55.8, 75.8, 108.7, 119.3, 121.3, 126.7, 126.9, 127.4, 127.7, 128.0, 128.5, 129.2, 140.7, 142.4, 143.0, 146.3.

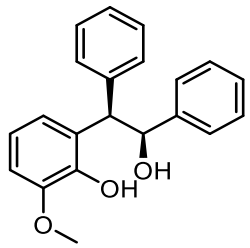

***syn*-25a**

***Syn* and *anti* 2-[1-(4-Bromo-phenyl)-2-hydroxy-2-phenyl-ethyl]-6-methoxy-phenol (*syn/anti*-25b)** (MW = 399 mg/mol) were obtained (259 mg, 0.65 mmol, 65%) from ***syn/anti*-23b,** as 3:1 *syn*/*anti* mixture, after 2h reaction time and column chromatography (40% Et_2O/EP).

Rf = 0.2 (40% Et_2O/EP).

^{1}H NMR (400 MHz, $CDCl_3$): δ (ppm) 3.78 (s, 3H, *syn* + *anti*), 4.71 (brs, 1H, *syn* + *anti*), 5.51 (brs, 1H, *syn* + *anti*), 5.80 (brs, 1H, *anti*), 5.85 (brs, 1H, *syn*), 6.65 (brs, 2H, *syn* + *anti*), 6.74 (m, 1H, *syn* + *anti*), 6.93 (brs, 1H, *syn* +*anti*), 7.23 (m, 3H, *syn* + *anti*), 7.32 (m, 4H, *syn* + *anti*), 7.41 (d, J = 8.1 Hz, 2H, *syn*), 7.48 (d, J = 7.7 Hz, 2H, *anti*) ^{13}C NMR (100 MHz, $CDCl_3$): δ (ppm) 51.9 (*syn*), 52.6 (*anti*), 55.9 (*syn*), 58.5 (*anti*), 75.2 (*anti*), 75.6 (*syn*), 108.8 (*anti*), 108.9 (*syn*), 117.2 (*syn*), 119.40 (*anti*), 119.43 (*syn*), 120.5 (*anti*), 121.2 (*anti*), 121.3 (*syn*), 126.7 (*syn*), 127.4 (*anti*), 127.5 (*syn*), 128.0 (*syn*), 128.6 (*anti*), 128.7 (*anti*), 129.1 (*anti*), 131.00 (*anti*), 131.07 (*syn*), 131.31 (*syn*), 132.29 (*syn* + *anti*), 139.8 (*syn*), 140.5 (*anti*), 141.3 (*anti*), 142.3 (*anti*), 142.9 (*syn*), 146.4 (*syn*), 155.1 (*syn* + *anti*).

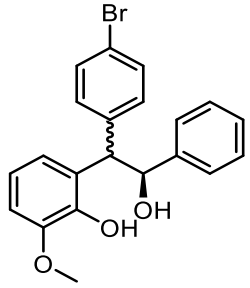

***syn/anti*-25b**

Rac *Syn* 5-bromo-2- (hydroxy-1,2-diphenylethyl) -3-methoxyphenol (rac *syn*-45) (MW = 398 g/mol, 27 mg, 0.07 mmol, 77%) and **rac *trans* 6-bromo-4-methoxy-2,3-diphenyl-2,3-dihydrobenzofuran (rac *trans*-47** (MW = 390 g/mol, 11 mg, 0.03 mmol, 31%) were obtained from **rac *syn*-43** (41 mg, 0.09 mmol) after 7 h reaction time and column chromatography (30% Et_2O/EP).

***Syn*-(1*S*,2*R*)-5-bromo-2-(hydroxy-1,2-diphenylethyl)-3-methoxyphenol (*syn*-(1*S*,2*R*)-45)** (MW = 398 g/mol, 4 mg, 0.01 mmol, 46%) and ***trans* (2*S*,3*S*)-6-bromo-4-methoxy-2,3-diphenyl-2,3-dihydrobenzofuran (*trans*-(2*S*,3*S*)-47)** (MW = 390 g/mol, 5 mg, 0.013 mmol, 54%) were obtained from **(1*S*,2*R*)-43** (11 mg, 0.024 mmol) after 2 h reaction time and column chromatography (30% Et_2O/EP).

***Syn* 5-bromo-2- (hydroxy-1,2-diphenylethyl) -3-methoxyphenol**

R_f = 0.3 (30% Et_2O/Hexane)

^{1}H NMR (400 MHz, C_6D_6); δ (ppm) 2.90 (s, 3H), 5.01 (brs, 1H), 5.15 (brs, 1H), 6.30 (brs, 1H), 6.90 (m, 9H), 7.20 (m,2H). ^{13}C NMR (100 MHz, C_6D_6); δ (ppm) 30.5, 66.4, 76.1, 107.0, 115.2, 117.8, 122.1, 126.9, 128.6, 128.6, 130.9, 143.4, 158.3, 159.2.

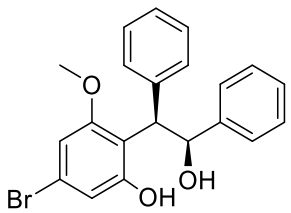

***syn*-45**

***Trans* 6-bromo-4-methoxy-2,3-diphenyl-2,3-dihydrobenzofuran**

R_f = 0.70 (30% Et_2O/Hexane)

^{1}H NMR (400 MHz, C_6D_6); δ (ppm) 4.53 (d, J = 5.5 Hz, 1H), 5.55 (d, J = 5.5 Hz, 1H), 6.48 (brs, 1H), 7.10 (m, 11H). ^{13}C NMR (100 MHz, C_6D_6); δ (ppm) 55.4, 56.6, 94.4, 107.6, 108.5, 116.4, 123.8, 126.0, 127.7, 129.4 (2C), 129.5 (2C), 142.3, 143.3, 158.0, 163.0.

$[\alpha]_D^{25}$ = +65 (c 1.2, CH_2Cl_2). 90% *ee*, HPLC conditions: Chiralpak IA column, 1% *i*PrOH/Hexane.

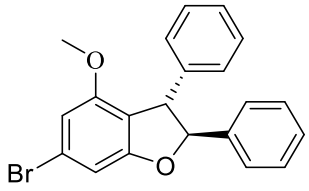

***trans*-47**

***Syn* 3-bromo-2-(2-(4-bromophenyl)-2-hydroxy-1-phenylethyl)-5-methoxyphenol (*syn*-46a)** (MW = 478 g/mol) was obtained (62 mg, 0.13 mmol, 90%) from ***syn*-44a** (80 mg, 0.15 mmol) after 1.5h reaction time and column chromatography (30% Et_2O/Hexane).

R_f = 0.25 (40% Et_2O/Hexane)
^{1}H NMR (400 MHz, C_6D_6): δ (ppm) 2.13 (brs, 1H), 3.02 (s, 3H), 4.97 (brs, 1H), 5.03 (brs, 1H), 6.50 (brs, 1H), 6.64 (brd, J = 8.0 Hz, 2H), 6.73 (brd, J = 3.0 Hz, 1H), 6.93 (m, 3H), 7.13 (m, 2H), 7.20 (brd, J = 8.0 Hz, 2H). ^{13}C NMR (100 MHz, C_6D_6); δ (ppm) 55.3, 60.5, 75.9, 104.3, 111.7, 121.5, 122.2, 127.6, 127.8, 128.3, 128.4, 130.8, 131.9, 138.5, 144.1, 158.3, 161.3.

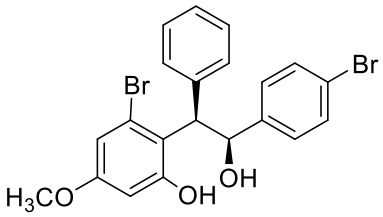

***syn*-46a**

***Syn*-3-bromo-2-(2-(4-bromophenyl)-1-(3,5-dibromophenyl)-2-hydroxyethyl)-5-methoxyphenol (*syn*-46b)** (MW = 635 g/mol, 20 mg, 0.032 mmol, 49%) and ***trans* 4-bromo-2-(4-bromophenyl)-6-methoxy-2,3-dihydrobenzofuran (*trans*-47b)** (MW = 618 g/mol, 17mg, 0.027 mmol, 41%) were obtained from ***syn*-44b** (42mg, 0.066 mmol) after 1 h reaction time and column chromatography (20% Et_2O/EP).

***Syn* 3-bromo-2-(2-(4-bromophenyl)-1-(3,5-dibromophenyl)-2-hydroxyethyl)-5-methoxyphenol (*syn*-46b)**

R_f = 0.1 (20% Et_2O/Hexane)
^{1}H NMR (400 MHz, $CDCl_3$): δ (ppm) 2.87 (brs, 1H), 3.72 (s, 3H), 4.95 (m, 1H), 5.62 (m, 1H), 6.32 (brs, 1H), 6.68 (brs, 1H), 7.20 (m, 3H), 7.41 (m, 3H), 7.52 (m, 1H). ^{13}C NMR (100 MHz,

$CDCl_3$); δ (ppm) 55.4, 74.1, 111.2, 119.4, 122.4, 122.8, 127.7, 128.0, 131.0, 131.2, 131.3, 131.5, 132.4, 133.5, 155.7, 159.7.

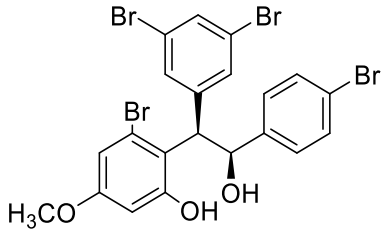

***syn*-46b**

***Trans* 4-bromo-2-(4-bromophenyl)-6-methoxy-2,3-dihydrobenzofuran (*trans*-47b)**

R_f =0.95 (20% Et_2O/Hexane)

^1H NMR (400 MHz, $CDCl_3$): δ (ppm) 3.82 (s, 3H), 4.31 (d, J = 5.0 Hz, 1H), 5.48 (d, J = 5.0 Hz, 1H), 6.53 (brs, 1H), 6.65 (brs, 1H), 7.15 (brd, J = 8.3 Hz, 2H), 7.23 (d, J = 1.7 Hz, 2H), 7.51 (brd, J = 8.3 Hz, 2H), 7.61 (m, 1H). ^{13}C NMR (100 MHz, $CDCl_3$); δ (ppm) 55.8, 57.5, 91.8, 95.9, 110.9, 119.9, 122.5, 123.4, 126.9, 129.7, 132.0, 133.1, 135.9, 139.4, 145.5, 161.2, 162.0.

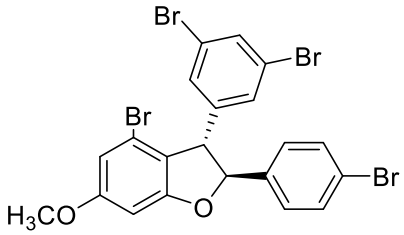

***trans* 47b**

2.7.1.11 Mitsunobu type cyclodehydration

General procedure

To a solution of the suitable 2-(2-hydroxyethyl)-phenol substrate (1 eq.) dissolved in anhydrous THF, PPh_3 (4 eq.) and DEAD (3 eq.) were added under inert atmosphere. The mixture was reacted at room temperature for the appropriate time. Then the solvent was evaporated under reduced pressure and the crude was purified by column chromatography on silica gel.

***Trans* 5-Methoxy-2,3-diphenyl-2,3-dihydro-benzofuran (*trans*-26a)** (MW = 302 g/mol) was obtained (30 mg, 76%) from ***syn*-24a** (43 mg, 0.13 mmol) after 1h reaction time and purification on silica gel (5% Et_2O/EP).

R_f = 0.6 (5% Et_2O/EP).

^{1}H NMR (400 MHz, $CDCl_3$): δ (ppm) 3.72 (s, 3H), 4.55 (d, J = 8.2 Hz, 1H), 5.53 (d, J = 8.2 Hz, 1H), 6.55 (brs, 1H), 6.79 (dd, J_1 = 8.6 Hz, J_2 = 2.3 Hz, 1H), 6.89 (d, J = 8.6 Hz, 1H), 7.19 (d, J = 7.2 Hz, 2H), 7.33 (m, 8H). ^{13}C NMR (100 MHz, $CDCl_3$): δ (ppm) 55.9, 58.3, 93.1, 109.6, 110.9, 114.0, 125.8, 127.2, 128.1, 128.3, 128.6, 128.8, 131.0, 140.7, 141.5, 153.9, 154.6.

***Trans* (2*R*,3*R*)-5-Methoxy-2,3-diphenyl-2,3-dihydro-benzofuran, (*trans* (2*R*,3*R*)-26a)** (MW = 302 g/mol) was obtained (43 mg, 0.14 mmol, 81%) from **(1*S*,2*R*)-24a** (53 mg, 0.17 mmol) after 1h reaction time and purification on silica gel (5% Et_2O/EP).

$[\alpha]_D^{25}$ - 10 (c 1.2 CH_2Cl_2), 50% *ee* HPLC conditions: Chiralpak IA column, 1% *i*PrOH/*n*-hexane, 0.5 mL/min; t_R 29.63 ((*R*,*R*) major) and 38.05 ((*S*,*S*) minor).

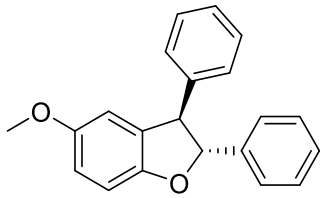

***trans* 26a**

***Trans* 4-Bromo-5-methoxy-2,3-diphenyl-2,3-dihydro-benzofuran (*trans* 26b)** (MW = 380 g/mol) was obtained (331 mg, 0.87 mmol, 87%) from ***syn*-24b** (399 mg, 1.0 mmol) after 5h reaction time and purification on silica gel (3% Et_2O/EP).

R_f = 0.5 (5% Et_2O/EP).

^{1}H NMR (400 MHz, $CDCl_3$): δ (ppm) 3.70 (s, 3H), 4.48 (d, J = 8.4 Hz, 1H), 5.43 (d, J = 8.4 Hz, 1H), 6.49 (brs, 1H), 6.77 (d, J = 8.5 Hz, 1H), 6.87 (d, J = 8.5 Hz, 1H), 7.04 (d, J = 8.2 Hz, 2H), 7.16 (m, 1H), 7.24-7.34 (m, 4H), 7.45 (d, J = 8.2 Hz, 2H). ^{13}C NMR (100 MHz, $CDCl_3$): δ (ppm) 56.0, 57.9, 93.0, 109.8, 110.8, 114.3, 121.3, 125.8, 127.5, 128.3, 128.6, 130.1, 132.0, 140.3, 140.4, 153.9, 154.7.

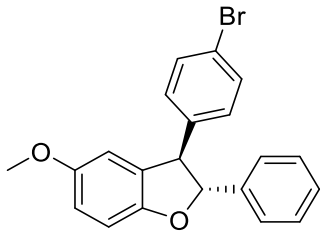

***trans* 26b**

***Cis* 4-Bromo-5-methoxy-2,3-diphenyl-2,3-dihydro-benzofuran (*cis* 26b)** (MW = 380 g/mol) was obtained (343 mg, 0.9 mmol, 90%) from ***anti*-24b** (399, 1.0 mmol) after 2h reaction time and purification on silica gel (20% Et_2O/EP).

R_f = 0.4 (20% Et_2O/EP).

^{1}H NMR (400 MHz, $CDCl_3$): δ (ppm) 3.73 (s, 3H), 4.81 (d, J = 9.2 Hz, 1H), 5.93 (d, J = 9.2 Hz, 1H), 6.67 (brs, 2H), 6.81 (d, J = 8.7 Hz, 1H), 6.88 (d, J = 8.2 Hz, 2H), 6.94 (d, J = 8.7 Hz,

1H), 7.04 (m, 2H), 7.11 (m, 1H), 7.19 (d, J = 8.2 Hz, 2H), 7.26 (brs, 1H). ^{13}C NMR (100 MHz, $CDCl_3$): δ (ppm) 54.2, 55.9, 88.2, 109.8, 111.5, 114.3, 126.3, 126.8, 127.9, 128.1, 129.0, 130.6, 131.1, 136.6, 138.4, 154.0, 154.8.

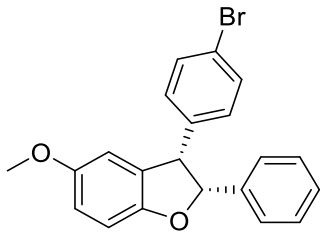

***cis* 26b**

***Trans* 3-(3,5-dibromo-phenyl)-5-methoxy-2-phenyl-2,3-dihydro-benzofuran (*trans* 26c)** (MW = 460 mg/mol) was obtained (6.8mg, 0.008 mmol, 78%) from ***syn*-24c** (10 mg, 0.02 mmol) after 22h reaction time and purification on silica gel (5% Et_2O/EP).

R_f = 0.3 (5% Et_2O/EP).

^{1}H NMR (400 MHz, $CDCl_3$): δ (ppm) 3.72 (s, 3H), 4.81 (d, J = 8.6 Hz, 1H), 5.87 (d, J = 8.6 Hz, 1H), 6.67 (m, 3H), 6.80 (dd, J_1 = 8.6 Hz, J_2 = 2.5 Hz, 1H), 6.93 (d, J = 8.6 Hz, 1H), 7.06 (brs, 4H), 7.32 (m, 2H). ^{13}C NMR (100 MHz, $CDCl_3$): δ (ppm) 54.4, 56.0, 87.2, 110.1, 111.5, 114.6, 122.2, 127.3, 128.1, 128.4, 129.0, 130.6, 132.7, 138.1, 141.8, 153.8, 155.1.

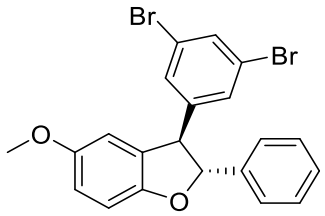

***trans* 26c**

***Trans* 7-methoxy-2,3-diphenyl-2,3-dihydro-benzofuran (*trans* 27a)** (MW = 302 g/mol) was obtained (24 mg, 58%) from ***syn*-25a** (54 mg, 0.14 mmol) after 1h reaction time and purification on silica gel (EP 100%).

R_f = 0.6 (EP 100%).

^{1}H NMR (400 MHz, $CDCl_3$): δ (ppm) 3.94 (s, 3H), 4.60 (d, J = 8.3 Hz, 1H), 5.58 (d, J = 8.3 Hz, 1H), 6.59 (m, 1H), 6.85 (m, 2H), 7.17 (d, J = 7.0 Hz, 2H), 7.28 (m, 8H). ^{13}C NMR (100 MHz, $CDCl_3$): δ (ppm) 56.0, 58.3, 93.6, 111.7, 117.3, 121.7, 126.0, 127.2, 128.1, 128.3, 128.5, 128.8, 131.3, 140.5, 141.6, 144.5, 148.2.

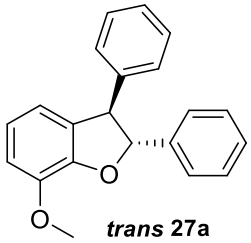

***trans* 27a**

***Trans* and *cis* 3-(4-bromo-phenyl)-7-methoxy-2-phenyl-2,3-dihydro-benzofuran (*trnas/cis* 27b)** (MW = 380 g/mol) were obtained (37 mg, 0.1 mmol, 80%) from ***syn/anti*-25b** (50 mg, 0.12 mmol) , as *trans*/*cis* = 3:1 mixture, after 2h reaction time and purification on silica gel (10% Et_2O/EP).

R_f = 0.5 (10% Et_2O/EP).

^1H NMR (400 MHz, $CDCl_3$): δ (ppm) 3.96 (brs, 3H, *trans* + *cis*), 4.55 (d, *J* = 9.1 Hz, 1H *cis*), 4.59 (d, *J* = 8.9 Hz, 1H *trans*), 5.53 (d, *J* = 8.9 Hz, 1H *trans*), 5.55 (d, *J* = 9.1 Hz, 1H, *cis*), 6.59 (brs, 1H, *trans* + *cis*), 6.88 (m, 2H, *trans* + *cis*), 7.06 (brs, 2H, *trans* + *cis*), 7.20 (m, 1H, *trans* + *cis*), 7.34 (brs, 4H, *trans* + *cis*), 7.46 (m, 2H, *trans* + *cis*). ^{13}C NMR (100 MHz, $CDCl_3$):characteristic signals δ (ppm) 56.1 (*trans* + *cis*), 57.9 (*trans*), 58.5 (*cis*), 93.0 (*cis*), 93.6 (*trans*), 111.7 (*trans*), 112.0 (*cis*), 117.2 (*trans*), 117.3 (*cis*), 121.3 (*trans*), 122.0 (*cis*), 122.1 (*trans*), 122.2 (*cis*), 130.7 (*trans*), 131.1 (*cis*), 139.5 (*trans*), 140.1 (*cis*), 140.6 (*trans*), 141.2 (*cis*), 144.5 (*trans*), 144.6 (*cis*), 148.0 (*cis*), 148.3 (*trans*)

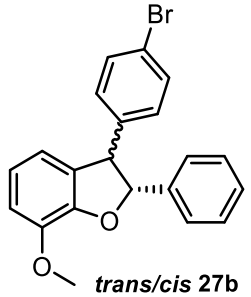

***trans/cis* 27b**

***Trans* 6-bromo-4-methoxy-2,3-diphenyl-2,3-dihydrobenzofuran (*trans*-47)** (MW = 380 g/mol) was obtained (12 mg, 0.03 mmol, 42%) from **rac *syn*-45** (29 mg, 0.073mmol) after 1h reaction time and purification on silica gel (30% Et_2O/Hexane)

R_f = 0.70 (30% Et_2O/Hexane)

^1H NMR (400 MHz, C_6D_6); δ (ppm) 4.53 (d, *J* = 5.5 Hz, 1H), 5.55 (d, *J* = 5.5 Hz, 1H), 6.48 (brs, 1H), 7.10 (m, 11H). ^{13}C NMR (100 MHz, C_6D_6); δ (ppm) 55.4, 56.6, 94.4, 107.6, 108.5, 116.4, 123.8, 126.0, 127.7, 129.4 (2C), 129.5 (2C), 142.3, 143.3, 158.0, 163.0.

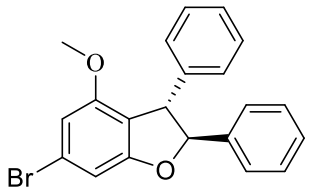

***trans*-47**

Trans* 4-bromo-2- (4-bromophenyl) -6-methoxy-3-phenyl-2,3-dihydrobenzofuran (*trans (MW = 460 g/mol) was obtained (33 mg, 0.071 mmol, 55%) from (62 mg, 0.13 mmol) after 4h reaction time and purification on silica gel (10% EtOAc/Hexane).

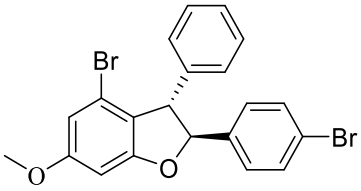

***trans*-48a**

2.7.2 General biological experimental

Roswell Park Memorial Institute 1640 (RPMI 1640), Dulbecco's Modified Eagle's medium (DMEM), L-glutamine, penicillin/streptomycin solution and lipopolysaccharide from *Salmonella enterica* serotype typhimurium (LPS) were obtained from Sigma-Aldrich (St. Louis, MO, USA). 6-Carboxy-2',7'-Dichlorodihydrofluorescein Diacetate (DCF-DA) and Alexa Fluor 488 Dye were purchased from Thermo Fisher Scientific (San Jose, CA, USA). The anti-NF-κB antibody (ab7970), anti-*β*-actin (ab8227), HRP goat anti-rabbit IgG antibody (ab205718) and Mounting Medium with DAPI (ab104139) were from abcam® (Cambridge, MA).

2.7.2.1 Cell lines and culture

A human monoblastic leukemia U937 cell line, obtained from ICLC Interlab Cell Line Collection, was maintained in suspension in Roswell Park Memorial Institute 1640 medium (RPMI 1640, Sigma-Aldrich, St. Louis, MO, USA) supplemented with 10% (v/v) fetal bovine serum, 2 mM L-glutamine, 100 U/ml penicillin and 100 μg/ml streptomycin at 37°C in humidified air with 5% CO_2.

Hek293 cells (Sigma) were cultured in Dulbecco's Modified Eagle's medium (DMEM, Sigma) containing 10% (v/v) fetal bovine serum, 2mM L-glutamine, 100 U/ml penicillin and 100 μg/ml streptomycin at 37°C in 5% CO_2.

Promonocytic U937 cells, where indicated, were activated with 200 ng/mL LPS from *Salmonella enterica* serotype typhimurium (LPS, Sigma–Aldrich, St. Louis, MO, United States). Cell viability was determined by using the automated handheld *Scepter 2.0 Cell Counter* (Merck Millipore, Switzerland).

2.7.2.2 *Sample's treatments and determination of cell viability by cell count*

The effect of dihydrobenzofurans on cell viability was determined by using a Millipore Scepter™ handheld automated cell counter (Merck Millipore, Darmstadt, Germany), according to the manufacturer's instructions. Briefly, U937 cells were seeded at a density of 5×10^3 cells per well in 96-well plates and treated with DMSO (vehicle) or tested compounds at different concentrations (0.01, 0.1 and 1 µM) for 72 h. After incubation, cells were collected and counted. Cell viability was calculated with respect to untreated cells by using the following equation: cell viability (%) = (mean absorbance in treated cells/mean absorbance in the untreated cells) × 100.

2.7.2.3 Western Blot Analysis

U937 cells were pretreated with DMSO (vehicle) or different compounds (0.01 µM) for 1 h and stimulated with LPS (200 ng/mL) for 3 h. Cells were lysed in Laemmli buffer and boiled at 100°C for 5 minutes. After being separated by 10% SDS-PAGE, the proteins of the samples were electroblotted onto nitrocellulose membranes as shown in our previous work.[i] Briefly, membrane was blocked for 1 hour in a Tris-buffered saline (TBS) solution containing 5% skimmed dry milk and 0.5% Tween 20 and then incubated at 4°C overnight with anti-NF-*κ*B/p65 (ab7970, Abcam, Cambridge, MA) and anti-*β*-actin (ab8227, Abcam) antibodies. The blot was incubated with HRP goat anti-rabbit IgG antibody (ab205718, Abcam) for 1 h and the immunoreaction was detected by using the horseradish peroxidase substrate *WesternBright™ ECL* (Advansta, Menlo Park, CA, USA).

2.7.2.4 Immunocytochemistry (ICC)

The expression of NF-kB p65 in Hek293 cells was examined by immunocytochemistry (ICC). Cells were seeded in 96 well-plate at 1 x 10^4 cells/well and triggered by 2 µg/mL of LPS in the presence or absence of compounds (0.01 µM) for 3 h. After treatment, the medium was removed and Hek293 cells were washed once with phosphate-buffered saline (PBS 1X), fixed for 15 min in 3% paraformaldehyde at room temperature, rinsed two times with ice-cold PBS, and permeabilized for 10 min with PBST (PBS supplemented with 0,25% Triton X-100). Cells were treated for 30 min with blocking buffer (PBST supplemented with 1% bovine serum albumin) and, finally, incubated overnight with primary antibody (anti-NF-κB/p65, ab7970, Abcam) at 4°C. Alexa Fluor 488 Dye (Thermo Fisher Scientific, San Jose, CA, USA) was used as secondary antibody. Cellular nuclei were visualized by DAPI staining. Images were examined and acquired on FLoid™ Cell Imaging Station (Thermo Fisher Scientific).

2.7.2.5 *ROS, NO and PGE_2 detection*

To determine ROS and NO levels, U937 cells were triggered by LPS in the presence or not of compounds (0.01 µM). After 24 h, ROS and NO concentrations were measured by using 6-carboxy-2',7'-dichlorodihydrofluorescein diacetate (DCF-DA, Thermo Fisher Scientific, San Jose, CA, USA) and 4-amino-5-methylamino-2',7'-difluorofluorescein diacetate (DAF-FM diacetate, Thermo Fisher Scientific), respectively. U937 cells were plated in 12 well-plate at 3

x 10^5 cells/well and triggered by 100 ng/ml of LPS in the presence or not of samples (0.01 µM). After 24 h, cells were collected in tubes, counted and centrifugated. The cell pellet was resuspended in PBS to have 10^5 cells/100 µL and incubated with DCF-DA in the dark. The fluorescence intensity was analyzed after 30 min of incubation by using GloMax plate reader (Promega, Madison, WI, USA).

Cell culture supernatants were used to assess prostaglandin E_2 (PGE_2) levels after 48 hours of exposure to LPS using DetectX® Prostaglandin E_2 High Sensitivity Immunoassay Kit (Arbor Assays, Ann Arbor, MI, USA) according to manufacturer's protocol.

CHAPTER 3. METAL-CATALYZED C-H FUNCTIONALIZATION OF DIARYLACETALDEHYDE

3.1 Introduction

The paradigm of synthesis, whether it be of small molecules or large natural products, is that one functional group must be converted into another. The fields of organic and inorganic chemistry revolve around this school of thought. However, functional group interconversion sequences have inherent flaws including the generation of significant waste, as the starting material must lose one functional group in place of another. Additionally, much effort is invested in the starting material's design, installation, protection, etc. To avoid this waste of materials and effort, using a functional group readily available in our chemical feedstocks is a desirable solution. One functional group that is ubiquitous is the C–H bond. Because functional groups are handles for reactivity, the C–H bond is rarely thought of as such (although that has been changing over the past two decades), and has even been labelled as the "un-functional group" because of its inherent stability.[113]

Bonds are broken and formed according to their reactivity, which is often quantified as bond dissociation energies (BDEs) or, in the special case of bonds to hydrogen, as acidity. The C–H bond is so unreactive because of its high pKa and high BDE.[114] The BDE decreases along the series C(sp)-H → C(sp2)-H → C(sp3)-H, and on passing from 1° → 2° → 3° → allylic C(sp3)-H bond, in line with the notion that this value is inversely proportional to the stability of the radicals obtained from homolytic dissociation of the bond. On the other hand, being acidity proportional to the stability of the corresponding deprotonated species, the pKa trend goes roughly in the opposite direction, with the obvious exception of the allyl C-H bond.[115]

Despite the strength of C–H bonds, there have been numerous examples of their cleavage in the literature, primarily with the aid of transition metals. In addition, the growing demand for enantiopure compounds in chemical and pharmaceutical industries has continued to spur the development of the asymmetric metal-catalyzed C-H functionalization, that provide a novel technique to prepare chiral molecules in an atom- and step-economical manner.[116]

Traditional directing group-assisted enantioselective C-H functionalization relies on the combined effects of the directing groups (DGs) that brings the metal in close proximity to the targeted C-H bond, chiral ligands and metal catalysts (Scheme 57).

---

[113] Alan, S. G.; Karen, I. G *Am. Chem. Soc*., **2009**, *885*, 1-43.

[114] Arndtsen, B. A.; Bergman, R. G.; Mobley, T. A.; Peterson, T. H. *Acc. Chem. Res.*, **1995**, *28*, 154.

[115] a) Liron, F.; Oble, J.; Lorion, M. M.; Poli, G. *Eur. J. Org. Chem.*, **2014**, 5863-5883; b) Engelin, C. J.; Fristrup, P.; *Molecules*, **2011**, *16*, 951-969; c) Liu, G.; Wu, Y. *Top. Curr. Chem*., **2010**, *292*, 195-209.

[116] a) Wencel-Delord,J.; Colobert, F. *Chem. Eur. J.* **2013**, *19*, 14010; b) Zheng, C.; You, S.-L. *RSC Adv.* **2014**, *4*, 6173; c) Newton, C. G.; Wang, S.-G.; Oliveira, C. C.; Cramer, N. *Chem. Rev*. **2017**, *117*, 8908; d) Saint-Denis, T. G.; Zhu, R.-Y.; Chen, G.; Wu, Q.-F.; Yu, J.-Q. *Science* **2018**, *359* e) Zhang, Q.; Shi, B.-F.; Chin*. J. Chem.* **2019**, *37*, 647; f) Loup, J.; Dhawa, U.; Pesciaioli, F.; Wencel-Delord, J.; Ackermann, L. *Angew. Chem. Int. Ed*. **2019**, *58*, 12803; *Angew. Chem*. **2019**, *131*, 12934.

To such end, directing groups such as pyridine, imines, amides, etc. have been effectively employed for a plethora of C-H activation reactions via the formation of five- or six-membered metallacycles **I**.

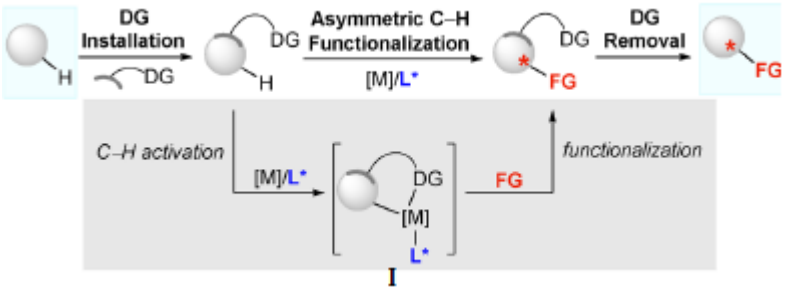

Scheme 57 Traditional directing group-assisted enantioselective C-H functionalization

Although by no doubt powerful methods, several challenges of this asymmetric process need to be emphasized. Firstly, extra steps for the stoichiometric introduction and subsequent removal of DGs that are not components of the target molecules diminish the overall efficacy. In particular, the removal of these DGs often encounters harsh conditions, thus limiting the application in structurally complex compounds, such as natural products or drug molecules. Secondly, since the DG itself acts as an efficient coordinating ligand, the identification of an external chiral ligand that can cooperatively (or to some extent, competitively) coordinate with transition metal catalyst to induce high enantiocontrol is extremely challenging.

To this end, the recent developments of chiral transient directing group (*c*TDG) strategy have demonstrated to be a promising alternative since it obviates the lengthy steps to install and remove external DGs in traditional directing group-assisted processes.[117] In addition, compared to the diastereoselective C-H functionalization strategy that relies on the use of stoichiometric, covalently attached chiral DG,[118] the *c*TDG strategy involves the use of catalytic chiral organocatalyst for the *in situ* formation of a transient chiral auxiliary, which serves as an efficient DG to coordinate with metal catalyst to enable C-H cleavage and ensure chiral induction during or after the C-H cleavage step. A generic catalytic cycle is summarized in Scheme 58. Initially, chiral organocatalyst **II** reversibly reacts with substrate **I** to form intermediate **III** bearing a transient chiral auxiliary, which coordinates to transition metal catalyst and assists the subsequent C-H cleavage, leading to the corresponding metallacycle **IV**. Intermediate **IV** then reacts with coupling reagent to give **V**. *In situ* deconstruction of the *c*TDG and decomplexation would afford the desired chiral product **VI** and release the chiral organocatalyst **II** and metal catalyst to close the catalytic cycle.

---

[117] a) Kim, D.-S.; Park, W.-J.; Jun, C.-H. *Chem. Rev.* **2017**, *117*, 8977; b) Gandeepan, P.; Ackerman, L. *Chem* **2018**, *4*, 199; c) St John-Campbell, S.; Bull, J. A. *Org. Biomol. Chem.* **2018**, *16*, 4582; d) Bhattacharya, T.; Pimparkar, S.; Maiti, D. *RSC Adv.* **2018**, *8*, 19456; e) Niu, B.; Yang, K.; Lawrence, B.; Ge, H. *ChemSusChem* **2019**, *12*, 2955; f) Wu, Y.-J.; Shi, B.-F. *Chin. J. Org. Chem.* **2020**.

[118] a) Giri, R.; Chen, X.; Yu, J.-Q. *Angew. Chem. Int. Ed.* **2005**, *44*, 2112; *Angew. Chem.* **2005**, *117*, 2150; b) Wesch, T.; Leroux, F. R.; Colobert, F. *Adv. Synth. Catal.* **2013**, *355*, 2139; c) Jerhaoui, S.; Chahdoura, F.; Rose, C.; Djukic, J.-P.; Wencel-Delord, J.; Colobert, F. *Chem. Eur. J.* **2016**, *22*, 17397; d) Ma, Y.-N.; Zhang, H.-Y.; Yang, S.-D. *Org. Lett.* **2015**, *17*, 2034.

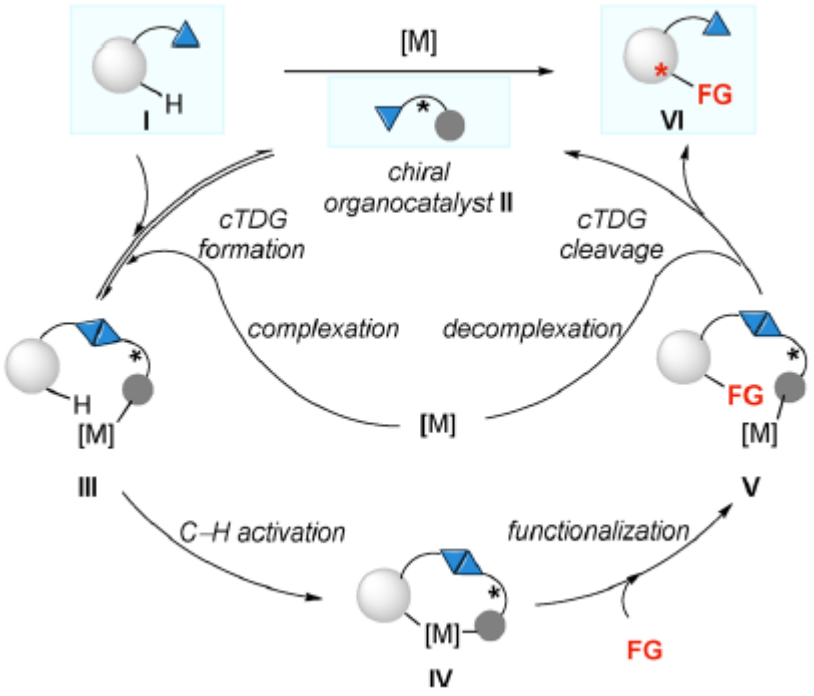

Scheme 58 Chiral transient directing group enabled enantioselective C-H functionalization

3.2 Goal of the work

In regio- and stereoselective nucleophilic ring opening reactions on *trans* diaryloxiranes **I** with $ArB(OH)_2/Et_2Zn$ system, we noted, in certain cases, the formation of diarylacetaldehydes **III** as side products *via* Meinwald rearrangement caused by Lewis acidic character of *in situ* generated arylethyl zinc (Scheme 59).

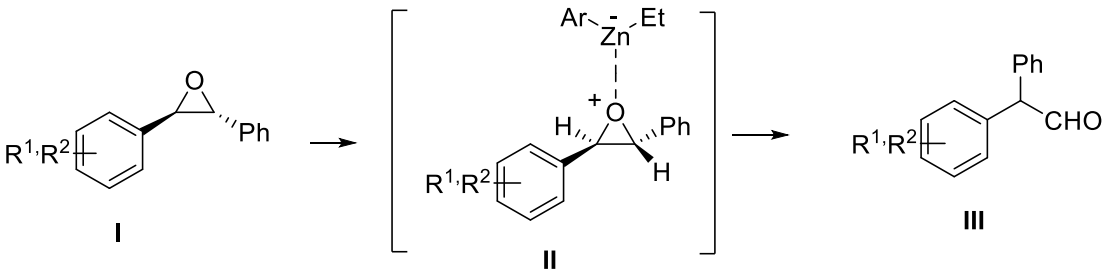

Scheme 59 Meinwald rearrangement of *trans* diaryloxiranes with $ArB(OH)_2/Et_2Zn$ system

During my doctoral period at *SynCat (Synthèse et Catalyse Asymétrique)*, a research group of *Université de Strasbourg*, in which major effors are focused on the metal-catalyzed C-H functionalization for asymmetric synthesis, the goal of the work was to investigate suitable conditions to perform the metal-catalyzed C-H functionalization on the diaryl acetaldehydes **II**, which derive by Meinwald rearrangement of the parent epoxide **I**. The compounds **III** could be

a new potential key intermediate for alternative route to 2,3-diaryl- 2,3-dihydrobenzofurans **V** by nucleophilic addition of arylmetallic compounds and subsequent cyclization (Scheme 60).

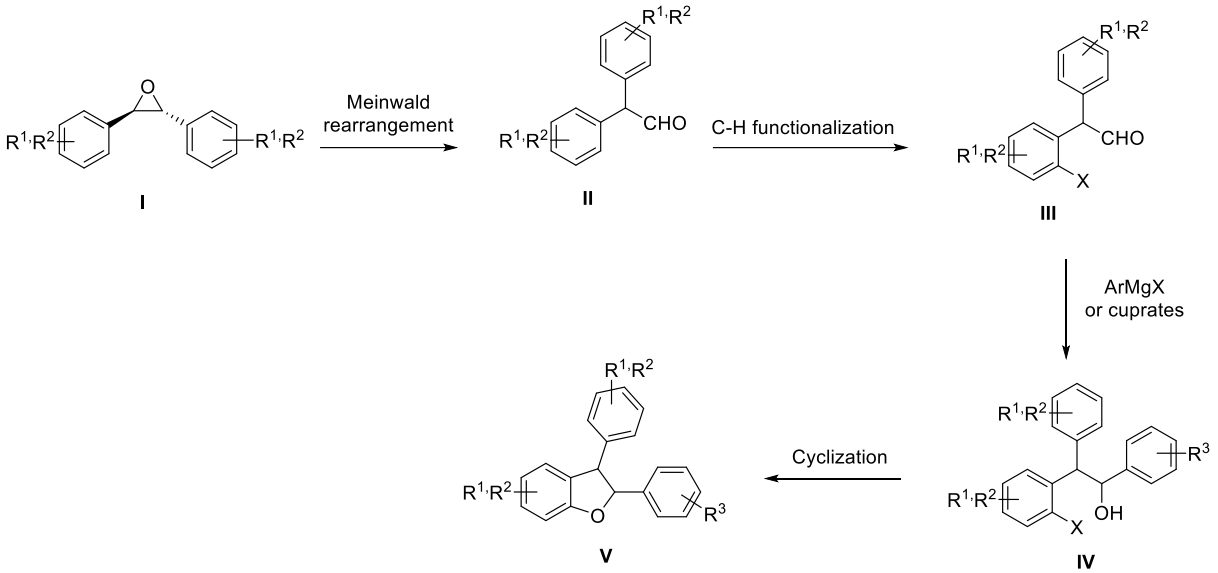

Scheme 60 Alternative route to 2,3-diaryl-2,3-dihydrobenzofuranes

3.3 Results and discussion

The study was focused on the metal-catalyzed C-H functionalization of the diphenylacetaldehyde model **56** that was obtained by a highly efficient Meinwald rearrangement of commercial available *trans*-diphenyloxirane **55** in presence of catalytic amounts of copper(II) tetrafluoroborate (Scheme 61).[119]

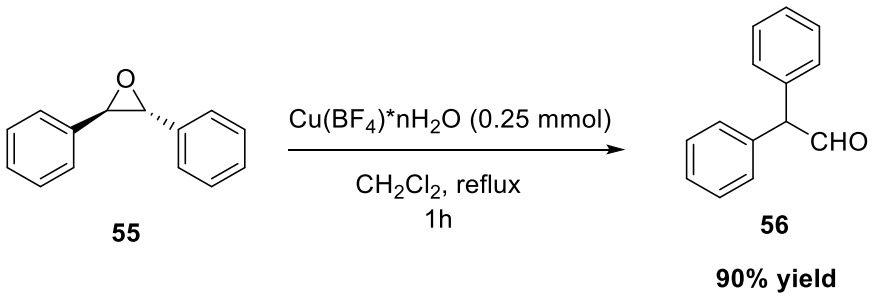

Scheme 61 Meinwald rearrangement of epoxide **55** by $Cu(BF_4)*nH_2O$

Firstly we decided to use the chiral transient directing group (*c*TDG) strategy, thanks to the numerous advantages already discussed in the introduction. In literature there are many examples of this strategy for the $C(sp^2)$-H activation, but unfortunately almost of them starting from aromatic aldehydes.

[119] Robinson, M. W. C.; Pillinger, K. S.; Mabbett, I.; Timms, D. A.; Graham, E. *Tetrahedron*, **2010**, *66*, 8377-8382.

In a recent paper, Shi and coworkers[120] reported the atroposelective synthesis of axially chiral biaryls by palladium-catalyzed C(sp^2)–H olefination, using *tert*-leucine as an inexpensive, catalytic, and transient chiral auxiliary. This strategy, in the presence of 10 mol% of $Pd(OAc)_2$, 20 mol% of *tert*-leucine and 10 mol% of the co-oxidant benzoquinone (BQ) at 60°C in HFIP/AcOH under O_2, provided a highly efficient and straightforward access to a broad range of enantioenriched biaryls (Scheme 62) in good yields (up to 98 %) with excellent enantioselectivities (95 to >99 % *ee*).

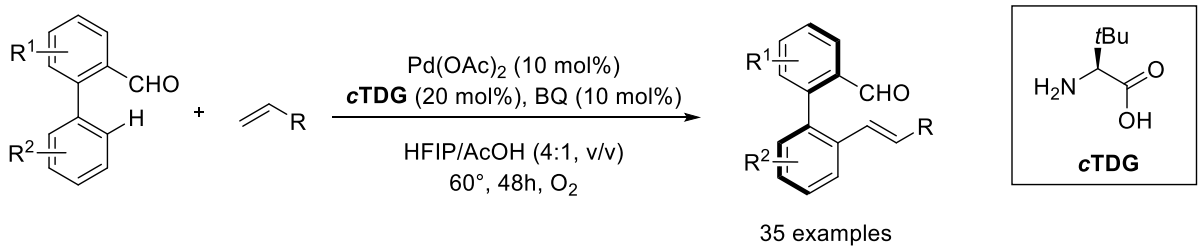

Scheme 62 Atroposelective synthesis of axially chiral biaryls by palladium-catalyzed C(sp^2)–H olefination *via* *c*TDG strategy

The proposed mechanism of this reaction is shown on scheme 63: 1) reaction of ***c*TDG** with biaryl aldehydes to form the imines **II** and **III**; 2) the preferential formation of an axially enantioenriched biaryl palladacycle **IV** with one imine diastereomer enhanced by steric interaction; 3) Heck-type reaction of **IV** with alkene to give **VI**; 4) hydrolysis of **VI** delivering the expected axially chiral biaryl **VII** and oxidation of Pd^0 to regenerate Pd^{II} species.

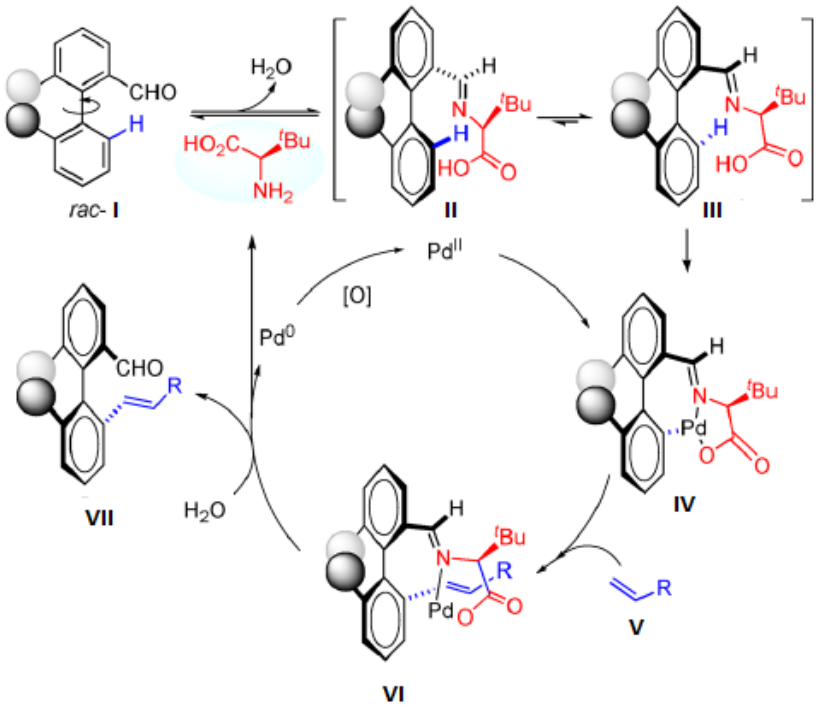

Scheme 63 Proposed mechanism of atroposelective synthesis of chiral biaryls through C-H olefination

[120] Yao, Q.-J.; Zhang, S.; Zhan, B.-B.; Shi, B.-F. *Angew. Chem. Int. Ed.* **2017**, *56*, 6617.

We tested this procedure using the same reaction conditions for the Pd-catalyzed C-H olefination of the diphenylacetaldehyde **56** with *n*-butylacrylate **57** (Scheme 64), but unfortunately we did not obtain the desired product **58** but only degradation products.

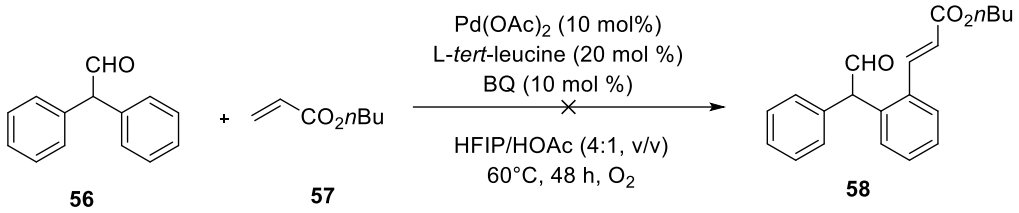

Scheme 64 Attempt for Pd-catalyzed C-H olefination of the diphenylacetaldehyde **56** *via* ***c*TDG**

Therefore, we investigated on different reaction conditions (Table 17), increasing the temperature and the amount of $Pd(OAc)_2$, L-*tert*-leucine and using three different silver salts as additive under nitrogen atmosphere instead of benzoquinone under oxygen atmosphere. Unfortunately, all these attempts afforded only degradation products.

Table 17 Variation in the reaction conditions for Pd-catalyzed C-H olefination of the diphenylacetaldehyde **56** *via* ***c*TDG**

Exp.	$Pd(OAc)_2$ (mol%)	L-*tert*-leucine (mol%)	Additive	Temp (°C)	Product
1	20	50	AgOAc	100	-
2	20	50	AgTFA	100	-
3	20	50	Ag_2CO_3	100	-

One reason for the unsuccessful of this procedure could rely on the lack of the reaction between L-*tert*-leucine and the diphenylacetaldehyde to form the imine **59**, which is a fundamental intermediate for starting the catalytic cycle, as shown on scheme 63. Perhaps it is due to the facile keto-enolic tautomerism of the diphenylacetaldehyde by the presence of strong acidic doubly benzylic hydrogen, α to the formyl group (Figure 36).

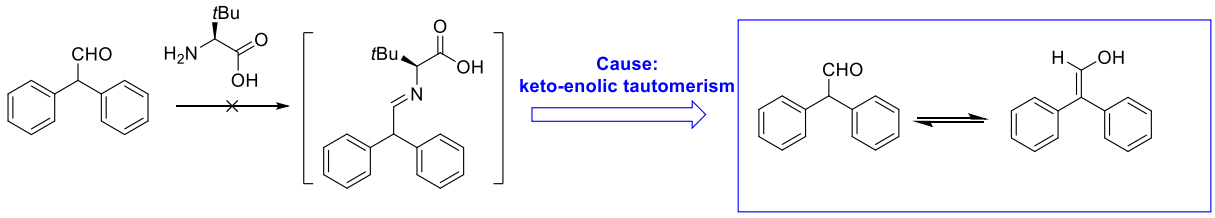

Figure 36 Likely key problem for Pd-catalyzed C-H olefination of the diphenylacetaldehyde **56**

To confirm our hypothesis we performed two classical procedure to form the imine on the diphenylacetaldehyde **56**; in the first we used DL-phenylalanine and 4 Å molecular sieves in toluene at reflux, while in the second procedure DL-phenylalanine was first converted in DL-phenylalanine sodium salt and then reacted with the aldehyde (Scheme 65). In both cases, as expected, only degradation products were obtained, confirming our hypothesis.

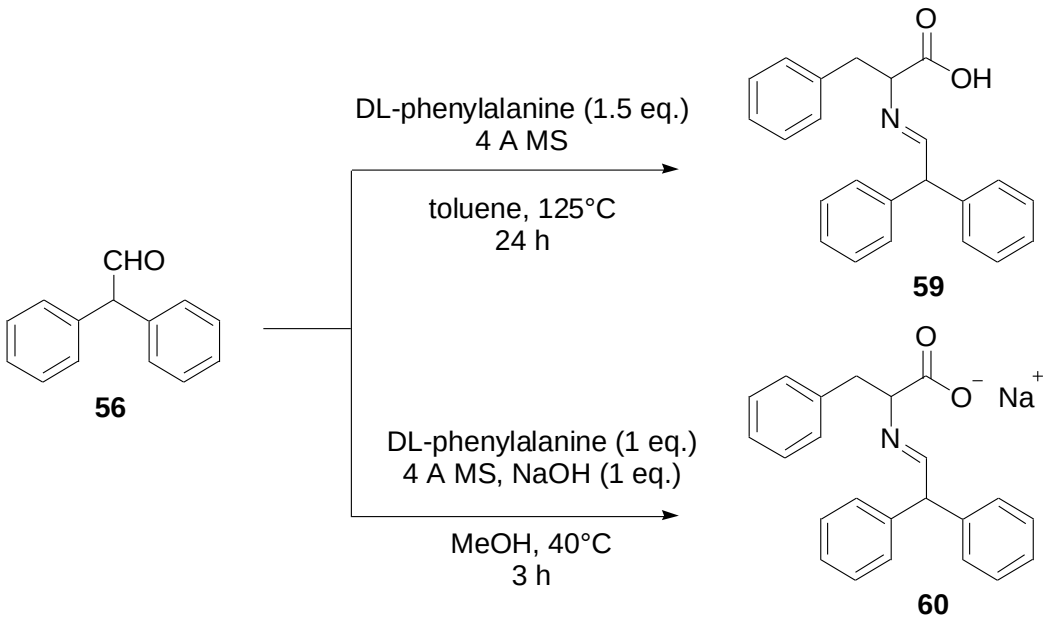

Scheme 65 Attempts for synthesis of imine

Therefore, we decided to test the Pd-catalyzed C-H olefination on the acetal **61**, which was prepared in moderate yield treating the diphenylacetaldehyde **56** with trimethyl orthoformate and *p*-TsOH·H_2O in methanol (Scheme 66).[121]

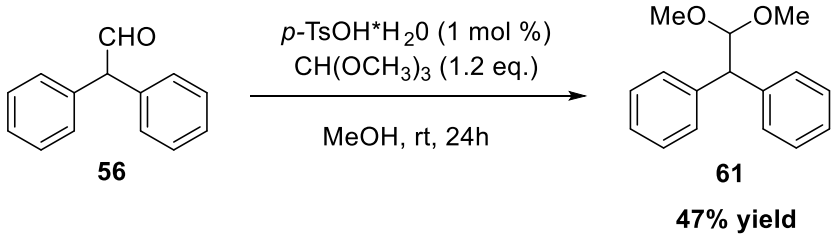

Scheme 66 Synthesis of acetal **61**

The acetal **61** in presence of HFIP can lose a methoxy group forming an oxonium species more reactive towards the amine to obtain the desired imine intermediate. The reaction was performed in two different experimental conditions (Scheme 67), but in all cases we obtained only degradation products.

[121] Rodríguez-Gimeno, A.; Cuenca, A. B.; Gil-Tomás, J.; Medio-Simon, M.; Olmos, A.; Asensio, G, *J. Org. Chem* **2014**, *79*, 8263-8270

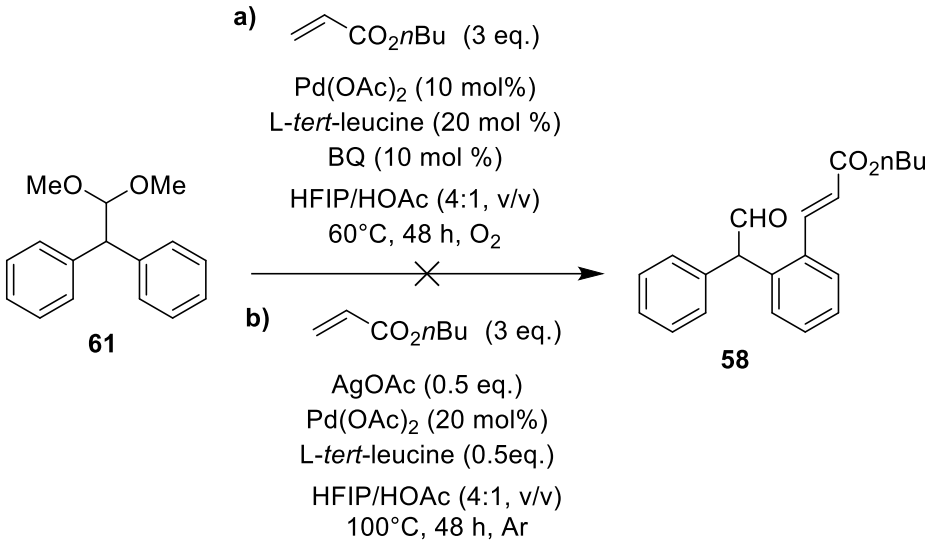

Scheme 67 Attempts for Pd-catalyzed C-H olefination of the acetal **61** *via* ***c*TDG**

After all these unsuccessful attempts, we decided to change the strategy switching to the traditional metal-catalyzed C-H functionalization *via* external directing group (DG).
Diphenyl-*N*-(8-quinolinyl)acetamide **63** bearing a bidentate donating group was prepared in good yield by reaction of diphenylacetyl chloride **62** with 8-aminoquinoline and triethylamine in CH_2Cl_2 (Scheme 68).[122]

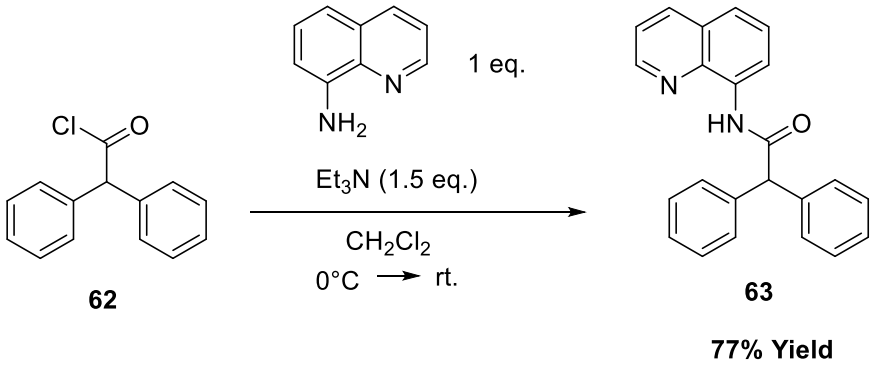

Scheme 68 Synthesis of amide **63**

We performed the Pd-catalyzed C-H olefination on diphenyl-*N*-(8-quinolinyl)acetamide **63** with *n*-butyl-acrylate **57** in presence of $Pd(OAc)_2$ (0.2 eq.) and silver acetate as co-oxidant (2 eq.) in HFIP/AcOH under N_2 at 60°C for 48h. The reaction did not afford the desired product **64**, but the product **65** which derives from double C-H activation: the Heck type reaction with the alkene and the subsequent intramolecular cyclization (Scheme 69). The structure **65** was confirmed by GC/MS analysis (MS (m/z, %): 463.10 [M^+]) and ^{1}H NMR analysis (in particular for the presence of a singlet instead a doublet of the stylbenic part).

[122] Liao, G.; Chem, H.-M.; Shi, B.-F. *Chem. Commun.* **2018**, *54*, 10859-10862.

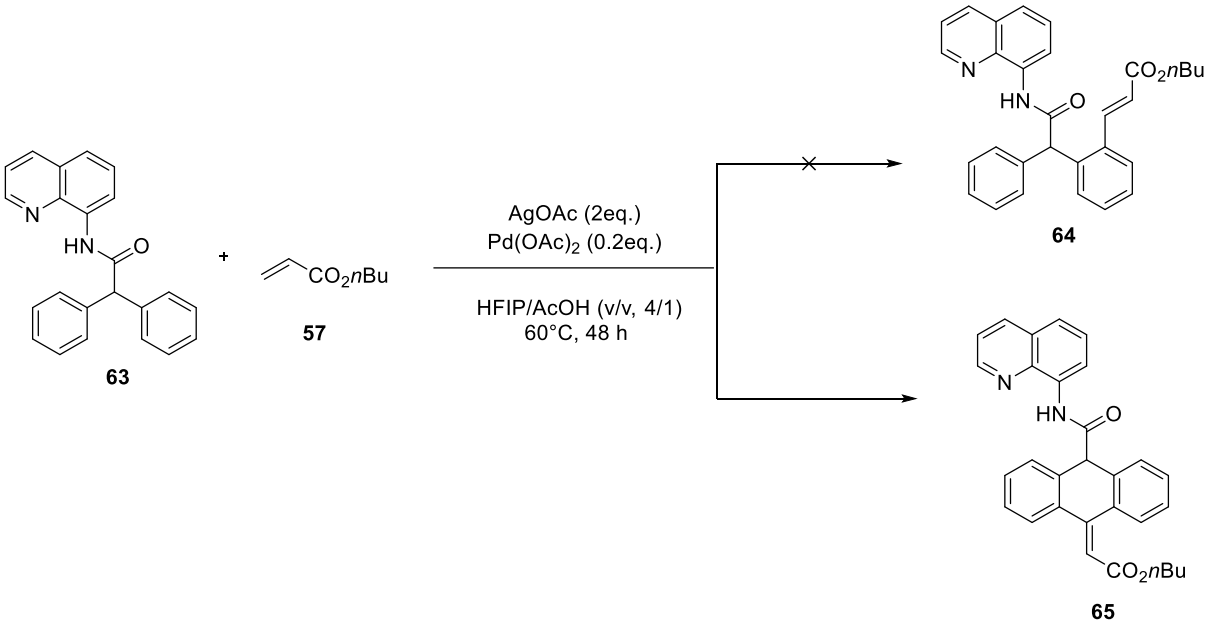

Scheme 69 Pd-catalyzed olefination of amide **63**

Since Pd-catalyzed C-H olefination *via* DG strategy did not give the desired product, we turned our attention towards two other types of C-H activation; the C-H iodination and the C-H acetoxylation.

In 2014, Colobert and coworkers[123] reported the synthesis of axially chiral biaryls by palladium-catalyzed C(sp^2)−H acetoxylation and iodination, using an enantiopure sulfoxide as both chiral auxiliary and bidentate directing group. The asymmetric direct acetoxylation, in the presence of $Pd(OAc)_2$ as catalyst, acetic acid (AcOH) as acetoxylating agent, persulfate ($(NH_4)_2S_2O_8$) as oxidant and a small amount of water in HFIP at room temperature, provided a highly efficient access to a broad range of biaryls (Scheme 70) in good yields and with excellent diastereoselectivities.

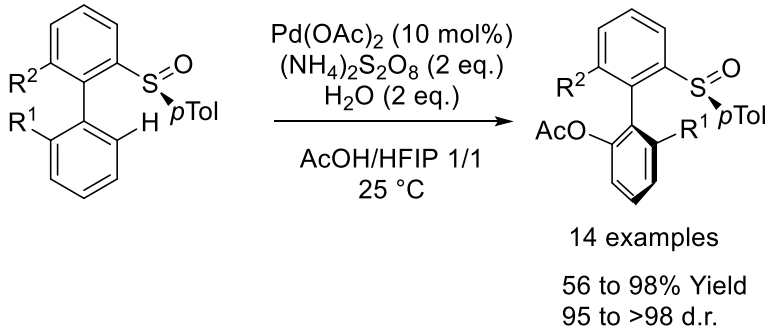

Scheme 70 Synthesis of axially chiral biaryls through sulfoxide-directed C-H acetoxylation

Encouraged by the efficiency of this diastereoselective acetoxylation reaction, they subsequently focused on proving a more general character of such an original asymmetric CH activation reaction, turned their attention toward an iodination reaction. Rapidly, they discovered that a simple replacement of the $(NH_4)_2S_2O_8$ oxidant by *N*-iodosuccinimide (NIS;

[123] Hazra, C. K.; Dherbassy, Q.; Wencel-Delord, J.; Colobert, F. *Angew. Chem. Int. Ed.* **2014**, *53*, 13871-13875.

1.3 equiv) led to a complete switch in the reactivity of catalytic system enabling smooth, mild, and highly diastereoselective C-I coupling (Scheme 71).

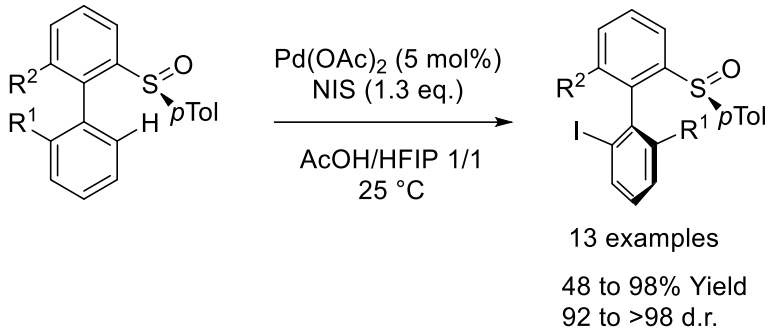

Scheme 71 Synthesis of axially chiral biaryls by sulfoxide-directed C-H iodination

We tested this procedures for the direct C-H acetoxylation and iodination of the diphenyl-*N*-(8-quinolinyl)acetamide **63**.

The acetoxylation reaction of diphenyl-*N*-(8-quinolinyl)acetamide **63** under the same condition reported in literature both at room temperature and 60 °C led to the starting material (Scheme 72).

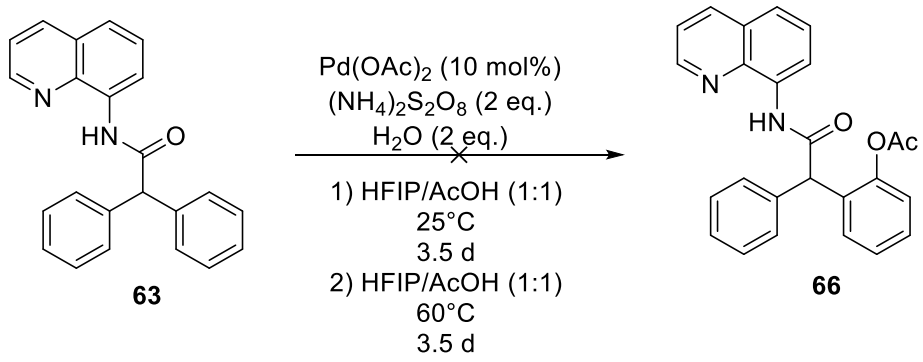

Scheme 72 Attempts for the Pd- catalyzed C-H acetoxylation of the diphenyl-*N*-(8-quinolinyl)acetamide **63**

The iodination reaction of diphenyl-*N*-(8-quinolinyl)acetamide **63** under the same condition reported in literature led to the product **67** in which the C-H iodination took place on the 8-quinolinamine instead on the desired phenyl group (Scheme 73).

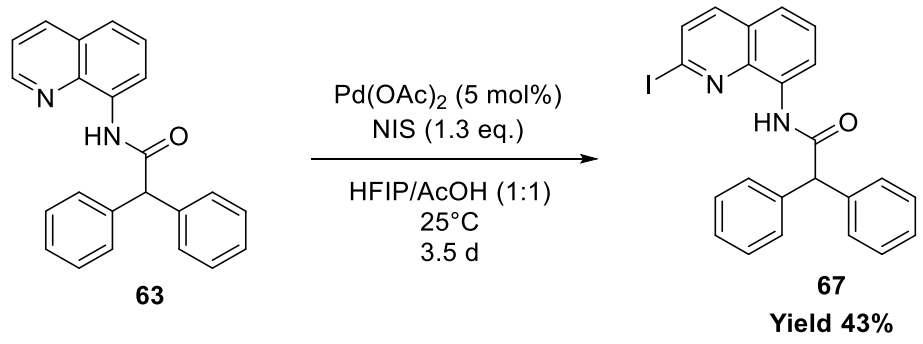

Scheme 73 Pd- catalyzed C-H iodination of the diphenyl-*N*-(8-quinolinyl)acetamide **63**

The structure **67** was confirmed by GC/MS analysis (MS (m/z, %): 464.10 [M^+]) and ^{1}H NMR analysis (the signals of aromatic part were still symmetric, this means that the iodine did not go on the phenyl but on 8-quinolinamine). Furthermore, the iodine could go both on C4 and C8 position of 8-quinolinamine (Figure 37).

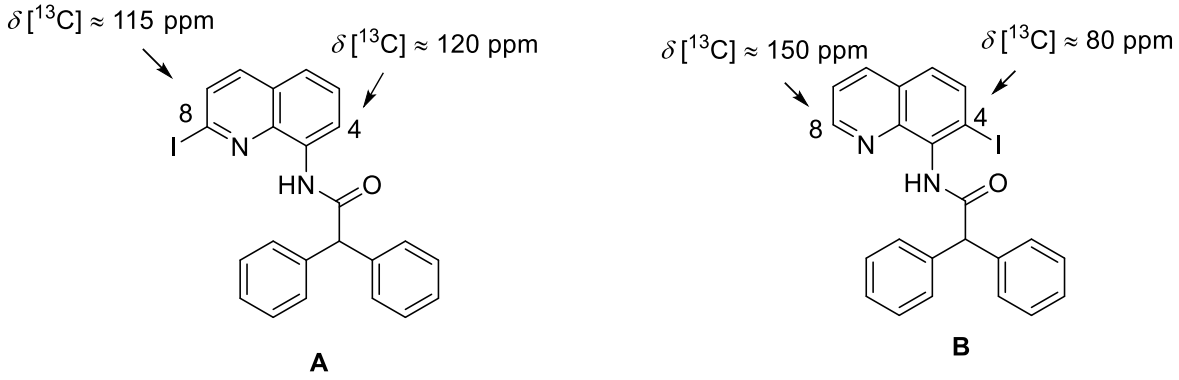

Figure 37 Predicted values of δ [^{13}C] of C4 and C8 in structure **A** and **B**

The type structure **A** of the product **67** was confirmed by a long-range ^{1}H/^{13}C correlation between N-H proton at 9.99 ppm with C4 carbon at 118 ppm (Figure 38).

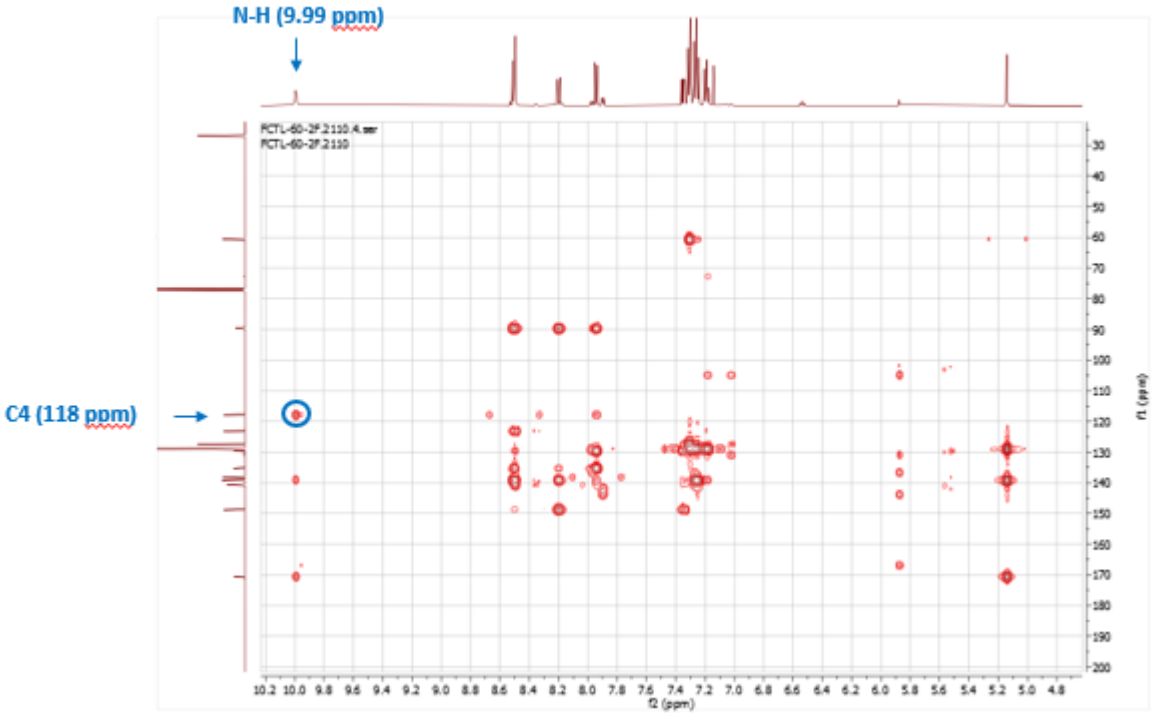

Figure 38 Diagnostic long-range ^{1}H/^{13}C correlation between N-H proton and C4 carbon of product **67**

The lack of good results using this strategy prompted us to test other procedures reported in literature, in which the same bidentate DG, the 8-aminoquinoline, was used.

In 2009, Liang and coworkers[124] disclosed Pd-Catalyzed acetoxylation of various *N*-(8-Quinolinyl)benzamides. The reaction in presence of $Pd(OAc)_2$ as catalyst and $PhI(OAc)_2$ as both acetoxylating agent and oxidant in $AcOH/Ac_2O$ at 150°C led to the desired acetoxylation products in good yields (Scheme 74).

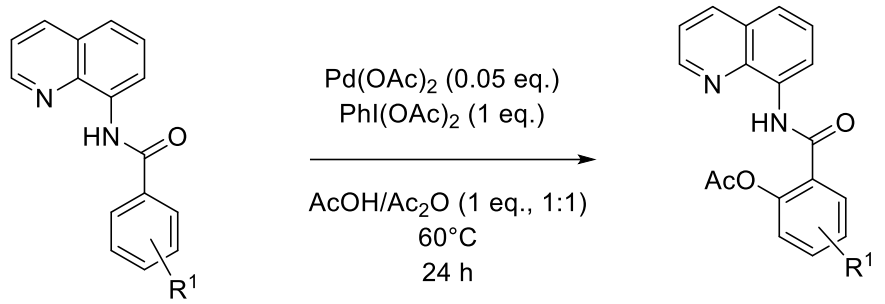

Scheme 74 Pd-catalyzed acetoxylation of various *N*-(8-Quinolinyl)benzamides

The C-H activation of the resulting acetoxylated products could be easily realized due to the selective coordination of the substrate bearing a *N,N* donor with the palladium catalyst, formation of two five-membered palladacyles, followed by an unstable Pd(IV) species that decompose *via* a reductive elimination pathway. Subsequent functionalization would be possible (Scheme 75).

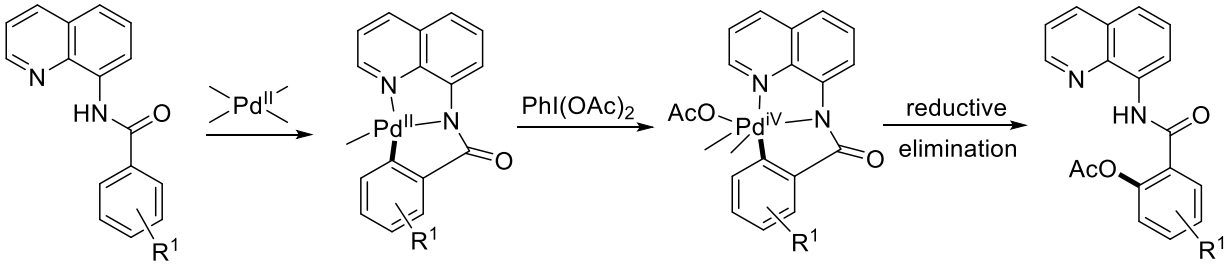

Scheme 75 Possible mechanism of Pd-catalyzed acetoxylation of *N*-(8-Quinolinyl)benzamides

The acetoxylation reaction of diphenyl-*N*-(8-quinolinyl)acetamide **63** under same conditions but at 60 °C instead of 150 °C afforded the product **68** in which the C-H acetoxylation took place on the 8-quinolinamine and not on the desired phenyl group (Scheme 76).

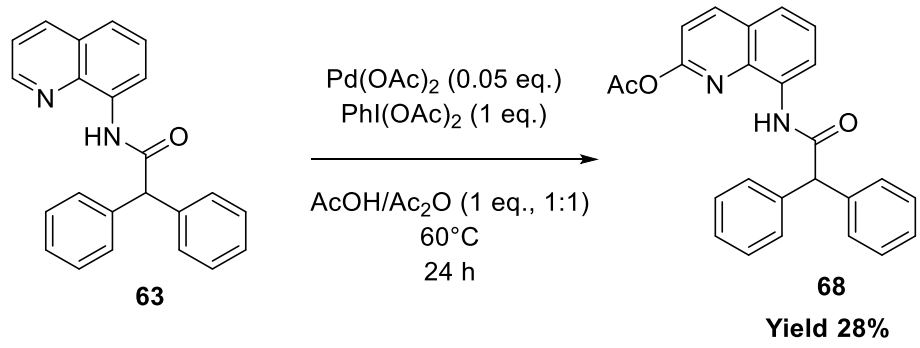

Scheme 76 Pd- catalyzed C-H acetoxylation of the diphenyl-*N*-(8-quinolinyl)acetamide **63**

[124] Gou, F.-R,; Wang, X.-C.; Huo, P.-F.; Bi, H.-P,; Guan, Z.-H,; Liang, Y.-M. *Org. Lett.*, Vol. **2009**, *11*, 5726-5729.

The structure **68** was confirmed by GC/MS analysis (MS (m/z, %): 396.10 [M^+]) and ^{1}H NMR analysis (the signals of aromatic part were still symmetric, this means that the iodine did not go on the phenyl but on 8-quinolinamine). Furthermore, the iodine could go both on C4 and C8 position of 8-quinolinamine (Figure 39).

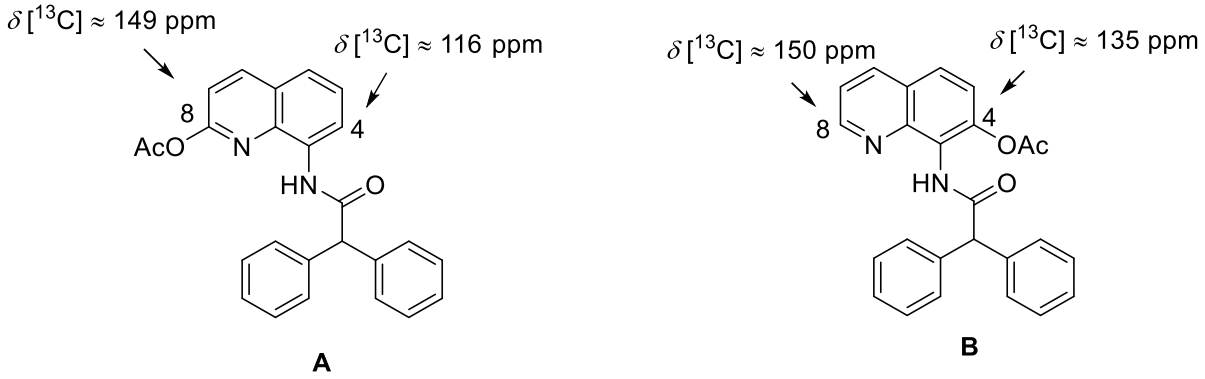

Figure 39 Predicted values of δ [^{13}C] of C4 and C8 in structure **A** and **B**

The structure **A** of the product **68** was confirmed by a long-range ^{1}H/^{13}C correlation between N-H proton at 10.03 ppm with C4 carbon at 115.9 ppm (Figure 40).

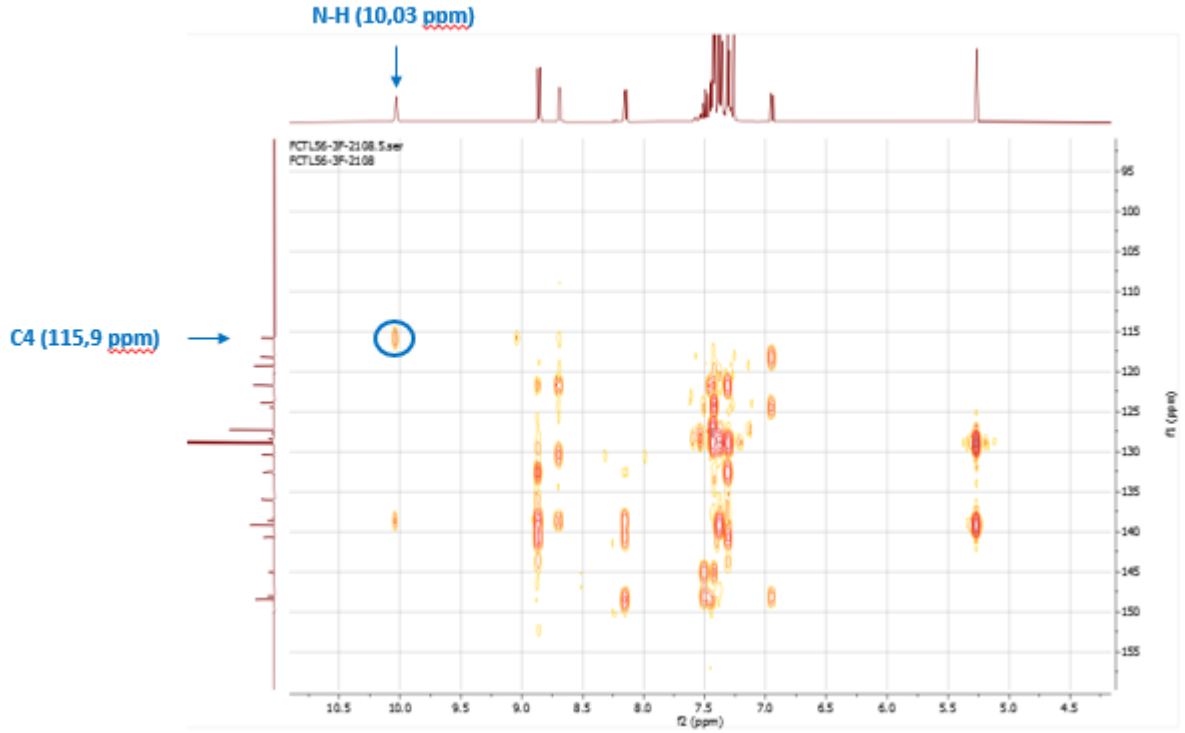

Figure 40 Diagnostic long-range ^{1}H/^{13}C correlation between N-H proton and C4 carbon of product **68**

In 2018, Kakiuchi and coworkers[125] reported the Pd-catalyzed C-H Iodination of various N-(8-Quinolinyl)benzamides. The reaction in presence of $Pd(OAc)_2$ as catalyst and I_2 as iodine source led to the desired iodinated products in moderate to good yields (Scheme 77).

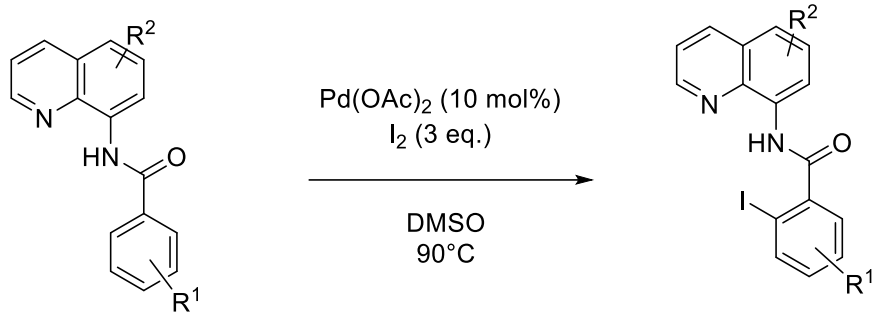

Scheme 77 Pd-catalyzed iodination of various *N*-(8-Quinolinyl)benzamides

The proposed catalytic cycle for the C-H iodination is shown on Scheme 78: the reaction of the palladium(II) catalyst with benzamide **I** provides palladium chelate species **II** via C-H bond cleavage; the reaction of **II** with I_2 gives iodination product **III** and generates HI.

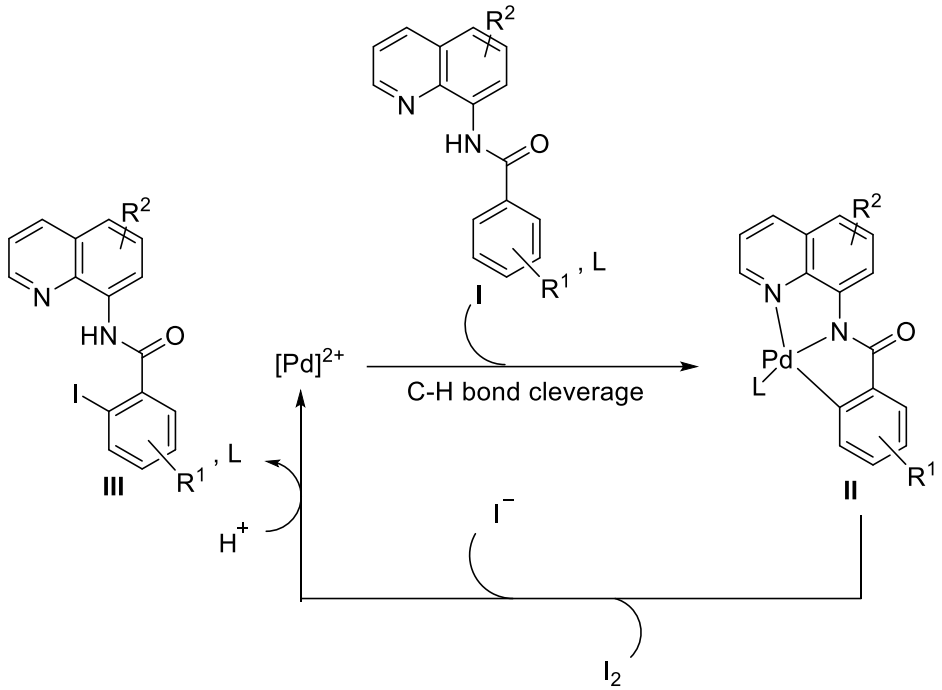

Scheme 78 Possible mechanism of Pd-catalyzed iodination of *N*-(8-Quinolinyl)benzamides

The iodination reaction of diphenyl-*N*-(8-quinolinyl)acetamide **63** under same conditions but at 60 °C instead of 90 °C, finally provided the desired iodinated product **69** (Scheme 79).

[125] Sano, K.; Kimura, N.; Kochi, T.; Kakiuchi, F. *Asian J. Org. Chem*. **2018**, *7*, 1311 – 1314.

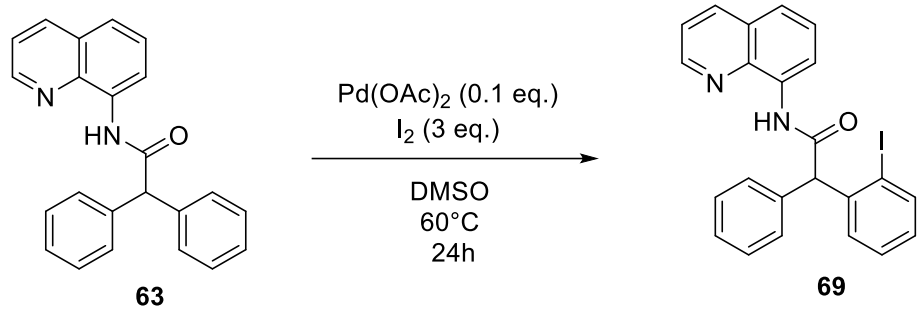

Scheme 79 Pd- catalyzed C-H iodination of the diphenyl-*N*-(8-quinolinyl)acetamide **63**

The structure **69** was confirmed by GC/MS analysis (MS (m/z, %): 464.10 [M^+]) and ^{1}H NMR analysis (the signals of aromatic part were dissymmetrical, this means that the iodine went on the phenyl group). A further confirmation was obtained by the direct (Figure 41) and long range (Figure 42) ^{1}H/^{13}C NMR experiments.

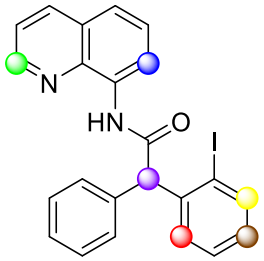

Figure 41 HSQC (direct ^{1}H/^{13}C NMR experiment) of **69**

From the HSQC spectra (Figure 41) the following correlations can be seen:

- **A:** proton at 8.78 ppm with the carbon at 116.52 ppm;
- **B:** protons at 8.05 ppm with the carbon at 148.28 ppm;
- **C:** proton at 7.45 ppm with the carbon at 140.24 ppm:
- **D:** proton at 7.16 ppm with the carbon at 129.39 ppm;
- **E:** protons at 6.96 ppm with the carbon at 129.26 ppm;
- **F:** proton at 5.61 ppm with the carbon at 69.29 ppm.

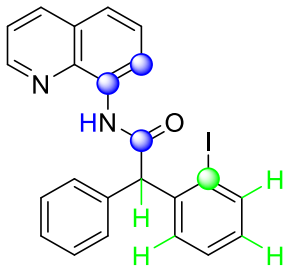

69

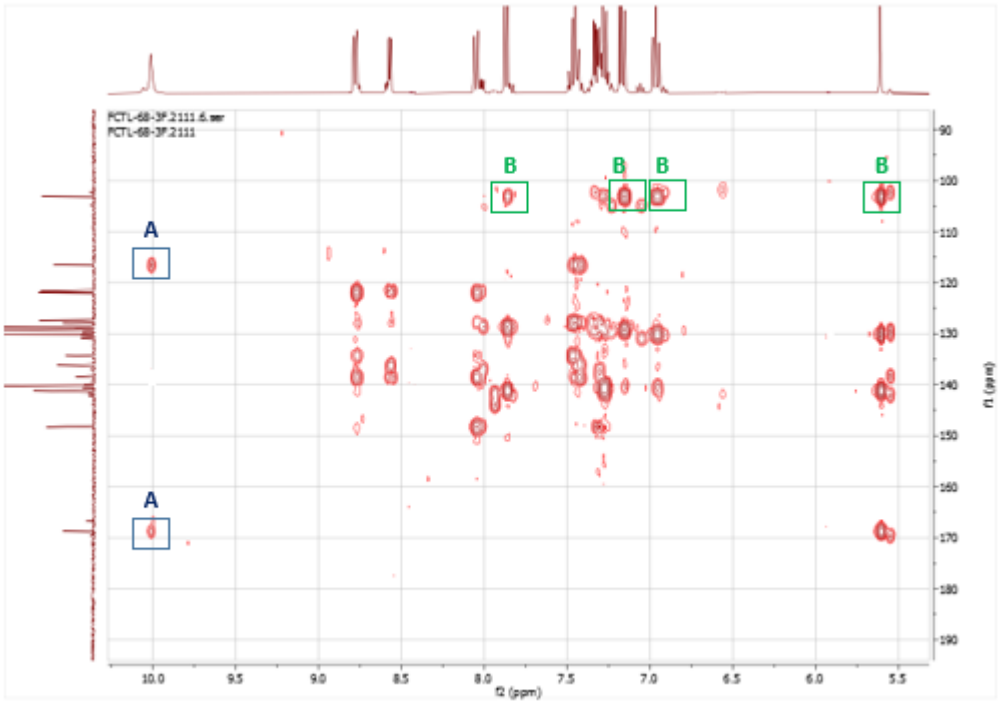

Figure 42 HMBC (long range $^{1}H/^{13}C$ NMR experiment) of **69**

From the HSQC spectra (Figure 42) the diagnostic correlations can be seen:

- **A:** proton at 10.01 ppm (N-H) with the carbons at 116.52 ppm (C4), 168.75 ppm (C=O);
- **B:** carbon at 103.11 ppm (C-I) with the protons at 7.87 ppm, 7.16 ppm, 6.96 ppm amd 5.61 ppm.

This last correlation, in particular, confirms the structure of the product **69**.

Encouraged by this result, we performed an enantioselective version of this reaction using the (*R*)-Monophos **70** as chiral ligand (Scheme 80).[126] Unfortunately, the reaction afforded the iodinated product **69** but without induction of chirality (HPLC analysis).

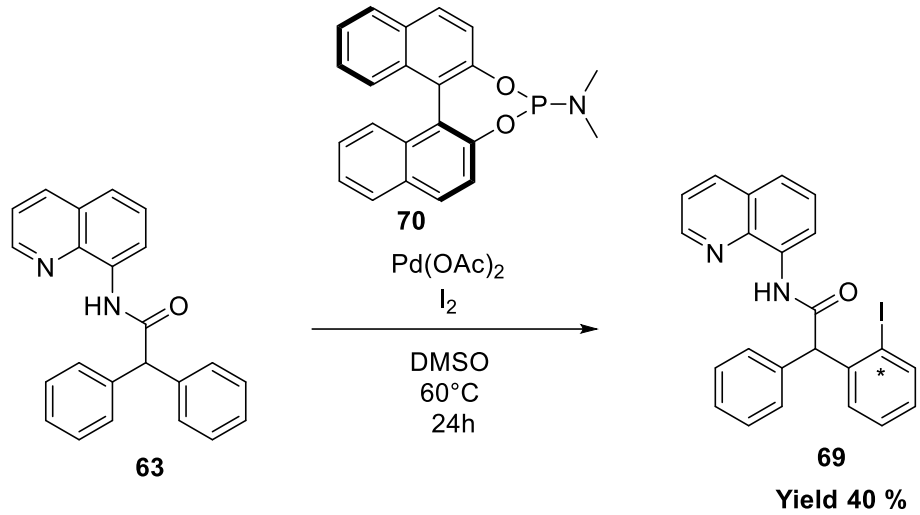

Scheme 80 Attempt of the enantioselective Pd- catalyzed C-H iodination of the diphenyl-*N*-(8-quinolinyl)acetamide **63**

In summary, the fist example of regioselective C-H iodinations of diphenyl-acetamide possessing the 8-aminoquinoline as directing group was developed. This kind of bidentate system has large potential for the exploration of other type of C-H activation reactions that have not been achieved by the transient directing group strategy.

3.4 Experimental procedures

3.4.1 General chemical experimental

Technical grade solvents for extraction and chromatography (cyclohexane, ethyl acetate and diethyl ether) were used without purification. All reagents, if commercially available, were purchased from standard suppliers (Sigma Aldrich, ABCR, Fluorochem, TCI, Alfa Aesar and Apollo scientific) and used without further purification unless otherwise stated. Air- and moisture- sensitive materials were stored, protected and handled under an atmosphere of argon, with appropriate glassware. Thin layer chromatography (TLC) was carried out using pre-coated silica gel sheets (Merck 60 F254). Flash column chromatography was performed on VWR silica gel (40–63 μm) using the indicated solvents. Spots were visualized by UV light irradiation. ^{1}H NMR (400 or 500 MHz), and ^{13}C NMR (100 or 125 MHz) spectra were recorded on Bruker Avance III HD 400 and 500 MHz instruments, respectively. Chemical shifts are reported as *δ*-

[126] Tong, H.-R.; Zheng, S.; Li, X.; Deng, Z.; Wang, H.; He, G.; Peng, Q.; Chen, G. *ACS Catal.* **2018**, 8, 11502−11512

values in parts per million (ppm) and are referred to partially deuterated chloroform, (chloroform $\delta[^1H]$ = 7.26 ppm and $\delta[^{13}C]$ = 77.0 ppm) Multiplicities were abbreviated as s (singlet), brs (broad signal), d (doublet), t (triplet), q (quartet), m (multiplet), dd (doublet of doublets), ddd (doublet of doublets of doublets). Coupling constants *J* were given in Hz. MS spectra were recorded on a GC/MS system consisting of a 5977E MSD single-quadrupole mass spectrometer with a 7820A GC by Agilent Technologies with EI (Electronic Impact) ion source. Enantiomeric excess was determined by HPLC analysis performed on a JASCO PU-1580 pump with a Varian 2550 UV detector and Daicel CHIRALCEL®-OD column (internal diameter 4.6 mm, column length 250 mm, particle size 10 µm).

3.4.1.1 Meinwald rearrangement

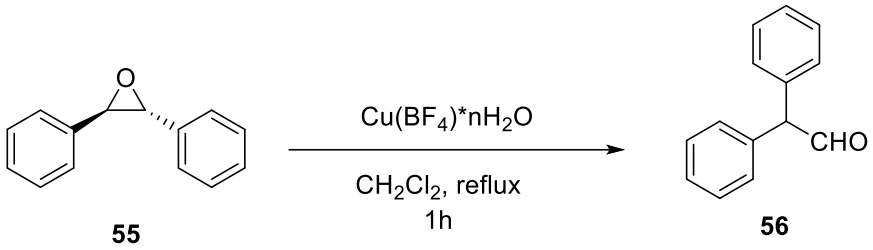

55 **56**

Copper tetrafluoroborate (255 mg, 0.25 mmol, 25 mol%) was added to a solution of *trans*-diphenyloxirane (196 mg, 0.95 mmol, 1 eq.) in dry dichloromethane (10 mL) at reflux. Upon completion of the reaction (TLC) the mixture was diluted with dichloromethane (30 mL) and washed with water (3x40 mL). The organic phase was dried over Na_2SO_4, and the solvent removed to give 2,2-diphenylacetaldehyde as an oil, which was used without purification (167 mg, 0,85 mmol, 90%).

^1H NMR (400 MHz, $CDCl_3$); δ (ppm) 4.81 (d, *J* = 4.0 Hz, 1H), 7.16 (t, *J* = 8.0 Hz, 4H), 7.23 (t, *J* = 8.0 Hz, 2H), 7.30 (t, *J* = 8.0 Hz, 4H), 9.88 (s, *J* = 4.0 Hz, 1H).

3.4.1.2 Pd-catalyzed C-H olefination via cTDG

Method A: To an oven-dried Schlenk tube the substrate (0.10 mmol), butyl acrylate (0.3 mmol), $Pd(OAc)_2$ (2.2 mg, 0.010 mmol), *L-tert*-leucine (2.6 mg, 0.02 mmol), BQ (1.1 mg, 0.01 mmol), were added in a mixture of HFIP (0.8 mL) and HOAc (0.2 mL). The tube was then charged with O_2, the mixture was stirred for 48 h at 60 °C followed by cooling. The resulting mixture was quenched by filtration through a celite pad and concentrated in vacuo. The residue was purified by preparative TLC using hexane/EtOAc as eluent.

Method B: To an oven-dried Schlenk tube the substrate (0.10 mmol), butyl acrylate (0.3 mmol), $Pd(OAc)_2$ (4.4 mg, 0.020 mmol), L-*tert*-leucine (6.5 mg, 0.05 mmol), Silver salt (0.2 mmol), were added in a mixture of HFIP (0.8 mL) and HOAc (0.2 mL). The tube was then charged with N_2, the mixture was stirred for 48 h at 100 °C followed by cooling. The resulting mixture was quenched by filtration through a celite pad and concentrated in vacuo. The residue was purified

by preparative TLC using hexane/EtOAc as the eluent.

3.4.1.3 Synthesis of imine

Method A: To a magnetically stirred mixture of diphenylacetaldehyde **56** (130 mg, 1 eq., 0.65 mmol) in toluene (4 mL), DL-phenylalanine (165 mg, 1.5 eq., 0.99 mmol) and 4 Å molecular silvers were added and the mixture was stirred at 125°C for 24h. The resulting mixture was filtered and concentrated *in vacuo*. The NMR of the crude was performed.

Method B: To a magnetically stirred mixture of DL-phenylalanine (115 mg, 1 eq., 0.7 mmol) in methanol (4 mL) and 4 Å molecular sieves , sodium hydroxide (165 mg, 1 eq., 0.7 mmol) was added and the mixture was stirred at 40°C for 1h and cooled to room temperature. Diphenylacetaldehyde **56** (140 mg, 1 eq., 0.7 mmol) was added and the mixture was stirred at 40°C for 2h. The resulting mixture was filtered and concentrated *in vacuo*. The NMR of the crude was performed**.**

3.4.1.4 Synthesis of dimethylacetal of diphenylacetaldehyde

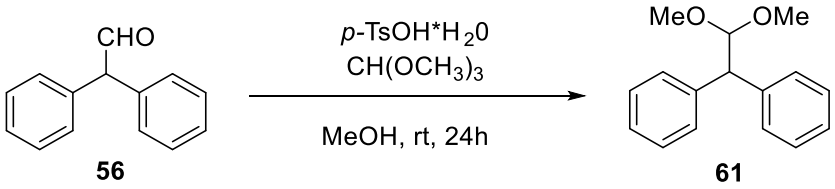

56 **61**

To a magnetically stirred mixture of diphenylacetaldehyde **56** (105 mg. 1 equiv, 0.55 mmol) and trimethyl orthoformate (106 mg, d = 0.97 g/mL, 70 µL, 1.2 equiv, 0.66 mmol) in methanol (1M), *p*-TsOH·H_2O (0.01 equiv, 1 mol %) was added and the mixture was stirred at room temperature for 24h. The mixture was extracted with H_2O/Et_2O. The combined Et_2O extracts were dried with Na_2SO_4 and concentrated under reduced pressure and the product **61** was obtained as colorless oil and used without purification (61 mg, 0.25 mmol, 47%).

^{1}H NMR (400 MHz, $CDCl_3$); δ (ppm) 3.32 (s, 6H), 4.25 (d, J = 8.0 Hz, 1H), 5.0 (d, J = 8.0 Hz, 1H), 7.20 (m, 2H), 7.30 (m, 8H).

3.4.1.5 Synthesis of amide

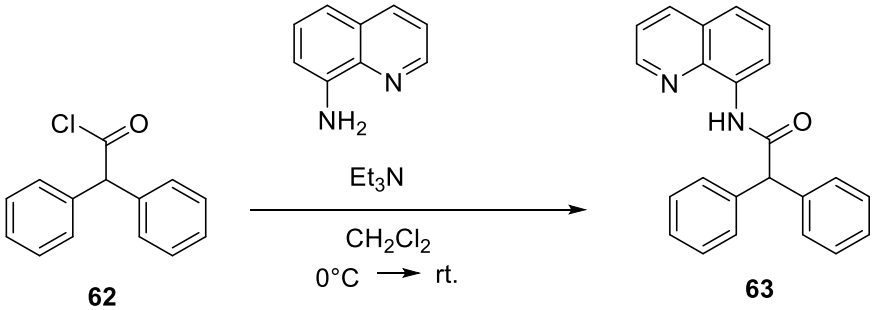

62 **63**

To a magnetically stirred solution of 8-quinolynamine (620 mg, 1 eq., 4.33 mmol) and Et_3N (0.66g, d = 0.728 g/mL, 0.9 mL, 1.5 eq., 6.5 mmol) in dry CH_2Cl_2 (10 mL) the solution of diphenylacetyl chloride (1g, 1 eq., 4.33 mmol) in dry CH_2Cl_2 (10 mL) was slowly added at 0 °C and the mixture was stirred at room temperature for 24h. The mixture was quenched by CH_2Cl_2 (15 mL), filtered through a pad of Celite to remove the undissolved salts and washed by CH_2Cl_2 (15 mL). The collected solution was washed by aqueous HCl (20 mL, 1M), satured $NaHCO_3$ (20 mL) and brine (20mL). The organic phase was dried with Na_2SO_4 and concentrated under reduced pressure. The crude was purified by flash column chromatography on silica gel (40% EtOAc/Hexane) to obtain diphenyl-*N*-(8-quinolinyl)acetamide **63** (1.12g, 3.33 mmol, 77%).

R_f = 0.4 (30% EtOAc/Hexane)

^{1}H NMR (400 MHz, $CDCl_3$); δ (ppm) 5.28 (s, 1H), 7.31 (m, 2H), 7.38 (m, 5H), 7.46 (m, 5H), 7.54 (m, 1H), 8.11 (d, *J* = 8.0 Hz, 1H), 8.67 (d, *J* = 4.0 Hz), 8.87 (d, *J* =8.0 Hz), 10.14 (s, 1H).

3.4.1.6 Pd-catalyzed C-H olefination via cTDG of diphenyl-N-(8-quinolinyl)acetamide

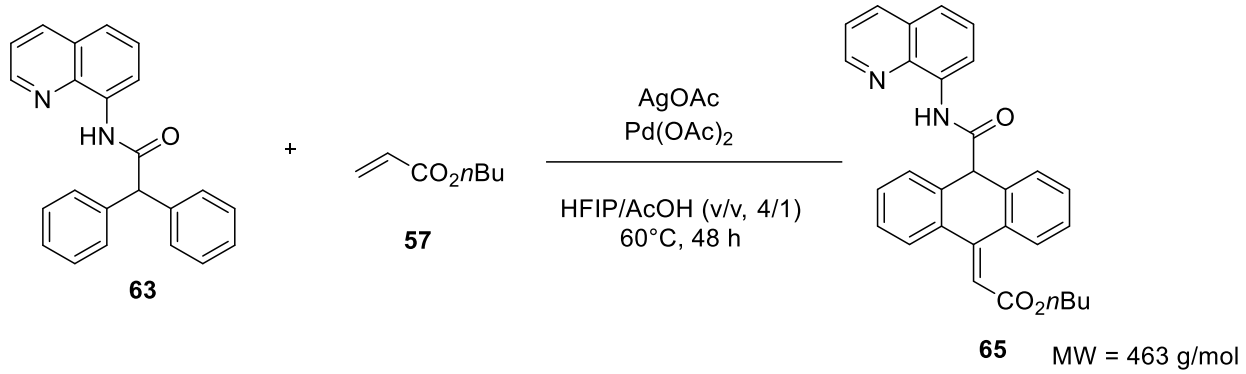

To an oven-dried Schlenk tube diphenyl-*N*-(8-quinolinyl)acetamide **63** (60 mg, 1 eq., 0.18 mmol), butyl acrylate (68 mg, 3 eq., 0.53 mmol), $Pd(OAc)_2$ (7.9 mg, 0.2 eq., 0.035 mmol) and AgOAc (59 mg, 0.2 eq., 0.35 mmol) were added in a mixture of HFIP (0.8 mL) and HOAc (0.2 mL). The tube was then charged with N_2, the mixture was stirred for 48 h at 60 °C followed by cooling. The resulting mixture was quenched by filtration through a celite pad and concentrated in vacuum. The residue was purified by preparative TLC (30% EtOAc/Hexane) to obtain butyl 2-(10-(quinolin-8-ylcarbamoyl)anthracen-9(10H)-ylidene)acetate **65**.

R_f = 0.3 (30% EtOAc/Hexane)

^{1}H NMR (400 MHz, $CDCl_3$); δ (ppm) 0.73 (t, *J* = 8.0 Hz, 3H), 1.10 (q, *J* =8.0 Hz, 2H), 1.38 (q, *J* = 8.0 Hz), 3.98 (t, *J* = 8.0 Hz, 3H), 5.20 (s, 1H), 6.52 (s, 1H), 7.34 (m, 2H), 7.42 (m, 6H), 7.63 (m, 1H), 7.67 (d, *J* =4.0 Hz, 1H), 7.79 (m, 1H), 7.92 (d, *J* =4.0 Hz, 1H), 8.04 (d, *J* = 4.0 Hz, 1H), 8.61 (d, *J* = 4.0 Hz, 1H), 9.88 (s, 1H). MS (m/z, %): 463 (0.3), 429 (1), 281 (19), 207 (100).

3.4.1.7 Pd-catalyzed directed C-H acetoxylation of diphenyl-N-(8-quinolinyl)acetamide

Method A: The reactions were performed under air. A sealed tube was successively charged with

diphenyl-*N*-(8-quinolinyl)acetamide **63** (68 mg, 1 eq., 0.2 mmol), $Pd(OAc)_2$ (10 mol%, 4.5 mg, 0.02 mmol), $(NH_4)_2S_2O_8$ (91.3 mg, 2 eq., 0.4 mmol). AcOH (530 µL, 46.5 eq., 9.3 mmol), HFIP (530 µL, 25.3 eq., 5.06 mmol), and H_2O (7.2 µL, 2.0 eq., 0.40 mmol) and the resulting suspension was stirred at 25 °C or 60°C. After 3.5 days analysis of an aliquot by TLC indicated no conversion and the presence of only starting diphenyl-*N*-(8-quinolinyl)acetamide **63.**

Method B: A solution of diphenyl-*N*-(8-quinolinyl)acetamide **63** (60 mg, 1 eq., 0.18 mmol), $Pd(OAc)_2$ (2.0 mg, 5 mmol%) in toluene (2.0 mL) was stirred in Schlenk tube. After 1 min of stirring $PhI(OAc)_2$ (114 mg, 2 eq., 0.35 mmol) and 1.0 equiv of HOAc/Ac2O (1:1) were added. The resulting mixture was then heated at 60°C for 24h. The reaction mixture was allowed to cool to room temperature and evaporated under reduced pressure. The crude was purified by preparative TLC (30% EtOAc/Hexane) to obtain the 8-(2,2-diphenylacetamido)quinolin-2-yl acetate **68** (20 mg, 0.05 mmol, 28%).

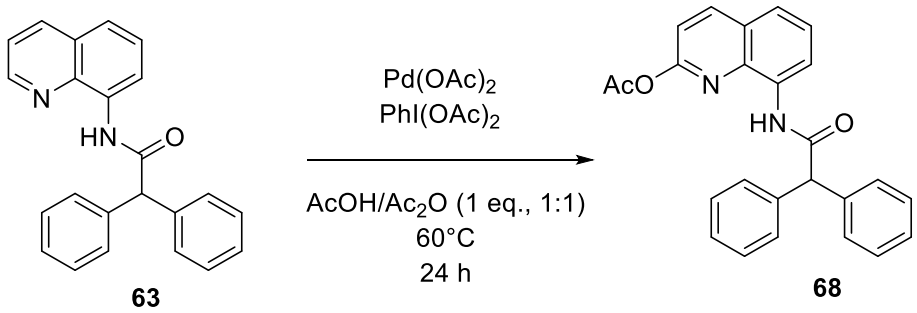

R_f = 0.25 (30% EtOAc/Hexane)

^{1}H NMR (400 MHz, $CDCl_3$); δ (ppm) 2.43 (s, 3H), 5.27 (s, 1H), 7.30 (m, 2H), 7.37 (m, 4H), 7.42 (m, 4H), 7.44 (dd, J_{AB} = 4.0 Hz, J_{AC} = 10.0 Hz 1H), 8.14 (d, J = 4.0 Hz, 1H), 8.69 (d, J = 4.0 Hz), 8.86 (d, J = 8.0 Hz), 10.03 (s, 1H). ^{13}C NMR (100 MHz, $CDCl_3$): δ (ppm) 21.5, 60.4, 115.9, 118,2, 119,3, 121.8, 123.9, 127.3, 128.4, 129.0, 130.4, 132.6, 136.0, 139.2, 148.5, 169.4, 130.4. MS (m/z, %): 396.1 (3), 229 (52), 187 (100).

3.4.1.8 Pd-catalyzed directed C-H iodination of diphenyl-N-(8-quinolinyl)acetamide

Method A: The reaction was performed under air. A sealed tube was successively charged with diphenyl-*N*-(8-quinolinyl)acetamide **63** (1.0 equiv, 0.2 mmol), $Pd(OAc)_2$ (5 mol%, 2.3 mg, 0.01 mmol), NIS (1.3 equiv, 58.5 mg, 0.26 mmol), AcOH (69.8 equiv, 800 µL, 13.96 mmol) and HFIP (38 equiv, 800 µL, 7.59 mmol). The resulting mixture was stirred at 25 °C until analysis of an aliquot by TLC showed complete conversion of the substrate. The mixture was quenched with saturated $NaHCO_3$ solution. Aqueous phase was extracted with ethyl acetate, the combined organic phases were washed with brine, dried over Na_2SO_4, filtrated and concentrated under vacuum. The crude was purified by preparative TLC (30% EtOAc/Hexane) to obtain *N*-(2-iodoquinolin-8-yl)-2,2-diphenylacetamide **67** (40mg, 0.083 mmol, 43%).

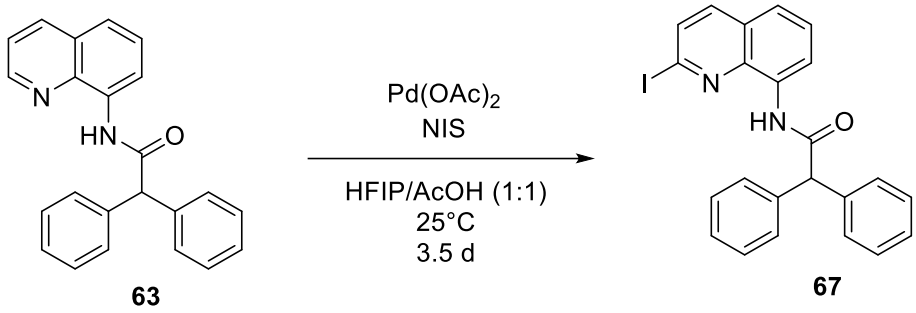

R_f = 0.3 (30% EtOAc/Hexane)

^{1}H NMR (400 MHz, $CDCl_3$); δ (ppm) 5.14 (s, 1H), 7.19 (m, 2H), 7.26 (m, 4H), 7.30 (m, 4H), 7.35 (dd, J_{AB} = 4.0 Hz, J_{AC} = 8.0 Hz 1H), 7.94 (d, J = 4.0 Hz, 1H), 8.20 (d, J = 8.0 Hz, 1H), 8.50 (m, 1H), 9.99 (s, 1H). ^{13}C NMR (100 MHz, $CDCl_3$): δ (ppm) 60.6, 112.8, 123.1, 127.4, 128.9. 129.0, 129.6, 135.3, 138.2, 139.1, 139.1, 148.2, 170.6. MS (m/z, %): 464.1 (7), 297 (100).

HSQC

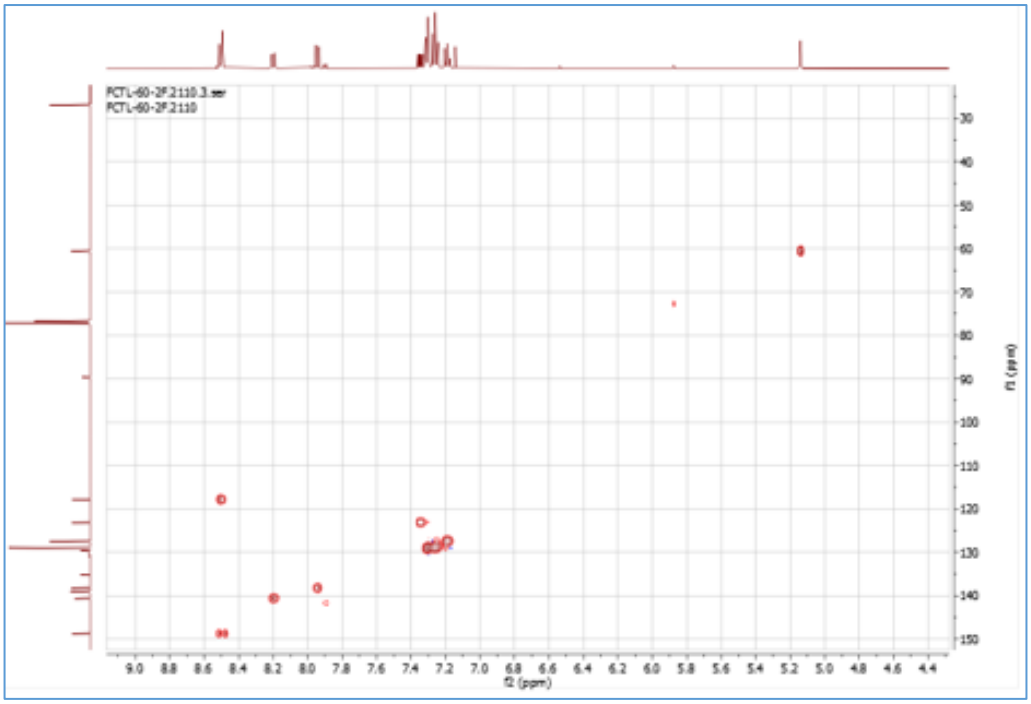

HMBC

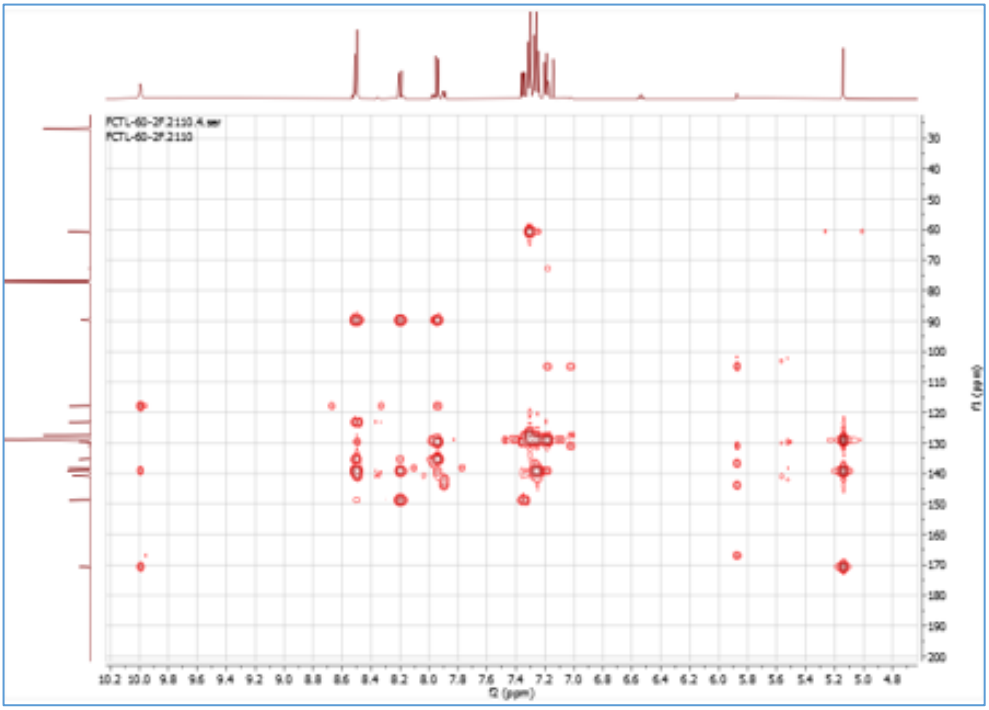

Method B: A bottom flask was charged with diphenyl-*N*-(8-quinolinyl)acetamide **63** (60 mg, 1 eq., 0.18 mmol), $Pd(OAc)_2$ (0.8 mg, 20 mol%, 0.020 mmol), I_2 (135 mg, 3 eq., 0.53 mmol), and DMSO (10 mL). The mixture was stirred at 60°C for 24h under air. Then, the mixture was quenched with an aqueous solution of $Na_2S_2O_3$ and with an aqueous solution of $NaHCO_3$. The solution was then extracted with EtOAc. The combined organic portions were washed with water and then with brine. The resulting solution was dried over anhydrous Na_2SO_4, filtered,

and concentrated under vacuum. The crude was purified by preparative TLC (30% EtOAc/Hexane) to obtain 2-(2-iodophenyl)-2-phenyl-*N*-(quinolin-8-yl)acetamide **69** (40mg, 0.086 mmol, 48%).

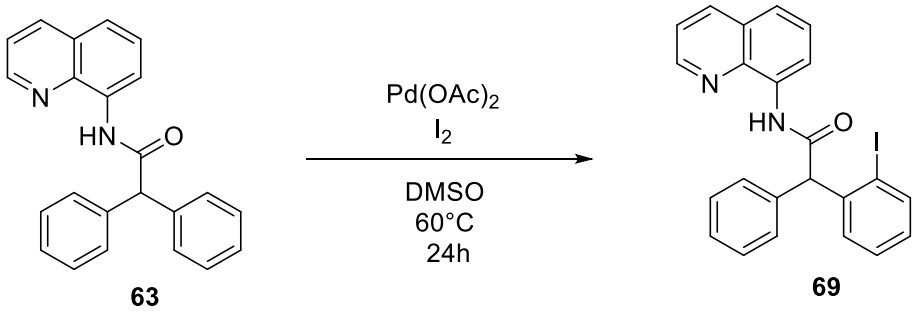

63 **69**

R_f = 0.3 (30% EtOAc/Hexane)

^{1}H NMR (400 MHz, $CDCl_3$); δ (ppm) 5.61 (s, 1H), 7.19 (m, 2H), 6.96 (t, J = 8.0 Hz, 2H), 7.16 (d, J = 8.0 Hz, 1H), 7.27 (d, J = 8.0 Hz, 1H), 7.31 (m, 3H), 7.33 (d, J = 8.0 Hz, 1H), 7.45 (m, 2H), 7.87 (d, J = 8.0 Hz, 1H), 8.05 (d, J = 8.0 Hz, 1H), 8.57 (d, J = 8.0 Hz, 1H),8.78 (d, J = 8.0 Hz, 1H), 10.01 (s, 1H). ^{13}C NMR (100 MHz, $CDCl_3$): δ (ppm) 69.3, 103.1, 116.5, 121.6, 122.0, 127.4, 127.9, 128.7, 128.9, 129.3, 129.4, 134.3, 136.2, 140.2, 141.2, 148.3, 168.7. MS (m/z, %): 464.1 (1.5), 171 (100).

CONCLUSIONS

During my PhD project, I have involved in three different studies.

In the first study (Chapter 1) the content of total polyphenol compounds and of *trans*-resveratrol into three different varieties of grape pomace *("Aglianico del Vulture", "Yuko" and "Piedirosso")* was analyzed using two different extraction procedures. The percentage of total polyphenols obtained for all three GP extracts was very good, so considering their innumerable beneficial properties for human health, these wine byproducts could be a potential matrices for the formulation of new drugs and supplements food. The HPLC-UV method applied for the quantification of *trans*-resveratrol in the three GP extracts gave a bad to quite good separation in the chromatographic runs. In the GP from *"Piedirosso"* analysis the peak of *trans*-resveratrol was not much resolved and for this reason the content of *trans*-resveratrol obtained could not be accurately evaluated. A better separation was obtained in the chromatographic runs of GP from *"Aglianico del Vulture"* and the content of *trans*-resveratrol was found quite in agreement with the results obtained in previous research on different red grape. Finally, the best separation was obtained in the chromatographic runs of GP from *"Yuko"*, in which the peak of *trans*-resveratrol was quite resolved and the content obtained very high.

In the second study (Chapter 2), taking advantage of the good preliminary results obtained in the regio- and stereoselective phenylation of oxo-substituted *trans* 2,3-diaryloxiranes with the phenylzinc reagent, the scope of this reaction using various aryl boronic acid was investigated. The ring-opening reaction of *ortho*-substituted *trans* 2,3-diaryloxiranes proved to be quite general in terms of regio- and stereoselectivity using different aryl boronic acids as nucleophile source, affording the *syn* aryl alcohols in good yields. Furthermore, the synthetic approach previously used for the preparation of *trans* 2,3-diphenyl-2,3-dihydrobenzofuran was successfully applied for the preparation of new seven methoxy-bromo derivatives of *trans*-2,3-diaryl-2,3-dihydrobenzofuran and for the preparation of three polyfunctionalized intermediates bearing 2,3-diaryl-2,3-dihydrobenzofuran structure towards the synthesis of Gnetin C and ε-Viniferin, even in enantioenriched form. The seven methoxy-bromo derivatives of *trans*-2,3-diaryl-2,3-dihydrobenzofuran was tested as anti-inflammatories in U937 cells. All compounds showed a significant role in inhibiting the NF-κB pathway and were able to restore normal ROS and NO level upon LPS activation. Moreover, regarding inhibition of ACLY and reduction of prostaglandin E2 production, enantioenriched *trans* 5-Methoxy-2,3-diphenyl-2,3-dihydro-benzofuran showed more potency than the racemic counterpart, thus suggesting a stereoselective interaction in this pathway.

In the third study (Chapter 3), the metal-catalyzed C-H functionalization on the diphenyl acetaldehyde, which could be a new potential key intermediate for alternative route to 2,3-diaryl- 2,3-dihydrobenzofurans, was investigated. The first attempts of Pd-catalyzed C-H olefination using L-*tert*-leucine as *c*TDG gave only degradation products because the reaction of amino acid with the diphenylacetaldehyde did not form the fundamental imine intermediate for the catalytic cycle. Instead, the traditional metal catalyzed reaction using 8-aminoquinoline as external donating group provided interesting results. The Pd-catalyzed C-H olefination of diphenyl-*N*-(8-quinolinyl)acetamide led to a product in which there was double C-H activation: the Heck type reaction with the alkene and the subsequent intramolecular cyclization. The Pd-catalyzed C-H acetoxylation using $PhI(OAc)_2$ as acetoxylating agent and the Pd-catalyzed C-H

iodination using NIS as iodinating agent of diphenyl-*N*-(8-quinolinyl)acetamide led to a products in which there were the C-H functionalization on the aminoquinoline. Finally the Pd-catalyzed C-H iodination of diphenyl-*N*-(8-quinolinyl)acetamide using I_2 as iodinating agent afforded the desired iodinated product in good yield.

LIST OF PUBLICATIONS

- T. Laurita, L. Chiummiento, M. Funicello, R. D'Orsi, D. Salemi, D. Tofani, P. Lupattelli "Regio- and Diastereoselective Organo-Zinc-Promoted Arylation of trans-2,3-Diaryloxiranes by Arylboronic Acids: Stereoselective Access to trans.2,3-Diphenyl-2,3-dihydrobenzofuran", *Eur. J. Org. Chem.* **2019,** 4397–4403.

- T. Laurita, R. D'Orsi, L. Chiummiento, M. Funicello, P. Lupattelli "Recent Advances in Synthetic Strategies to 2,3-Dihydrobenzofurans" *Synthesis* 2020**,** *52***,** 1451-1477.

- R. D'Orsi, F. Morrongiello, T. Laurita, M. Funicello, P. Lupattelli, L. Chiummiento "Regio- and DIastereo-Selective Biomimetic Synthesis of (±)-ε-Viniferin by NIS and Resveratrol" *Chemistry Select.*, **2021**, *6*, 6863-6866.

- T. Laurita, I. Pappalardo, L. Chiummiento, R. D'Orsi, M. Funicello, A. Santarsiero, M. Marsico, V. Infantino, S. Todisco, P Lupattelli " Synthesis of new methoxy derivatives of *trans* 2,3-diaryl-2,3-dihydrobenzofurans and evaluation of their anti-inflammatory activity" *Bioorg. Med. Chem. Lett.* **2021**, *49*, 128264.

- R. D'Orsi, M. Funicello, T. Laurita, P. Lupattelli, F. Berti, L. Chiummiento "The Pseudo-Symmetric *N*-benzyl Hydroxyethylamine Core in a New Serie of Heteroarylcarboxyamide HIV-1 Inhibitors: Synthesis, Molecular Modeling and Biological Evaluation" *Biomolecules* **2021**, *11*, 1584.

CONTRIBUTION TO CONFERENCES

- T. Laurita, R. D'Orsi, M. Funicello, L. Chiummiento, P. Lupattelli "*From diariloxiranes to dihydrobenzofurans: a story of a ring opening and cyclization"*, I Virstual Symposium on Pericycloc Reaction and Synthetic of Carbo- and Heterocyclic Sistems-2020 (**ORAL**)
- T. Laurita, M. Funicello, L. Chiummiento, P. Lupattelli "*Regio- and diasteroselective organo-zinc promoted arylation of trans 2,3-diaryloxiranes by arylboronic acids: stereoselective access to trans 2,3-diaryl-2,3-dihydrobenzofuran"* XXXIX Congresso Nazionale della divisione organica della Società chimica Italiana-2019, Torino, Italy (**POSTER**)

ACKNOWLEDGEMENTS

During my PhD I had the great pleasure to work with wonderful and professional people and I would like to express my gratitude to each of them, for the fundamental research experience they have granted me.

Foremost, I would like to express my sincere gratitude to my tutor Prof. Paolo Lupattelli for the continuous support of my Ph.D study and research, for his patience, motivation, enthusiasm, and immense knowledge. He has been a true mentor for me, an essential point of reference giving me a constant human, scientific and moral support.

My sincere thanks go also to Dr. Lucia Chiummiento for her collaboration, her human support and her constructive and critical opinions; and to Prof. Maria Funicello for her disponibility and kidness.

I wish also thanks to all Osun Solutions S.r.l. staff: Antonella, Catia, Anna and in particular Filomena for her precious help and for being a fundamental guide during this experience.

A great acknowledgement to Prof. Françoise Colobert, Dr. Gilles Hanquet, Dr. Sabine Choppin and Dr. Joanna Wencel-Delord for hosting me for six months in their Syncat group at the University of Strasbourg and leading me working on diverse project. I am grateful to all the people who helped me in that period, in particular Matteo Lanzi for his scientific and moral support.

I am also grateful to all the friends and people with whom I shared part of my research, in particular the "CollegheAmiche": Marisabel, Giulia, Francesca, Rosarita and Gerarda.
A great thanks go to my friend Rosarita: we shared troubles and happiness since bachelor degree up to this important goal. Thank you for always supporting and helping me over the years.

My special thanks go to my best friends Stefania, Donato and Francesca for the continuous encouragement and support but above all you for hepling me not to forget to enjoy the many others beautiful things that life has to offer.

I deeply feel I have to express my great gratitude to all my family, because they never left me alone. I want to thank my parents for the patience, my brother Luigi and my sister Antonietta for their support and encouragement throughout my study.

In the end, the most important person I want to thank is my niece Irene, because she is the most precious treasure of my life.